

Analysis of bird flight calls from the German North and Baltic Seas

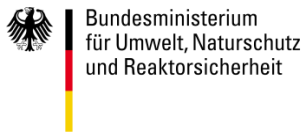
Report from the ProBIRD project

Jorg Welcker
Raúl Vilela



Husum, June 2018

Funded by



Bundesministerium für Umwelt, Naturschutz und nukleare Sicherheit (BMU)
Stresemannstraße 128-130
10117 Berlin, Germany

Coordinated and supported by



Bundesamt für Seeschifffahrt und Hydrographie (BSH)
Federal Maritime and Hydrographic Agency
Bernhard-Nocht-Straße 78
20359 Hamburg, Germany

The research project “ProBIRD” (FKZ UM15 86 2000) is funded by BMU (Ressortforschungsplan 2015).

Responsibility for the content of this report lies entirely with the authors.

Authors



Dr. Jorg Welcker and Dr. Raúl Vilela
BioConsult SH GmbH & Co. KG
Schobüller Str. 36
25813 Husum, Germany

Citation

Welcker, J. & Vilela, R. 2018. Analysis of bird flight calls from the German North and Baltic Seas. Final Report – June 2018. BioConsult SH, Husum. 128 pp.

Contents

1 SUMMARY.....1

2 INTRODUCTION.....3

3 MATERIALS & METHODS5

3.1 Data collection5

3.2 Data analysis8

3.2.1 Phenology8

3.2.2 Spatial correlation of call rates8

3.2.3 Mass migration9

3.2.4 Spatial gradients10

3.2.5 Weather11

4 RESULTS13

4.1 Phenology13

4.2 Spatial correlation of call rates17

4.3 Correlation of mass migration22

4.4 Gradient of call intensities23

4.4.1 Gradient between North and Baltic Sea23

4.4.2 Gradient with distance to shore within the North Sea26

4.5 Weather models29

4.5.1 Model performance and importance of explanatory variables29

4.5.2 Species-specific results37

5 DISCUSSION42

5.1 Seasonality43

5.2 Spatial correlation.....44

5.3 Mass migration45

5.4	Gradient of call intensities	45
5.5	Weather models	46
6	LITERATURE.....	50
A	APPENDIX.....	54
A.1	Data summary.....	54
A.2	Spatial correlation of call rates	58
A.3	Spatial gradients	60
A.4	Weather models	69

List of figures

Figure 2.1	Location of the study sites in the EEZ of the German North and Baltic Sea.....	5
Figure 2.2	Microphone systems used at OSS ‘Butendiek’ and OSS ‘Nordsee Ost’ (left) and on FINO1 (right, from OREJAS et al. 2005).....	7
Figure 2.3	Histogram of mean call intensities per night [calls/h] of all species combined.	9
Figure 2.4	Left panel: cumulative number of calls [%] per time [%]. Two values are indicated: 71 % of calls were recorded in only 5 % of the nights; 90 % of the calls were recorded in 14 % of the nights. Right panel: Mean call intensities per night sorted in ascending order to illustrate the definition of ‘mass migration’ (median * 100) and ‘high call intensities’ (median * 25).....	10
Figure 3.1	Species composition of flight calls recorded between 2008 and 2015 in the German EEZ of the North and Baltic Sea.....	13
Figure 3.2	Phenology of call rates (calls*h ⁻¹) of two wader species in the German EEZ of the North and Baltic Sea. Call rates were standardized between years and projects and plotted as 3-day moving average. In addition the time period with the inner 90% of calls (red dashed lines) per season are given (see text for details).....	14
Figure 3.3	Phenology of call rates (calls*h ⁻¹) of four thrush species in the German EEZ of the North and Baltic Sea. See Figure 3.2 and text for details.	15
Figure 3.4	Phenology of call rates (calls*h ⁻¹) of four passerine species in the German EEZ of the North and Baltic Sea. See Figure 3.2 and text for details.	16

Figure 3.5 Relationship between distance between sites and the correlation of call rates (Spearman’s rank correlation coefficient rho) of the combined data of two species of waders (Common Sandpiper and Dunlin) for spring (upper panel) and fall (lower panel). Correlation coefficients were calculated based on days with simultaneous observations of each pair of projects and years. The number of days a coefficient is based on is indicated by symbol size (minimum number of days = 5). Left panel: linear regression for data from the North Sea; right panel: mean correlation coefficient [± SE] for North Sea sites (open symbol) and for comparisons between North and Baltic Sea (filled symbols). 19

Figure 3.6 Relationship between distance between sites and the correlation of call rates (Spearman’s rank correlation coefficient rho) of the combined data of four thrush species (Blackbird, Song Thrush, Redwing and Fieldfare) for spring (upper panel) and fall (lower panel). For details see Figure 3.5 and Materials & Methods. 20

Figure 3.7 Relationship between distance between sites and the correlation of call rates (Spearman’s rank correlation coefficient rho) of the combined data of four passerine species (Robin, Starling, Meadow Pipit and Skylark) for spring (upper panel) and fall (lower panel). For details see Figure 3.5 and Materials & Methods. 21

Figure 3.8 Relationship between distance between sites and the correlation of call rates (Spearman’s rank correlation coefficient rho) of the combined data of four thrush species (Blackbird, Song Thrush, Redwing and Fieldfare). The relationship differed between seasons (spring vs. fall) and with observation method (observer only vs. mixed data observer/microphone systems). Predicted values based on an additive linear model are indicated for the different factor levels. 22

Figure 3.9 Left panel: relationship between the distance between wind farms and the predicted probability [± SE] of coincidence of high call intensities at these sites. Data restricted to North Sea only. Right panel: relationship between the distance between wind farms and the predicted probability of coincidence of mass migration events. Data from both North and Baltic Seas. Predicted probabilities are based on generalized linear models with binomial error structure (see text for further details). Filled symbols represent distances between sites at which high migration intensities coincided, open symbols distances at which high call intensities did not coincide. 23

Figure 3.10 Call intensities (calls/h, log transformed) of waders simultaneously measured in the Baltic and North Sea. Box plots indicate the median (bold black bar) and the interquartile range (box), the whiskers extend to the most extreme data points which are no more than 1.5 times the interquartile range, open symbols indicate values outside 1.5 times the interquartile range. Additionally, the results of paired Wilcoxon rank-sum tests (** p < 0,001; * p < 0,01; * p < 0,05; - p > 0,05) and the sample size of paired observations are given above the box plots. Results are shown separately for spring (lower left panel) and fall (lower right panel), as well as for comparisons restricted to the same developmental phase of the wind farms (upper right panel) and for all data combined (upper left panel). 24

Figure 3.11 Call intensities (calls/h, log transformed) of thrushes simultaneously measured in the Baltic and North Sea. See Figure 3.10 for further details. 25

Figure 3.12 Call intensities (calls/h, log transformed) of other passerine species simultaneously measured in the Baltic and North Sea. See Figure 3.10 for further details. 26

Figure 3.13 Relationship of the difference in call rates between two sites and their difference in distance to shore for the species group of waders. The results of a linear regression are given above the plot. Left panel: during spring migration; right panel: during fall migration.	27
Figure 3.14 Relationship of the difference in call rates between two sites and their difference in distance to shore for thrushes. The results of a linear regression are given above the plot. Left panel: during spring migration; right panel: during fall migration.	28
Figure 3.15 Relationship of the difference in call rates between two sites and their difference in distance to shore for other passerine species. The results of a linear regression are given above the plot. Left panel: during spring migration; right panel: during fall migration.	28
Figure 3.16 Examples of partial dependence plots of time from midnight. Upper panel: Blackbird in fall (left) and Redwing in spring (right). Lower panel: Skylark in fall (left) and Meadow Pipit in fall (right).	31
Figure 3.17 Examples of partial dependence plots of TWC and δ TWC. Upper panel: Redwing in spring (left) and Song Thrush in spring (right). Mid panel: Redwing in fall (left) and Song Thrush in fall (right). Lower panel: δ TWC of Skylark in fall (left) and Starling in spring (right).	32
Figure 3.18 Examples of partial dependence plots of CWC for spring and fall. Upper panel: Blackbird in spring (left) and Robin in spring (right). Lower panel: Starling in fall (left) and Song Thrush in fall (right).	33
Figure 3.19 Examples of partial dependence plots of cloud cover for spring (upper panels) and fall (lower panels). Upper panel: Blackbird in spring (left) and Fieldfare in spring (right). Lower panel: Blackbird in fall (left) and Robin in fall (right).	34
Figure 3.20 Examples of partial dependence plots of rain. Upper panel: Blackbird (right) and Redwing (left) in spring. Lower panel: Meadow Pipit in spring (left) and Common Sandpiper in fall (right).	35
Figure 3.21 Examples of partial dependence plots of ambient temperature (left) and interaction plots of ambient temperature with Julian day (right). Upper panel: Fieldfare in spring, mid panel: Meadow pipit in fall, and lower panel: Robin in fall.	36
Figure A. 1 Relationship between distance between sites and the correlation of call rates (Spearman’s rank correlation coefficient rho) of two wader species for spring and fall. For details see Figure 3.5 and Materials & Methods.	58
Figure A. 2 Relationship between distance between sites and the correlation of call rates (Spearman’s rank correlation coefficient rho) of four thrush species for spring and fall. For details see Figure 3.5 and Materials & Methods.	59
Figure A. 3 Relationship between distance between sites and the correlation of call rates (Spearman’s rank correlation coefficient rho) of four passerine species for spring and fall. For details see Figure 3.5 and Materials & Methods.	60
Figure A. 4 Call intensities (calls/h, log transformed) of the Common Sandpiper simultaneously measured in the Baltic and North Sea. See Figure 3.10 for further details.	61
Figure A. 5 Call intensities (calls/h, log transformed) of the Dunlin simultaneously measured in the Baltic and North Sea. See Figure 3.10 for further details.	61

Figure A. 6 Call intensities (calls/h, log transformed) of the Blackbird simultaneously measured in the Baltic and North Sea. See Figure 3.10 for further details. 62

Figure A. 7 Call intensities (calls/h, log transformed) of the Redwing simultaneously measured in the Baltic and North Sea. See Figure 3.10 for further details. 62

Figure A. 8 Call intensities (calls/h, log transformed) of the Song Thrush simultaneously measured in the Baltic and North Sea. See Figure 3.10 for further details. 63

Figure A. 9 Call intensities (calls/h, log transformed) of the Fieldfare simultaneously measured in the Baltic and North Sea. See Figure 3.10 for further details. 63

Figure A. 10 Call intensities (calls/h, log transformed) of the Skylark simultaneously measured in the Baltic and North Sea. See Figure 3.10 for further details. 64

Figure A. 11 Call intensities (calls/h, log transformed) of the Meadow Pipit simultaneously measured in the Baltic and North Sea. See Figure 3.10 for further details. 64

Figure A. 12 Call intensities (calls/h, log transformed) of the Robin simultaneously measured in the Baltic and North Sea. See Figure 3.10 for further details. 65

Figure A. 13 Call intensities (calls/h, log transformed) of the Starling simultaneously measured in the Baltic and North Sea. See Figure 3.10 for further details. 65

Figure A. 14 Relationship of the difference in call rates between two sites and their difference in distance to shore for Common Sandpiper and Dunlin. The results of a linear regression are given above the plot. Left panel: during spring migration; right panel: during fall migration. 66

Figure A. 15 Relationship of the difference in call rates between two sites and their difference in distance to shore for Blackbird, Redwing, Song Thrush and Fieldfare. The results of a linear regression are given above the plot. Left panel: during spring migration; right panel: during fall migration. ... 67

Figure A. 16 Relationship of the difference in call rates between two sites and their difference in distance to shore for Skylark, Meadow Pipit, Robin and Starling. The results of a linear regression are given above the plot. Left panel: during spring migration; right panel: during fall migration. 68

Figure A. 17 *Common Sandpiper spring, continued on next page.* 69

Figure A. 18 *Common Sandpiper spring, continued on next page.* 70

Figure A. 19 Common Sandpiper spring: Top left panel shows the Standardized Error Variable Importance (%IncMSE) plot. Top right panel shows the multi-way importance plot. Below are the partial dependence plots for each variable included in the model (note the different scales of the partial effect on the y-axis). In the lower panels interaction plots are shown: TWC vs CWC, TWC vs Julian day, TWC vs hour from midnight and Julian day vs ambient temperature. Colours of the interaction plots represent the predicted bird call rate (square root transformed) for each combination of effects. 71

Figure A. 20 Common Sandpiper fall: Top left panel shows the Standardized Error Variable Importance (%IncMSE) plot. Top right panel shows the multi-way importance plot. Below are the partial dependence plots for each variable included in the model (note the different scales of the partial effect on the y-axis). In the lower panels interaction plots are shown: TWC vs CWC, TWC vs Julian day, TWC vs hour from midnight and Julian day vs ambient temperature. Colours of the interaction plots represent the predicted bird call rate (square root transformed) for each combination of effects. 74

Figure A. 21 Dunlin spring: Top left panel shows the Standardized Error Variable Importance (%IncMSE) plot. Top right panel shows the multi-way importance plot. Below are the partial dependence plots for each variable included in the model (note the different scales of the partial effect on the y-axis). In the lower panels interaction plots are shown: TWC vs CWC, TWC vs Julian day, TWC vs hour from midnight and Julian day vs ambient temperature. Colours of the interaction plots represent the predicted bird call rate (square root transformed) for each combination of effects. 77

Figure A. 22 Dunlin fall: Top left panel shows the Standardized Error Variable Importance (%IncMSE) plot. Top right panel shows the multi-way importance plot. Below are the partial dependence plots for each variable included in the model (note the different scales of the partial effect on the y-axis). In the lower panels interaction plots are shown: TWC vs CWC, TWC vs Julian day, TWC vs hour from midnight and Julian day vs ambient temperature. Colours of the interaction plots represent the predicted bird call rate (square root transformed) for each combination of effects. 80

Figure A. 23 Blackbird spring: Top left panel shows the Standardized Error Variable Importance (%IncMSE) plot. Top right panel shows the multi-way importance plot. Below are the partial dependence plots for each variable included in the model (note the different scales of the partial effect on the y-axis). In the lower panels interaction plots are shown: TWC vs CWC, TWC vs Julian day, TWC vs hour from midnight and Julian day vs ambient temperature. Colours of the interaction plots represent the predicted bird call rate (square root transformed) for each combination of effects. 83

Figure A. 24 Blackbird fall: Top left panel shows the Standardized Error Variable Importance (%IncMSE) plot. Top right panel shows the multi-way importance plot. Below are the partial dependence plots for each variable included in the model (note the different scales of the partial effect on the y-axis). In the lower panels interaction plots are shown: TWC vs CWC, TWC vs Julian day, TWC vs hour from midnight and Julian day vs ambient temperature. Colours of the interaction plots represent the predicted bird call rate (square root transformed) for each combination of effects. 86

Figure A. 25 Redwing spring: Top left panel shows the Standardized Error Variable Importance (%IncMSE) plot. Top right panel shows the multi-way importance plot. Below are the partial dependence plots for each variable included in the model (note the different scales of the partial effect on the y-axis). In the lower panels interaction plots are shown: TWC vs CWC, TWC vs Julian day, TWC vs hour from midnight and Julian day vs ambient temperature. Colours of the interaction plots represent the predicted bird call rate (square root transformed) for each combination of effects. 89

Figure A. 26 Redwing fall: Top left panel shows the Standardized Error Variable Importance (%IncMSE) plot. Top right panel shows the multi-way importance plot. Below are the partial dependence plots for each variable included in the model (note the different scales of the partial effect on the y-axis). In the lower panels interaction plots are shown: TWC vs CWC, TWC vs Julian day, TWC vs hour from midnight and Julian day vs ambient temperature. Colours of the interaction plots represent the predicted bird call rate (square root transformed) for each combination of effects. 92

Figure A. 27 Song Thrush spring: Top left panel shows the Standardized Error Variable Importance (%IncMSE) plot. Top right panel shows the multi-way importance plot. Below are the partial dependence plots for each variable included in the model (note the different scales of the partial effect on the y-axis). In the lower panels interaction plots are shown: TWC vs CWC, TWC vs Julian day, TWC vs hour from midnight and Julian day vs ambient temperature. Colours of the interaction plots represent the predicted bird call rate (square root transformed) for each combination of effects. 95

Figure A. 28 Song Thrush fall: Top left panel shows the Standardized Error Variable Importance (%IncMSE) plot. Top right panel shows the multi-way importance plot. Below are the partial dependence plots for each variable included in the model (note the different scales of the partial effect on the y-axis). In the lower panels interaction plots are shown: TWC vs CWC, TWC vs Julian day, TWC vs hour from midnight and Julian day vs ambient temperature. Colours of the interaction plots represent the predicted bird call rate (square root transformed) for each combination of effects. 98

Figure A. 29 Fieldfare spring: Top left panel shows the Standardized Error Variable Importance (%IncMSE) plot. Top right panel shows the multi-way importance plot. Below are the partial dependence plots for each variable included in the model (note the different scales of the partial effect on the y-axis). In the lower panels interaction plots are shown: TWC vs CWC, TWC vs Julian day, TWC vs hour from midnight and Julian day vs ambient temperature. Colours of the interaction plots represent the predicted bird call rate (square root transformed) for each combination of effects. 101

Figure A. 30 Fieldfare fall: Top left panel shows the Standardized Error Variable Importance (%IncMSE) plot. Top right panel shows the multi-way importance plot. Below are the partial dependence plots for each variable included in the model (note the different scales of the partial effect on the y-axis). In the lower panels interaction plots are shown: TWC vs CWC, TWC vs Julian day, TWC vs hour from midnight and Julian day vs ambient temperature. Colours of the interaction plots represent the predicted bird call rate (square root transformed) for each combination of effects. 104

Figure A. 31 Meadow Pipit spring: Top left panel shows the Standardized Error Variable Importance (%IncMSE) plot. Top right panel shows the multi-way importance plot. Below are the partial dependence plots for each variable included in the model (note the different scales of the partial effect on the y-axis). In the lower panels interaction plots are shown: TWC vs CWC, TWC vs Julian day, TWC vs hour from midnight and Julian day vs ambient temperature. Colours of the interaction plots represent the predicted bird call rate (square root transformed) for each combination of effects. 107

Figure A. 32 Meadow Pipit fall: Top left panel shows the Standardized Error Variable Importance (%IncMSE) plot. Top right panel shows the multi-way importance plot. Below are the partial dependence plots for each variable included in the model (note the different scales of the partial effect on the y-axis). In the lower panels interaction plots are shown: TWC vs CWC, TWC vs Julian day, TWC vs hour from midnight and Julian day vs ambient temperature. Colours of the interaction plots represent the predicted bird call rate (square root transformed) for each combination of effects. 110

Figure A. 33 Skylark spring: Top left panel shows the Standardized Error Variable Importance (%IncMSE) plot. Top right panel shows the multi-way importance plot. Below are the partial dependence plots for each variable included in the model (note the different scales of the partial effect on the y-axis). In the lower panels interaction plots are shown: TWC vs CWC, TWC vs Julian day, TWC vs hour from midnight and Julian day vs ambient temperature. Colours of the interaction plots represent the predicted bird call rate (square root transformed) for each combination of effects. 113

Figure A. 34 Skylark fall: Top left panel shows the Standardized Error Variable Importance (%IncMSE) plot. Top right panel shows the multi-way importance plot. Below are the partial dependence plots for each variable included in the model (note the different scales of the partial effect on the y-axis). In the lower panels interaction plots are shown: TWC vs CWC, TWC vs Julian day, TWC vs hour from midnight and Julian day vs ambient temperature. Colours of the interaction plots represent the predicted bird call rate (square root transformed) for each combination of effects. 116

Figure A. 35 Robin spring: Top left panel shows the Standardized Error Variable Importance (%IncMSE) plot. Top right panel shows the multi-way importance plot. Below are the partial dependence plots for each variable included in the model (note the different scales of the partial effect on the y-axis). In the lower panels interaction plots are shown: TWC vs CWC, TWC vs Julian day, TWC vs hour from midnight and Julian day vs ambient temperature. Colours of the interaction plots represent the predicted bird call rate (square root transformed) for each combination of effects. 119

Figure A. 36 Robin fall: Top left panel shows the Standardized Error Variable Importance (%IncMSE) plot. Top right panel shows the multi-way importance plot. Below are the partial dependence plots for each variable included in the model (note the different scales of the partial effect on the y-axis). In the lower panels interaction plots are shown: TWC vs CWC, TWC vs Julian day, TWC vs hour from midnight and Julian day vs ambient temperature. Colours of the interaction plots represent the predicted bird call rate (square root transformed) for each combination of effects. 122

Figure A. 37 Starling spring: Top left panel shows the Standardized Error Variable Importance (%IncMSE) plot. Top right panel shows the multi-way importance plot. Below are the partial dependence plots for each variable included in the model (note the different scales of the partial effect on the y-axis). In the lower panels interaction plots are shown: TWC vs CWC, TWC vs Julian day, TWC vs hour from midnight and Julian day vs ambient temperature. Colours of the interaction plots represent the predicted bird call rate (square root transformed) for each combination of effects. 125

Figure A. 38 Starling fall: Top left panel shows the Standardized Error Variable Importance (%IncMSE) plot. Top right panel shows the multi-way importance plot. Below are the partial dependence plots for each variable included in the model (note the different scales of the partial effect on the y-axis). In the lower panels interaction plots are shown: TWC vs CWC, TWC vs Julian day, TWC vs hour from midnight and Julian day vs ambient temperature. Colours of the interaction plots represent the predicted bird call rate (square root transformed) for each combination of effects. 128

List of tables

Table 2.1 Study sites (wind farm locations), bird call recording systems and sample sizes of the data set used in this study. In addition, years with available data and the developmental phase of the wind farms during data collection (B – baseline, C – construction, O – operation) is given. 6

Table 3.1 Main migration periods (time periods with inner 90% of calls, see text) and peak for spring and fall migration in the German EEZ of the North and Baltic Sea..... 17

Table 3.2 Mean correlation coefficients (Spearman’s rank correlation coefficient rho) for correlations of call rates between sites within the North Sea and between sites across the North and Baltic Sea for the different species and species groups. In addition, sample sizes (number of correlations within the North Sea and between the North and Baltic Sea, respectively) are given. Bold values indicate significant differences according to a non-parametric Wilcoxon rank-sum test (where applicable). 18

Table 3.3 Summary of model results by species and season. N hours is the number of hours observed, % Var. expl. is the percentage of variance explained by the model. In addition, for each predictor variable the ranked “Standardized Error Variable Importance” is indicated (see Materials & Methods for details). 30

Tab. A 1 List of species and number of calls recorded in the time between 2008 and 2015 at 13 locations in the German EEZ of the North and Baltic Sea (see text for details). Species selected for further analyses are shaded in grey. 54

1 SUMMARY

A large number of migrating birds cross the offshore waters of the German North and Baltic Sea each year on the way from their breeding grounds to their wintering areas and back. The majority of these birds, particularly songbirds, migrate during the night.

With the increasing development of offshore wind farms in the German Exclusive Economic Zone (EEZ) the potential impact of wind turbines on nocturnal migrants has come into focus. However, information on temporal and spatial patterns of nocturnal migrants at offshore locations is still scarce, especially regarding information on species level.

Many species produce specific flight calls during migration. Although the number of these calls may not necessarily be proportional to the number of birds migrating the recording of flight calls is the only method readily available to collect information on nocturnal migration behavior for single species.

Here we use data from 13 different offshore wind farm sites in the German EEZ of the North and Baltic Sea collected during eight years (2008 – 2015) to analyze temporal and spatial patterns of nocturnal bird migration in this area. The main aims of the study were i) to test whether and to what extent call rates and events of mass migration correlate across sites and regions, ii) to test the hypotheses of a gradient of migration intensities between the North and Baltic Sea, and with increasing distance to shore within the North Sea, and iii) to determine the effect of weather conditions on call rates in our study area. Out of 127 species recorded we selected 10 species for further analyses: four thrush species (Blackbird, Redwing, Song Thrush and Fieldfare), four other passerine species (Skylark, Meadow Pipit, Robin and Starling) as well as two species of waders (Dunlin and Common Sandpiper).

For these species we found that the overall correlation of call intensities was relatively high (mean Spearman rank correlation coefficient over all species and project-years: 0.42 ± 0.02 SE) yet varied substantially between species, seasons and between the North and Baltic Sea. Notably, the correlation strength declined with increasing distance between sites in thrushes and waders. The spatial relationship of events of mass migration, defined as call intensities $> 100 \times$ median call rate, was similar. While events of mass migration coincided with a probability of approx. 70% for sites in close vicinity, the probability dropped to about 20% at 100 km distance between sites indicating that the correlation of mass migration was not higher than that of ordinary call intensities.

Simultaneous observations in the North and Baltic Sea showed that call rates of thrushes and the other passerine species studied were systematically higher in the Baltic Sea. With respect to a gradient within the North Sea results differed between seasons and species. Our data indicated that in fall call rates declined with increasing distance to shore for all species groups. However, in spring an opposite relationship was evident for thrushes. In spring call rates of this species group increased with increasing distance to shore, while the relationship was negative for the other passerine species and call rates were independent of distance to shore in waders. These results suggest that no general gradient exists with the EEZ of the German North Sea with respect to call rates. It also needs to be noted that distance to shore generally explained only a small proportion of the variance indicating that other factors have to be considered to explain variability among sites.

We used Random Forest regression models to determine the effect of a number of meteorological and time-related variables on call rates. Model performance varied substantially among species with between 1.2 and 66.8% of the variance explained. Generally, call rates varied between study years, with Julian day and in the course of the night. Other factors included in the analyses such as study site, developmental stage of the wind farm and the company responsible for data collection were of minor importance.

Contrary to expectations based on knowledge of the temporal pattern of nocturnal migration intensities, call rates generally increased in the course of the night with maximum intensities usually being reached in the hours before dawn. This suggests that birds may reduce flight altitude towards the end of the night and/or increase call activity itself when in search of a stop-over site.

Atmospheric parameters had strong effects on call rates that were largely consistent across species but varied to some extent between migration periods. Call rates increased with increasing tailwind usually in a stepwise fashion with birds tolerating moderate headwinds in fall but not in spring. This could reflect the relatively scarce occurrence of tailwinds in fall with predominating southwesterly winds in the study area. Seaward crosswinds also increased call intensities indicating partial drift of birds to offshore locations.

Call rates correlated positively with cloud cover. In both spring and fall highest call intensities were recorded with completely overcast skies. In contrast to spring, call rates in fall were also elevated with clear skies. These results suggest that birds loose altitude when visibility of the sky is limited and perhaps additionally increase call activity itself in these conditions. High call rates with clear skies are likely to be related to high migration intensities. Sufficient visibility of the stars is regarded as a factor favoring high migration activity.

The relationship between call rates and ambient temperature suggested that temperature primarily affected the timing of migration. In spring, high call rates early in the season were often conditional on high ambient temperatures. In fall low temperatures stimulated early migration while high temperatures delayed the timing of migration.

These results suggest that high call rates occur both during unfavorable conditions (crosswinds, overcast skies, rain) but also during favorable conditions (tailwinds, clear skies). As nocturnal migrants are often supposed to incur a high risk of collision at offshore structures during deteriorating flight conditions high call rates may not necessarily be a good indicator of such situations.

2 INTRODUCTION

Millions of songbirds migrate twice a year between their breeding range in Scandinavia and northern Russia and their wintering grounds in southern Europe and Africa (BERTHOLD et al. 2003). The majority of these birds migrate during the night.

Diurnally migrating passerines usually avoid migrating over large expanses of water. Hence, their migration routes are generally guided by the topography of the landscape. Due to their reluctance to cross open water, diurnal migrating land birds are usually recorded offshore in relatively low numbers only. In the southern North Sea, migration intensities of this group of species are substantially higher along the coast compared to offshore locations such as Heligoland (HÜPPOP et al. 2009).

In contrast, nocturnal migration is thought to be largely independent of the landscape. Instead, nocturnal migrants follow a general migration direction (about 200° - 235° in fall in the region of the German North and Baltic Sea; BELLEBAUM et al. 2010; HÜPPOP & HILGERLOH 2012) unguided by the coastline or other topographical features (e.g. EASTWOOD 1967; ZEHNDER et al. 2001; but see also BRUDERER & LIECHTI 1998; GESICKI et al. 2016). This migration pattern is referred to as “broad front migration” (BERTHOLD et al. 2003). On their broad front migration nocturnal migrants regularly cross larger bodies of water like the North and Baltic Seas. The total number of nocturnal passerine migrants has been estimated at about 100 million for the North Sea (40 – 150 million; OREJAS et al. 2005; BSH 2015) and at about 500 million (fall) and 200-300 million (spring), respectively, for the western Baltic Sea (BERTHOLD 2000; BELLEBAUM et al. 2010; BSH 2014).

During migration nocturnal migrants are susceptible to collisions with man-made structures (LONGCORE et al. 2008; STRICKLAND et al. 2011; LONGCORE et al. 2012; HÜPPOP et al. 2016). It is generally assumed that the risk of collision is particularly high at illuminated structures and during periods of inclement weather and poor visibility (AVERY et al. 1977; EVANS OGDEN 1996; GEHRING et al. 2009; KERLINGER et al. 2010). With the rapid development of offshore wind farms in recent years the risk of collision for nocturnally migrating birds may substantially increase. However, while there is evidence that the collision risk of nocturnal migrants at onshore wind turbines is relatively low (KRIJGSVELD et al. 2009; GRÜNKORN et al. 2016; WELCKER et al. 2017), there is a paucity of information with respect to the situation at offshore wind farms. As it is largely impossible to collect direct evidence of bird collisions at offshore wind turbines even with state-of-the-art technology it is of paramount importance to improve our knowledge on the temporal and spatial patterns of nocturnal bird migration in offshore areas as well as on the factors affecting these patterns and the associated collision risk.

Direct observations of nocturnal migrants are difficult to obtain (e.g. moonwatching; LIECHTI et al. 1995; BERTHOLD et al. 2003). Therefore, instrument-based indirect methods such as radar or infrared devices are often used to quantify bird migration during the night (EASTWOOD 1967; BRUDERER 1997a; ZEHNDER et al. 2001; SHAMOUN-BARANES et al. 2014). However, these methods usually only allow for distinguishing between birds and other biological signals (such as bats or insects) or, in the case of radars that obtain data on wing beat frequency, the identification of species groups (ZAUGG et al. 2008). Recording of flight calls is the only method that provides information on the taxonomic identity of migrant species.

Many species of nocturnally migrating birds produce species-specific flight calls during migration (FARNSWORTH 2005). The function of these flight calls is not well understood. They have been suggested to serve flock maintenance, help orientation or stimulate migration activity (FARNSWORTH et al. 2004; FARNSWORTH 2005). At least in some species flight calls are also given in other contexts than migration (MUNDINGER 1970; TAOKA & OKUMURA 1990; FARNSWORTH 2005, 2007). However, there is also a large number of species that do not or only occasionally utter flight calls during migration (FARNSWORTH 2005). With respect to Palearctic passerines these are notably *sylviid* and *Acrocephalidae* warblers, leaf warblers (*Phylloscopus* spec.) and most Old World flycatchers (*Muscicapidae*), among others.

A large number of studies have used flight calls to derive information on the activity of nocturnal migrants (SMITH et al. 2014; e.g. SANDERS & MENNILL 2014; GESICKI et al. 2016; VAN DOREN et al. 2017). However, flight calls may not necessarily reflect migration intensities, i.e. call rates may not be proportional to the number of birds aloft (HORTON et al. 2015a). Atmospheric conditions like temperature, humidity or precipitation as well as the time of day may affect call rates independently of migration intensities (FARNSWORTH 2005; HÜPPOP & HILGERLOH 2012; SMITH et al. 2014; HORTON et al. 2015b). In addition, artificial light may alter the propensity of nocturnal migrants to produce flight calls (WATSON et al. 2016).

We used data from 13 different sites in the German North and Baltic Sea collected over a span of eight years (2008 – 2015) to analyze temporal and spatial patterns of nocturnal bird migration in this area. Specifically, we selected data of 10 species (eight passerines and two wader species) to determine phenological patterns and main migration periods. We tested whether and to what extent call rates and events of mass migration correlate across sites and regions. In addition, we tested the hypotheses that i.) systematic differences exist in species-specific migration intensities between the North and Baltic Sea; and that ii.) migration intensities decrease with increasing distance to shore within the German North Sea. Finally, we determined the influence of weather conditions on call rates in our study area.

3 MATERIALS & METHODS

3.1 Data collection

Data on flight calls were collected at 11 locations in the German EEZ of the south-eastern North Sea (German Bight) and at two locations in the Baltic Sea during the years 2008 – 2015 (Figure 3.1). The different locations were sampled in different years during that period and for different lengths of time (Table 3.1). Only at one location (FINO1) data were collected during all years of the study period. In total the dataset comprised 48 location-years of data (Table 3.1).

Within each year data acquisition was restricted to the main migration period in spring and fall which were defined as the time periods between 01/03 – 31/05 (spring) and 15/07 – 30/11 (fall). With the exception of FINO1 where data were collected continuously during the migration periods of the years 2008 – 2012, bird calls were recorded during approx. 20 to 60 nights per year (Table 3.1).

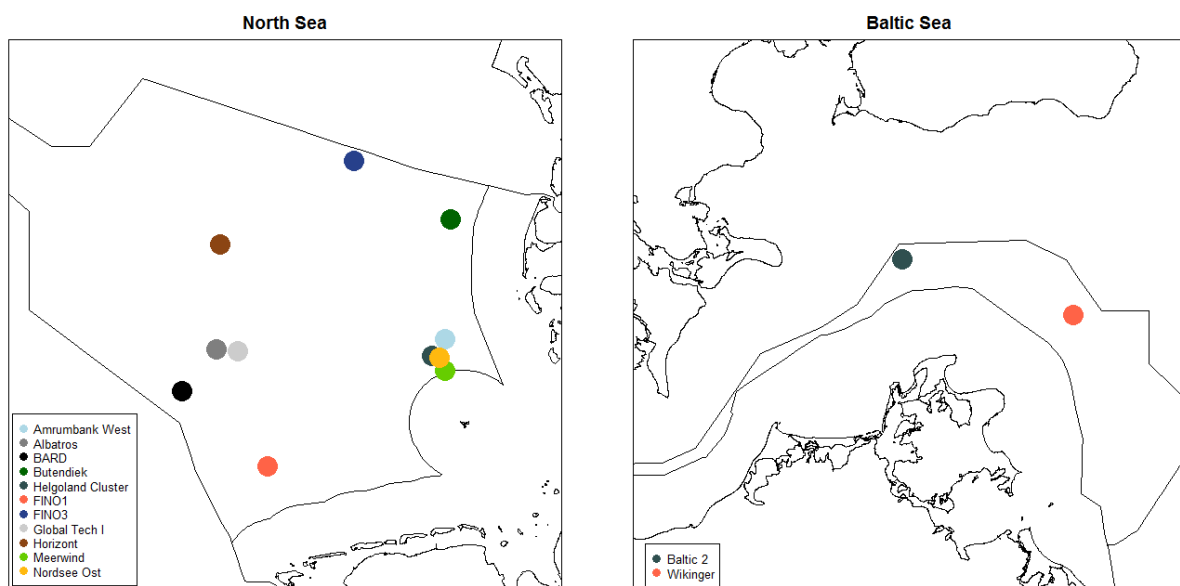


Figure 3.1 Location of the study sites in the EEZ of the German North and Baltic Sea.

The data used in this study were collected within larger bird migration monitoring programs as part of pre-construction environmental impact assessments as well as effect studies during the construction and operational phases of offshore wind farms (OWF) (Table 3.1). Four different companies participated in data collection (BioConsult SH GmbH & Co. KG, IBL Umweltplanung GmbH, Institut für Angewandte Ökosystemforschung GmbH and Avitec Research GbR). As methods to record bird flight calls had to comply with requirements issued by the German Maritime and Hydrographic Agency (BSH) as detailed in BSH (2013) data collection was standardized across the different companies involved.

Table 3.1 Study sites (wind farm locations), bird call recording systems and sample sizes of the data set used in this study. In addition, years with available data and the developmental phase of the wind farms during data collection (B – baseline, C – construction, O – operation) is given.

Location	Recording system	N _{years}	N _{nights}	Years with data	Phase (years)
Albatros	observer	2	122	2008 - 2009	B (2)
Amrumbank West	observer	3	107	2011 - 2012, 2014	B (2); C (1)
Baltic 2	observer	3	104	2013 - 2015	C (3)
BARD	observer	6	306	2010 - 2015	C (3); O (3)
Butendiek	observer	3	143	2011, 2014 - 2015	B (1), C (2)
Butendiek	microphone (2)	1	23	2015	O (1)
Cluster Helgoland	microphone (2)	1	31	2015	O (1)
FINO1	microphone (1)	8	1258	2008 - 2015	B (1), C (1), O (6)
FINO3	observer	4	111	2011, 2013 - 2015	B (1), C (2), O (1)
Global Tech I	observer	5	247	2009, 2012 - 2015	B (1), C (3), O (1)
Horizont	observer	2	119	2009 - 2010	B (2)
Meerwind	observer	4	139	2010 – 2011, 2013 - 2014	B (2), C (2)
Nordsee Ost	observer	4	203	2010, 2012 - 2014	B (1), C (3)
Wikinger	observer	2	121	2014 - 2015	B (2)
TOTAL		48	3034	2008 - 2015	B (16), C (19), O (13)

Principally, data were collected by two different methods: observer-based recordings and automatic audio system recordings.

Observer-based recordings

In the time between civil dusk and civil dawn one observer recorded all flight calls during two observation periods each hour. Observation periods usually lasted 15 min, at some locations during the years 2008 – 2012 observation periods were of 10 min duration. Flight calls were identified to the lowest possible taxa. Calls of species that typically consist of up to several syllables were noted as one call. Observations were usually conducted onboard of anchored vessels with the exception of the location FINO3 where observers stayed on a research platform.

Audio system recordings

At the locations FINO1, Cluster Helgoland and Butendiek (2015), flight calls were recorded by automatic audio systems installed on research platforms (FINO1) and Offshore Substations (“OSS”, Cluster Helgoland and Butendiek), respectively. At FINO1 the audio system was based on a single Sennheiser ME67 long shotgun condenser microphone capsule (40 – 20 000 Hz; HÜPPOP & HILGERLOH 2012). At each of the other locations two Monacor ECM-30A unidirectional electret microphone modules were used (Figure 3.2). Microphones were placed in weatherproof housing

and affixed to the working deck of the respective platforms avoiding the vicinity of sources of technical noise to the largest possible degree.



Figure 3.2 Microphone systems used at OSS 'Butendiek' and OSS 'Nordsee Ost' (left) and on FINO1 (right, from OREJAS et al. 2005).

The detection range of both systems is unknown. It is likely to be species dependent and to vary with the level of background noise. Systems with two microphones were installed at close proximity on the platform but pointed in opposite directions. Hence, the detection range of these systems is likely to be larger compared to those with single microphones. In general, the detection range for most songbirds is assumed to be up to a few hundred meters (FARNSWORTH et al. 2004; HÜPPOP & HILGERLOH 2012).

The software AROMA (automatic recording of migrating aves, see HILL & HÜPPOP (2008) and HÜPPOP & HILGERLOH (2012) for details) was used to filter out technical and environmental (wind, rain) noise to a large degree. Bird calls were stored as audio files (WAV, 16 bit, 22 Hz) on a local hard disk. Audio files had a maximum length of 5 sec, and bird calls were stored on a single file if the time between calls exceeded 1.5 sec. At a later date, audio files were evaluated by specially trained ornithologists and bird calls were identified to the lowest possible taxa.

The vessels and platforms involved in this study were illuminated in accordance with marine traffic safety regulations. It is well known that light structures may attract nocturnal migrants particularly at sea. The extent to which species analyzed in this report were attracted by illuminated observation platforms is unknown and cannot be quantified. Yet, as illumination regimes varied only to a small degree between vessels, relative differences between sites and time periods are likely to remain unaffected.

3.2 Data analysis

As data were collected by different companies data formats varied and raw data was not available from all location-years. This led to differences in data analysis particularly with respect to the data collected with different microphone systems.

Bird call rates (calls/h) were calculated for each hour with observations separately for each species and for all species combined. As the data from FINO1 did not include the number of calls registered by the audio system but only qualitative information about the species recorded on each audio file, the number of files per hour containing calls of the respective species was used as a proxy for call rates at this location.

Call rates per night were calculated as the mean of the hourly values for each night and location. Incomplete nights with hourly values covering less than 75% of the total length of the night were excluded from the dataset.

For further analyses data from 10 species were selected. Selection was based on the total number of calls recorded throughout the study period and the constancy with which the given species were observed across all locations and years (Tab. A 1). Thus four species of thrushes (Blackbird *Turdus merula*, Redwing *Turdus iliacus*, Song Thrush *Turdus philomelos* and Fieldfare *Turdus pilaris*), four other passerine species (Skylark *Alauda arvensis*, Meadow Pipit *Anthus pratensis*, Robin *Erithacus rubecula* and Starling *Sturnus vulgaris*) as well as two species of waders (Dunlin *Calidris alpina* and Common Sandpiper *Actitis hypoleucos*) were selected.

3.2.1 Phenology

To determine the general phenological pattern of the selected species in the German EEZ of the North and Baltic Sea we calculated mean standardized call intensities for each Julian day (night). Call intensities were log-transformed and standardized across years and sites to avoid uneven leverage of single years or nights with high call rates. However, as the distribution of call intensities was highly right-skewed, log-transformation did not result in a normal distribution of data and hence standardization did not completely remove a larger influence of single nights with unusually high call rates. Phenologies were plotted as the three-day moving average for each species.

We defined the main migration period in spring and fall for each species as the inner time interval with 90% of calls, i.e. we removed time periods with 5% of calls at the beginning and at the end of the spring and fall migration season. All further analyses were performed on the data restricted to the main migration periods for each species.

3.2.2 Spatial correlation of call rates

To calculate the correlation of call rates between different sites we first selected all nights with simultaneous observations in at least two different sites. We then calculated the correlation coefficient ρ based on Spearman's rank correlation for each pair of sites and years with at least five nights of simultaneous observations. To determine the spatial extent of the correlation of call rates between sites we regressed the correlation coefficients ρ against the spatial distance be-

tween locations for which ρ was calculated. The sample size of the pairwise correlations was included as weights in the regression analysis.

To test for systematic differences in the relationship between correlation strength and distance among sites we included migration season (spring vs. fall), recording system (observer only vs. combination of audio systems and observers) and developmental stage of the OWF (same phase only vs. mix of phases) as explanatory factors in the models. Due to limited sample size this was done for the combined data of the four thrush species and the two wader species only.

3.2.3 Mass migration

We evaluated the possibility to derive a data-driven definition of ‘mass migration’. To this end we calculated daily call rates for all species combined using observer-based recordings only. Histograms and cumulative plots of call rates were examined for signs of a bimodal distribution or any other distribution that would allow the definition of a cut-off value to distinguish between ‘mass migration events’ and ‘ordinary’ call intensities.

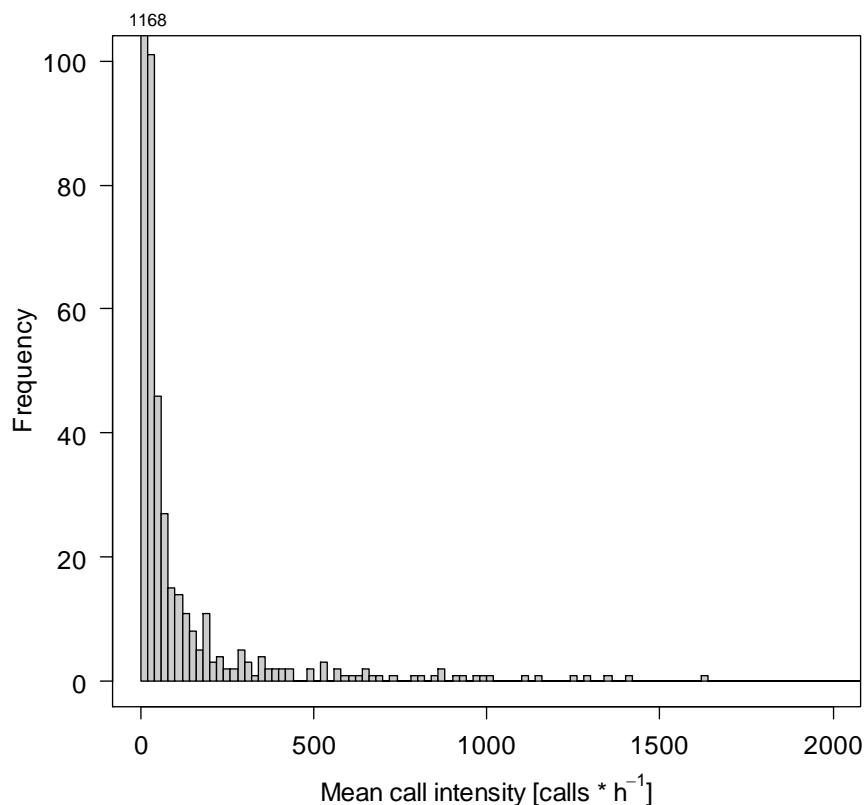


Figure 3.3 Histogram of mean call intensities per night [calls/h] of all species combined.

However, the distribution of the call rate data was highly right-skewed but continuous (Figure 3.3 and Figure 3.4) and hence the definition of ‘mass migration’ had to be derived independently of the distribution of the data.

We arbitrarily chose the cut-off value for ‘mass migration’ at 100 times the median call rate which corresponded to 186.7 calls/h. ‘High call intensities’ were defined as > 25 times the median call rate (46.7 calls/h; Figure 3.4). These cut-off values were exceeded in 4.9% and 12.4% of the nights, respectively.

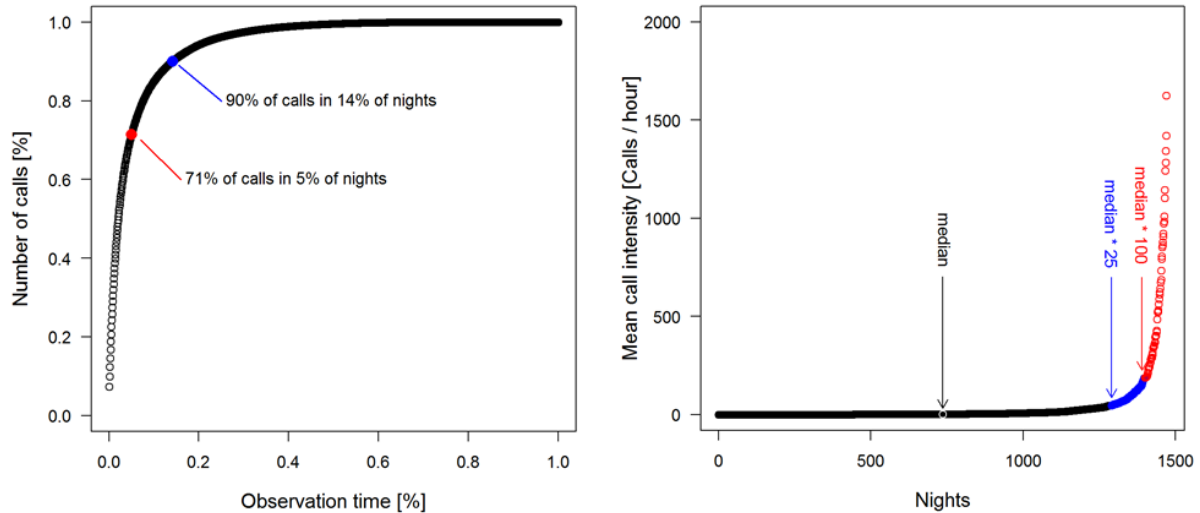


Figure 3.4 Left panel: cumulative number of calls [%] per time [%]. Two values are indicated: 71 % of calls were recorded in only 5 % of the nights; 90 % of the calls were recorded in 14 % of the nights. Right panel: Mean call intensities per night sorted in ascending order to illustrate the definition of ‘mass migration’ (median * 100) and ‘high call intensities’ (median * 25).

The definition of mass migration as 100 times the median value and high call intensities as 25 times the median value were applied to the data of the species group of thrushes. This resulted in a threshold value for mass migration of 266.7 calls/h which was exceeded in 4.8% of the nights. The threshold value for ‘high migration intensities’ corresponded to 66.7 calls/h for thrushes which was exceeded in 14.3% of the nights.

We then tested whether the occurrence of mass migration was correlated across locations. To do this we estimated the effect of distance among sites on the probability of coincidence of mass migration by fitting a generalized linear model with binomial error distribution and logit link function.

3.2.4 Spatial gradients

We tested for a systematic spatial gradient in call intensities between the German EEZ of the North Sea and the EEZ of the Baltic Sea, and for a gradient with distance to shore within the North Sea for all 10 species. To determine differences between the North and Baltic Sea we ran paired Wilcoxon tests on call rates from nights for which simultaneous observations were available from both areas. To determine the gradient with distance to shore within the North Sea we ran least-squares linear regressions between the difference in call rates (log-transformed) between sites

and the difference in distance to shore between these sites. Simultaneous observations with call rates of zero at both sites were excluded prior to analyses.

3.2.5 Weather

Weather data

We used in-situ weather observations collected by the bird observers simultaneously with recordings of flight calls as meteorological variables in our analyses. Data were collected once or twice per hour and included ambient temperature (°C), visibility (km), rain (as a qualitative measure yes/no), cloud coverage (8/8), wind speed (m/s) and wind direction (cardinal point). As visibility was often difficult to estimate during the night this variable contained a large proportion of missing values and thus was removed from the analysis.

Based on information on wind direction and speed we calculated the tailwind component (TWC [m/s]) and crosswind component (CWC [m/s]) following ZEHNDER et al. (2001) and HÜPPOP & HILGERLOH (2012):

$$TWC = \cos(OWD - TWD) \cdot WS \quad (\text{eq. 1})$$

$$CWC = \sin(OWD - TWD) \cdot WS \quad (\text{eq. 2})$$

where OWD is the observed wind direction, TWD is the tailwind direction and WS is the wind speed. We assumed a mean migration direction of 225° in fall and 45° in spring. Positive TWC values correspond to supportive winds (tailwind), negative TWC values correspond to headwinds. The CWC describes the wind component perpendicular to the main migration direction. Positive CWC values correspond to a crosswind component from the left of the bird, negative values from the right. In relation to the assumed direction of the migrating birds positive CWC values translate to shoreward (northwesterly) winds in spring and seaward (southeasterly) winds in fall and vice versa.

In addition we calculated the variable δTWC as the difference between the average TWC value at the current and the previous night. This variable indicated increasing or decreasing TWC corresponding to improving or deteriorating wind conditions.

For all weather parameters mean hourly values were calculated if more than one observation per hour was available.

In addition to atmospheric parameters, two variables accounting for temporal patterns in migration were included in the analyses. To capture the phenological pattern within the spring and fall migration periods we included Julian day in the models. As migration intensities are known to vary systematically within the course of the night we also included the variable “hour from midnight” (HÜPPOP & HILGERLOH 2012). Finally, the variables study year (“year”), project location (“project”), the company responsible for data collection (“lab”) and the developmental stage of the wind farm (“phase”) were included as factors to account for these potential sources of variation.

Models

As nights with high call intensities are rare events the distribution of call rates was highly right-skewed (see chapter 3.2.3). Conventional parametric statistics such as generalized linear models (GLM) or generalized additive models (GAM) often used in similar studies based on radar data (ZEHNDER et al. 2001; ERNI et al. 2002; VAN BELLE et al. 2007; KEMP 2012) were therefore not suited for our data. Hence, we used random forest (RF) regression (BREIMAN 2001), in which the mean prediction of the “forest” is based on the predictions of a large number of individual decision trees (i.e., 500–2000). Each decision tree in the forest is built on a bootstrap sample of the original data and the forest prediction is the dominant class of the class predictions of the individual trees (majority vote). Observations not included in the bootstrap samples used to build individual trees (out-of-bag or OOB data) are used to calculate an unbiased error rate and variable importance, so that no cross-validation is needed (PRASAD et al. 2006; CUTLER et al. 2007). As main characteristics, RF is a quick algorithm, robust to include a large number of correlated variables (ARCHER & KIMES 2008) and it does not make any prior assumptions about the data. At the same time, it has been proven to attain higher predictive performances than other methods commonly used for ecological prediction (BREIMAN 2001; PRASAD et al. 2006; CUTLER et al. 2007; CRISCI et al. 2012).

For each model different variable importance metrics were calculated. The “Standardized Error Variable Importance” (%IncMSE) is computed from permuting the OOB data: For each tree containing a specific variable, the prediction error on the out-of-bag data is recorded (mean squared error for regression). Then the same is done for all decision trees not containing this variable. The differences are then averaged over all trees and normalized by the standard deviation of the differences. In addition, a multi-way importance plot was generated for each model. This plot summarizes different variable importance scores. Each variable is represented in a scatter plot with the number of times that each variable is the root of the regression tree (*times_a_root*) represented on the y-axis and the mean minimum depth (average position of the variable in the regression trees) on the x-axis. The size of dots reflects the number of nodes split on the variable.

Call rates [calls/h] were square root transformed and used as the response variable. Separate models were run for spring and fall. Data included in the model were restricted to the main migration period of the respective species (see Table 4.1).

All analyses were performed in R 3.4.2. (R CORE TEAM 2016) using the “rfUtilities” package (EVANS & MURPHY 2018) and the “randomForest” package (LIAW & WIENER 2002).

4 RESULTS

In total the dataset comprised 524,895 bird calls of 127 species. 8,867 of these calls (1.7%) were not identified to species level (Tab. A 1). 68.7% of all calls were recorded by observers, 31.3% were recorded by automatic audio systems.

The species composition was dominated by thrushes (69.3%, see Figure 4.1), mainly Redwing (38.9% of all thrushes), Blackbird (37.8%), Song Thrush (17.1%) and Fieldfare (6.1%). Other passerine species constituted 22.4% of all calls with Robin (31.8% of all other passerines), Starling (19.6%), Goldcrest (19.4%) and Skylark (12.3%) being the most common species of this group (Tab. A 1). Waders, gulls and other non-passerine species such as geese, ducks and terns were recorded less often.

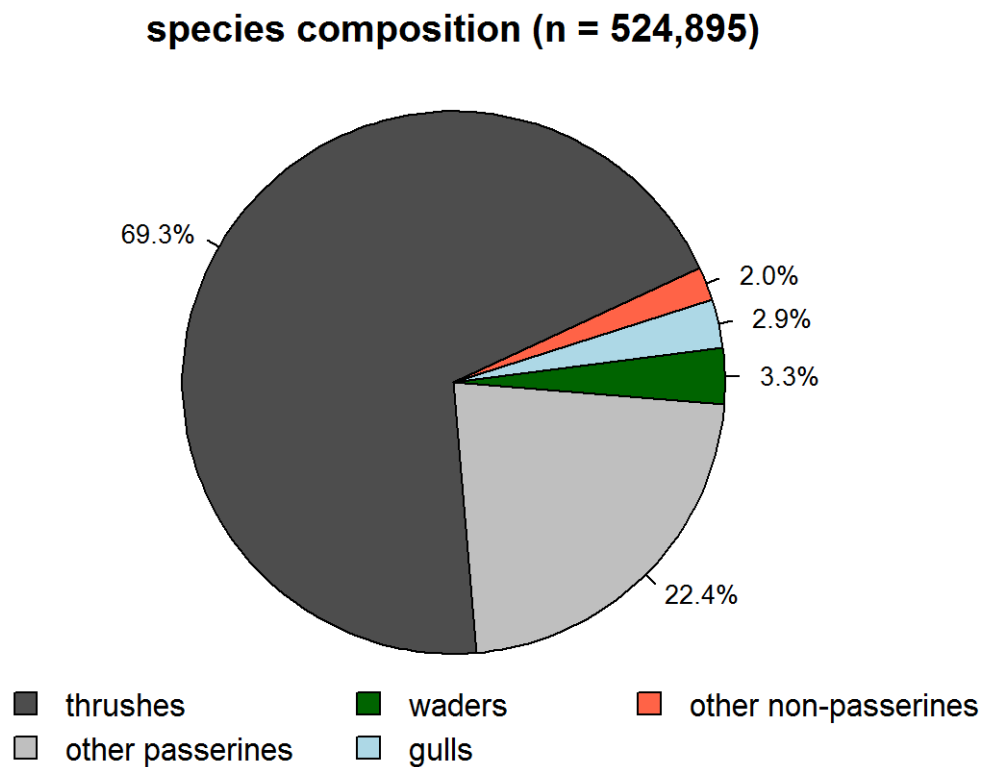


Figure 4.1 Species composition of flight calls recorded between 2008 and 2015 in the German EEZ of the North and Baltic Sea.

4.1 Phenology

With the exception of the Dunlin all species covered in this report showed a pronounced phenological pattern during both spring and fall migration (see Figure 4.3, Figure 4.4 and Figure 4.2). The time period of the inner 90% of calls (defined as the main migration period) varied between species and lasted between 31 and 89 days in spring and between 38 and 111 days in fall (Table 4.1).

Maximum call rates of thrushes and other passerine species were reached between mid-March and mid-April in spring and between early October and early November in fall (Table 4.1). Migration of Common Sandpipers peaked in mid-May and early August, respectively.

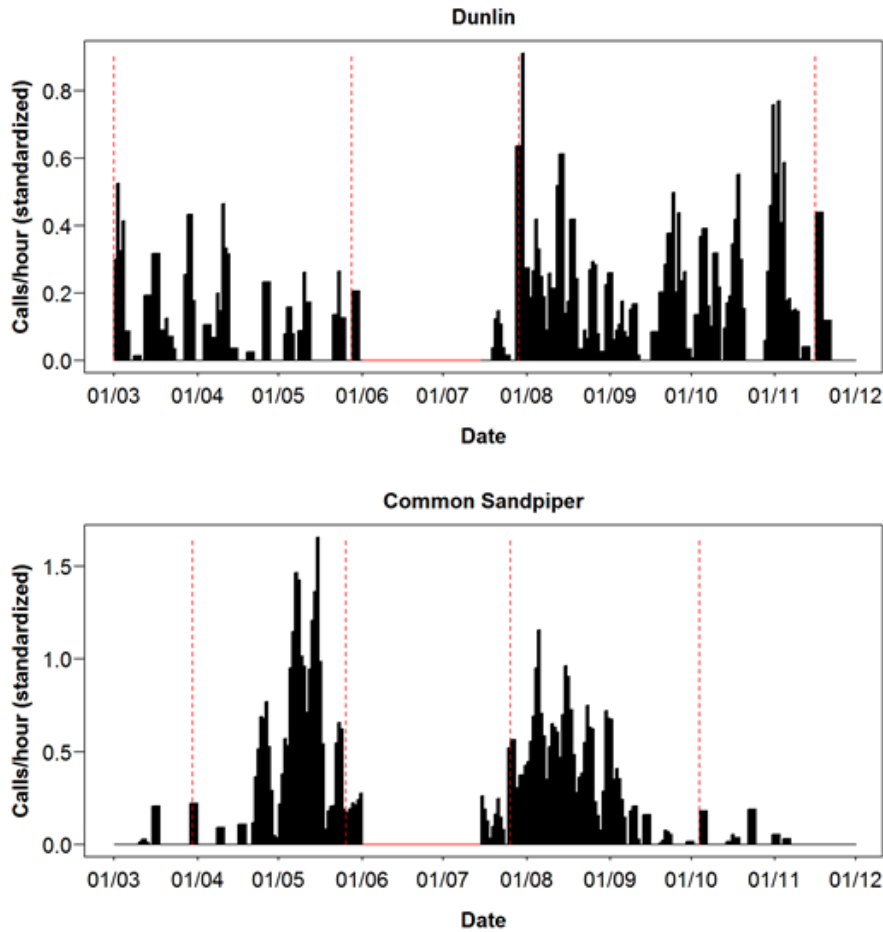


Figure 4.2 Phenology of call rates ($\text{calls} \cdot \text{h}^{-1}$) of two wader species in the German EEZ of the North and Baltic Sea. Call rates were standardized between years and projects and plotted as 3-day moving average. In addition the time period with the inner 90% of calls (red dashed lines) per season are given (see text for details).

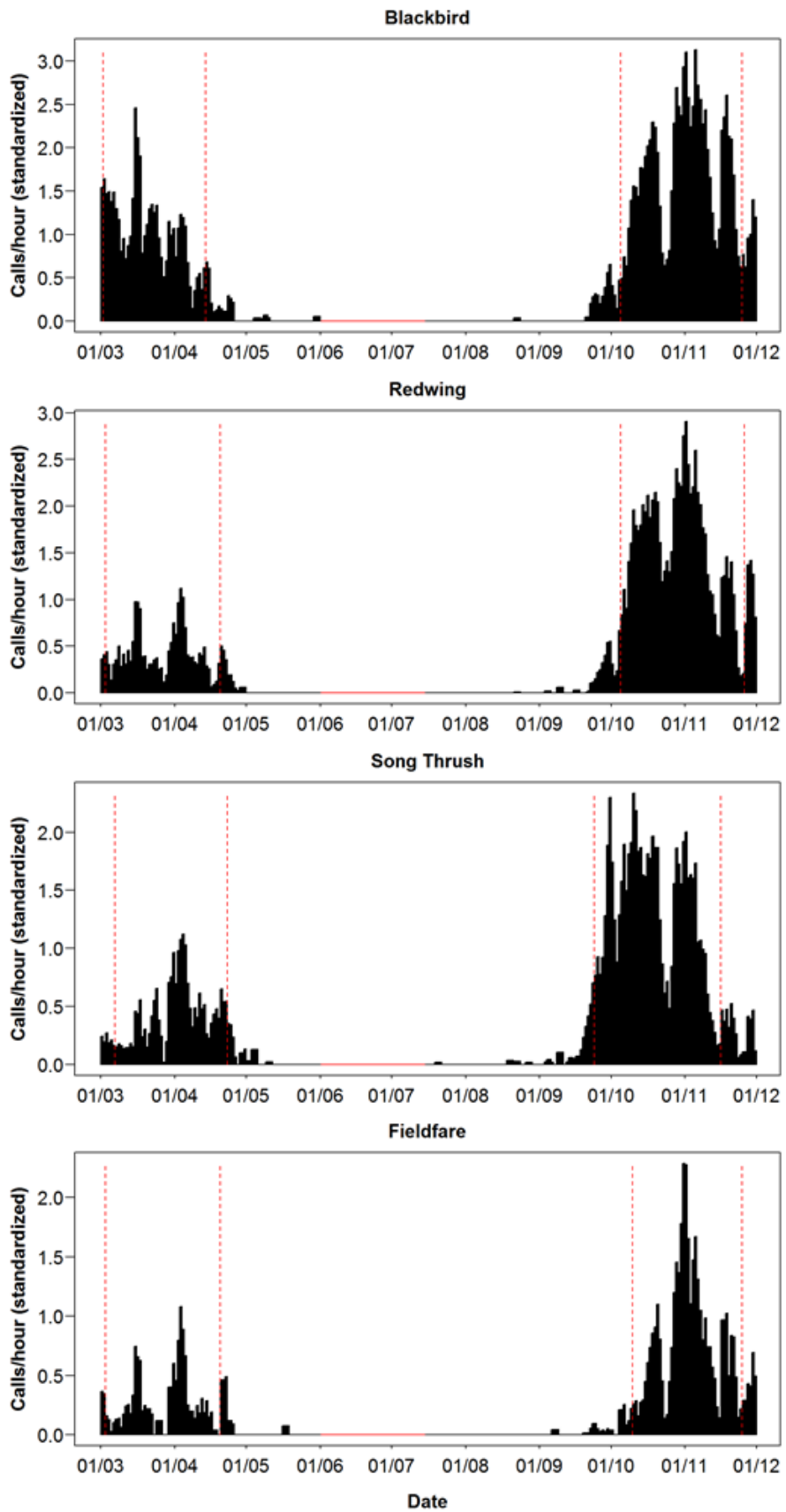


Figure 4.3 Phenology of call rates (calls* h^{-1}) of four thrush species in the German EEZ of the North and Baltic Sea. See Figure 4.2 and text for details.

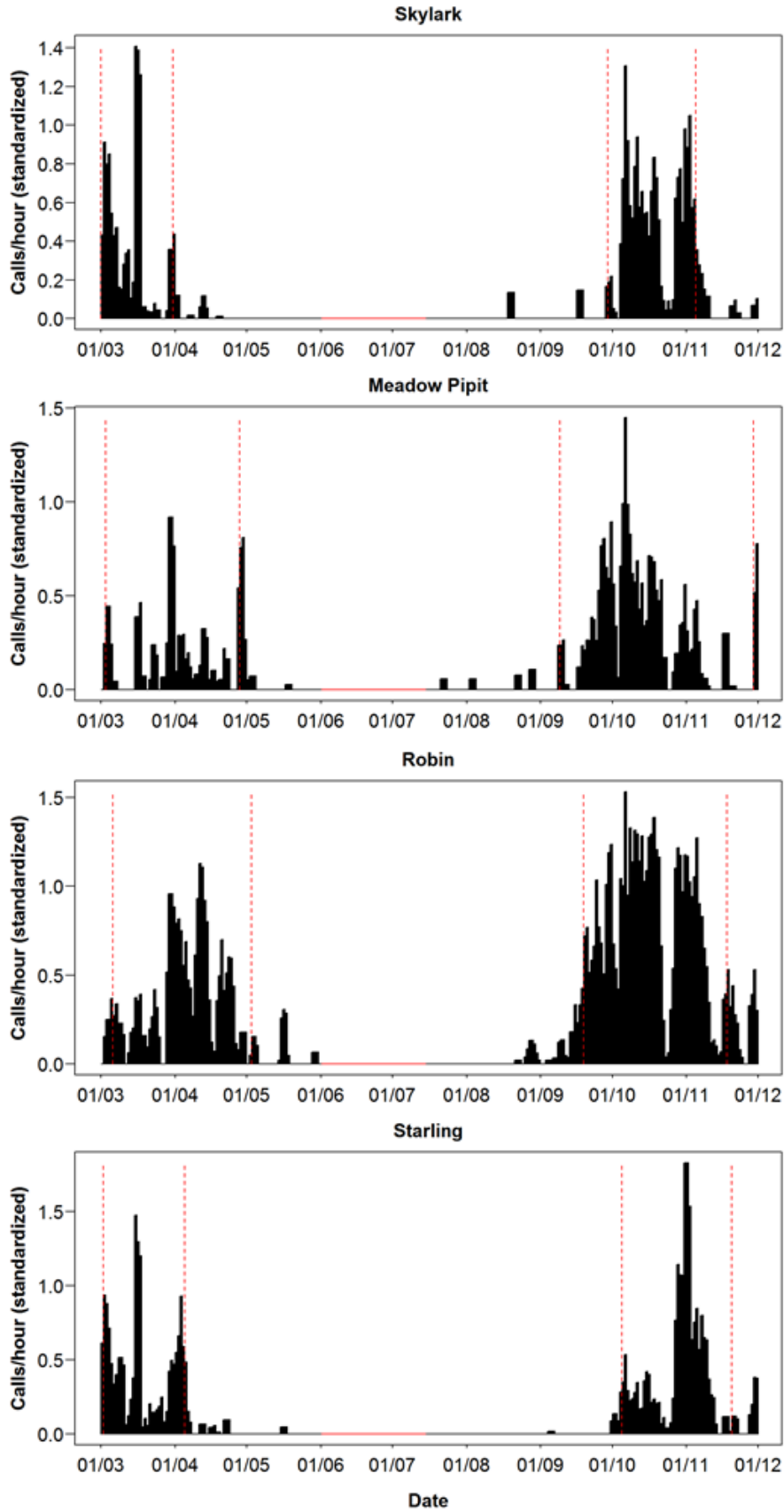


Figure 4.4 Phenology of call rates (calls* h^{-1}) of four passerine species in the German EEZ of the North and Baltic Sea. See Figure 4.2 and text for details.

Table 4.1 *Main migration periods (time periods with inner 90% of calls, see text) and peak for spring and fall migration in the German EEZ of the North and Baltic Sea.*

species	main migration period (90% of calls) and date of peak			
	spring	peak	fall	peak
Dunlin	01/03 – 28/05	02/03	29/07 – 16/11	30/07
Common Sandpiper	30/03 – 26/05	15/05	26/07 – 04/10	05/08
Skylark	01/03 – 31/03	15/03	29/09 – 05/11	06/10
Meadow Pipit	03/03 – 28/04	29/03	09/09 – 29/11	06/10
Robin	06/03 – 03/05	11/04	19/09 – 18/11	06/10
Blackbird	02/03 – 14/04	15/03	05/10 – 25/11	05/11
Fieldfare	03/03 – 20/04	03/04	10/10 – 25/11	31/10
Song Thrush	07/03 – 23/04	04/04	24/09 – 16/11	10/10
Redwing	03/03 – 20/04	03/04	05/10 – 26/11	01/11
Starling	02/03 – 05/04	15/03	05/10 – 20/11	01/11

4.2 Spatial correlation of call rates

Overall, the spatial correlation of call intensities was relatively high. The mean correlation coefficient (ρ) calculated over all species and project-years was 0.42 (± 0.02 SE, $n = 314$). However, there were differences in the strength of the correlation with respect to season, locations and species. Generally, the correlation was significantly higher between sites within the North Sea than between sites across the North and Baltic Sea (Table 4.2; $W = 8736$, $p < 0.001$). Due to the limited dataset from the Baltic comparisons within the Baltic Sea were not possible. In addition, the correlation was stronger in fall compared to spring, at least within the North Sea (Table 4.2; $W = 6287$, $p = 0.018$). When looking at the different species and species groups separately, similar pattern were evident in most cases though statistical significance was only reached in a few instances (Table 4.2).

Table 4.2 Mean correlation coefficients (Spearman's rank correlation coefficient rho) for correlations of call rates between sites within the North Sea and between sites across the North and Baltic Sea for the different species and species groups. In addition, sample sizes (number of correlations within the North Sea and between the North and Baltic Sea, respectively) are given. Bold values indicate significant differences according to a non-parametric Wilcoxon rank-sum test (where applicable).

Species	Season	Mean rho North Sea	N North Sea	Mean rho Baltic/North Sea	N Baltica
Waders	spring	0.29	15	0.79	1
	fall	0.30	25	0.05	3
Common Sandpiper	spring	0.27	11	0.79	1
	fall	0.33	15	0.13	2
Dunlin	spring	0.35	4	-	0
	fall	0.22	10	-0.09	1
Thrushes	spring	0.44	44	0.50	2
	fall	0.61	90	0.19	29
Blackbird	spring	0.51	12	-	0
	fall	0.65	25	0.18	7
Redwing	spring	0.37	16	0.50	2
	fall	0.65	25	0.15	8
Song Thrush	spring	0.45	10	-	0
	fall	0.57	25	0.04	8
Fieldfare	spring	0.53	6	-	0
	fall	0.57	15	0.44	6
Other passerines	spring	0.38	28	0.64	1
	fall	0.44	61	0.05	15
Meadow Pipit	spring	-0.13	1	-	0
	fall	0.22	16	0.07	3
Skylark	spring	0.64	4	-	0
	fall	0.70	9	-	0
Robin	spring	0.35	16	0.64	1
	fall	0.49	23	0.17	9
Starling	spring	0.39	7	-	0
	fall	0.46	13	-0.30	3
All species	total	0.47	263	0.17	51
	spring	0.40	87	0.61	4
	fall	0.51	176	0.14	47

The relationship between correlation strength and distance between sites within the North Sea varied between species. Waders and Thrushes showed a significant steep decline of correlation strength with increasing distance between sites in both spring and fall (Figure 4.5 and Figure 4.7). For these species predicted correlation coefficients were generally high at close range (>0.8 with the exception of thrushes in spring) but reached values below 0.5 at distances of >100 km be-

tween sites. This pattern was generally evident also when looking at the different species of these species groups separately (Figure A. 1 and Figure A. 2).

However, for the other passerine species correlation coefficients were highly variable across project-years yet independent of the distance between sites (Figure 4.7 and Figure A. 3).

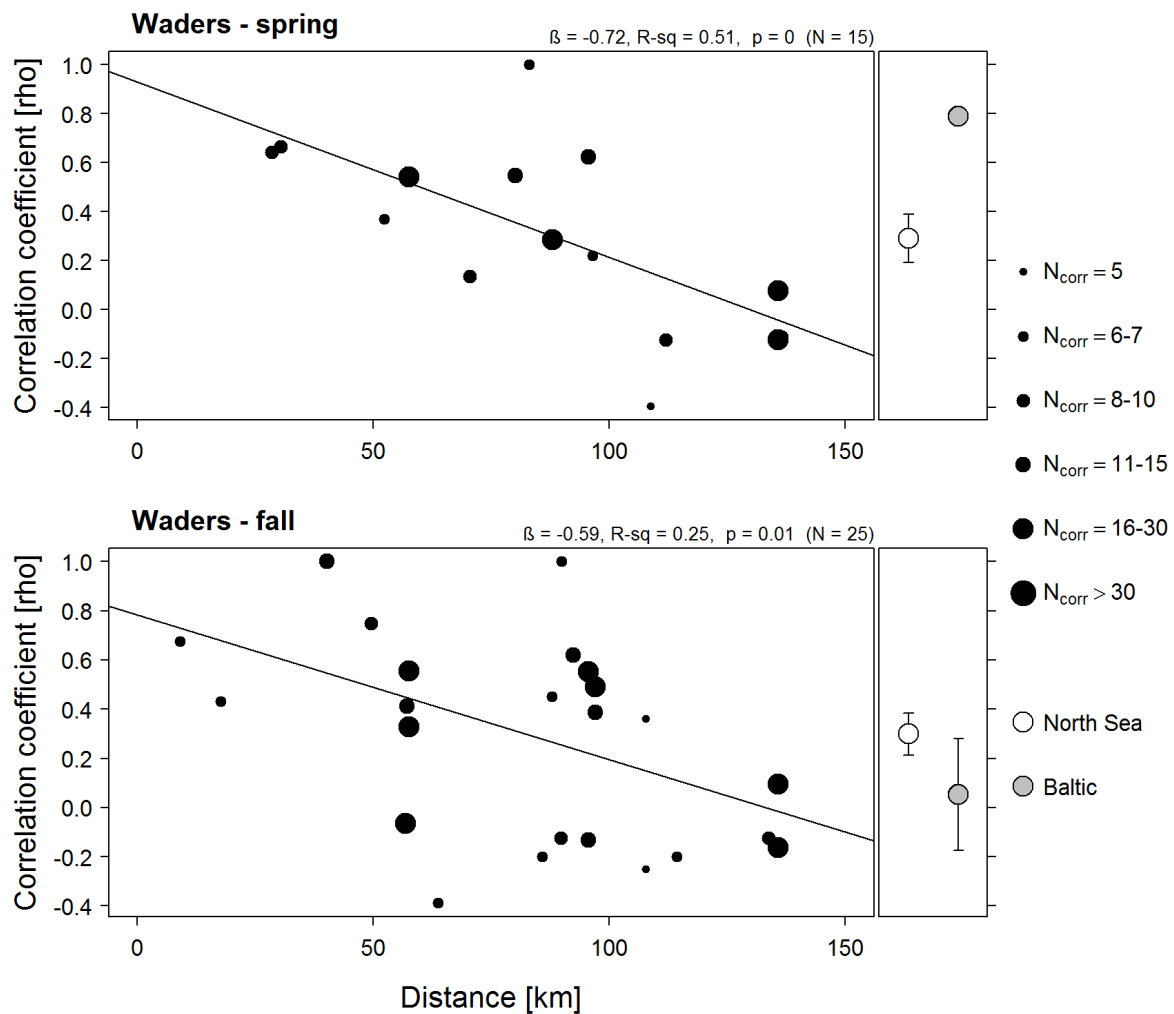


Figure 4.5 Relationship between distance between sites and the correlation of call rates (Spearman’s rank correlation coefficient rho) of the combined data of two species of waders (Common Sandpiper and Dunlin) for spring (upper panel) and fall (lower panel). Correlation coefficients were calculated based on days with simultaneous observations of each pair of projects and years. The number of days a coefficient is based on is indicated by symbol size (minimum number of days = 5). Left panel: linear regression for data from the North Sea; right panel: mean correlation coefficient \pm SE for North Sea sites (open symbol) and for comparisons between North and Baltic Sea (filled symbols).

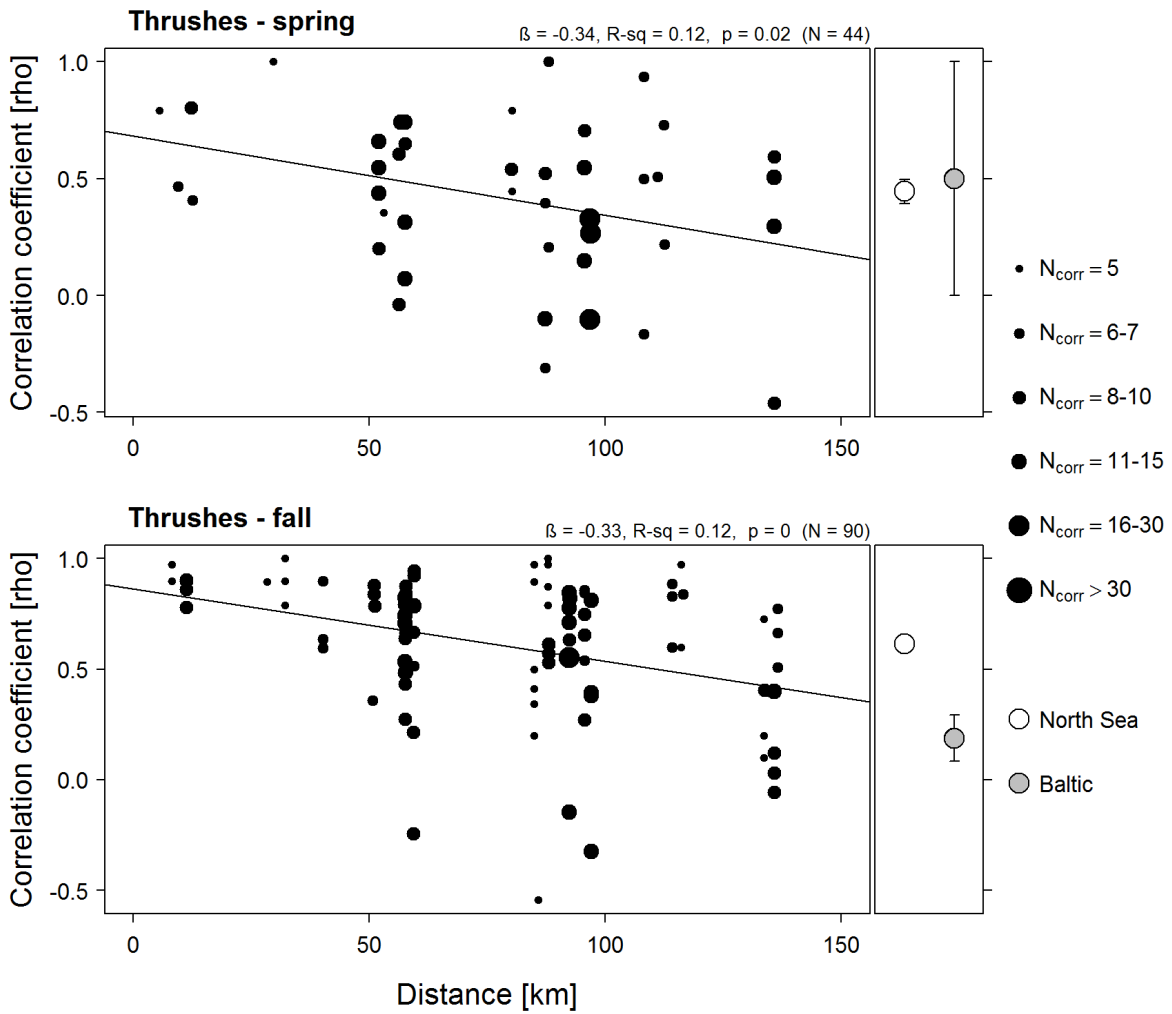


Figure 4.6 Relationship between distance between sites and the correlation of call rates (Spearman's rank correlation coefficient rho) of the combined data of four thrush species (Blackbird, Song Thrush, Redwing and Fieldfare) for spring (upper panel) and fall (lower panel). For details see Figure 4.5 and Materials & Methods.

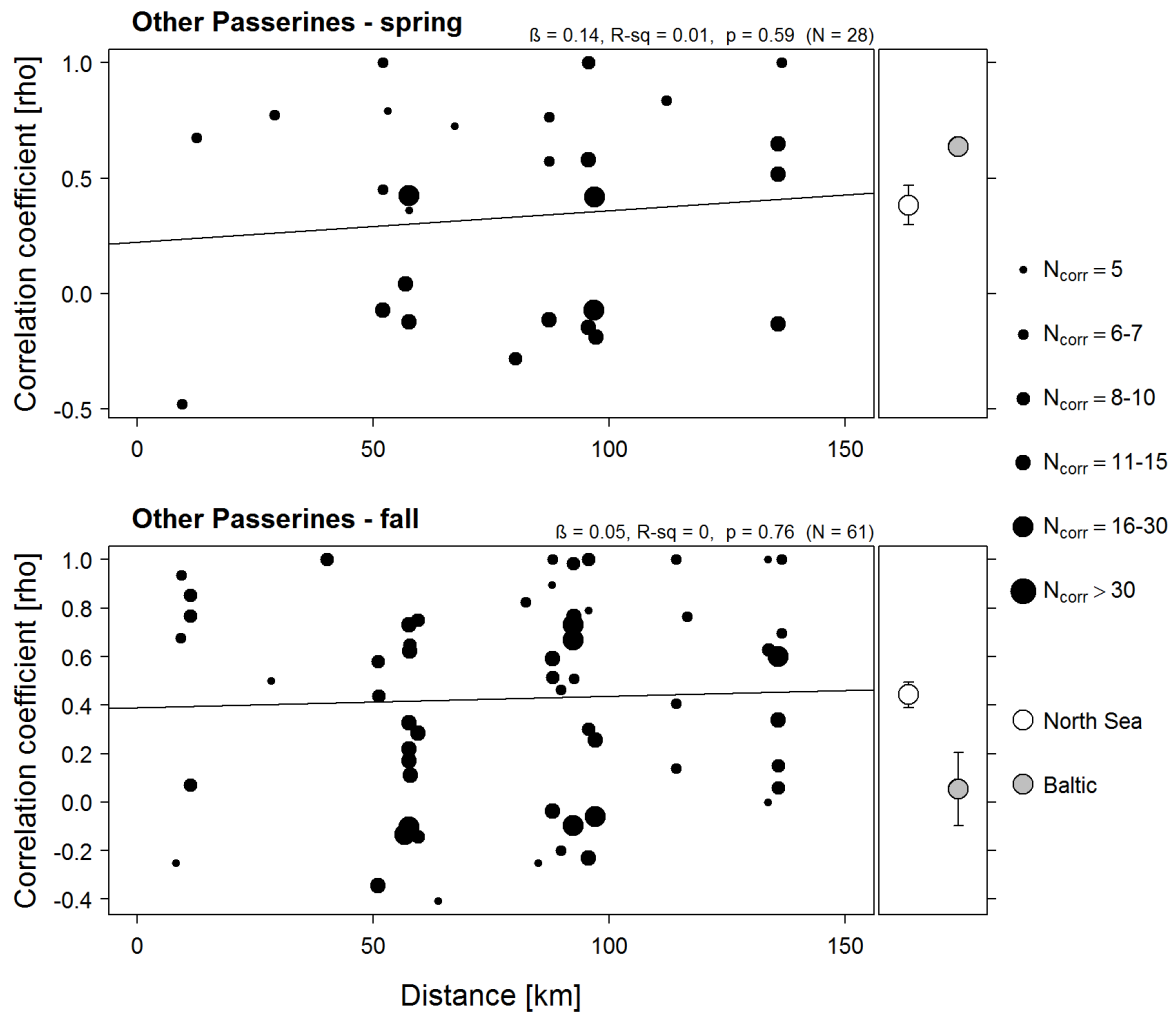


Figure 4.7 Relationship between distance between sites and the correlation of call rates (Spearman's rank correlation coefficient rho) of the combined data of four passerine species (Robin, Starling, Meadow Pipit and Skylark) for spring (upper panel) and fall (lower panel). For details see Figure 4.5 and Materials & Methods.

The data of thrushes were used to test for an effect of season (spring vs. fall), observation method (observer vs. microphone systems) and developmental phase of the wind farm (baseline, construction and operation). The degree of the decline of correlation strength with distance between sites did not differ with season (interaction distance * season, LRT: $F = 0.09, p = 0.77$) or method (interaction distance * method, LTR: $F = 0.18, p = 0.67$). Also, the development stage of the wind farm had no effect on the relationship between correlation coefficient and distance (LTR, $F = 0.77, p = 0.51$). However, correlation strength was significantly lower in spring compared to fall ($t = -3.10, p = 0.002$) and significantly lower for data including both observation methods compared to observer-based data only ($t = -2.53, p = 0.012$; see Figure 4.8).

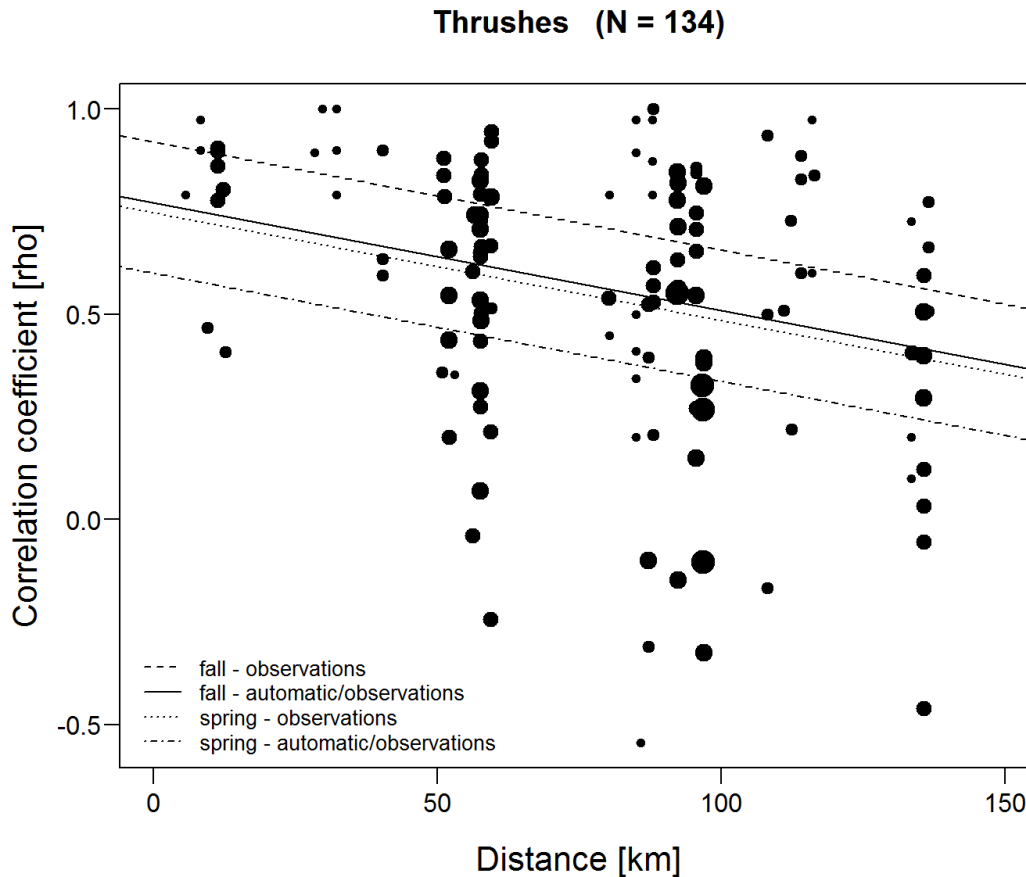


Figure 4.8 Relationship between distance between sites and the correlation of call rates (Spearman's rank correlation coefficient rho) of the combined data of four thrush species (Blackbird, Song Thrush, Redwing and Fieldfare). The relationship differed between seasons (spring vs. fall) and with observation method (observer only vs. mixed data observer/microphone systems). Predicted values based on an additive linear model are indicated for the different factor levels.

4.3 Correlation of mass migration

The probability of simultaneous occurrence of mass migration of thrushes declined markedly with increasing distance between sites (Figure 4.9; GLM: $z = -1.74$, $p = 0.082$). While the predicted probability of coincidence was about 60-70% for sites in close proximity, the probability decreased to about 10% at 100 km distance between sites. The data contained no case in which mass migration was simultaneously recorded in the North and Baltic Sea resulting in the predicted probability of coincidence of mass migration of zero at all distances >300 km between sites.

The analysis of high call intensities within the North Sea showed similar results (Figure 4.9). The probability of coincidence of high call intensities significantly decreased with increasing distance between sites (GLM: $z = -2.67$, $p = 0.008$).

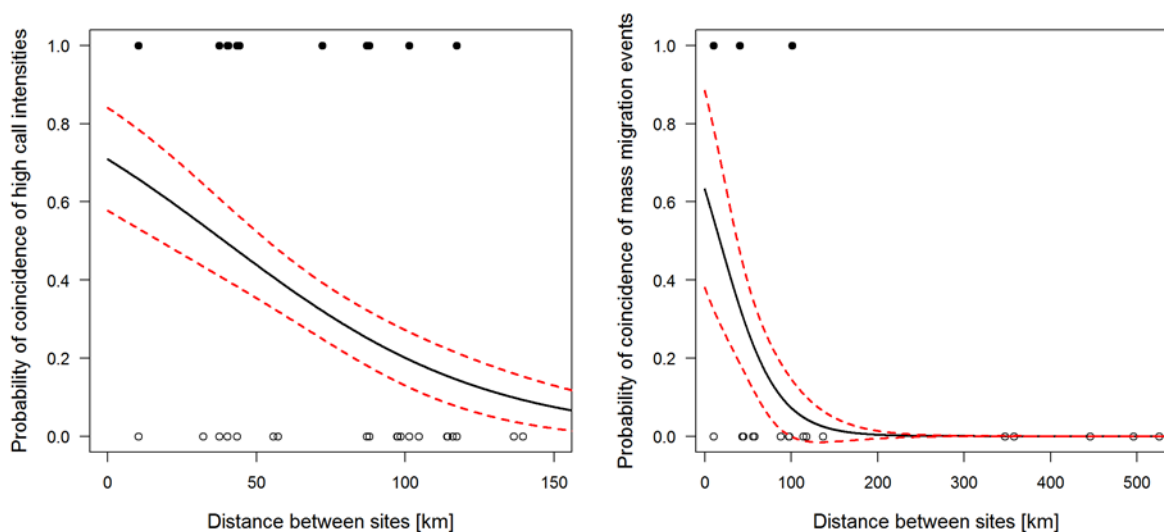


Figure 4.9 Left panel: relationship between the distance between wind farms and the predicted probability [\pm SE] of coincidence of high call intensities at these sites. Data restricted to North Sea only. Right panel: relationship between the distance between wind farms and the predicted probability of coincidence of mass migration events. Data from both North and Baltic Seas. Predicted probabilities are based on generalized linear models with binomial error structure (see text for further details). Filled symbols represent distances between sites at which high migration intensities coincided, open symbols distances at which high call intensities did not coincide.

4.4 Gradient of call intensities

4.4.1 Gradient between North and Baltic Sea

The comparison of call rates from simultaneous observations in the Baltic and North Sea showed varying results for the different species groups and species. The call rates of waders did not differ systematically between the Baltic and the North Sea (Figure 4.10). This was also true when analyzing the data of the Common Sandpiper and Dunlin separately (Figure A. 4 and Figure A. 5).

In contrast, call rates of thrushes were significantly higher at sites in the Baltic compared to the North Sea (Figure 4.11). Overall, the mean call rate of thrushes was 31% higher in the Baltic. This pattern was consistent for both spring and fall and independent of the development stage of the wind farm during which the data were collected. Results were also largely consistent for the four thrush species individually (Figure A. 6 to Figure A. 9).

Likewise, the call rates of the other passerine species were on average 71% higher in the Baltic compared to the North Sea (Figure 4.12). However, this pattern was only evident relating to Robin and, to a lesser degree, Skylark (Figure A. 12 and Figure A. 10). In contrast, call intensities of Meadow Pipits and Starlings did not show any systematic differences between sites in the Baltic and North Sea (Figure A. 11 and Figure A. 13).

Waders

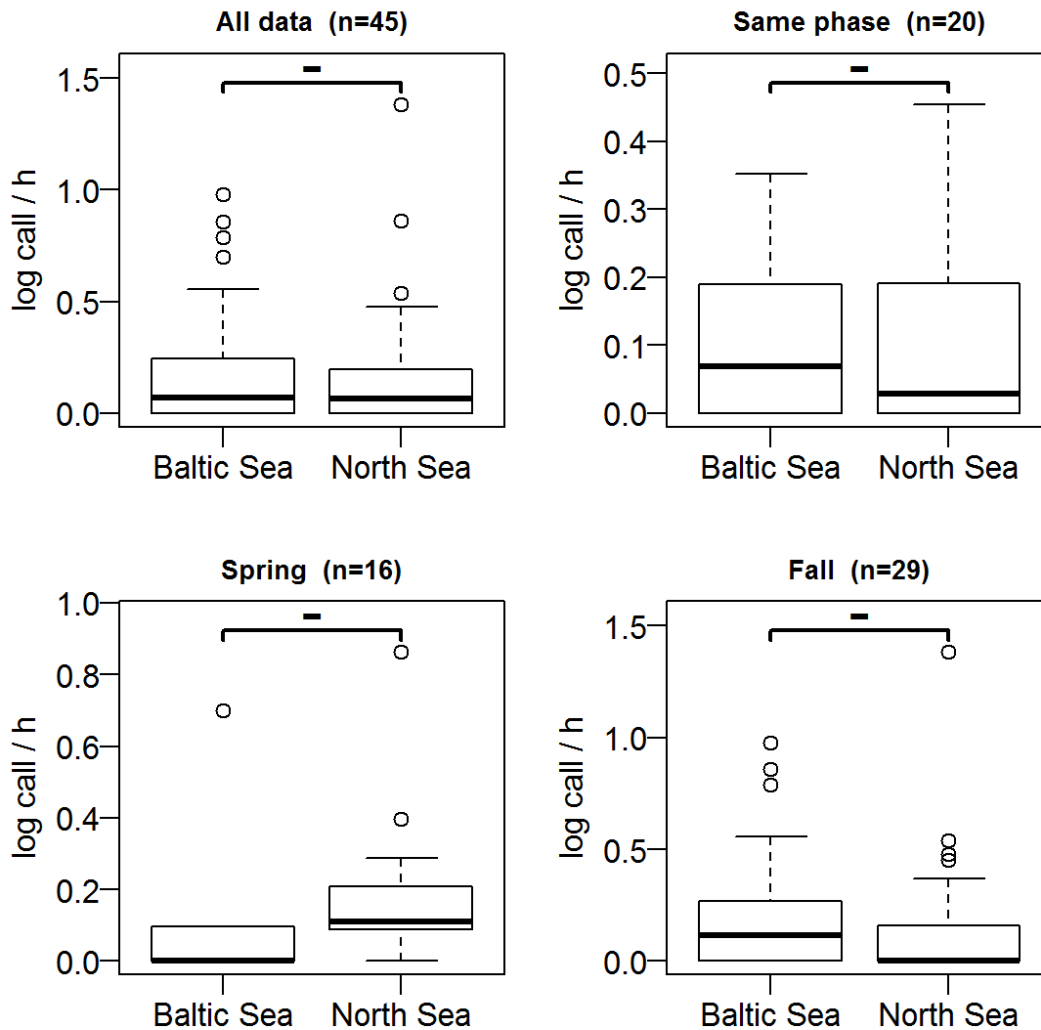


Figure 4.10 Call intensities (calls/h, log transformed) of waders simultaneously measured in the Baltic and North Sea. Box plots indicate the median (bold black bar) and the interquartile range (box), the whiskers extend to the most extreme data points which are no more than 1.5 times the interquartile range, open symbols indicate values outside 1.5 times the interquartile range. Additionally, the results of paired Wilcoxon rank-sum tests (** $p < 0,001$; ** $p < 0,01$; * $p < 0,05$; - $p > 0,05$) and the sample size of paired observations are given above the box plots. Results are shown separately for spring (lower left panel) and fall (lower right panel), as well as for comparisons restricted to the same developmental phase of the wind farms (upper right panel) and for all data combined (upper left panel).

Thrushes

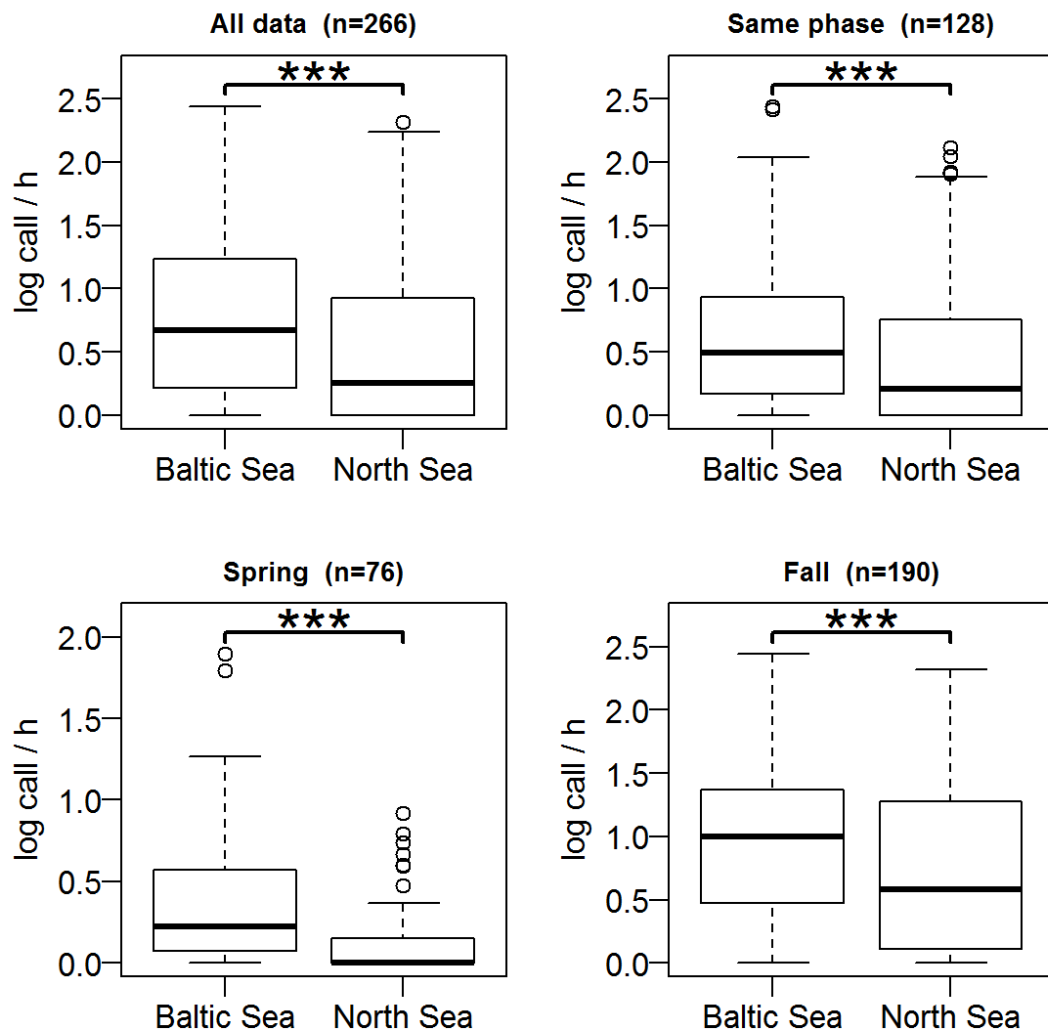


Figure 4.11 Call intensities (calls/h, log transformed) of thrushes simultaneously measured in the Baltic and North Sea. See Figure 4.10 for further details.

Other Passerines

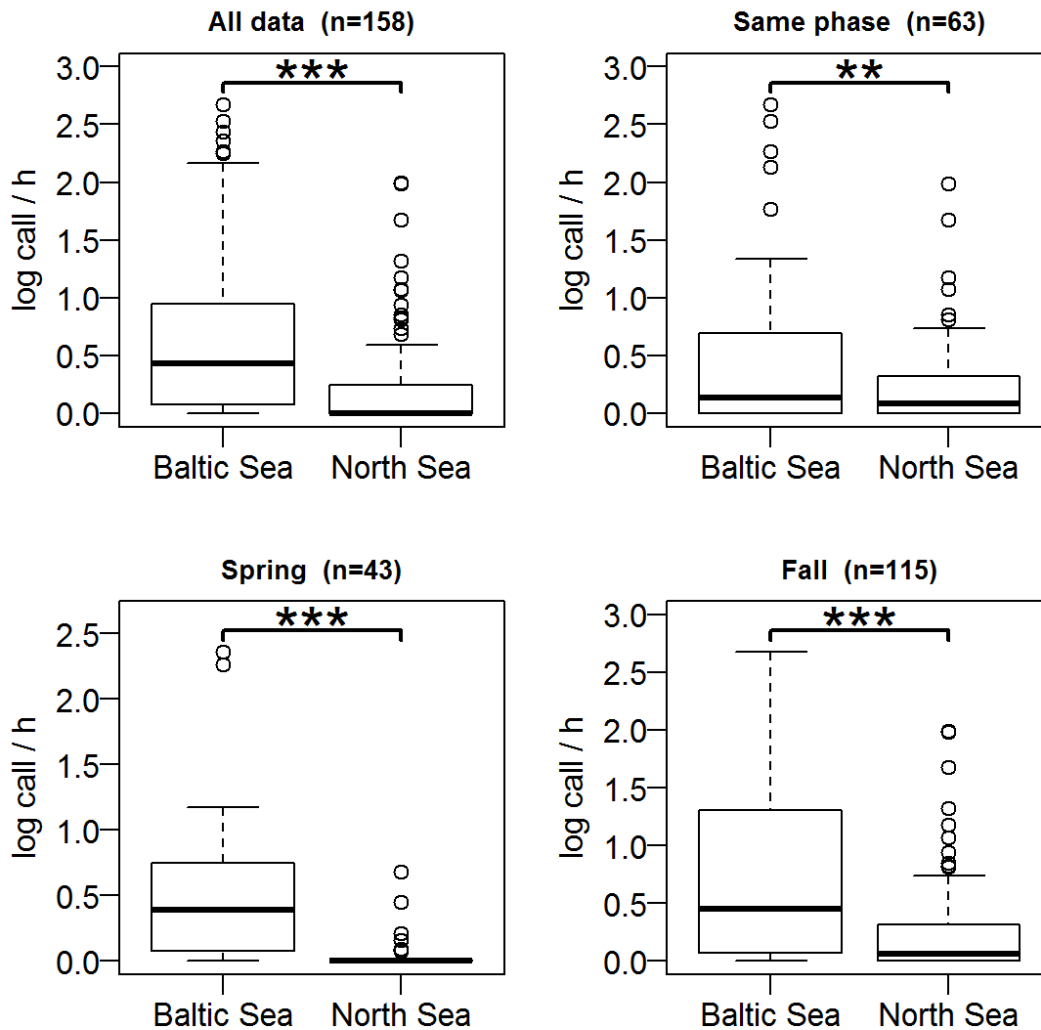


Figure 4.12 Call intensities (calls/h, log transformed) of other passerine species simultaneously measured in the Baltic and North Sea. See Figure 4.10 for further details.

4.4.2 Gradient with distance to shore within the North Sea

Different patterns also emerged with respect to a gradient of call intensities with distance to shore within the North Sea. Results differed between species groups and species, and between migration seasons.

There was no evidence of a gradient of call rates with distance to shore for waders in spring (Figure 4.13). During fall migration however, there was a significant negative relationship between the difference in call rates between sites and the difference in distance to shore suggesting that call rates declined with increasing distance to the mainland. This result was mainly driven by the

Dunlin which showed a marked decrease of δ call rates with increasing δ difference (Figure A. 14). In the Common Sandpiper there was a non-significant trend of a similar relationship.

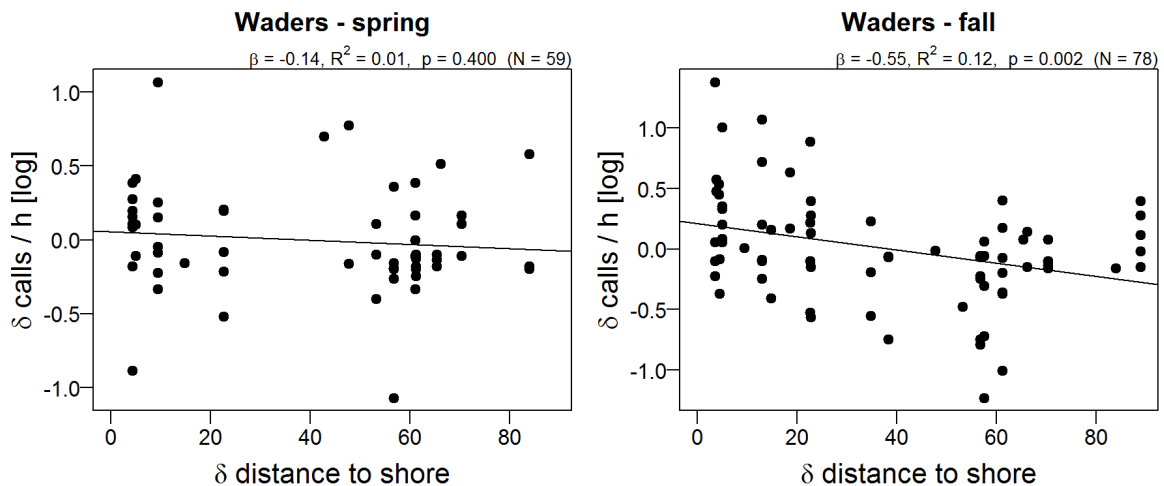


Figure 4.13 Relationship of the difference in call rates between two sites and their difference in distance to shore for the species group of waders. The results of a linear regression are given above the plot. Left panel: during spring migration; right panel: during fall migration.

For thrushes, the gradient with distance to shore differed distinctly between migration seasons. In spring, there was a significant positive relationship between δ call rates and δ difference to shore (Figure 4.14) indicating higher call intensities of thrushes at sites further offshore. This was the case in all thrush species except the Song Thrush for which call rates were independent of the distance to shore in spring (Figure A. 15). In contrast, there was an opposite relationship in fall. Here, δ call rates decreased significantly with increasing δ difference to shore suggesting higher call rates at sites closer to shore. A negative relationship between δ call rates and δ difference to shore was evident for all individual thrush species but only in Redwing was this relationship statistically significant (Figure A. 15).

Data from the species group of other passerines indicated a decrease of call rates with increasing distance to shore for both the spring and fall migration period. In both seasons, the difference in call intensities between sites decreased with increasing difference in distance to shore between those sites (Figure 4.15). In general, all four species of the species group 'other passerines' showed the same pattern, yet the strength of the relationship differed between species (Figure A. 16).

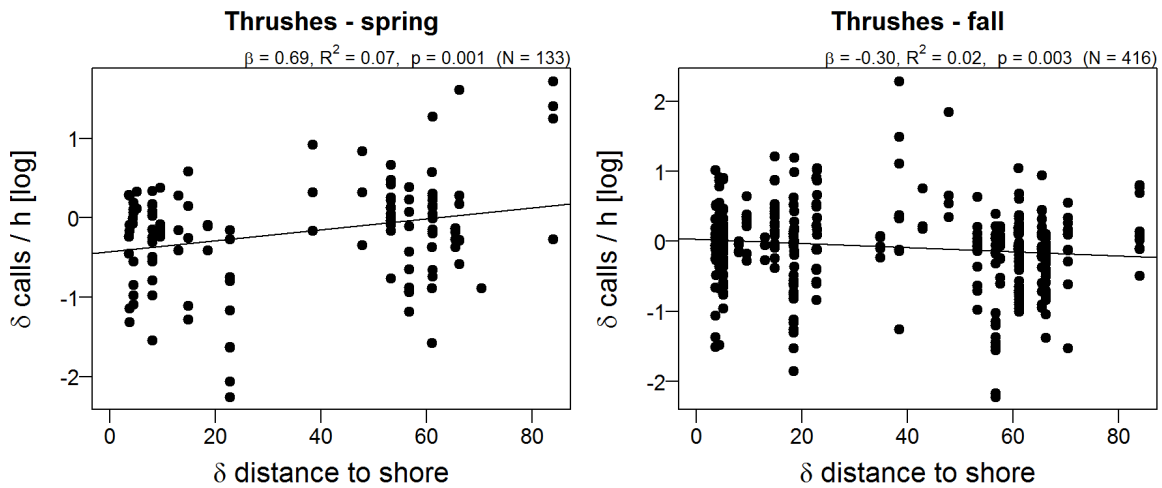


Figure 4.14 Relationship of the difference in call rates between two sites and their difference in distance to shore for thrushes. The results of a linear regression are given above the plot. Left panel: during spring migration; right panel: during fall migration.

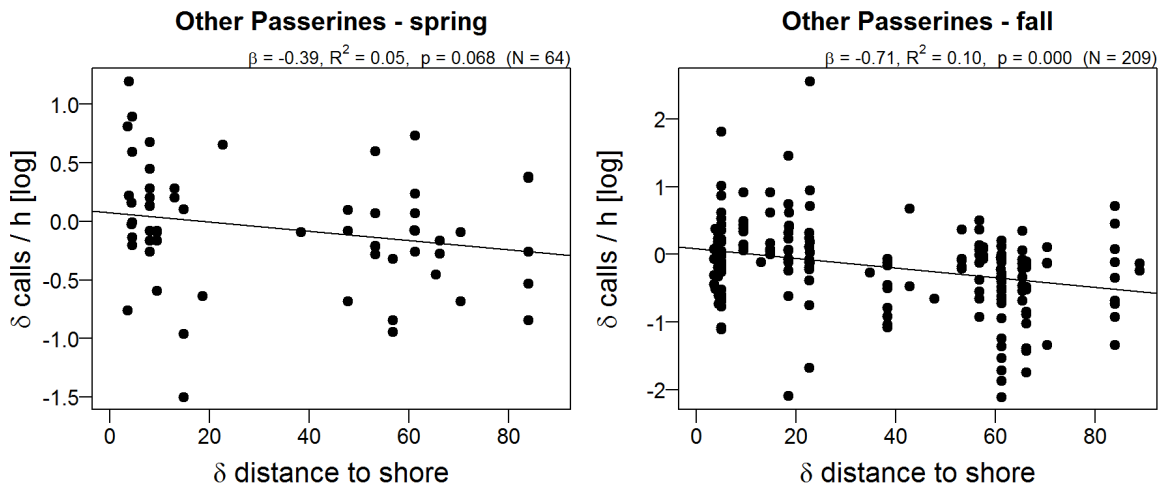


Figure 4.15 Relationship of the difference in call rates between two sites and their difference in distance to shore for other passerine species. The results of a linear regression are given above the plot. Left panel: during spring migration; right panel: during fall migration.

4.5 Weather models

4.5.1 Model performance and importance of explanatory variables

Model performance was highly variable depending on species and season (Table 4.3). In general, a higher percentage of the variance in call rates was explained in fall (43.9%) compared to spring (31.3%). With respect to species, model performance was best for the four thrushes and Robin (mostly more than 50% variance explained). Models also explained a considerable part of the variance in call rates of Starlings and Skylarks. Model performance for Waders and Meadow Pipit however was poor with variables explaining only between 1% and 17% of the variance (Table 4.3).

The relative importance of the different explanatory variables also differed between species and seasons. However, some general patterns emerged. In most cases, the time related variables Julian day and hour from midnight were important predictors. While Julian day accounted for the phenological pattern within the main migration periods of the respective species, hour from midnight captured the temporal pattern within the night.

Table 4.3 Summary of model results by species and season. N hours is the number of hours observed, % Var. expl. is the percentage of variance explained by the model. In addition, for each predictor variable the ranked “Standardized Error Variable Importance” is indicated (see Materials & Methods for details).

		Spp	N hours	% Var expl.	TWC	CWC	Δ TWC	Clouds	Rain	Temp.	Hour	Day	Year	Project	Phase	Lab	
SPRING	Waders	CS	2821	1.2	3	4	8	5	10	2	6	1	12	11	9	7	
		Du	4523	6.2	1	2	6	9	11	7	3	8	4	5	12	10	
	Thrushes	Bb	2296	60.2	4	7	10	2	6	9	1	3	5	8	11	12	
		Rw	2632	57.3	1	7	10	2	8	6	3	5	4	9	11	12	
		SoT	2540	47.3	5	7	9	1	10	8	3	2	6	4	11	12	
		Ff	2629	30.9	10	9	7	1	5	3	2	4	6	8	11	12	
	Other passerines	MP	3047	3.1	2	9	11	7	6	3	4	1	5	8	12	10	
		Sk	1627	31.6	2	3	5	6	9	8	1	4	11	7	12	10	
		Ro	2967	42.1	5	7	9	2	11	3	8	1	6	4	10	12	
		St	1812	32.9	10	2	7	4	9	3	1	5	6	8	11	12	
	Mean		2689	31.3	4.3	5.7	8.2	3.9	8.5	5.2	3.2	3.4	6.5	7.2	11	10.9	
	FALL	Waders	CS	3863	14.7	3	2	8	4	12	6	9	1	10	5	11	7
			Du	7419	7.0	1	3	8	6	11	4	12	2	7	5	9	10
Thrushes		Bb	4067	65.3	3	5	9	7	12	8	1	2	6	4	10	11	
		Rw	4075	64.4	2	7	9	5	12	8	3	1	6	4	10	11	
		SoT	4140	64.4	1	8	9	5	12	6	2	3	7	4	10	11	
		Ff	3654	57.2	1	8	10	7	12	6	2	4	3	5	9	11	
Other passerines		MP	6000	17.2	2	9	8	7	12	3	4	1	6	5	10	11	
		Sk	2808	45.4	2	7	9	4	12	3	5	1	6	8	10	11	
		Ro	4902	66.8	1	6	7	9	12	5	2	3	8	4	10	11	
		St	3820	36.9	3	4	5	6	8	2	9	1	10	7	11	12	
Mean		4475	43.9	1.9	5.9	8.2	6	11.5	5.1	4.9	1.9	6.9	5.1	10	10.6		
Mean		3582	37.6	3.1	5.8	8.2	5.0	10.0	5.2	4.1	2.7	6.7	6.2	10.5	10.8		

Call rates generally increased in the course of the night, yet the onset of this increase varied considerably among species and seasons (Figure 4.16). Highest call rates were usually reached shortly before sunrise. In some cases, the relationship between call rates and time from midnight was U-shaped with higher call intensities at the beginning and end of the night (Figure 4.16).

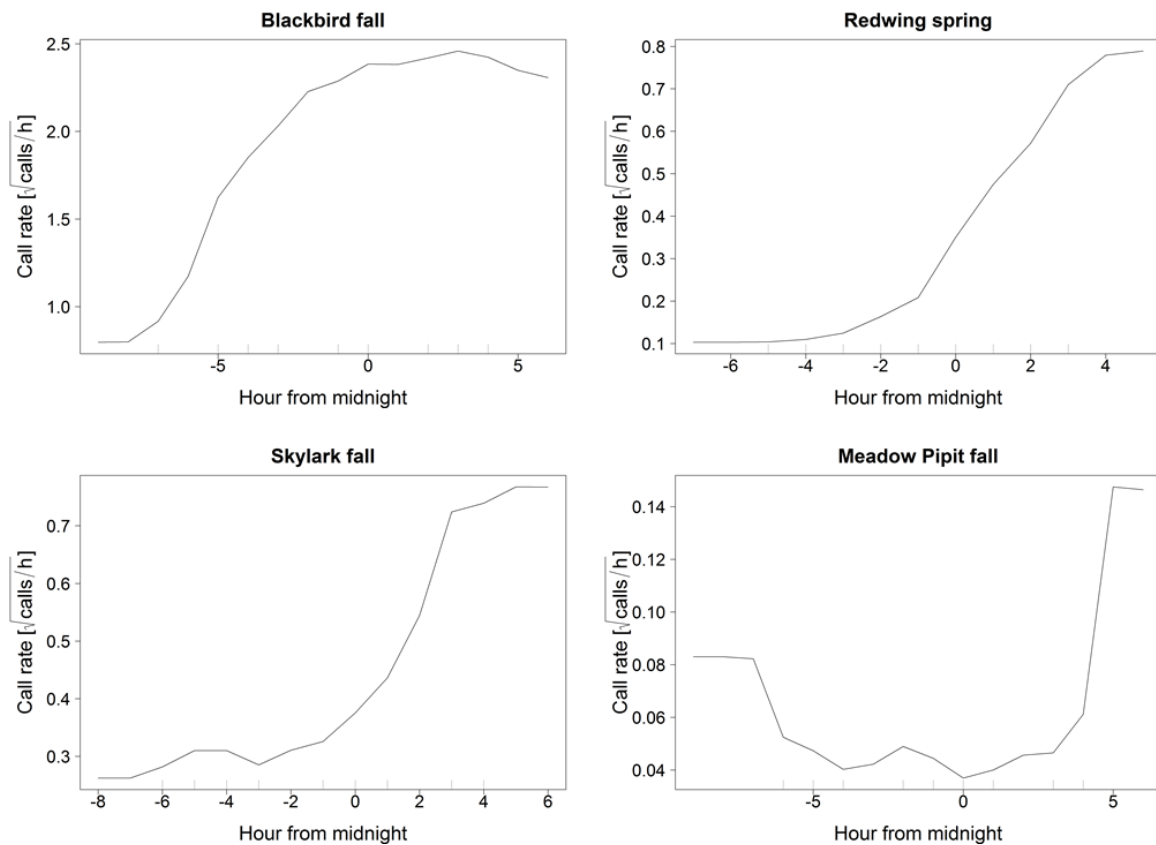


Figure 4.16 Examples of partial dependence plots of time from midnight. Upper panel: Blackbird in fall (left) and Redwing in spring (right). Lower panel: Skylark in fall (left) and Meadow Pipit in fall (right).

Of the meteorological parameters, TWC was consistently an important explanatory variable (Table 4.3). Call rates often increased sharply with increasing TWC (Figure 4.17). The value of TWC at which this steep increase occurred varied between about -5 m/s and 10 m/s. The abrupt increase often ensued at higher TWC values in spring compared to fall, particularly in thrushes. δ TWC generally was a poor predictor of call rates with low importance scores in most models (Table 4.3). The relationship of δ TWC with call rates was usually U-shaped with higher call intensities at low and high δ TWC values (Figure 4.17).

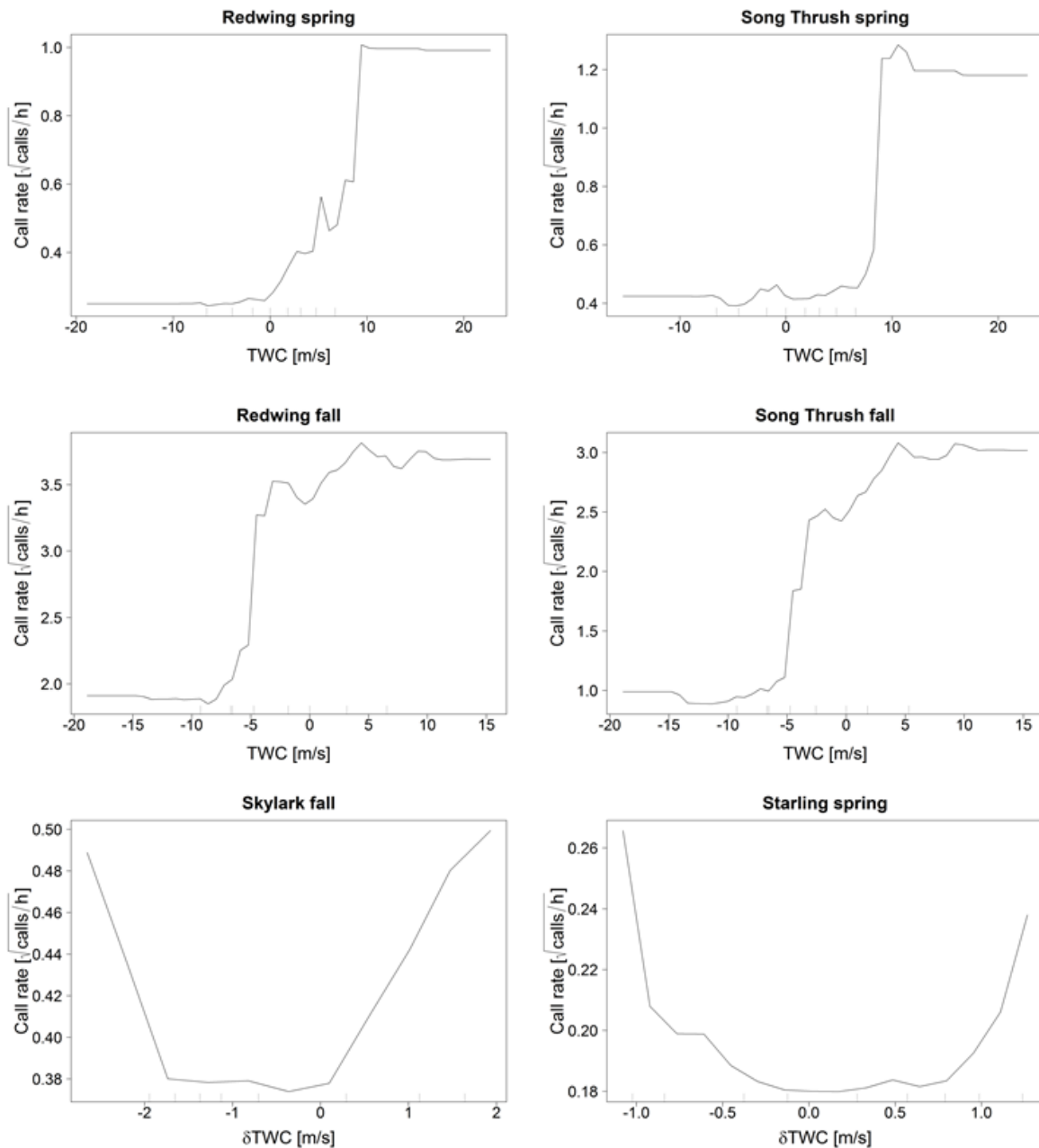


Figure 4.17 Examples of partial dependence plots of TWC and δ TWC. Upper panel: Redwing in spring (left) and Song Thrush in spring (right). Mid panel: Redwing in fall (left) and Song Thrush in fall (right). Lower panel: δ TWC of Skylark in fall (left) and Starling in spring (right).

CWC was of less importance than TWC overall and in most cases showed a distinct season-specific pattern (Figure 4.18). While during spring call rates increased with increasingly negative CWC values, the opposite pattern was evident in most cases in fall. This means that in both spring and fall call rates generally increased with southeasterly winds.

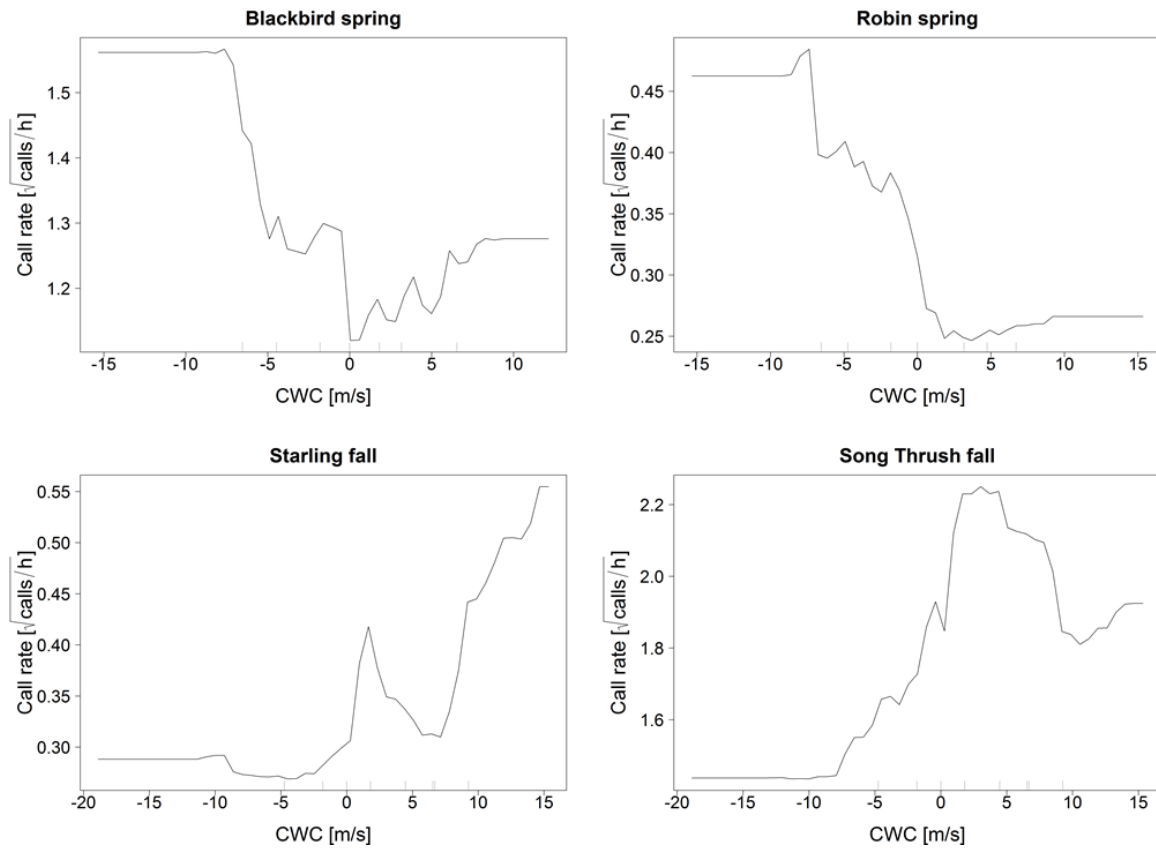


Figure 4.18 Examples of partial dependence plots of CWC for spring and fall. Upper panel: Blackbird in spring (left) and Robin in spring (right). Lower panel: Starling in fall (left) and Song Thrush in fall (right).

Cloud cover was also an important predictor of call rates. The relationship differed between spring and fall (Figure 4.19). In spring call rates usually showed low call intensities with clear and partly cloudy skies and a steep increase at high cloud cover values. In fall the relationship was mostly U-shaped with lowest call rates at partly cloudy skies (Figure 4.19).

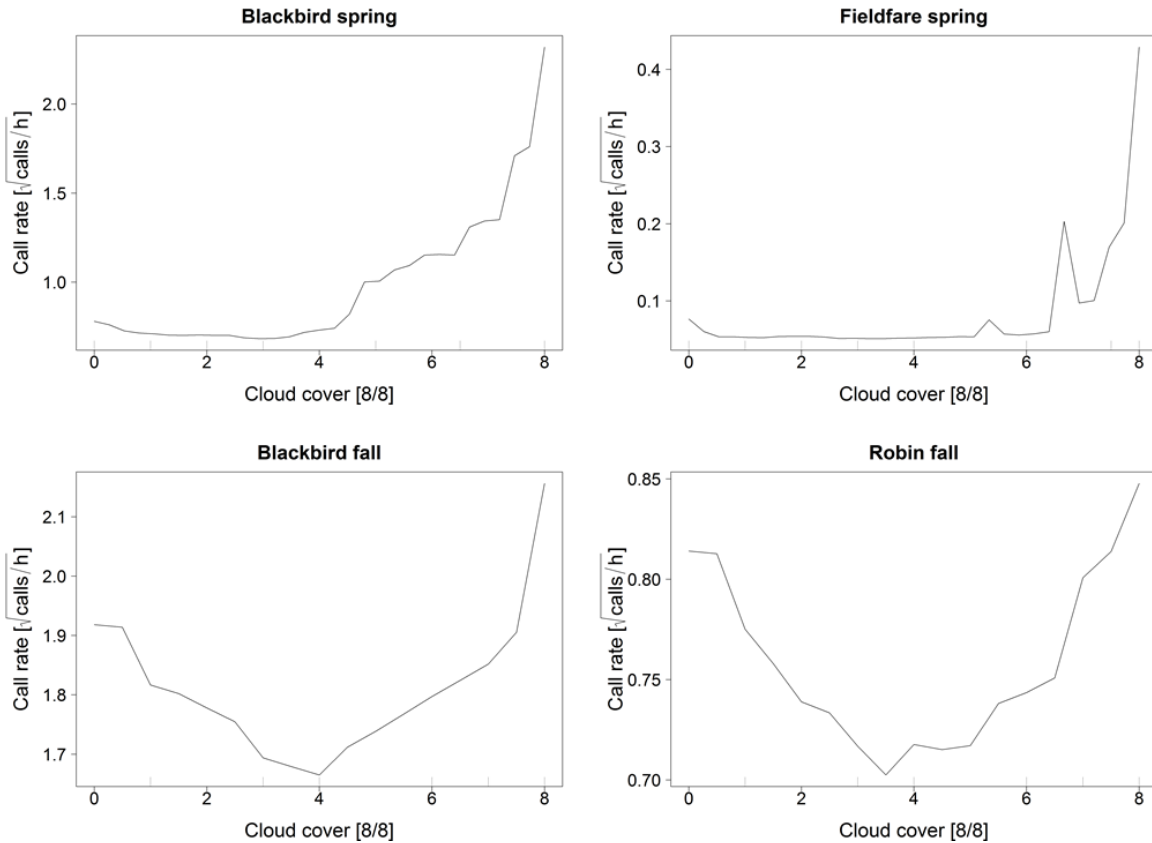


Figure 4.19 Examples of partial dependence plots of cloud cover for spring (upper panels) and fall (lower panels). Upper panel: Blackbird in spring (left) and Fieldfare in spring (right). Lower panel: Blackbird in fall (left) and Robin in fall (right).

Rain was the least important meteorological predictor in most models but appeared to have a stronger effect on call rates in spring compared to fall (Table 4.3). In most cases the relationship showed a clear pattern with increasing call intensities with an increasing proportion of rain during the hour of observation (Figure 4.20).

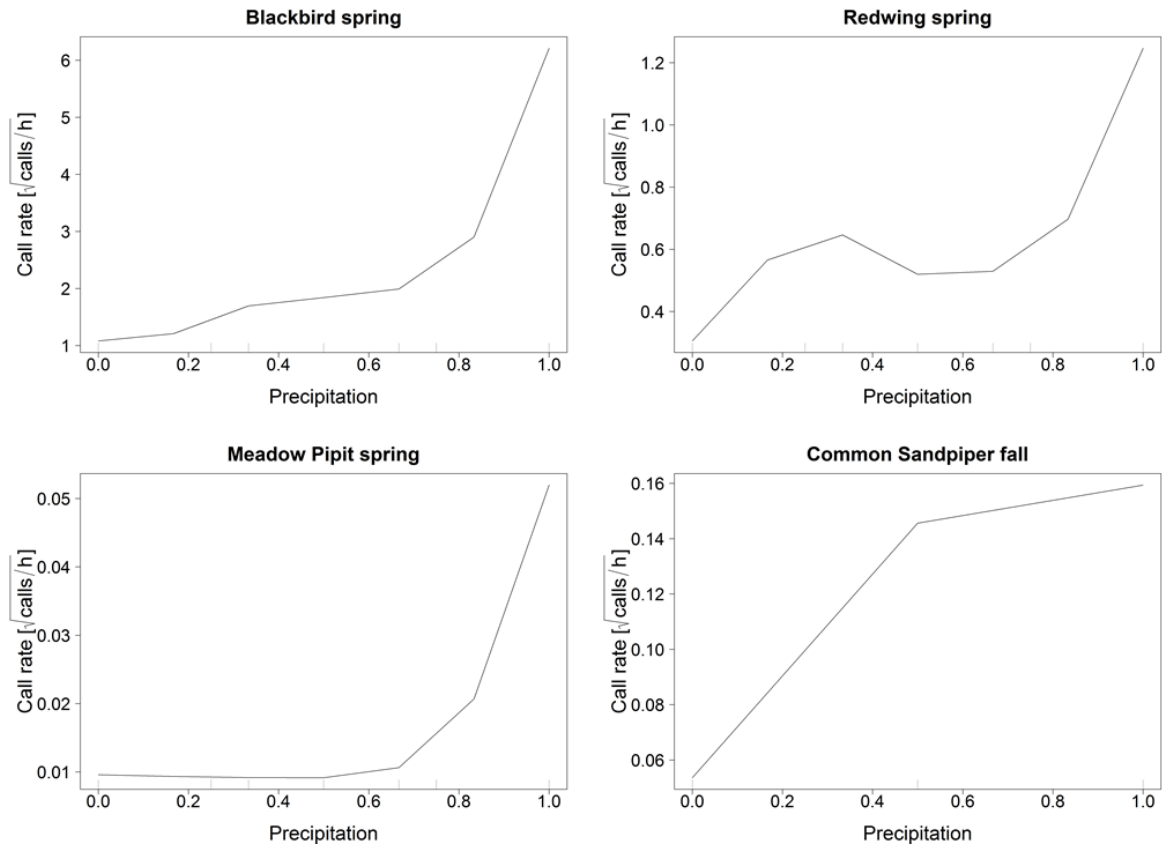


Figure 4.20 Examples of partial dependence plots of rain. Upper panel: Blackbird (right) and Redwing (left) in spring. Lower panel: Meadow Pipit in spring (left) and Common Sandpiper in fall (right).

Ambient temperature was an important meteorological parameter in most models yet the shape of the relationship varied substantially across models. The influence of temperature on call intensities was often easier to interpret when interaction plots between temperature and Julian day were considered (Figure 4.21). These plots indicated that ambient temperature at least in some cases had a strong effect on the seasonal pattern of call rates. For example, the onset of spring migration of the Fieldfare was dependent on temperatures above 5°C (Figure 4.21, upper panel). On the other hand, high call intensities at the end of the fall season only occurred when temperatures were above about 13°C in Meadow Pipits and Robins (Figure 4.21, mid and lower panel).

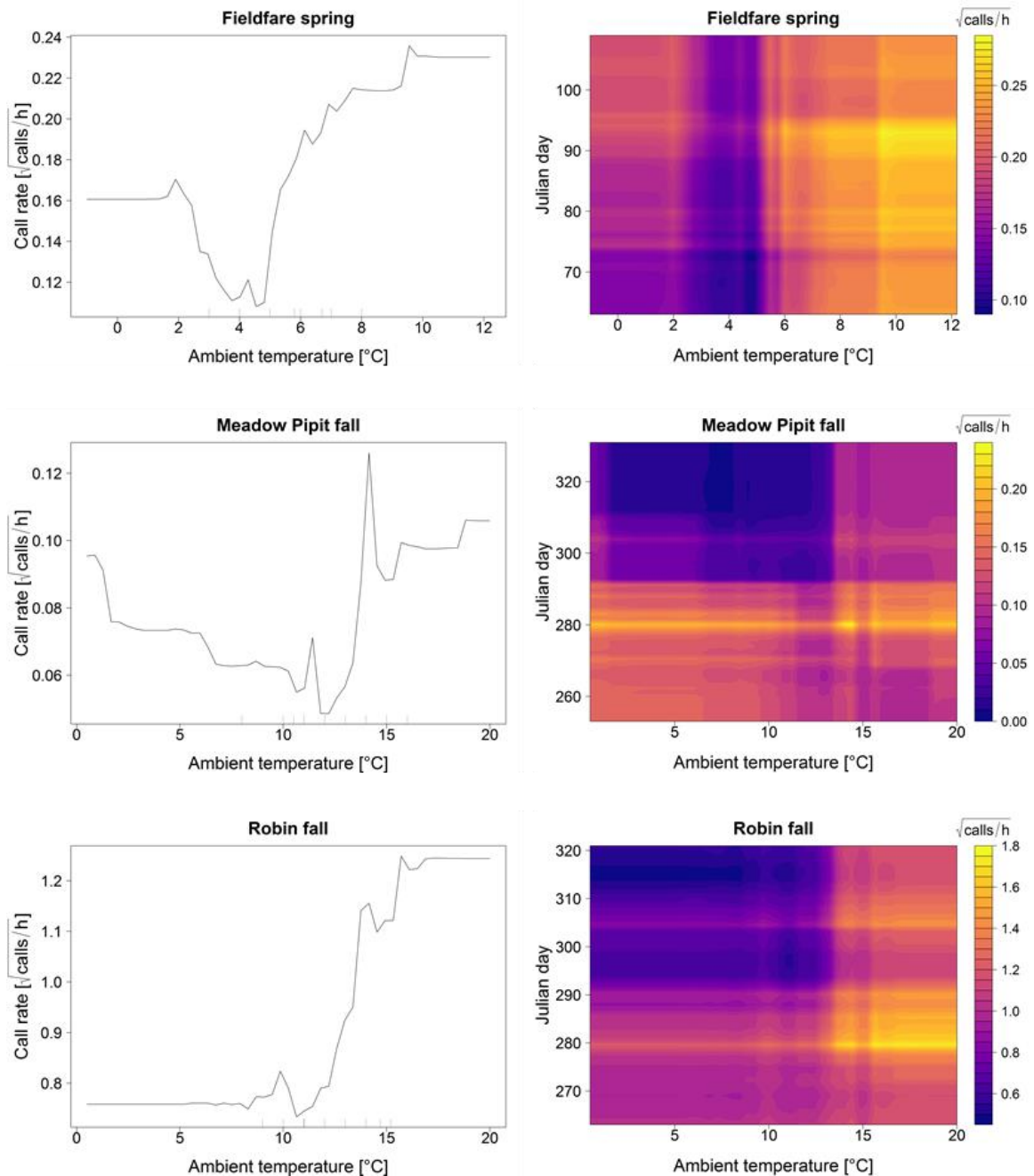


Figure 4.21 Examples of partial dependence plots of ambient temperature (left) and interaction plots of ambient temperature with Julian day (right). Upper panel: Fieldfare in spring, mid panel: Meadow pipit in fall, and lower panel: Robin in fall.

Of the four factors (year, project location, phase and lab) included in the modelling process, year and/or location were important predictors in most cases indicating high variability of call rates across years and locations. In contrast, the role of developmental phase of wind farms and the lab responsible for data collection was minor. These factors had a low “Standardized Error Variable Importance” in all models and results were inconsistent between models and seasons (Table 4.3, see also Appendix A.4).

4.5.2 Species-specific results

Common Sandpiper

For the spring migration period, the model performed very poorly explaining only 1.2% of the variance (Table 4.3 and Figure A. 19). Call activity of Common Sandpiper in spring was apparently affected by variables not considered in the analysis. Of the variables included Julian day was the most important. Other variables included were ambient temperature, hour from midnight, CWC, TWC and cloud cover which generally showed the characteristic relationships outlined in chapter 4.5.1.

For the fall migration period, explanatory variables explained 14.7% of the variance. Again, Julian day was the most important variable, followed by wind components, cloud cover and project location (Table 4.3 and Figure A. 20). Call intensities increased with increasing TWC with a distinct step between about 7-10 m/s. The relationship with δ TWC, CWC and ambient temperature was U-shaped. Also, the relationship with cloud cover was roughly U-shaped with highest call rates when skies were completely overcast. Interaction plots showed that TWC had a strong effect on the seasonal pattern. Call rates were highest early in the season when TWC values exceeded 10 m/s. In addition, call rates increased in the course of the night with low rates until approx. 2 h before midnight and maximum rates before dawn.

Dunlin

During both spring and fall migration, variance explained by the model was very low with 6.2% and 7.0%, respectively.

During spring migration, wind components, hour from midnight and year were the most relevant explanatory variables (Table 4.3 and Figure A. 21). Julian day and TWC were the main predictors during fall migration (Table 4.3 and Figure A. 22). Positive TWC during the early season resulted in highest call rates.

Blackbird

For spring migration, the model explained 60.2% of the variance. Cloud cover, precipitation and TWC were the most important meteorological variables. The time related components of Julian day and hour from midnight also played an important role (Table 4.3 and Figure A. 23).

Visibility had a strong influence with higher bird call rates detected during periods with rain and cloud covered skies. Call rates increased steeply at positive TWC and negative CWC values. Call rates varied considerably with hour from midnight with about twenty times higher call rates close to dawn compared to the early part of the night.

For fall migration, the model explained 65.3% of the variance of the data. Of the meteorological variables TWC, CWC and cloud cover were most relevant. Again, the time related components Julian day and hour from midnight were important predictors (Table 4.3 and Figure A. 23).

The relationship of call rates with TWC was similar to the situation in spring yet the increase of call rates commenced at lower TWC values (-5 m/s vs. 0 m/s in spring). Also the relationship with CWC

and cloud cover differed between seasons. In fall, highest call rates were detected at positive CWC values. The relationship with cloud cover was U-shaped indicating high call intensities when skies were clear or completely overcast. Interaction plots suggested that both TWC and ambient temperature had an effect on the phenological pattern particularly during the first part of the season. Up to Julian day 300 (27th of October) high call intensities only occurred at TWC > -4 m/s. Yet, during the main part of fall migration (approx. Julian day 300 - 315) call intensities were largely independent of TWC (Figure A. 24). Likewise, the onset of fall migration depended on ambient temperature. High call rates early in the season were only detected when ambient temperature was below approx. 8°C. Again, during the peak migration period end of October /early November, call rates were independent of ambient temperature (Figure A. 24).

Redwing

The spring model explained 57.3% of the variance with TWC, cloud cover, hour from midnight and year being the main explanatory variables. Call rates increased steeply about two hours before midnight, and at dawn reached values about 50-fold higher than during the first hours of the night. There was also a prominent step in call intensities at TWC values > 9 m/s. In addition, call rates were substantially higher at negative CWC values than when CWC was positive. Also, low visibility conditions (cloudy skies and precipitation) increased call intensities about 10-fold. The effect of temperature seemed to depend on Julian day. While at the onset of spring migration high call intensities were only reached at temperatures above approx. 7°C, towards the end of the season, call rates were largely independent of ambient temperature (Figure A. 25).

For fall migration, Julian day, TWC and hour from midnight were the main explanatory variables. Project location, year and cloud cover were also relevant variables. In total, the fall model explained 64.4% of the variance.

Call rates increased with increasing TWC in a marked step at -5 m/s. However, an interaction plot showed that the effect of TWC depended on Julian day. Up to about Julian day 300 TWC had a strong impact on call rates. During the peak phase of migration and particularly towards the end of the season the effect of TWC was minor. Additionally, call rates generally increased markedly at the end of the night with roughly 20-fold higher call intensities than at its start. However, an interaction plot with TWC showed that the pattern during a night was strongly affected by TWC. Under favorable TWC conditions high call intensities were also reached in the hours before midnight (Figure A. 26). The relationship of call rates with cloud cover was mildly U-shaped with highest call intensities during cloudy conditions and to a much lesser extent during clear skies.

Song Thrush

For spring migration, cloud cover, Julian day and hour from midnight were the main predictor variables. TWC, air temperature and project site were also relevant. In total, the model explained 47.3% of the variance during the spring season.

Call rates increased during the course of a night reaching 40-fold higher values at the end of the night compared to the start. Call rates were also about 15 times higher with a high degree of cloud cover compared to clear skies. In addition, call intensities were positively related to TWC

and ambient temperature. The relationship of call rates with TWC showed a steep increase at TWC above approx. 9 m/s (Figure A. 27).

In fall, model predictive performance increased to 64.4% of explained variance. By far the most important predictor was TWC followed by hour from midnight and Julian day. Other relevant variables included cloud cover and ambient temperature as well as project location and year.

The relationships of call intensities with cloud cover, TWC and CWC showed seasonal differences in particular (Figure A. 28). As in spring, call rates were positively related to TWC yet the onset of the increase occurred at lower TWC values in fall (-5 m/s) than in spring (9 m/s). In contrast to spring, the relationship with cloud cover was U-shaped with high call rates during either clear or completely overcast skies. While in spring call rates were higher at negative CWC values, in fall call rates were higher at positive CWC values.

Fieldfare

During spring migration, performance of the model was 30.9% of variance explained. Main explanatory variables included cloud cover, air temperature, hour from midnight and Julian day.

Call rates increased steeply during the second half of the night and with completely overcast skies (Figure A. 29). Call rates were about 50 times higher at the end of the night compared to its start and 15 times higher with complete cloud cover compared to clear skies. Furthermore, call intensities increased with increasingly positive TWC values with a particularly steep increase between 7 and 10 m/s. The effect of ambient temperature was highest during the early and mid-part of the spring season with a strong increase in call rates above 5°C. At the end of the season the effect of temperature was negligible.

The fall model explained 57.2% of the variance, selecting TWC, hour from midnight, year, Julian day and project location as the main explanatory variables.

Bird call intensities increased steadily during the night until dawn and also increased with increasing TWC. In contrast to spring, in fall call intensities started to increase at TWC values > -5 m/s with another step at about 7 m/s (Figure A. 30). Again, the effect of ambient temperature seemed to depend on Julian day. During the early and mid-part of the spring season call rates were higher at temperatures < 8°C while the opposite was true for the end of the season.

Call rates were highly variable across years in both spring and fall. In contrast to the situation in fall, heterogeneity across years in spring appeared not to be stochastic but indicated a systematic decrease of call rates during the study period.

Meadow Pipit

Model performance for this species was generally low, achieving 17.2% of variance explained during the fall season and only 3.1% during the spring season.

Despite the low explanatory power of the models the relationship of call rates of the Meadow Pipit with meteorological variables was largely consistent with the other species (Figure A. 31 and Figure A. 32). However, the relationship of call intensities with hour from midnight differed dis-

tinctly from all other study species. Particularly in fall this relationship was U-shaped with high call rates shortly after dusk and prior to dawn.

Skylark

For the spring season, the model explained 31.6% of the variance. Relevant variables were wind components, hour from midnight and Julian day. Call intensity of the Skylark increased sharply with CWC values < -5 m/s. There was a positive relationship with TWC indicating a mild increase in call rates with positive TWC. Calls of Skylark were almost exclusively detected in the second half of the night, call rates at the end of the night were about 25-fold higher than at the beginning (Figure A. 33).

With 45.4% variance explained the model for the fall season performed considerably better than for spring. Main predictors included Julian day, TWC, air temperature, clouds and hour from midnight.

Call rates increased with increasing TWC in two steps, at -5 m/s and at 9 m/s (Figure A. 34). With respect to hour from midnight, there was a prominent increase of call rates in the second half of the night. The effect of ambient temperature depended strongly on Julian day. Temperature had only a negligible impact on call rates until the end of the season when call intensities increased considerably at temperatures < 9°C.

Robin

The model for the Robin in fall achieved the best performance of all species, reaching 66.8% of variance explained. With 42.1% variance explained the spring model also reached high explanatory power.

During spring, Julian day, cloud conditions, ambient temperature, project and TWC were relevant predictors. In line with the results of most other species, call rates in spring increased sharply with positive TWC and negative CWC and were substantially higher when the sky was overcast in comparison to clear skies (Figure A. 35). Also, call rates increased in the course of the night with highest intensities in the second half of the night. The effect of ambient temperature was largely independent of Julian day. Call rates were generally higher at temperatures above 6°C throughout the season.

Main predictors for the fall season were TWC, hour from midnight, Julian day, project and ambient temperature.

Of these, TWC was the dominant predictor. Call rates increased about 10-fold from -5 m/s to 0 m/s TWC and stayed high for all positive TWC values (Figure A. 36). CWC had a much lower effect, call rates increased mildly at positive CWC values indicating southeasterly winds in fall. The relationship with cloud cover was U-shaped. Call intensities increased continually during the first half of the night and remained high throughout the second part of the night. Also, call rates were higher at ambient temperatures above 13°C although this effect applied mostly to second part of the fall season.

Starling

Model performance for the Starling was very similar for both seasons with 32.9% and 36.9% of variance explained for spring and fall, respectively.

During the spring season, main predictors were hour from midnight, CWC, ambient temperature and cloud cover. Prior to midnight call rates were generally low but increased continually during the second half of the night at the end of which call rates were more than 50 times higher than at the beginning. Also, during hours with continuous rain call rates of the Starling were about 40-fold higher than during hours with no precipitation. Call rates showed a pronounced increase at ambient temperatures higher than 6°C yet the magnitude of this effect was comparatively low. Likewise, call rates increased slightly with CWC >5 m/s (Figure A. 37).

Similar to spring, call rates of Starling in fall increased with the proportion of rain during the hour of observation. The relationship with cloud cover was U-shaped. In addition call rates increased during the second part of the night. The relationship of call rates with TWC showed an unusual pattern with higher call rates at negative TWC values. Yet there was a positive relationship with δ TWC indicating higher call rates when TWC values increased. Call rates also increased at positive CWC values.

5 DISCUSSION

In this study we integrated data of bird flight calls from 13 different locations across the German EEZ of the North and Baltic Sea over a span of eight years. This gave us the unprecedented opportunity to comprehensively analyze temporal and spatial patterns as well as causes of variation of flight calls of nocturnal migrants in this region. However, it has to be kept in mind that several factors contributed to high heterogeneity in the data. Firstly, four different companies and a large number of observers were involved in data collection. Even though acquisition methods were standardized to a large degree through a detailed description of the requirements by the “Standard – Investigation of the Impacts of Offshore Wind Turbines on the Marine Environment (StUK4)” issued by the BSH (BSH 2013), differences in effort per hour, the definition of a call in species that produce a series of notes, or whether or not to count calls that are thought to be uttered by the same individual bird are known factors that added noise to the data. As the lab responsible for data collection was often confounded with project location and/or project year it was difficult to determine whether systematic differences in call rates between labs occurred. Yet, the fact that the factor “lab” was generally of negligible importance in random forest analyses suggests that the effect of differences between labs on our results was minor.

In addition, data were collected during all three developmental stages of wind farms, baseline, construction and operation. Particularly during the operational phase bird call rates may be affected by OWF. The sign of the response (attraction vs. avoidance) however may be context dependent and may also vary between species (DREWITT & LANGSTON 2006; HÜPPOP et al. 2006; SCHULZ et al. 2014; DIERSCHKE et al. 2016). In our data no clear pattern was evident with respect to an effect of developmental stage. We did not find an effect of stage on the correlation of call rates between sites. Also, stage was generally of low importance in random forest models. The minor effect of stage on call rates could be related to the often rather large distances between the sites of data collection and the wind farms themselves. With the exception of the projects “Butendiek” and “Cluster Helgoland”, ship-based and platform-based data collection took place between approx. 0.5 – 2 km outside the construction site or wind farm. As many species, particularly passerines, may respond to a wind farm at close range, these distances might have been too large to detect differences. In addition, due to the very high variability of call rates on different temporal and spatial scales, comparing call rates across different years and sites has little power to detect differences with respect to the developmental stage of a wind farm. Comparative study designs linking simultaneously collected data inside and outside a wind farm may be a more promising approach to do so (SCHULZ et al. 2014; WELCKER & NEHLS 2016).

Finally, data were collected by two different methods, observer-based recordings and digital audio systems. As these data were not directly comparable this reduced the data available for quantitative analyses. Acquisition method was also an important factor in qualitative analyses. For example, rank correlations of call rates were significantly lower when data of both methods were included in the analysis. Differences in species-specific detection range as well as diverging effects of factors like weather and environmental noise on detectability may be responsible for the reduced comparability between methods.

Due to several reasons it is not possible to equate call rates with migration intensities or to directly compare call intensities between species. The propensity to utter flight calls may depend on several factors independently of the number of migrating birds, such as precipitation, visibility

conditions or time of day (see Chapter 3.5; FARNSWORTH 2005; HÜPPOP & HILGERLOH 2012; HORTON et al. 2015a; b) and may also be affected by the observation platform and/or its illumination (EVANS OGDEN 1996; WATSON et al. 2016). Furthermore, the inclination of birds to produce flight calls as well as the audibility and, consequently, the detection range of calls varies between species. The call rates reported in this study can therefore only be regarded as an indirect proxy of flight activity of the respective species close (not more than a few hundred meter) to the observation sites.

Out of the 127 species recorded we selected 10 species (8 passerines and 2 waders) for further analysis. Selection was based on the number of calls and the constancy with which the species were recorded across sites and years. Not all of the selected species can be regarded as obligate nocturnal migrants. The passerine species Skylark, Starling and particularly the Meadow Pipit migrate partly or predominantly (Meadow Pipit) during the day. Especially the regular and numerous recordings of Meadow Pipits may therefore be related to an attraction to boats or platforms as potential staging opportunities at sea.

Although Dunlins and Common Sandpipers migrate primarily during the night they are thought to usually fly at high altitudes outside the range of acoustic recordings at sea (GREEN 2004). Observations of these species might therefore to a larger degree be “accidental” and less representative of the migration behavior of these species.

5.1 Seasonality

With the exception of Dunlin, call rates of all species showed a clear seasonal pattern in both spring and fall. The main migration period, defined as the inner time period with 90% of calls (HÜPPOP & HILGERLOH 2012) lasted 6-8 weeks in most cases.

In contrast, call rates of the Dunlin seemed to vary stochastically in both migration seasons. The reason for this lack of seasonal pattern remains speculative. As discussed above, Dunlins may mainly migrate outside the range of acoustic recordings at sea suggesting that recordings at sea are predominantly of accidental nature. The lack of pattern could also be related to the fact that Dunlins use the tidal flats of the Waddensea in large numbers as a staging site throughout spring and fall. Flight calls recorded offshore might be related to movements of birds between staging sites rather than birds on long-distance migration and thus show less of a seasonal pattern. In contrast, flight calls of Dunlin recorded on Heligoland show a clear phenological pattern with peaks in March and August thought to be related to the arrival of birds in the Waddensea (DIERSCHKE et al. 2011).

For all other species for which comparable data is available, the seasonal patterns observed in our study correspond well with data from Heligoland (DIERSCHKE et al. 2011) and a research platform in the southeastern North Sea (FINO1; HÜPPOP et al. 2012; HÜPPOP & HILGERLOH 2012).

The study period given by the StUK (BSH 2013) encompasses the time periods between 01/03 – 31/05 (spring) and 15/07 – 30/11 (fall). Our results indicate that for some species and seasons a considerable part of the migration activity occurs outside these time periods. Specifically, the spring main migration period of Blackbird, Skylark and Starling appears to commence before 01/03 (Figure 4.3 and Figure 4.4). Likewise, the fall main migration period of Blackbird and Redwing seems to extend beyond the end of November (Figure 4.3). Comparable data collected

throughout the year support this view (DIERSCHKE et al. 2011; HÜPPOP et al. 2012; HÜPPOP & HILGERLOH 2012). For instance, the main fall migration period of Blackbird and Redwing, calculated in a similar way as in our study, extended to the 13th of December at the FINO1 platform in the southeastern North Sea (HÜPPOP & HILGERLOH 2012).

The main migration periods of the thrushes and the other passerine species show a multi-peak pattern particularly in fall with periods of high call rates interspersed with time periods with little call activity. For example, the fall migration of Blackbirds is interrupted by three distinct periods with low call intensities (22.-25/10, 12.-15/11 and 23.-26/11) which in turn causes three apparent peaks in call intensities (Figure 4.3). While at first sight this might be interpreted as a temporal separation of the migration of different sub-populations of this species the comparison of patterns shows that periods with low call intensities occurred simultaneously in all species. This suggests that periods of low call intensities are at least partly related to an artifact due to unequal observation effort or observation conditions. Indeed, during the main migration period the mean number of observation days per calendar day was significantly lower for time periods with low call intensities compared to all other days (7.5 days vs. 12.8 days, t test: $t = -8.5$, $p < 0.0001$). As nights with high call rates are rare events (Figure 3.4) the probability of recording such an event increases with effort. The apparent periods with low call intensities during the main migration periods can therefore be regarded as a consequence of the highly right-skewed distribution of the data the effect of which was not completely removed by the standardization procedure and the calculation of moving averages (see chapter 3.2.1).

5.2 Spatial correlation

The correlation of call rates among project-years varied substantially between seasons, species and across space. Overall, correlation was weaker during spring compared to fall. This might reflect differences in migration strategies between seasons. During spring migration, many species migrate on average faster and at higher altitudes (Berthold et al. 2003) which may affect the detection probability of flight calls. In addition, sample sizes were generally smaller during spring which may have contributed to the seasonal differences in correlations.

The correlation strength between sites depended strongly on the distance between those sites. Generally, correlations within the North Sea were higher than between the North and Baltic Sea, reflecting the difference in distances among sites (mean distance among sites in the North Sea: 82.0 km; mean distance of sites between North and Baltic Sea: 417.1 km). Also, there was a strong negative relationship between correlation strength and distance between sites within the North Sea for most species. This result was corroborated by the analysis of the correlation of mass migration. The probability of coincidence of mass migration or high call intensities showed a similar decline with increasing distance between locations. Hence, the low correlation between distant sites was not caused by stochastic variation of call rates during nights with low call activity (the vast majority of nights) but also applied to nights with exceptionally high call rates.

The concept of broad front migration predicts consistent migration patterns over large spatial scales. Hence we would expect strong spatial correlation of call rates within the study area, particularly within the North Sea. However, our results suggest that patterns of the nocturnal migration of many species may vary at smaller spatial scales than previously thought. An alternative

explanation could be related to factors other than migration intensity known to affect bird call rates such as local weather conditions. Specifically, locally varying visibility or cloud cover may influence flight altitude and hence detectability as well as general call activity (FARNSWORTH 2005). As a consequence this may reduce correlation of call rates across sites. These two explanatory approaches are not mutually exclusive. Similar analyses based on radar data, a more direct proxy of migration intensities, may help to distinguish between these two hypotheses.

Remarkably, correlation strength of the four passerines Skylark, Robin, Meadow Pipit and Starling varied considerably among project-years, yet was independent of the distance between project locations. As discussed above, due to their at least partly diurnal migration behaviour, data of these species is likely to contain more variability related to factors other than migration intensity. In addition, sample sizes for most of these species, particularly in spring, were low.

5.3 Mass migration

The distribution of nightly call intensities was highly right-skewed but continuous. We did not find any indication of a bimodal or multi-modal distribution that would allow establishing a data driven cut-off value to distinguish between nights with “mass migration” and nights with “ordinary call intensities”. This means that any definition of mass migration, at least as far as bird call data is concerned, needs to be based on considerations other than the distribution of the data.

For the purpose of this study we arbitrarily defined mass migration as mean nightly call rates >100 times the median call rate. Based on this definition roughly 5% of the nights were regarded as mass migration events. Applying this criterion would result on average in 11.5 nights of mass migration per year (in the seasonal migration periods as given by the StUK). It needs to be noted that the outcome of applying a criterion based on a multiple of a median value largely depends on the distribution of the data. For example, as radar data is likely to be less right-skewed in comparison to flight call data, the application of the same criterion would result in a smaller proportion of nights being labelled as mass migration events.

5.4 Gradient of call intensities

Estimates of the total number of nocturnally migrating passerines passing over the western part of the Baltic Sea and the eastern part of the North Sea indicated a larger number of birds migrating over the Baltic Sea each spring and fall (OREJAS et al. 2005; BELLEBAUM et al. 2010; BSH 2014, 2015). This could result in higher mean migration intensities in the Baltic region compared to the North Sea. The multi-year, multi-site data available for this study gave us the opportunity to test this hypothesis. Comparing simultaneously conducted recordings of call rates revealed systematic differences between sites in the North and Baltic Sea for some species. In line with the prediction, call rates of the thrush species, the Robin and Skylark were significantly higher in the Baltic. Differences were consistent in both spring and fall and held when only data within the same developmental stage of the wind farms was used. In contrast, call rates of Common Sandpiper, Meadow Pipit and Starling did not differ systematically between the two regions. Dunlin was the only species that showed a tendency for higher call rates in the North Sea.

These differences could be related to inter-specific differences in migration routes. For example, Starlings are known to winter in increasing numbers in the British Isles (BAIRLEIN et al. 2014) which

may lead to a high number of these birds crossing the southern North Sea in easterly and westerly direction in spring and fall, respectively. Dunlins use the Waddensea as an important staging area (see above). High call rates of this species may be related to some extent to movements between those areas. However, the lack of difference between North and Baltic Sea in some species could be associated with call rates of these species being to a larger degree affected by factors other than migration intensity (see above).

It is often assumed that within the German EEZ of the North Sea migration intensities of nocturnal migrants decrease with increasing distance to shore. While for diurnal migration there is evidence that migration intensities along the coast are usually higher than at offshore locations for most species (e.g. Heligoland, HÜPPOP et al. 2009), due to a paucity of data this hypothesis has rarely been tested for nocturnal migration (JELLMANN 1977; KNUST et al. 2003; BSH 2015).

Our study shows ambiguous results with respect to a gradient in call rates within the German Bight. For fall migration, data of all species groups supported the notion of decreasing call intensities with increasing distance to shore although the strength of the relationship was slight in some species. In spring, however, thrushes showed an opposite gradient with increasing call rates with increasing distance to shore. Results for waders did not indicate the existence of a gradient in spring while the data of the passerine species Robin, Skylark, Meadow Pipit and Starling suggested a similar gradient in spring as in fall. Consequently, our data suggest that there is no universal gradient in migration intensities within the German Bight. Instead, spatial patterns of migration in the North Sea may be species specific and may differ between the spring and fall migration periods perhaps reflecting different seasonal migration strategies. However, it also needs to be noted that in all cases distance to shore explained only a small proportion of the variance indicating that other factors played a more important role than distance to shore.

5.5 Weather models

We used in-situ weather data collected directly at the sites of the bird observations. In comparison to reanalysis datasets (e.g. HIRLAM or NECP) that are often used when no local weather information is available (HÜPPOP & HILGERLOH 2012; KEMP 2012) in-situ data better reflects local conditions especially for factors like cloud cover or precipitation that are known to vary locally to a large extent and are less well predicted by reanalysis data. However, direct weather observations by bird observers may have several disadvantages. First, several atmospheric parameters like barometric pressure and humidity that are known to be important variables explaining variability in migration intensities (GEIL et al. 1974; ZEHNDER et al. 2001; VAN BELLE et al. 2007) or call rates (HÜPPOP & HILGERLOH 2012) were not available to us. Second, instruments used to record weather parameters on board of the ships are likely to be less precise and less well calibrated than those used by professional weather stations. For example, this resulted also data on wind components to be divided in only eight categories. Finally, due to missing values not all bird observations could be included in the analyses.

However, even without potentially important variables and with less precise measurements, model performance was comparable to previous studies on radar data or call rates (ZEHNDER et al. 2001; ERNI et al. 2002; VAN BELLE et al. 2007; HÜPPOP & HILGERLOH 2012). This also suggests that additional sources of error in our multi-year, multi-site data such as the involvement of different

labs and a large number of individual observers in data collection were either well accounted for in the models (labs) or were only of minor importance.

As our data were strongly right-skewed parametric models such as GLM or GAM which have often been used when investigating the relationship between bird migration and atmospheric parameters were not suitable for this study. In contrast to many linear regression models, random forest regressions can handle noisy and correlated variables and is robust to overfitting (Fox et al. 2017). In addition, this approach captures very well non-linear relationships. Due to the large size of our dataset, random forest models yielded clear and distinct functional relationships between call rates and meteorological and time-related variables that allowed us to identify seasonal and species-specific differences for some of the most common nocturnal migrants in the German EEZ.

Call rates increased in the course of the night in nearly all species and seasons. Maximum call intensities were usually reached shortly before dawn. The onset of this increase differed between species. For example, while in Blackbird, Song Thrush and Robin call rates increased well before midnight, this increase was shifted to around midnight (e.g. Starling, Fieldfare) or to the hours before dawn (e.g. Skylark) in other species. Our results for thrushes are in close accordance to findings of HÜPPOP & HILGERLOH (2012) from an offshore site in the south-eastern North Sea (FINO1). Most nocturnal migrants are thought to commence migration at or shortly after sunset. For thrushes, mean departure time was about ½ h after sunset at a location in southern Sweden (ALERSTAM 1976). The delayed onset of call recordings in our data could partly be related to the offshore location of the study sites. The minimum distance to shore varied between 30 and 120 km for our study sites. Assuming a flight speed of approx. 12 m/s (43.2 km/h; BRUDERER 1997b; LIECHTI & BRUDERER 1998) the earliest nocturnal migrants cannot be expected before 1-3 h after sunset at these locations. However, the high and often increasing number of calls after midnight that have been reported in several studies (GRABER 1968; FARNSWORTH et al. 2004; HÜPPOP & HILGERLOH 2012) are at odds with the general temporal pattern of nocturnal migration. Many studies have shown that migration intensities usually peak before midnight and decrease in the second part of the night (ALERSTAM 1976; ZEHNDER et al. 2001; FARNSWORTH et al. 2004; KEMP 2012). It has been suggested that the temporal pattern of flight calls may be related to decreasing flight altitudes after midnight or may reflect behavioral changes as birds may be in search for stop-over sites at the end of the night (HÜPPOP & HILGERLOH 2012).

Species-specific differences in the temporal pattern may reflect differences in migration strategies. The late and very steep increase of call rates at the end of the night in e.g. Starling, Fieldfare and Skylark may be related to differences in temporal migration patterns of these species which are not strictly nocturnal migrants but migrate to a varying degree also during the day. This is also the likely explanation for the U-shaped pattern found in the Meadow pipit that preferentially migrates during the day.

Overall, TWC was the most important atmospheric variable in our analyses. With only few exceptions our results show that call rates increased sharply with supporting winds. Call intensities were up to 10 times higher with tailwinds compared to headwinds. While in fall call rates already increased at mild headwinds (starting at approx. -5 m/s TWC), in spring this increase usually occurred at positive TWC values (tailwind). It has been suggested that during fall birds might accept slightly unfavorable wind conditions as due to predominating westerly and southwesterly winds in north and central Europe favorable winds do not occur often and costs of delaying migration might exceed costs of accepting moderate headwinds (KARLSSON et al. 2011; HÜPPOP & HILGERLOH

2012). Nocturnally migrating passerines are thought to be able to compensate completely for wind drift up to 4-5 m/s (BRUDERER et al. 1989; ZEHNDER et al. 2001; ÅKESSON et al. 2002). This corresponds well with increasing call rates at TWC > -5 m/s in our study suggesting that birds may be hesitant to cross open water at wind conditions for which they may not be able to fully compensate.

Higher selectivity for favorable winds in spring indicates that birds can be more “picky” as favorable winds occur more often in that season. In several models a steep increase of call rates was found at a TWC of 10 m/s. The air speed of nocturnally migrating passerines in calm conditions has been estimated at 12 m/s (BRUDERER 1997b). This may indicate that, if possible, birds select wind conditions that compensate completely for the aerodynamic drag of their active flight.

Changes in TWC (δ TWC) were of less importance. The strongest relationship was found in the Robin where higher call rates were recorded with increasing TWC and also with decreasing TWC. This suggests that more calls were recorded when wind conditions improved substantially but also when wind conditions deteriorated. This pattern has been related to changing conditions in the course of the night. Birds may commence migration under favorable conditions but may encounter deteriorating conditions while at sea forcing them to reduce flight height and hence get recorded more frequently at sea level (HÜPPOP & HILGERLOH 2012). However, our results do not indicate that this is a regularly occurring phenomenon as otherwise we would expect a negative relationship with δ TWC or TWC more often in our data.

In comparison to TWC the effect of CWC was less pronounced and more variable among species. However, species for which CWC was an important predictor variable of call rates consistently showed a negative relationship in spring and a positive relationship in fall. In most cases a steep increase or decrease of call rates occurred at CWC of 0 m/s in spring and fall, respectively, indicating higher call rates with seaward crosswinds (southeasterly winds) in both seasons. Higher call rates with seaward crosswinds are probably a consequence of wind drift which is assumed to happen more often in nocturnal than diurnal migrants (LIECHTI 2006).

It has to be noted that the effect of wind components hinges crucially on the main migration direction assumed. We generally assumed a southwesterly migration (225°) in fall and a northeasterly direction (45°) in spring. We are aware that this is a somewhat rough estimation with different species presumably deviating from this assumption to a varying degree (BAIRLEIN et al. 2014). We also assumed similar migration directions for the North and Baltic Sea although it is likely that differences occur. We chose this approach because in-situ wind data was collected on the scale of cardinal and ordinal wind directions (i.e. 8 categorical directions) and hence both variables were on a comparable scale. It is likely that that fine-scale information on wind direction and migration direction would have increased the explanatory power of our models (KEMP 2012). A poor approximation of the actual migration direction might have contributed to the limited model performance, particularly with respect to the wind components, in some species (e.g. Common Sandpiper, Dunlin, Starling).

The relationship between cloud cover and call rates was consistent between species but differed between seasons. In spring, call rates were low with partly cloudy and clear skies and increased steeply with increasing cloud cover. In contrast, the relationship was U-shaped in fall indicating high call intensities also when skies were cloudless. Several studies have suggested that call rates

may be directly affected by cloud cover, ceiling height and humidity (GRABER & COCHRAN 1960; GRABER 1968; FARNSWORTH 2005; HÜPPOP & HILGERLOH 2012). In addition, when visibility is low birds may get attracted to sources of artificial light and hence may be recorded disproportionately at the observation platforms (EVANS OGDEN 1996; KERLINGER et al. 2010; VAN DOREN et al. 2017). Complete cloud cover particularly in combination with low ceiling height is known to reduce flight altitude in nocturnal migrants which increases detectability of call rates. Hence higher call rates may not only be related to higher call activity itself but also to a larger number of birds aloft at low altitudes. This is supported by the U-shaped relationship in fall suggesting high call rates during clear conditions. Clear skies enhance orientation capabilities of nocturnal migrants and hence are usually associated with higher migration intensities (BERTHOLD 2000). The fact that call rates remained low with clear skies in spring may reflect difference in flight heights between seasons. As birds usually migrate at higher altitudes in spring they are likely to fly outside the detection range for flight calls in that season.

Precipitation had only a minor effect on call rates overall. When it was included in the model, the relationship of call rates with rain was positive. This contrasts with several studies investigating the effect of rain on nocturnal migration intensities. These studies usually report a negative relationship (ERNI et al. 2002; VAN BELLE et al. 2007). However, similar to cloud cover and low cloud ceiling, precipitation may increase call activity itself (GRABER & COCHRAN 1960; DIERSCHKE 1989) as well as forcing birds to descend to lower altitudes.

Ambient temperature was an important predictor in most models yet the relationship varied to some extent between species and seasons. Considering the interaction between ambient temperature and Julian day some general patterns emerged. In spring, call rates mostly increased at higher ambient temperatures and this effect was often more pronounced during the early part of the season. This suggests that the timing of spring migration, particularly the onset of migration, was contingent on temperature being sufficiently high (e.g. approx. 5-7°C in Fieldfare and Redwing). Contrary, in fall high call rates at the beginning of the season depended on low ambient temperatures (e.g. Blackbird, Fieldfare). The opposite pattern was evident at the end of the fall season when high call rates occurred only when temperature was still high (Robin, Fieldfare). Thus, low temperatures advanced the onset of fall migration while high temperatures deferred the end of it. These results correspond well with a number of studies that showed a strong dependency of migration phenology on temperature particularly with respect to directional changes due to climate change (HÜPPOP & HÜPPOP 2003; LEHIKOINEN et al. 2004; JONZÉN et al. 2006).

In summary, the opportunity to combine flight call data from a number of sites and years led to new insights in the temporal and spatial patterns of nocturnal migration in the German EEZ and corroborated some previous results. We could demonstrate that call rates vary considerably in space and time. Despite the general concept of broad front migration, the spatial correlation of call rates deteriorated already at a scale of 50-100 km distance between sites. Our results also suggest that events of mass migration do not necessarily occur uniformly at the scale of the North Sea or even the whole German EEZ but may usually be a more localized event. Our data support the notion of higher migration intensities of many passerine species in the Baltic but results were ambiguous with respect to a general gradient with distance to shore in the North Sea. Finally, high call rates were related to unfavorable flight conditions (overcast skies, crosswind, rain) but also to favorable conditions (tailwind, clear skies) indicating that call rates are not necessarily a good indicator of situations with an increased collision risk of nocturnal migrants at offshore structures.

6 LITERATURE

- ÅKESSON, S., WALINDER, G., KARLSSON, L. & EHNBOOM, S. (2002): Nocturnal migratory flight initiation in reed warblers *Acrocephalus scirpaceus*: effect of wind on orientation and timing of migration. *Journal of Avian Biology* 33/4, S: 349–357.
- ALERSTAM, T. (1976): Nocturnal migration of thrushes (*Turdus spp.*) in southern Sweden. *Oikos* 27, S: 457–475.
- ARCHER, K. J. & KIMES, R. V. (2008): Empirical characterization of random forest variable importance measures. *Computational Statistics & Data Analysis* 52/4, S: 2249–2260.
- AVERY, M., SPRINGER, P. F. & CASSEL, J. F. (1977): Weather influences on nocturnal bird mortality at a North Dakota tower. *The Wilson Bulletin* 89/2, S: 291–299.
- BAIRLEIN, F., DIERSCHKE, J., DIERSCHKE, V., SALEWSKI, V., GEITER, O., HÜPPOP, K., KÖPPEN, U. & FIEDLER, W. (2014): Atlas des Vogelzugs: Ringfunde deutscher Brut- und Gastvögel. Aula-Verlag.
- BELLEBAUM, J., GRIEGER, C., KLEIN, R., KÖPPEN, U., KUBE, J., NEUMANN, R., SCHULZ, A., SORDYL, H. & WENDELN, H. (2010): Ermittlung artbezogener Erheblichkeitsschwellen von Zugvögeln für das Seegebiet der südwestlichen Ostsee bezüglich der Gefährdung des Vogelzuges im Zusammenhang mit dem Kollisionsrisiko an Windenergieanlagen. Abschlussbericht, Forschungsvorhaben des Bundesministeriums für Umwelt, Naturschutz und Reaktorsicherheit (FKZ 0329948). IfaÖ, LUNG MV/Neu Broderstorf (DEU), S: 333.
- BERTHOLD, P. (2000): Vogelzug. Eine aktuelle Gesamtübersicht. (4., stark überarb. und erw. Aufl. Auflage). Wissenschaftliche Buchgesellschaft/Darmstadt, 280 Seiten. ISBN: 978-3-534-13656-8.
- BERTHOLD, P., GWINNER, E. & SONNENSCHNEIN, E. (Hrsg.) (2003): Avian migration. Springer/Berlin, Heidelberg & New York, 610 Seiten.
- BREIMAN, L. (2001): Random forests. *Machine learning* 45/1, S: 5–32.
- BRUDERER, B. (1997a): The study of bird migration by radar. Part 1: The technical basis. *Naturwissenschaften* 84/1, S: 1–8.
- BRUDERER, B. (1997b): The study of bird migration by radar. Part 2: Major achievements. *Naturwissenschaften* 84/2, S: 45–54.
- BRUDERER, B. & LIECHTI, F. (1998): Flight behaviour of nocturnally migrating birds in coastal areas - crossing or coasting. *Journal of Avian Biology* 29/4, S: 499–507.
- BRUDERER, B., LIECHTI, F. & ERICH, D. (1989): Radarbeobachtungen über den herbstlichen Vogelzug in Süddeutschland. *Vogel und Luftverkehr* 9, S: 174–194.
- BUNDESAMT FÜR SEESCHIFFFAHRT UND HYDROGRAPHIE (Hrsg.) - **BSH** (2013): Standard - Untersuchung der Auswirkungen von Offshore-Windenergieanlagen auf die Meeresumwelt (StUK 4). Hamburg & Rostock (DEU), 86 Seiten.
- BUNDESAMT FÜR SEESCHIFFFAHRT UND HYDROGRAPHIE (Hrsg.) - **BSH** (2014): Bundesfachplan Offshore für die deutsche ausschließliche Wirtschaftszone der Ostsee 2013 und Umweltbericht. Nr. 7602, Hamburg & Rostock (DEU), S: 225.
- BUNDESAMT FÜR SEESCHIFFFAHRT UND HYDROGRAPHIE (Hrsg.) - **BSH** (2015): Bundesfachplan Offshore für die deutsche ausschließliche Wirtschaftszone der Nordsee 2013/2014 und Umweltbericht. Nr. 7603, Hamburg & Rostock (DEU), S: 195.
- CRISCI, C., GHATTAS, B. & PERERA, G. (2012): A review of supervised machine learning algorithms and their applications to ecological data. *Ecological Modelling* 240, S: 113–122.
- CUTLER, D. R., EDWARDS JR, T. C., BEARD, K. H., CUTLER, A., HESS, K. T., GIBSON, J. & LAWLER, J. J. (2007): Random forests for classification in ecology. *Ecology* 88/11, S: 2783–2792.
- DIERSCHKE, V. (1989): Automatisch-akustische Erfassung des nächtlichen Vogelzuges bei Helgoland im Sommer 1987. *Vogelwarte* 35/1989, S: 115–131.
- DIERSCHKE, J., DIERSCHKE, V., HÜPPOP, K., HÜPPOP, O. & JACHMANN, K. F. (2011): Die Vogelwelt der Insel Helgoland. (1. Auflage). Druckwerkstatt Schmittstraße/Helgoland (DEU), 632 Seiten.

- DIERSCHKE, V., FURNESS, R. W. & GARTHE, S. (2016): Seabirds and offshore wind farms in European waters: Avoidance and attraction. *Biological Conservation* 202, S: 59–68.
- DREWITT, A. L. & LANGSTON, R. H. . (2006): Assessing the impacts of wind farms on birds. *Ibis* 148, S: 29–42.
- EASTWOOD, E. (1967): Radar ornithology. Methuen & Co Ltd./London (GBR), 278 Seiten.
- ERNI, B., LIECHTI, F., UNDERHILL, L. G. & BRUDERER, B. (2002): Wind and rain govern the intensity of nocturnal bird migration in central Europe - a log-linear regression analysis. *Ardea* 90/1, S: 155–166.
- EVANS, J. S. & MURPHY, M. A. (2018): rfUtilities, R package version 2.1-3.
- EVANS OGDEN, L. J. (1996): Collision course: the hazards of lighted structures and windows to migrating birds. World Wildlife Fund Canada & Fatal Light Awareness Programm/Ontario (CAN).
- FARNSWORTH, A. (2005): Flight calls and their value for future ornithological studies and conservation research. *The Auk* 122/3, S: 733–746.
- FARNSWORTH, A. (2007): Flight calls of wood-warblers are not exclusively associated with migratory behaviors. *The Wilson Journal of Ornithology* 119/3, S: 334–341.
- FARNSWORTH, A., GAUTHREAUX, JR., S. A. & VAN BLARICOM, D. (2004): A comparison of nocturnal call counts of migrating birds and reflectivity measurements on Doppler radar. *Journal of Avian Biology* 35/4, S: 365–369.
- FOX, E. W., HILL, R. A., LEIBOWITZ, S. G., OLSEN, A. R., THORNBRUGH, D. J. & WEBER, M. H. (2017): Assessing the accuracy and stability of variable selection methods for random forest modeling in ecology. *Environmental monitoring and assessment* 189/7, S: 316.
- GEHRING, J., KERLINGER, P. & MANVILLE, A. M. (2009): Communication towers, lights, and birds: successful methods of reducing the frequency of avian collisions. *Ecological Applications* 19/2, S: 505–514.
- GEIL, S., NOER, H. & RABØL, J. (1974): Forecast models for bird migration in Denmark. *Report published by Bird Strike Committee Denmark*.
- GESICKI, D. V., JAMALI, M. M. & BINGMAN, V. P. (2016): Coastal and offshore counts of migratory sparrows and warblers as revealed by recordings of nocturnal flight calls along the Ohio coast of Lake Erie. *The Wilson Journal of Ornithology* 128/3, S: 503–509.
- GRABER, R. R. (1968): Nocturnal migration in Illinois: different points of view. *The Wilson Bulletin* 80/1, S: 36–71.
- GRABER, R. R. & COCHRAN, W. W. (1960): Evaluation of an aural record of nocturnal migration. *The Wilson Bulletin* 72/3, S: 253–273.
- GREEN, M. (2004): Flying with the wind-spring migration of Arctic-breeding waders and geese over South Sweden. *Ardea* 92/2, S: 145–159.
- GRÜNKORN, T., BLEW, J., COPPACK, T., KRÜGER, O., NEHLS, G., POTIEK, A., REICHENBACH, M., VON RÖNN, J., TIMMERMANN, H. & WEITEKAMP, S. (2016): Ermittlung der Kollisionsraten von (Greif-)Vögeln und Schaffung planungsbezogener Grundlagen für die Prognose und Bewertung des Kollisionsrisikos durch Windenergieanlagen (PROGRESS). Schlussbericht zum durch das Bundesministerium für Wirtschaft und Energie (BMWi) im Rahmen des 6. Energieforschungsprogrammes der Bundesregierung geförderten Verbundvorhaben PROGRESS, FKZ 0325300A-D. S: 332.
- HILL, R. & HÜPPOP, O. (2008): Birds and bats: automatic recording of flight calls and their value for the study of migration. *BfN-Skripten* 234, S: 135–141.
- HORTON, K. G., SHRIVER, W. G. & BULER, J. J. (2015a): A comparison of traffic estimates of nocturnal flying animals using radar, thermal imaging, and acoustic recording. *Ecological Applications* 25/2, S: 390–401.
- HORTON, K. G., STEPANIAN, P. M., WAINWRIGHT, C. E. & TEGELER, A. K. (2015b): Influence of atmospheric properties on detection of wood-warbler nocturnal flight calls. *International Journal of Biometeorology* 59/10, S: 1385–1394.
- HÜPPOP, O., DIERSCHKE, J., EXO, K. M., FREDRICH, E. & HILL, R. (2006): Bird migration studies and potential collision risk with offshore wind turbines. *Ibis* 148/s1, S: 90–109.

- HÜPPOP, K., DIERSCHKE, J., HILL, R. & HÜPPOP, O. (2012): Jahres- und tageszeitliche Phänologie der Vogelrufaktivität über der Deutschen Bucht. *Vogelwarte* 50/2, S: 87–108.
- HÜPPOP, O. & HILGERLOH, G. (2012): Flight call rates of migrating thrushes: effects of wind conditions, humidity and time of day at an illuminated offshore platform. *Journal of Avian Biology* 43/1, S: 85–90.
- HÜPPOP, O., HILL, R., HÜPPOP, K. & JACHMANN, F. (2009): Auswirkungen auf den Vogelzug - Begleitforschung im Offshore-Bereich auf Forschungsplattformen in der Nordsee (FINOBIRD), Abschlussbericht. Institut für Vogelforschung „Vogelwarte Helgoland“/Helgoland (DEU), S: 278.
- HÜPPOP, O. & HÜPPOP, K. (2003): North Atlantic Oscillation and timing of spring migration in birds. *Proceedings of the Royal Society of London B: Biological Sciences* 270/1512, S: 233–240.
- HÜPPOP, O., HÜPPOP, K., DIERSCHKE, J. & HILL, R. (2016): Bird collisions at an offshore platform in the North Sea. *Bird Study* 63/1, S: 1–10.
- JELLMANN, J. (1977): Radarbeobachtungen zum Frühjahrszug über Nordwestdeutschland und die südliche Nordsee im April und Mai 1971. *Vogelwarte* 29, S: 135–149.
- JONZÉN, N., LINDÉN, A., ERGON, T., KNUDSEN, E., VIK, J. O., RUBOLINI, D., PIACENTINI, D., BRINCH, C., SPINA, F. & KARLSSON, L. (2006): Rapid advance of spring arrival dates in long-distance migratory birds. *Science* 312/5782, S: 1959–1961.
- KARLSSON, H., NILSSON, C., BÄCKMAN, J. & ALERSTAM, T. (2011): Nocturnal passerine migration without tailwind assistance. *Ibis* 153/3, S: 485–493.
- KEMP, M. U. (2012): How birds weather the weather: avian migration in the mid-latitudes (*Disser-tation*). Universiteit van Amsterdam / Amsterdam (NLD), 207 S.
- KERLINGER, P., GEHRING, J. L., ERICKSON, W. P., CURRY, R., JAIN, A. & GUARNACCIA, J. (2010): Night migrant fatalities and obstruction lighting at wind turbines in North America. *The Wilson Journal of Ornithology* 122/4, S: 744–754.
- KNUST, R., DAHLHOFF, P., GABRIEL, J., HEUERS, J., HÜPPOP, O. & WENDELN, H. (2003): Untersuchungen zur Vermeidung und Verminderung von Belastungen der Meeresumwelt durch Offshore-Windenergieanlagen im küstenfernen Bereich der Nord-und Ostsee - Offshore-WEA, Abschlussbericht. Nr. Forschungsbericht 20097106, UBA-FB 000478, Umweltbundesamt/Berlin (DEU), Umweltforschungsplan des Bundesministeriums für Umwelt, Naturschutz und Reaktorsicherheit, S: 603.
- KRIGSVELD, K. L., AKERSHOEK, K., SCHENK, F., DIJK, F. & DIRKSEN, S. (2009): Collision risk of birds with modern large wind turbines. *Ardea* 97/3, S: 357–366.
- LEHIKONEN, E., SPARKS, T. H. & ZALAKEVICIUS, M. (2004): Arrival and departure dates. *Advances in ecological research* 35, S: 1–31.
- LIAW, A. & WIENER, M. (2002): Classification and regression by randomForest. *R news* 2/3, S: 18–22.
- LIECHTI, F. (2006): Birds: blowin' by the wind? *Journal of Ornithology* 147/2, S: 202–211.
- LIECHTI, F. & BRUDERER, B. (1998): The relevance of wind for optimal migration theory. *Journal of Avian Biology* 29, S: 561–568.
- LIECHTI, F., BRUDERER, B. & PAPROTH, H. (1995): Quantification of nocturnal bird migration by moonwatching: Comparison with radar and infrared observations. *Journal of Field Ornithology* 66/4, S: 457–468.
- LONGCORE, T., RICH, C. & GAUTHREUX JR, S. A. (2008): Height, guy wires, and steady-burning lights increase hazard of communication towers to nocturnal migrants: a review and meta-analysis. *The Auk* 125/2, S: 485–492.
- LONGCORE, T., RICH, C., MINEAU, P., MACDONALD, B., BERT, D. G., SULLIVAN, L. M., MUTRIE, E., GAUTHREUX JR, S. A., AVERY, M. L., CRAWFORD, R. L., MANVILLE II, A. M., TRAVIS, E. R. & DRAKE, D. (2012): An estimate of avian mortality at communication towers in the United States and Canada. *PLoS ONE* 7/4, S: e34025.
- MUNDINGER, P. C. (1970): Vocal imitation and individual recognition of finch calls. *Science* 168/3930, S: 480–482.

- OREJAS, C., SCHROEDER, A., JOSCHKO, T., DIERSCHKE, J., EXO, K. M., FRIEDRICH, E., HILL, R., HÜPPOP, O., POLLEHNE, F., ZETTLER, M. L. & BOCHERT, R. (2005): Ökologische Begleitforschung zur Windenergienutzung im Offshore-Bereich auf Forschungsplattformen in der Nord- und Ostsee (BeoFINO), BMU 0327526-Abschlußbericht. Alfred Wegener Institut für Polar- und Meeresforschung/Bremerhaven (DEU), S: 354.
- PRASAD, A. M., IVERSON, L. R. & LIAW, A. (2006): Newer classification and regression tree techniques: bagging and random forests for ecological prediction. *Ecosystems* 9/2, S: 181–199.
- R CORE TEAM (2016): R: A Language and Environment for Statistical Computing. R Foundation for Statistical Computing/Vienna, Austria.
- SANDERS, C. E. & MENNILL, D. J. (2014): Acoustic monitoring of nocturnally migrating birds accurately assesses the timing and magnitude of migration through the Great Lakes. *The Condor* 116/3, S: 371–383.
- SCHULZ, A., DITTMAN, T. & COPPACK, T. (2014): Erfassung von Ausweichbewegungen von Zugvögeln mittels Pencil Beam Radar und Erfassung von Vogelkollisionen mit Hilfe des Systems VARS. StUKplus Schlussbericht. Rostock, Im Auftrag des Bundesamts für Seeschifffahrt und Hydrographie (BSH), S: 89.
- SHAMOUN-BARANES, J., ALVES, J. A., BAUER, S., DOKTER, A. M., HÜPPOP, O., KOISTINEN, J., LEIJNSE, H., LIECHTI, F., VAN GASTEREN, H. & CHAPMAN, J. W. (2014): Continental-scale radar monitoring of the aerial movements of animals. *Movement Ecology* 2/1, S: 9.
- SMITH, A. D., PATON, P. W. & MCWILLIAMS, S. R. (2014): Using nocturnal flight calls to assess the fall migration of warblers and sparrows along a coastal ecological barrier. *PLOS ONE* 9/3, S: e92218.
- STRICKLAND, M., ARNETT, E., ERICKSON, W., JOHNSON, D., JOHNSON, G., MORRISON, M., SHAFFER, J. & WARREN-HICKS, W. (2011): Comprehensive guide to studying wind energy/wildlife interactions. *Prepared for the National Wind Coordinating Collaborative, Washington, DC, USA.*
- TAOKA, M. & OKUMURA, H. (1990): Sexual differences in flight calls and the cue for vocal sex recognition of swinhoe's storm-petrels. *The Condor* 92, S: 571–575.
- VAN BELLE, J., SHAMOUN-BARANES, J., VAN LOON, E. & BOUTEN, W. (2007): An operational model predicting autumn bird migration intensities for flight safety. *Journal of Applied Ecology* 44/4, S: 864–874.
- VAN DOREN, B. M., HORTON, K. G., DOKTER, A. M., KLINCK, H., ELBIN, S. B. & FARNSWORTH, A. (2017): High-intensity urban light installation dramatically alters nocturnal bird migration. *Proceedings of the National Academy of Sciences* 114/42, S: 11175–11180.
- WATSON, M. J., WILSON, D. R. & MENNILL, D. J. (2016): Anthropogenic light is associated with increased vocal activity by nocturnally migrating birds. *The Condor* 118/2, S: 338–344.
- WELCKER, J., LIESENJOHANN, M., BLEW, J., NEHLS, G. & GRÜNKORN, T. (2017): Nocturnal migrants do not incur higher collision risk at wind turbines than diurnally active species. *Ibis* 159/2, S: 366–373.
- WELCKER, J. & NEHLS, G. (2016): Displacement of seabirds by an offshore wind farm in the North Sea. *Marine Ecology Progress Series* 554, S: 173–182.
- ZAUGG, S., SAPORTA, G., VAN LOON, E., SCHMALJOHANN, H. & LIECHTI, F. (2008): Automatic identification of bird targets with radar via patterns produced by wing flapping. *Journal of The Royal Society Interface* 5/26, S: 1041–1053.
- ZEHNDER, S., ÅKESSON, S., LIECHTI, F. & BRUDERER, B. (2001): Nocturnal autumn bird migration at Falsterbo, South Sweden. *Journal of Avian Biology* 32/3, S: 239–248.

A APPENDIX

A.1 Data summary

Tab. A 1 *List of species and number of calls recorded in the time between 2008 and 2015 at 13 locations in the German EEZ of the North and Baltic Sea (see text for details). Species selected for further analyses are shaded in grey.*

species	calls percent	calls total	calls observations only	calls microphones only
Redwing	26.96	141,521	76,010	65,511
Blackbird	26.15	137,270	83,021	54,249
Song Thrush	11.81	62,003	49,179	12,824
Robin	7.13	37,407	35,460	1,947
Starling	4.40	23,118	22,111	1,007
Goldcrest	4.34	22,800	18,853	3,947
Fieldfare	4.19	22,012	9,536	12,476
Skylark	2.76	14,501	13,598	903
Lesser black-backed Gull	1.39	7,317	7,126	191
Common Scoter	0.94	4,939	4,939	0
Brambling	0.65	3,433	1,625	1,808
Eurasian Siskin	0.65	3,412	3,308	104
Common Gull	0.56	2,931	1,176	1,755
Common Chaffinch	0.54	2,843	1,931	912
Green Sandpiper	0.43	2,239	2,187	52
Common Sandpiper	0.37	1,916	1,545	371
Golden Plover	0.35	1,857	1,474	383
Meadow Pipit	0.35	1,823	1,208	615
Dunlin	0.30	1,599	1,477	122
Redshank	0.30	1,577	1,231	346
Oystercatcher	0.28	1,467	1,343	124
Black-headed Gull	0.27	1,438	705	733
Common Reed Bunting	0.27	1,395	942	453
Curlew	0.22	1,143	989	154
Wood Sandpiper	0.20	1,066	1,056	10
Tree Pipit	0.16	833	829	4
Ringed Plover	0.16	830	800	30
Common Tern	0.15	782	770	12
Kittiwake	0.14	759	759	0
Barnacle Goose	0.14	719	718	1
Whimbrel	0.13	672	563	109
Mistle Thrush	0.12	644	526	118
Herring Gull	0.11	580	570	10

species	calls percent	calls total	calls observations only	calls microphones only
Snipe	0.10	543	530	13
Lapwing	0.10	541	392	149
Greenshank	0.09	475	391	84
Bar-tailed Godwit	0.08	441	397	44
Hawfinch	0.08	438	438	0
Dunnock	0.08	418	175	243
Arctic Tern	0.06	314	314	0
Knot	0.05	271	221	50
Sandwich Tern	0.05	263	121	142
Great black-backed Gull	0.05	259	150	109
Waxwing	0.04	226	115	111
Guillemot	0.04	200	130	70
Barn Swallow	0.04	193	41	152
White Wagtail	0.03	176	128	48
Greylag Goose	0.03	169	158	11
Grey Plover	0.03	156	143	13
Common Chiffchaff	0.02	127	78	49
Grey Heron	0.02	126	33	93
Eurasian Teal	0.02	108	96	12
White-fronted Goose	0.02	101	94	7
Mediterranean Gull	0.02	99	0	99
Pink-footed Goose	0.02	96	80	16
Lapland Longspur	0.02	91	90	1
Yellow Wagtail	0.02	82	81	1
Common Crane	0.02	80	80	0
Grey Wagtail	0.01	78	54	24
Purple Sandpiper	0.01	69	60	9
Common Redstart	0.01	60	60	0
Brent Goose	0.01	60	57	3
Black-tailed Godwit	0.01	56	53	3
Sanderling	0.01	54	47	7
Snow Bunting	0.01	51	50	1
Rock Pipit	0.01	48	43	5
Spotted Flycatcher	0.01	44	44	0
Great Tit	0.01	43	40	3
Woodcock	0.01	39	39	0
Willow Warbler	0.01	32	29	3
Black Redstart	0.01	32	29	3
Ring Ouzel	0.01	31	2	29
Pied Flycatcher	0.01	31	31	0
Temminck's Stint	0.01	30	30	0
Winter Wren	0.01	30	5	25
Turnstone	0.01	28	24	4

species	calls percent	calls total	calls observations only	calls microphones only
Wigeon	0.00	26	15	11
Northern Gannet	0.00	25	25	0
Western Jackdaw	0.00	22	2	20
Curlew Sandpiper	0.00	19	18	1
Common Redpoll	0.00	17	12	5
Kentish Plover	0.00	17	17	0
Fulmar	0.00	16	16	0
Wood Pigeon	0.00	16	16	0
Little Stint	0.00	15	13	2
Long-tailed Duck	0.00	14	14	0
Avocet	0.00	14	1	13
Little Gull	0.00	13	13	0
Eurasian Blackcap	0.00	12	12	0
Common Moorhen	0.00	12	0	12
Common Linnet	0.00	10	6	4
Yellow-browed Warbler	0.00	10	0	10
Little Ringed Plover	0.00	9	8	1
Woodlark	0.00	9	7	2
Short-eared Owl	0.00	9	9	0
Spotted Redshank	0.00	8	3	5
Horned Lark	0.00	8	6	2
Great Cormorant	0.00	6	3	3
European Greenfinch	0.00	5	5	0
Whooper Swan	0.00	5	5	0
Yellowhammer	0.00	4	4	0
Tufted Duck	0.00	4	4	0
Pintail	0.00	4	4	0
Caspian Gull	0.00	4	4	0
European Goldfinch	0.00	4	3	1
Mallard	0.00	4	4	0
Eider	0.00	3	3	0
Eurasian Bullfinch	0.00	3	3	0
Icterine Warbler	0.00	2	2	0
Mute Swan	0.00	2	2	0
Ruff	0.00	2	2	0
Northern Wheatear	0.00	2	2	0
Red-throated Diver	0.00	2	2	0
Eurasian Collared Dove	0.00	2	2	0
Water Rail	0.00	2	0	2
Dusky Warbler	0.00	1	0	1
Red-breasted Merganser	0.00	1	1	0
Red-necked Phalarope	0.00	1	1	0
Red-throated Pipit	0.00	1	1	0

species	calls percent	calls total	calls observations only	calls microphones only
Barn Owl	0.00	1	1	0
Sabine's Gull	0.00	1	0	1
Great Skua	0.00	1	1	0
Broad-billed Sandpiper	0.00	1	1	0
Marsh Sandpiper	0.00	1	1	0
Kestrel	0.00	1	1	0
Peregrine	0.00	1	1	0
Little Bunting	0.00	1	0	1
passerine sp.	0.45	2,351	2,262	89
thrush sp.	0.27	1,419	1,190	229
Arctic/Common Tern	0.24	1,277	977	300
unidentified bird	0.19	995	364	631
gull sp.	0.19	974	973	1
large gull sp.	0.13	698	698	0
wader sp.	0.06	299	243	56
Blackbird/Redwing	0.05	287	152	135
tern sp.	0.04	220	215	5
black-backed gull sp.	0.02	96	96	0
duck sp.	0.02	82	62	20
unidentified Fringilla finch	0.01	39	0	39
goose sp.	0.01	33	32	1
plover sp.	0.01	27	27	0
redstart sp.	0.01	27	27	0
unidentified finch	0.00	10	8	2
Razorbill/Guillemot	0.00	8	8	0
unidentified tit	0.00	7	0	7
Whooper/Bewick's Swan	0.00	3	0	3
curlew sp.	0.00	2	2	0
owl sp.	0.00	2	2	0
lark sp.	0.00	2	2	0
pipit sp.	0.00	2	2	0
skua sp.	0.00	2	2	0
Phylloscopus warbler sp.	0.00	1	1	0
diver sp.	0.00	1	1	0
unidentified sandpiper	0.00	1	1	0
Herring/Common Gull	0.00	1	1	0
dove sp.	0.00	1	1	0
TOTAL	100.00	524,895	360,363	164,532

A.2 Spatial correlation of call rates

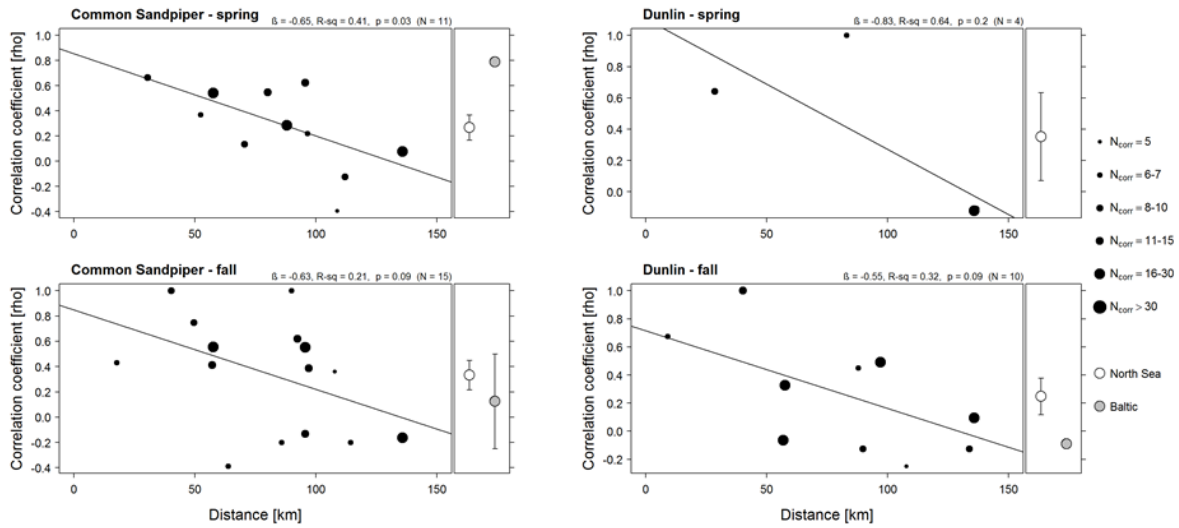


Figure A.1 Relationship between distance between sites and the correlation of call rates (Spearman's rank correlation coefficient rho) of two wader species for spring and fall. For details see Figure 4.5 and Materials & Methods.

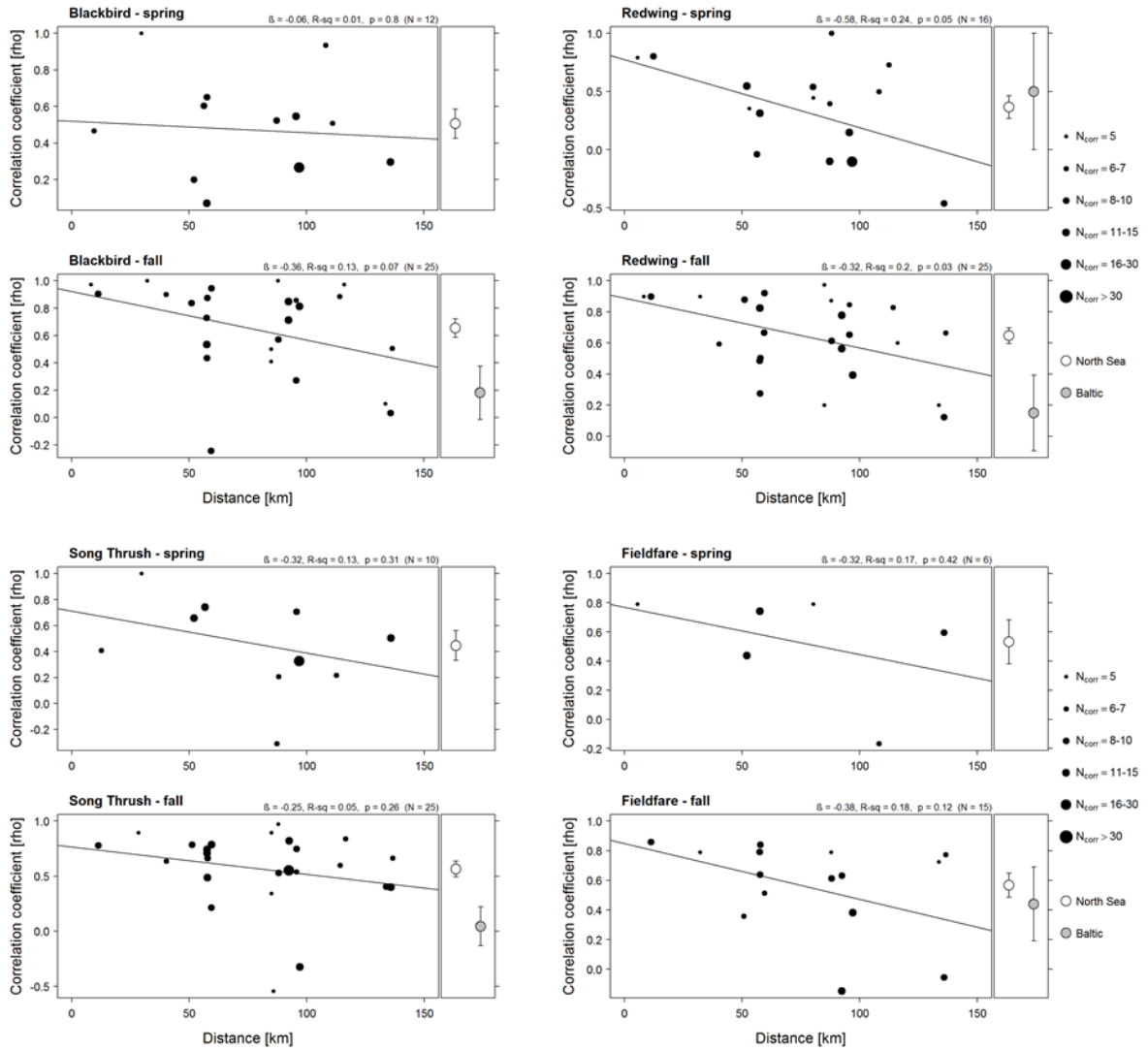


Figure A. 2 Relationship between distance between sites and the correlation of call rates (Spearman's rank correlation coefficient rho) of four thrush species for spring and fall. For details see Figure 4.5 and Materials & Methods.

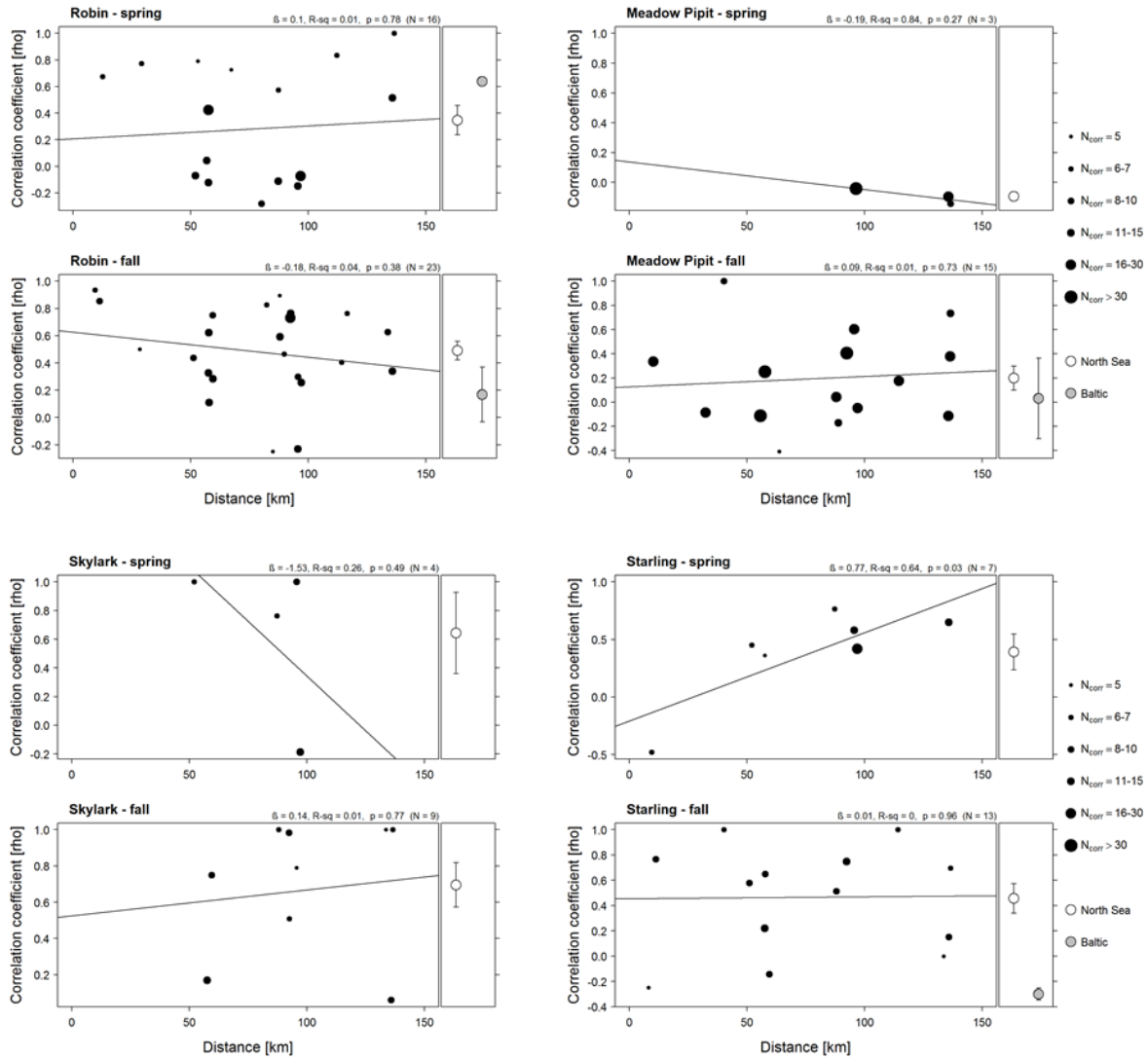


Figure A.3 Relationship between distance between sites and the correlation of call rates (Spearman's rank correlation coefficient rho) of four passerine species for spring and fall. For details see Figure 4.5 and Materials & Methods.

A.3 Spatial gradients

Common Sandpiper

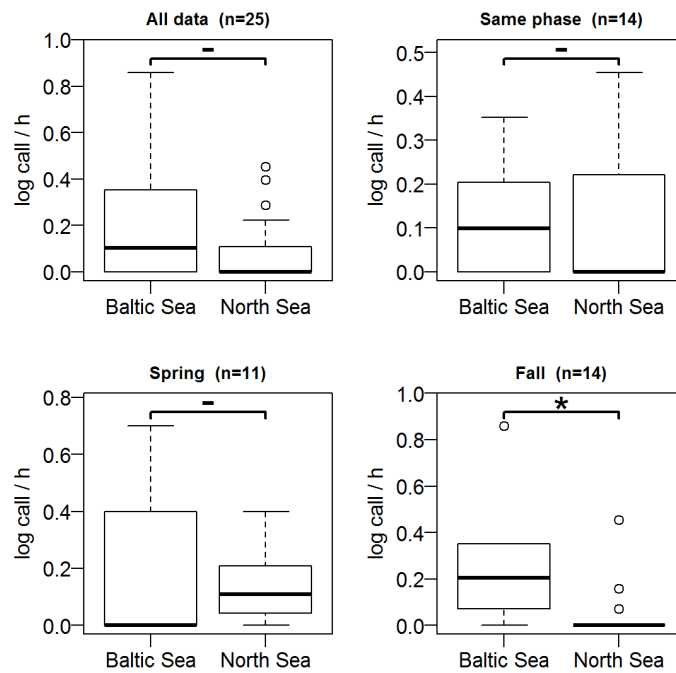


Figure A. 4 Call intensities (calls/h, log transformed) of the Common Sandpiper simultaneously measured in the Baltic and North Sea. See Figure 4.10 for further details.

Dunlin

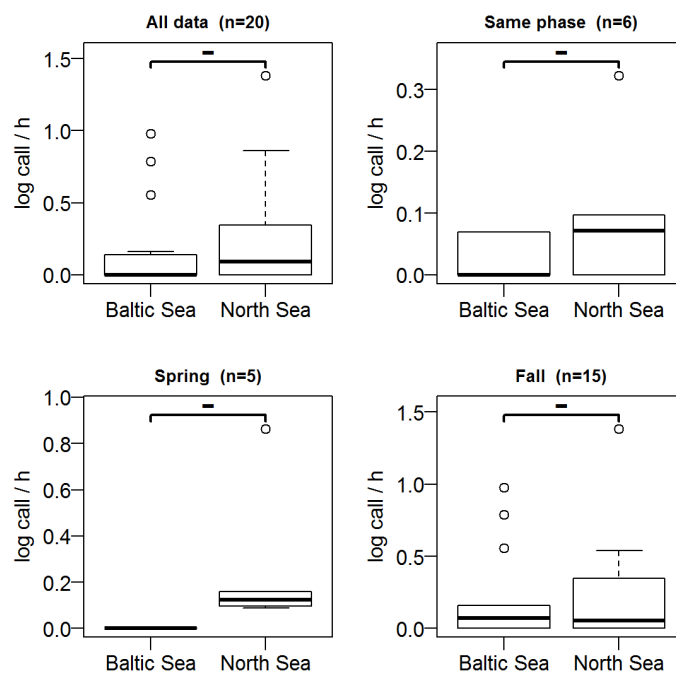


Figure A. 5 Call intensities (calls/h, log transformed) of the Dunlin simultaneously measured in the Baltic and North Sea. See Figure 4.10 for further details.

Blackbird

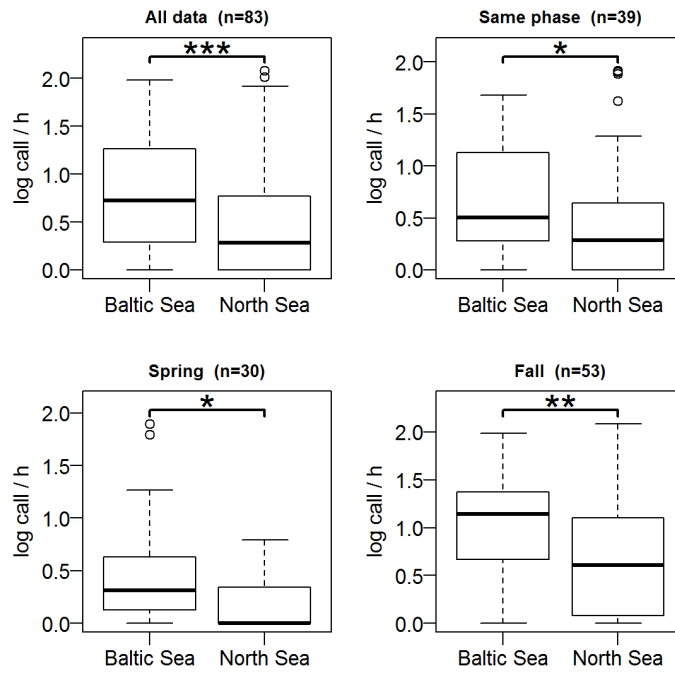


Figure A. 6 Call intensities (calls/h, log transformed) of the Blackbird simultaneously measured in the Baltic and North Sea. See Figure 4.10 for further details.

Redwing

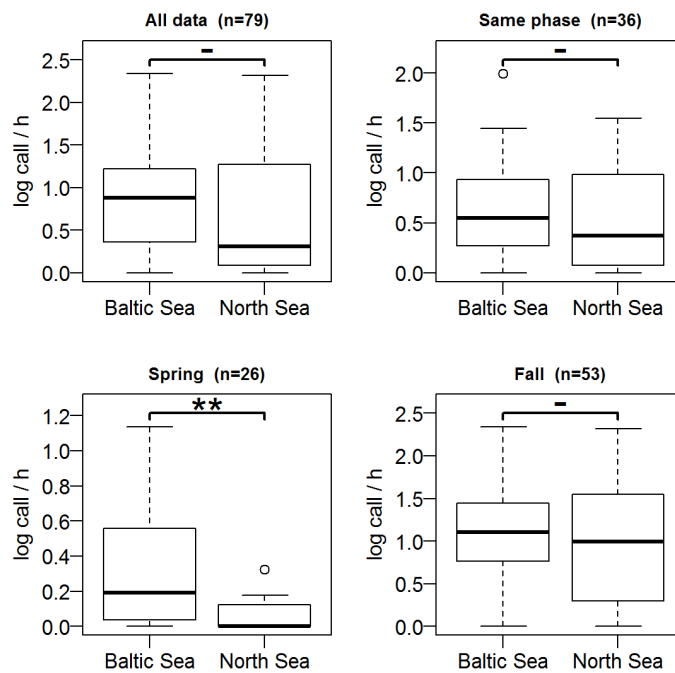


Figure A. 7 Call intensities (calls/h, log transformed) of the Redwing simultaneously measured in the Baltic and North Sea. See Figure 4.10 for further details.

Song Thrush

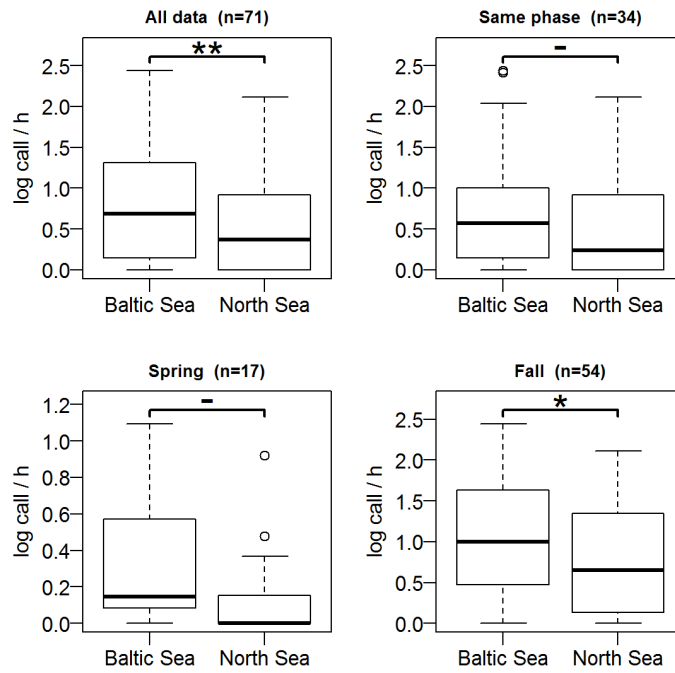


Figure A. 8 Call intensities (calls/h, log transformed) of the Song Thrush simultaneously measured in the Baltic and North Sea. See Figure 4.10 for further details.

Fieldfare

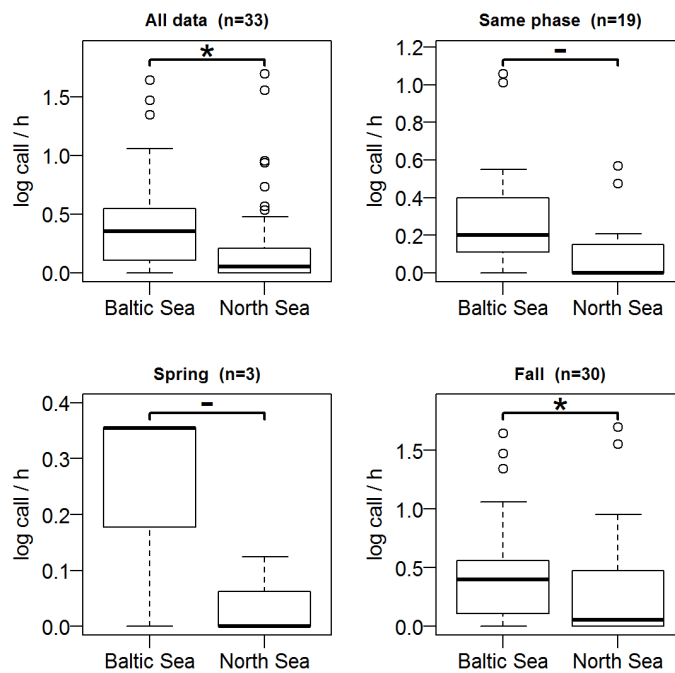


Figure A. 9 Call intensities (calls/h, log transformed) of the Fieldfare simultaneously measured in the Baltic and North Sea. See Figure 4.10 for further details.

Skylark

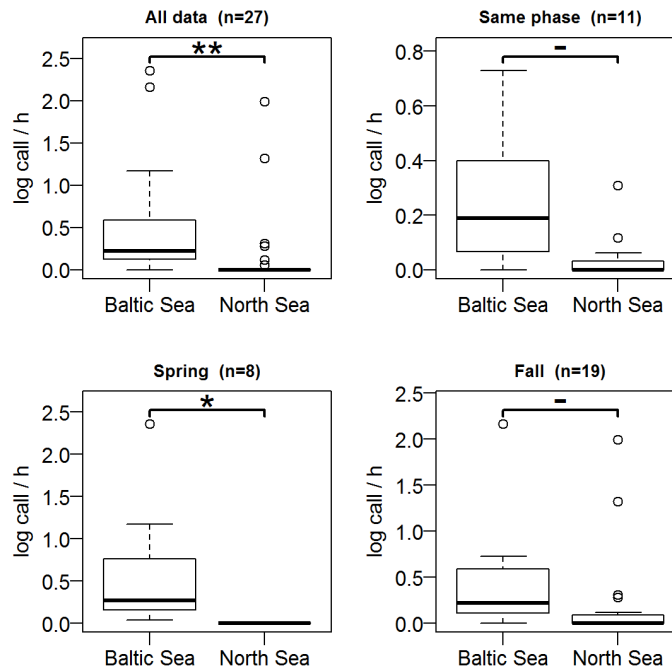


Figure A. 10 Call intensities (calls/h, log transformed) of the Skylark simultaneously measured in the Baltic and North Sea. See Figure 4.10 for further details.

Meadow Pipit

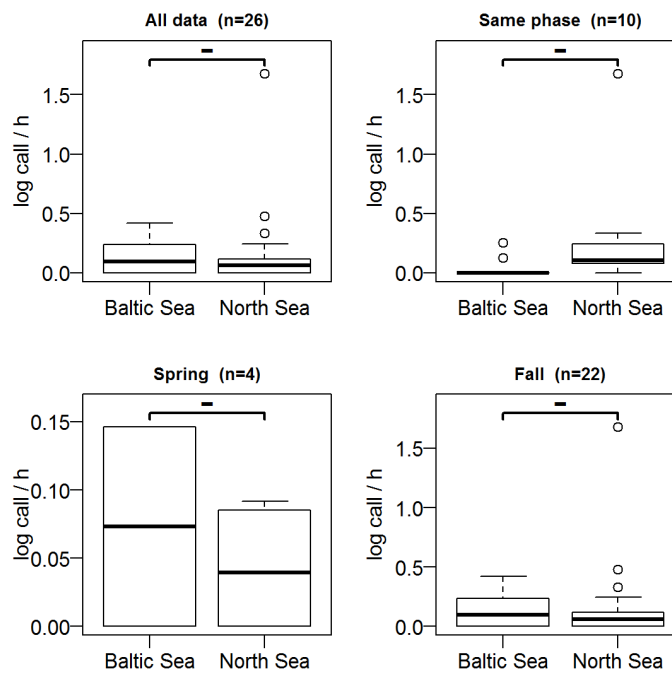


Figure A. 11 Call intensities (calls/h, log transformed) of the Meadow Pipit simultaneously measured in the Baltic and North Sea. See Figure 4.10 for further details.

Robin

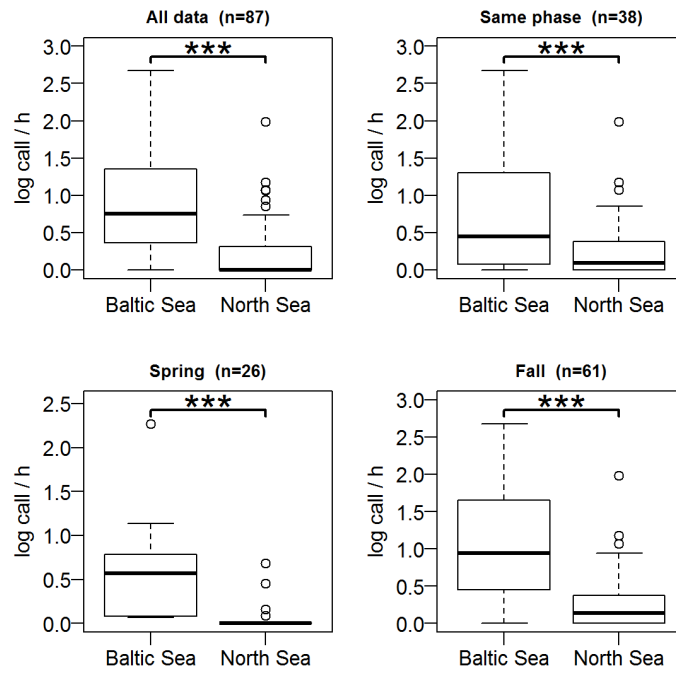


Figure A. 12 Call intensities (calls/h, log transformed) of the Robin simultaneously measured in the Baltic and North Sea. See Figure 4.10 for further details.

Starling

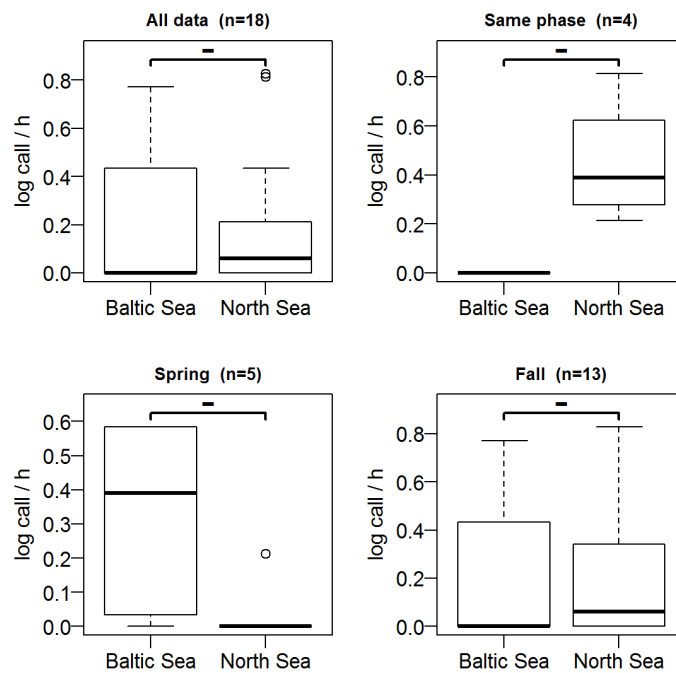


Figure A. 13 Call intensities (calls/h, log transformed) of the Starling simultaneously measured in the Baltic and North Sea. See Figure 4.10 for further details.

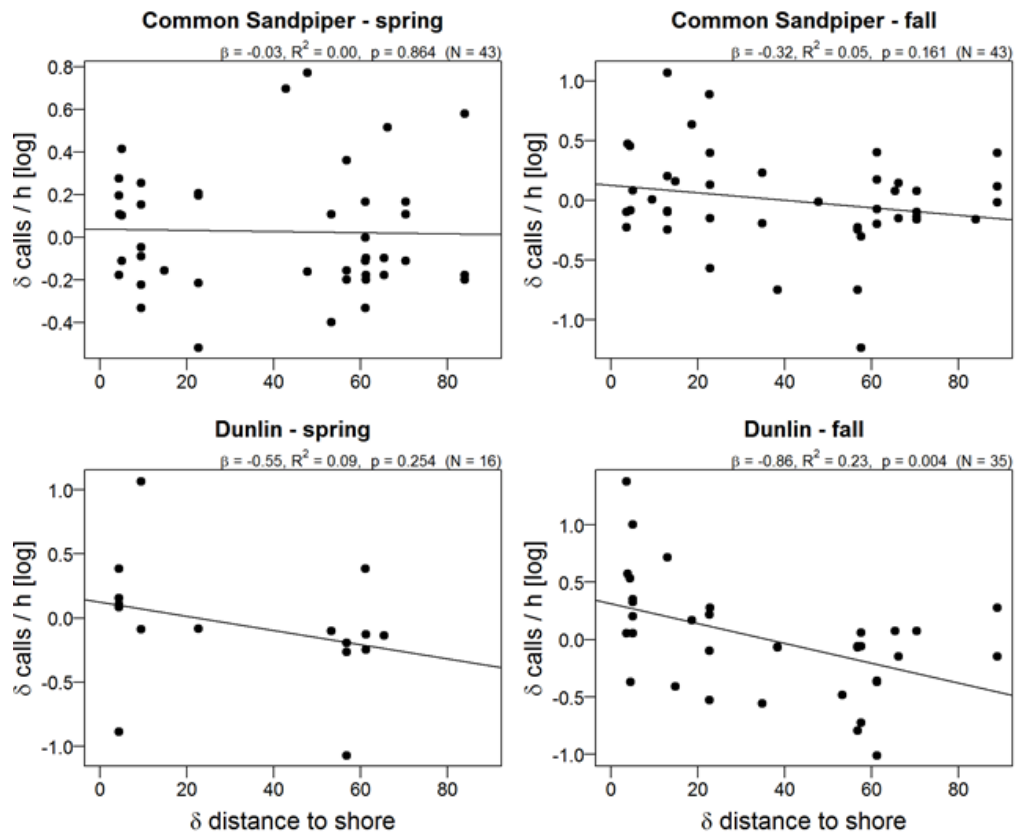


Figure A. 14 Relationship of the difference in call rates between two sites and their difference in distance to shore for Common Sandpiper and Dunlin. The results of a linear regression are given above the plot. Left panel: during spring migration; right panel: during fall migration.

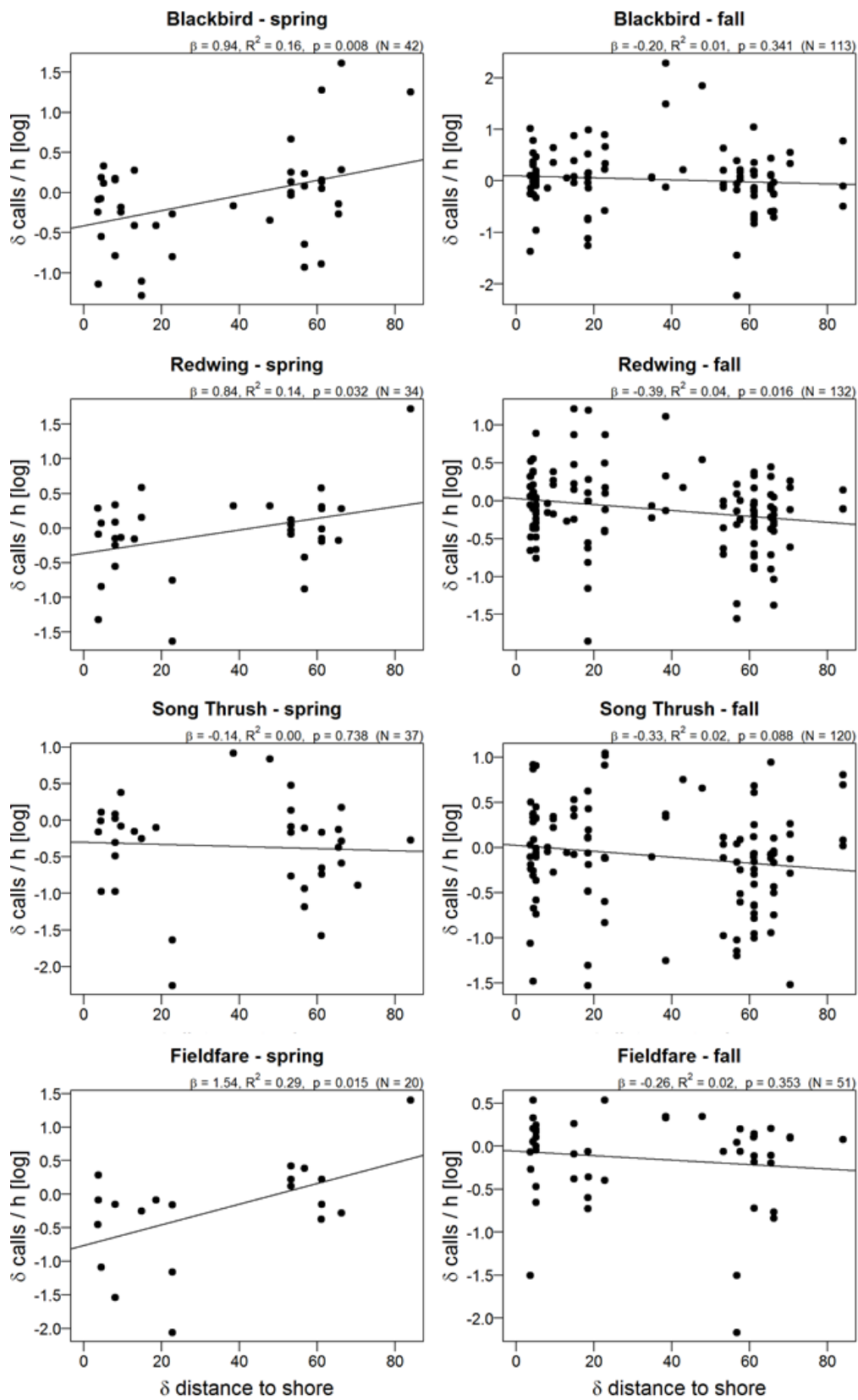


Figure A. 15 Relationship of the difference in call rates between two sites and their difference in distance to shore for Blackbird, Redwing, Song Thrush and Fieldfare. The results of a linear regression are given above the plot. Left panel: during spring migration; right panel: during fall migration.

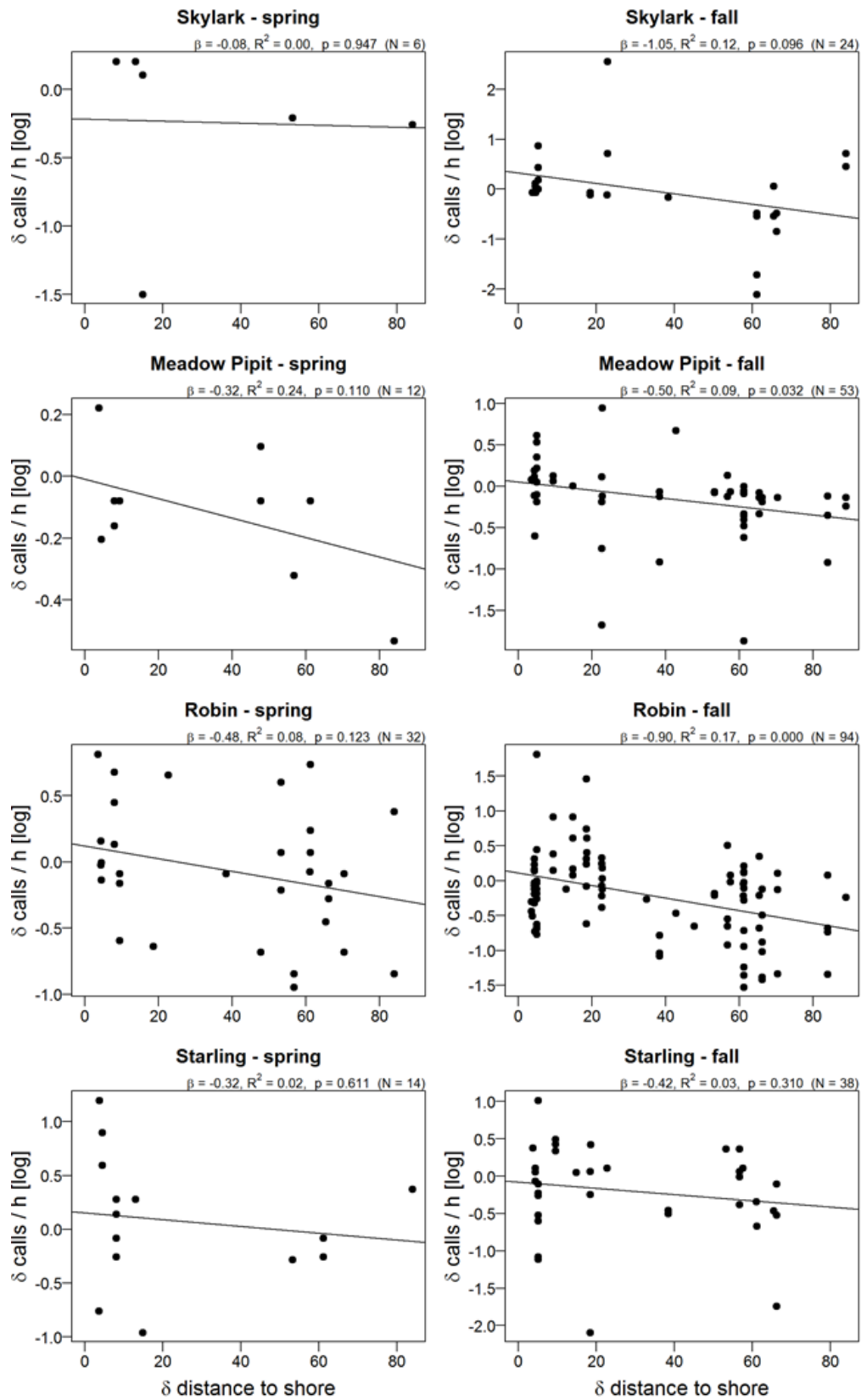


Figure A. 16 Relationship of the difference in call rates between two sites and their difference in distance to shore for Skylark, Meadow Pipit, Robin and Starling. The results of a linear regression are given above the plot. Left panel: during spring migration; right panel: during fall migration.

A.4 Weather models

Common Sandpiper

Spring

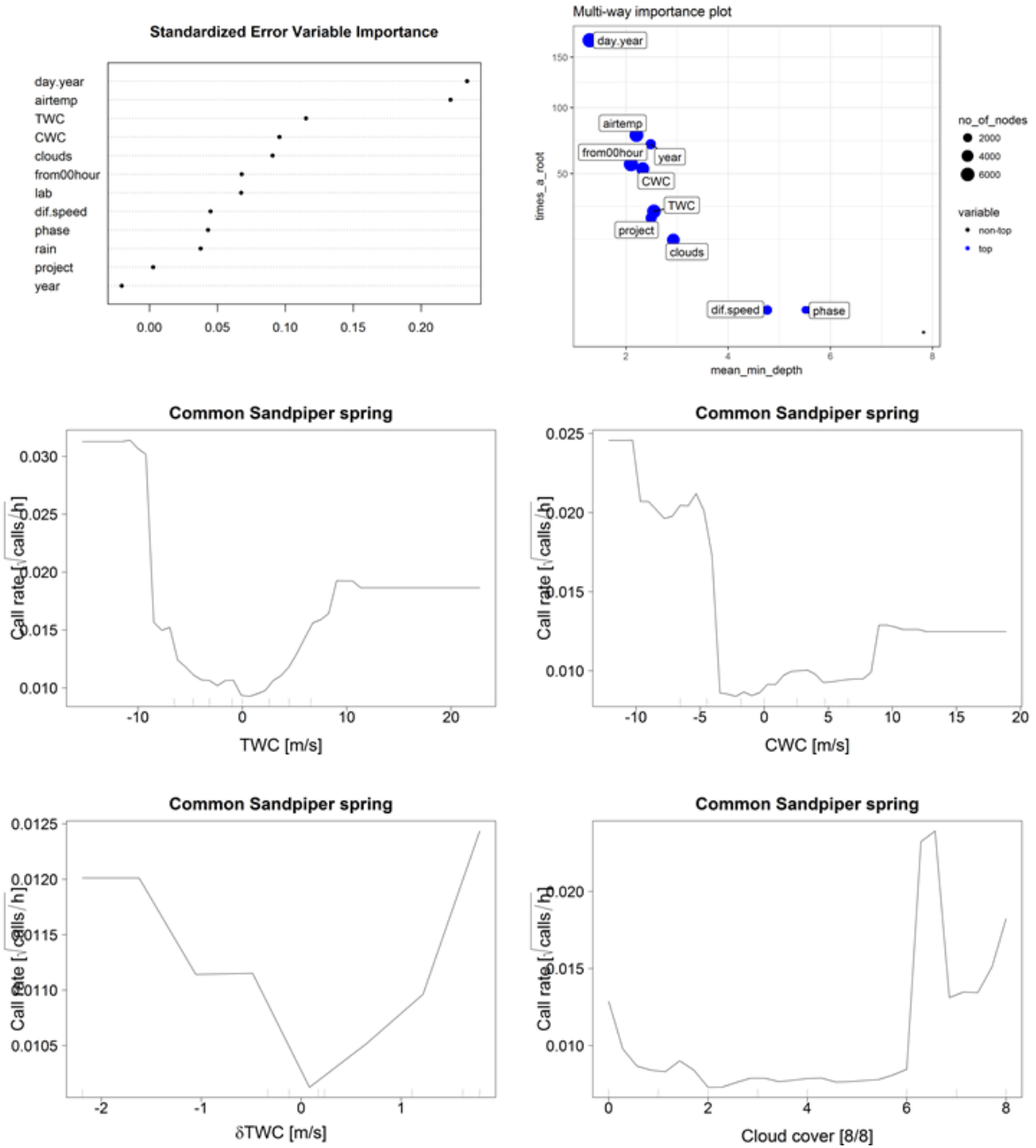


Figure A. 17 Common Sandpiper spring, continued on next page.

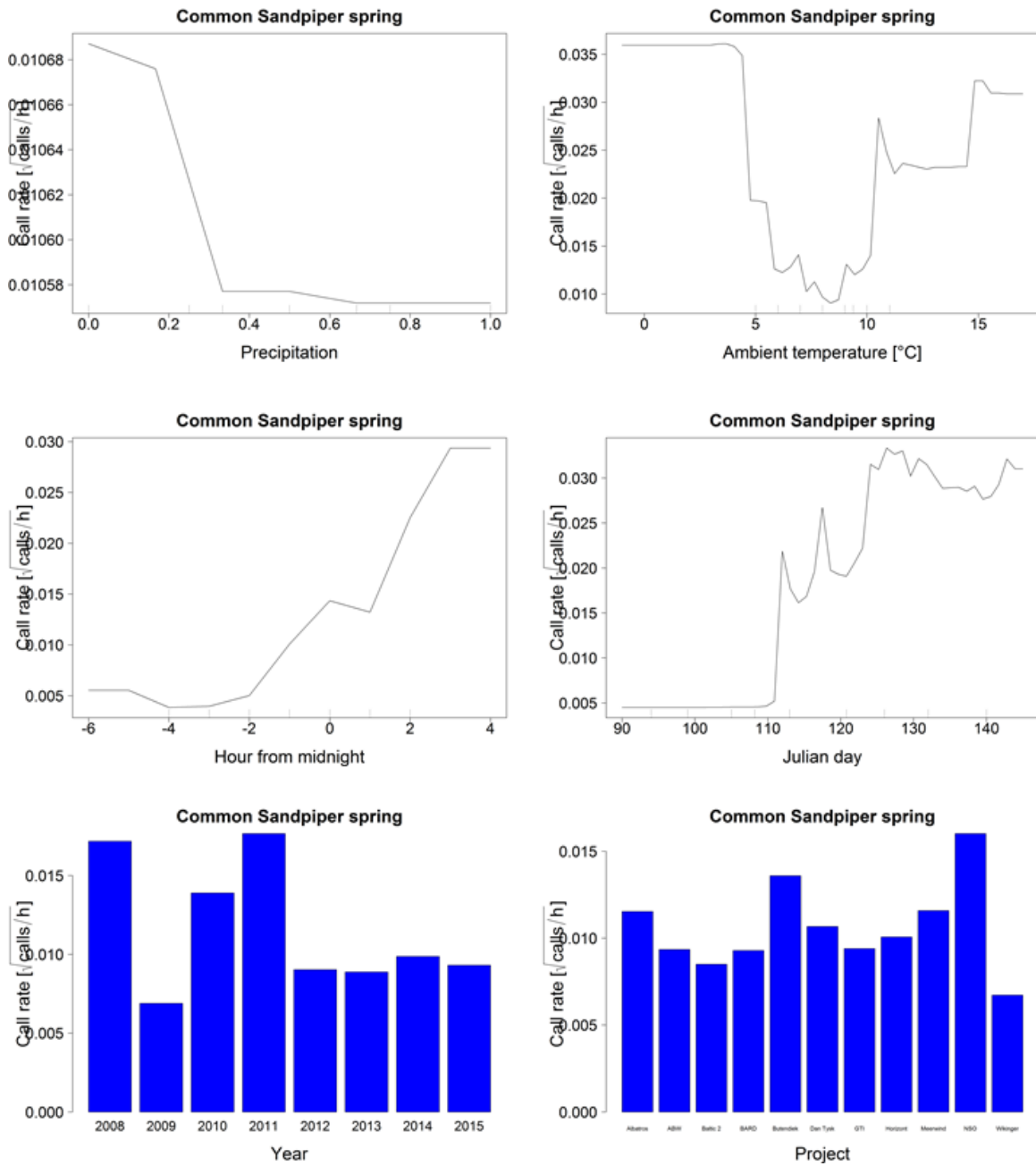


Figure A. 18 Common Sandpiper spring, continued on next page.

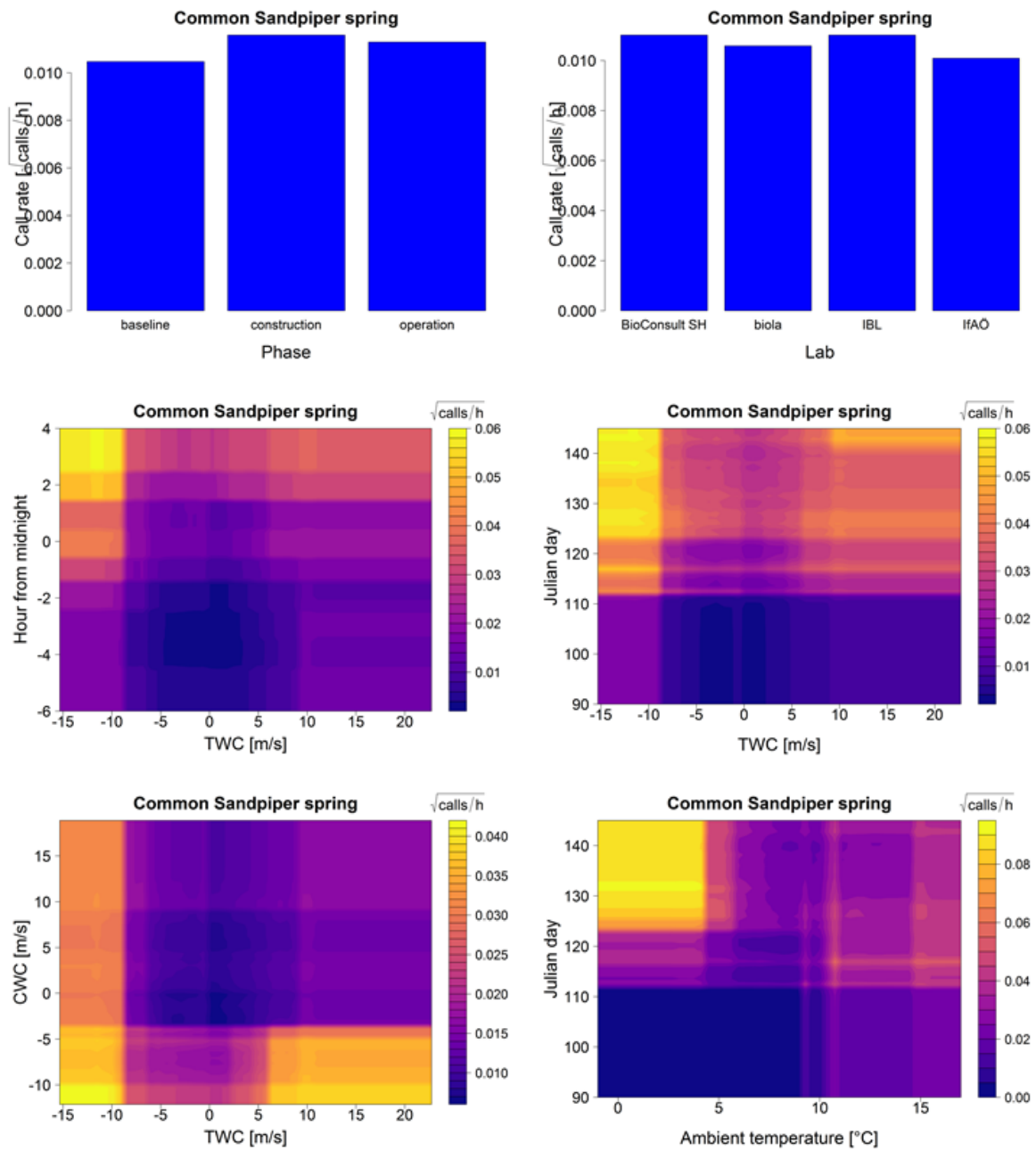


Figure A. 19 Common Sandpiper spring: Top left panel shows the Standardized Error Variable Importance (%IncMSE) plot. Top right panel shows the multi-way importance plot. Below are the partial dependence plots for each variable included in the model (note the different scales of the partial effect on the y-axis). In the lower panels interaction plots are shown: TWC vs CWC, TWC vs Julian day, TWC vs hour from midnight and Julian day vs ambient temperature. Colours of the interaction plots represent the predicted bird call rate (square root transformed) for each combination of effects.

Fall

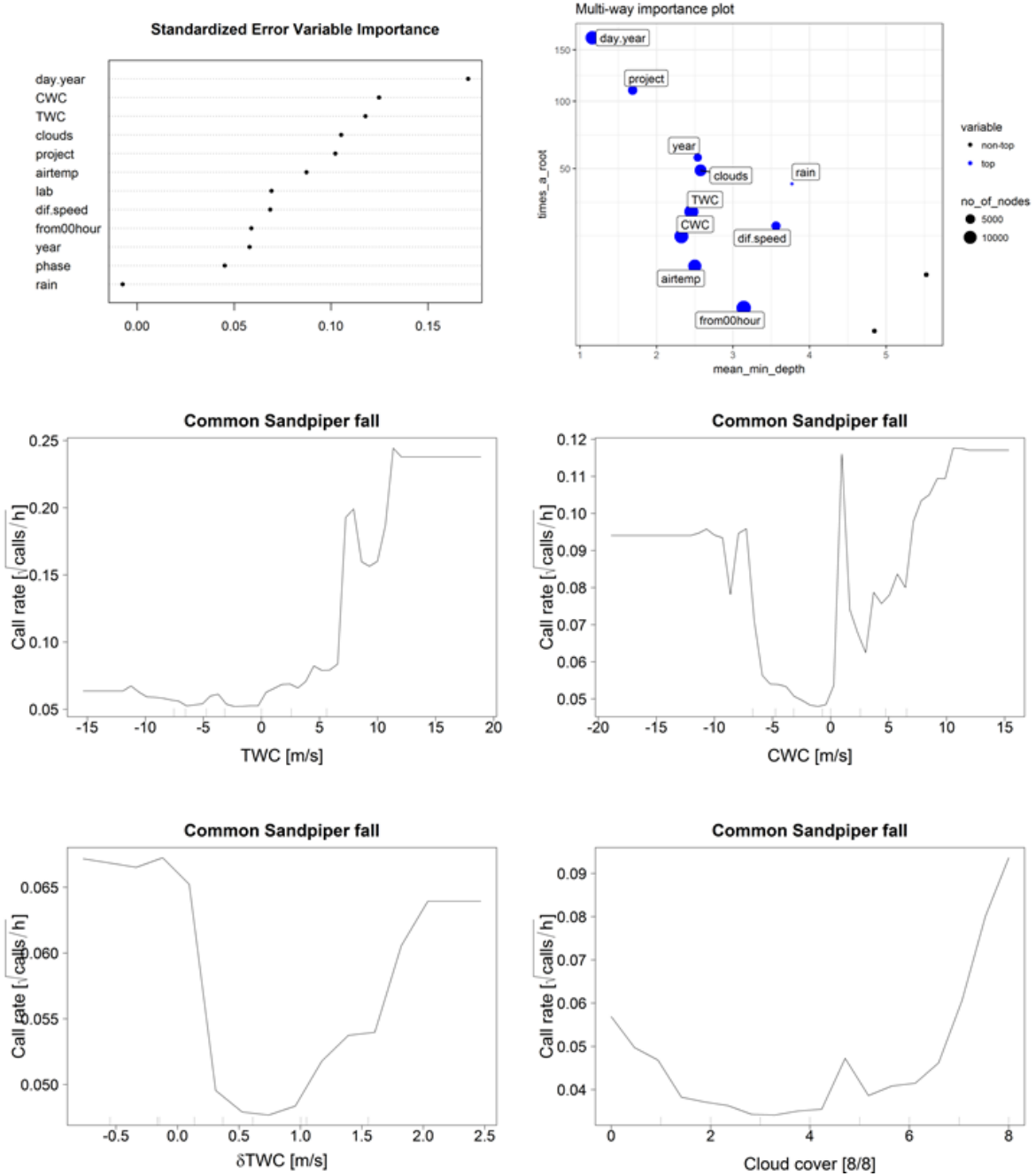


Figure A. 18 Common Sandpiper fall, continued on next page.

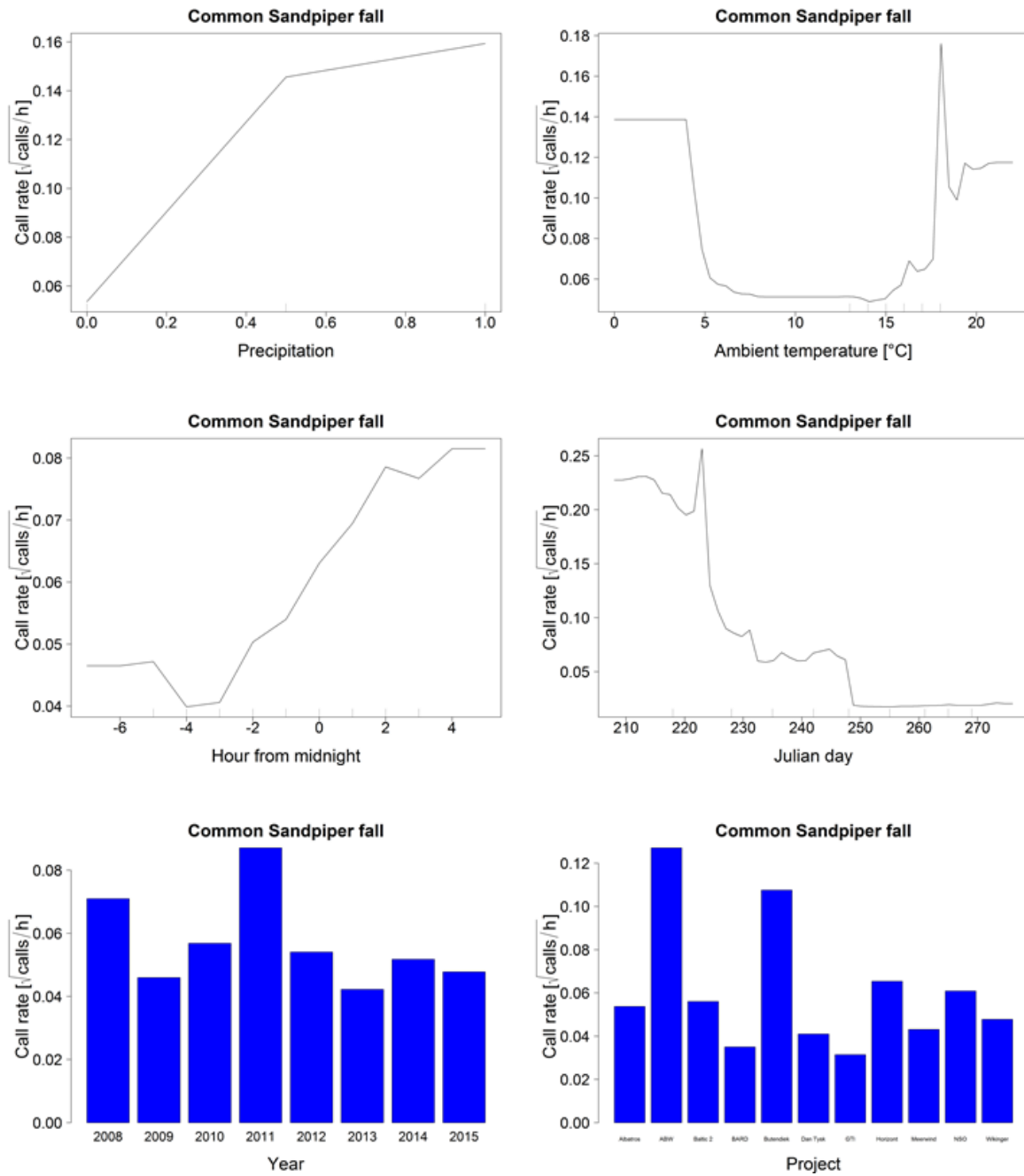


Figure A. 18 Common Sandpiper fall, continued on next page.

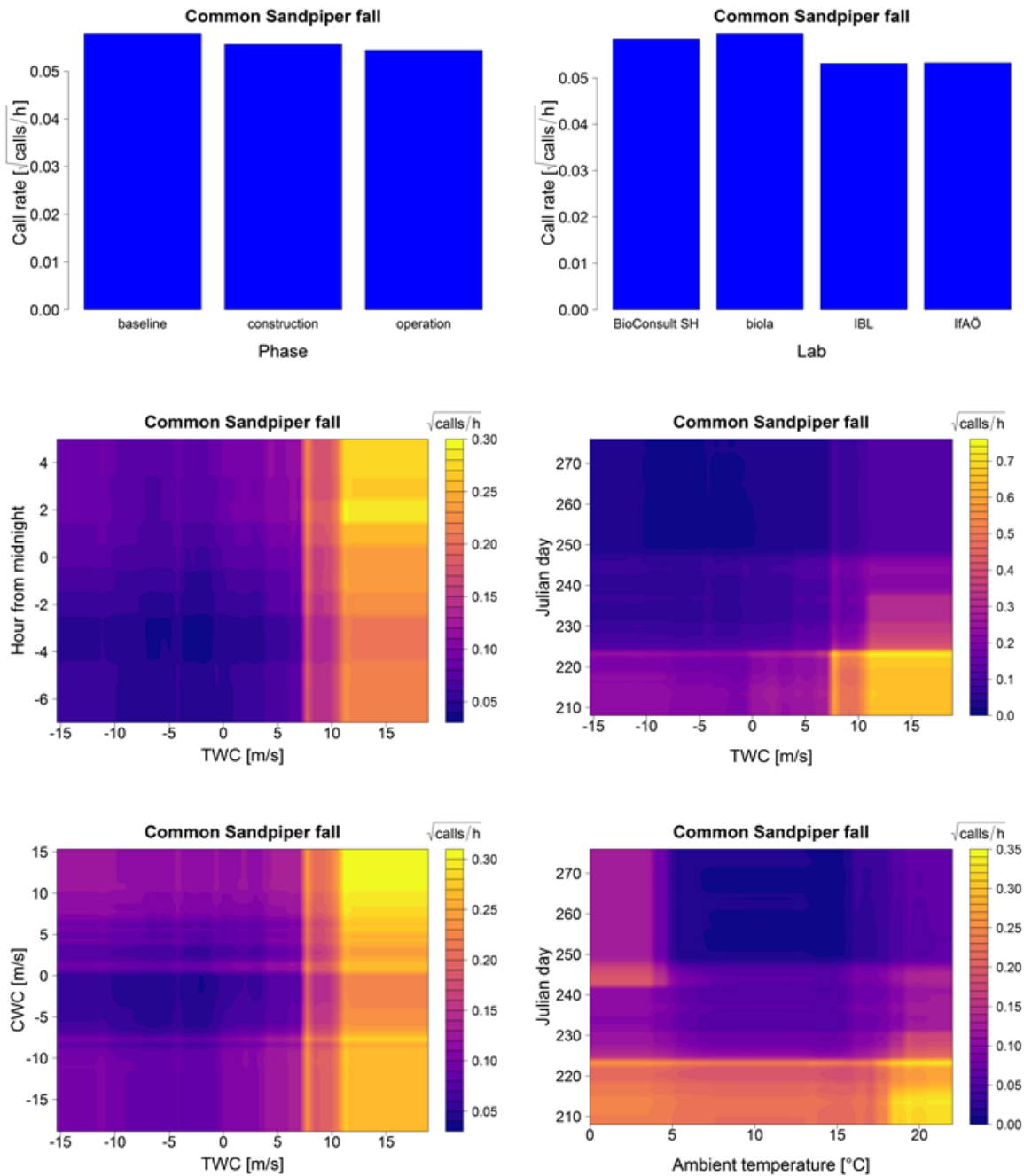


Figure A. 20 Common Sandpiper fall: Top left panel shows the Standardized Error Variable Importance (%IncMSE) plot. Top right panel shows the multi-way importance plot. Below are the partial dependence plots for each variable included in the model (note the different scales of the partial effect on the y-axis). In the lower panels interaction plots are shown: TWC vs CWC, TWC vs Julian day, TWC vs hour from midnight and Julian day vs ambient temperature. Colours of the interaction plots represent the predicted bird call rate (square root transformed) for each combination of effects.

Dunlin

Spring

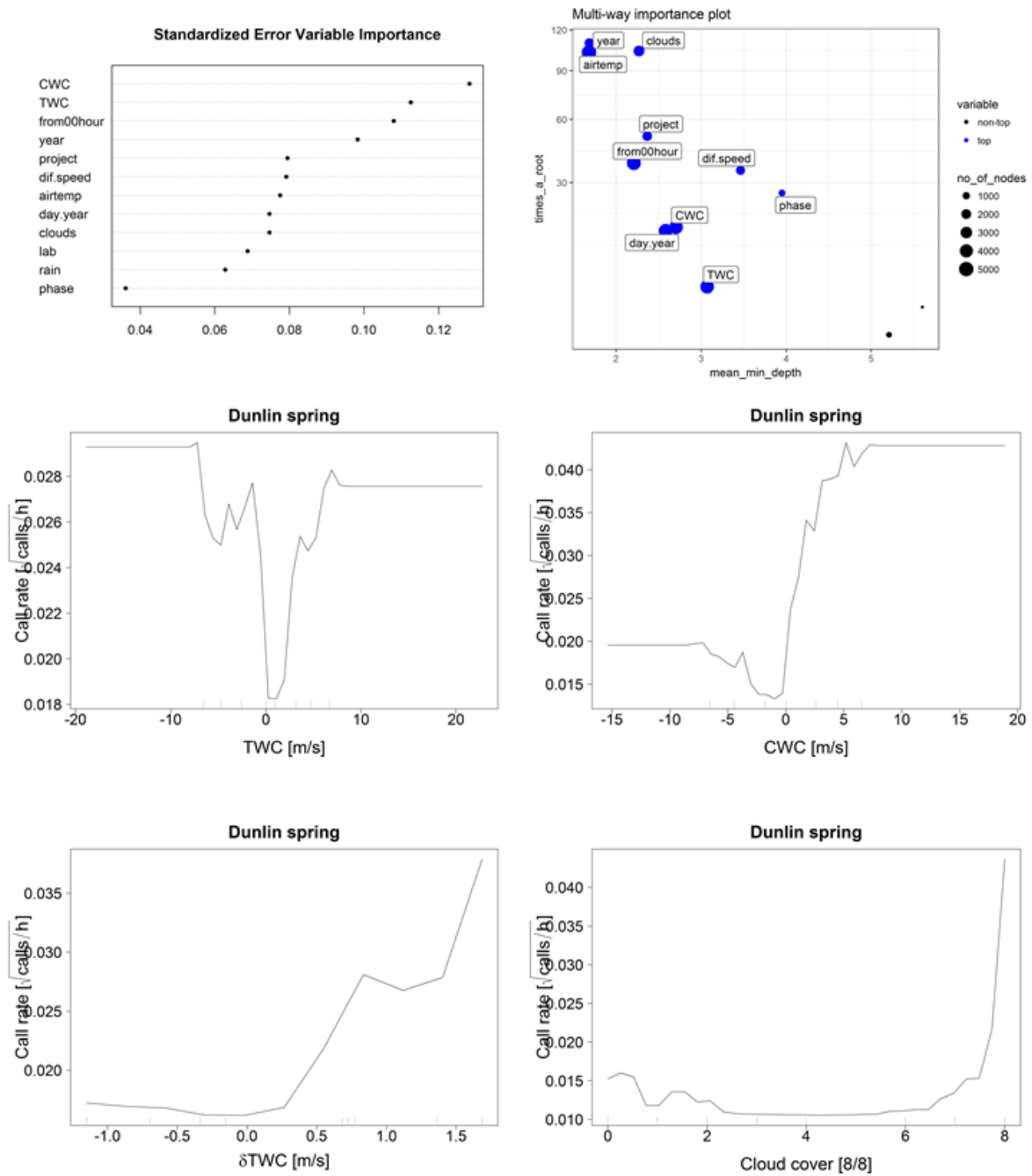


Figure A. 19 Dunlin spring, continued on next page.

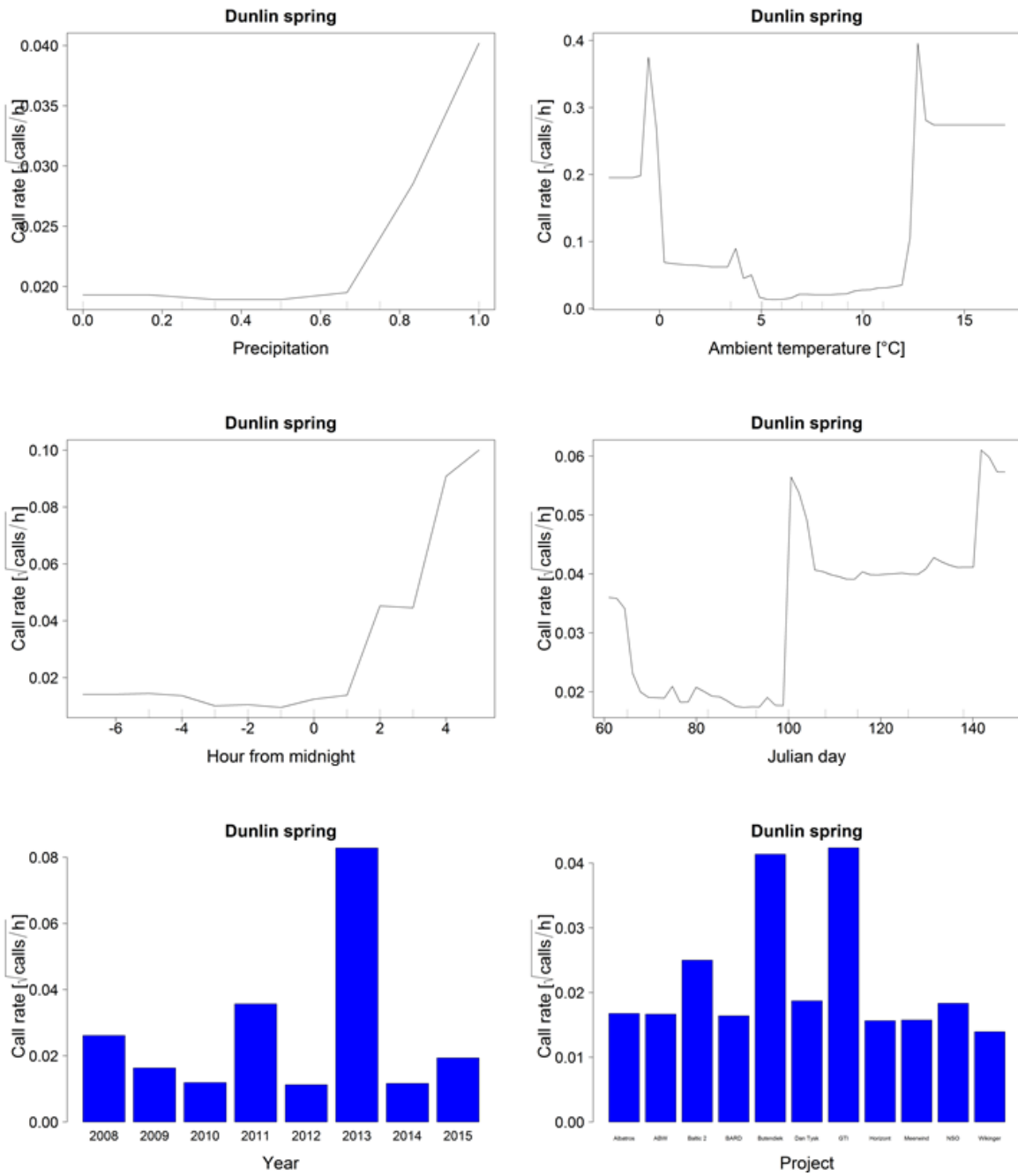


Figure A. 19 Dunlin spring, continued on next page.

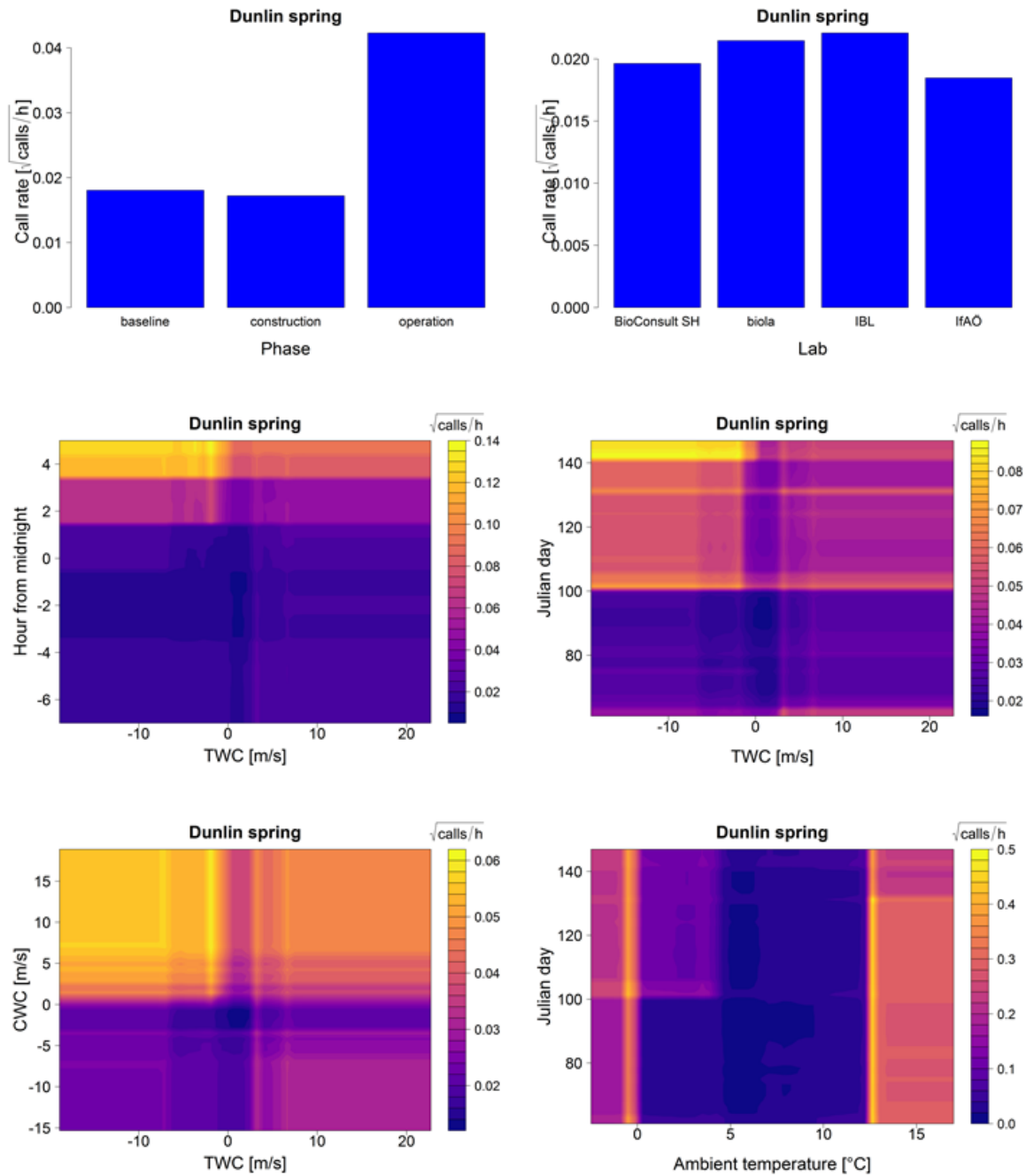


Figure A. 21 *Dunlin spring*: Top left panel shows the Standardized Error Variable Importance (%IncMSE) plot. Top right panel shows the multi-way importance plot. Below are the partial dependence plots for each variable included in the model (note the different scales of the partial effect on the y-axis). In the lower panels interaction plots are shown: TWC vs CWC, TWC vs Julian day, TWC vs hour from midnight and Julian day vs ambient temperature. Colours of the interaction plots represent the predicted bird call rate (square root transformed) for each combination of effects.

Fall

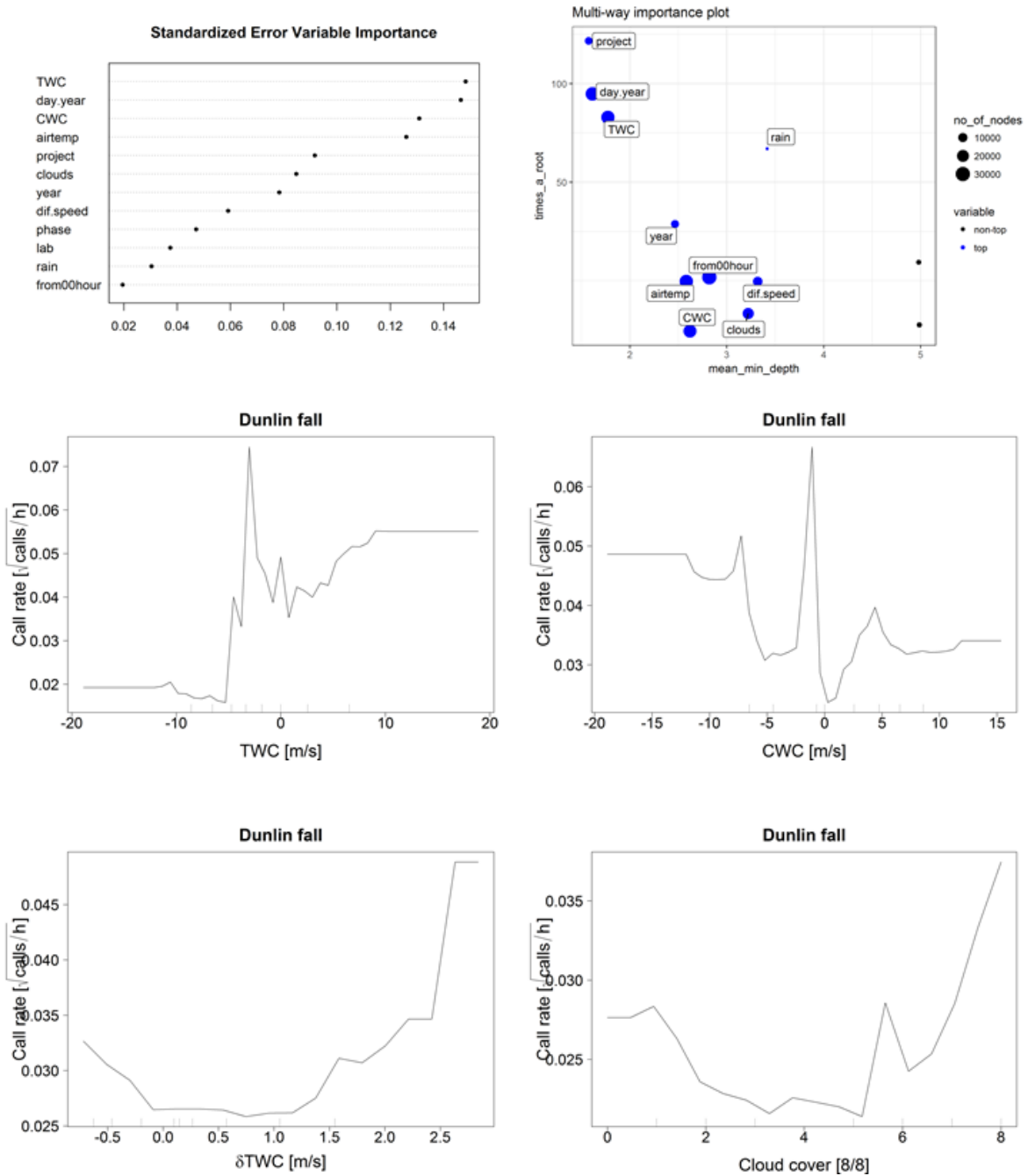


Figure A.20 Dunlin fall, continued on next page.

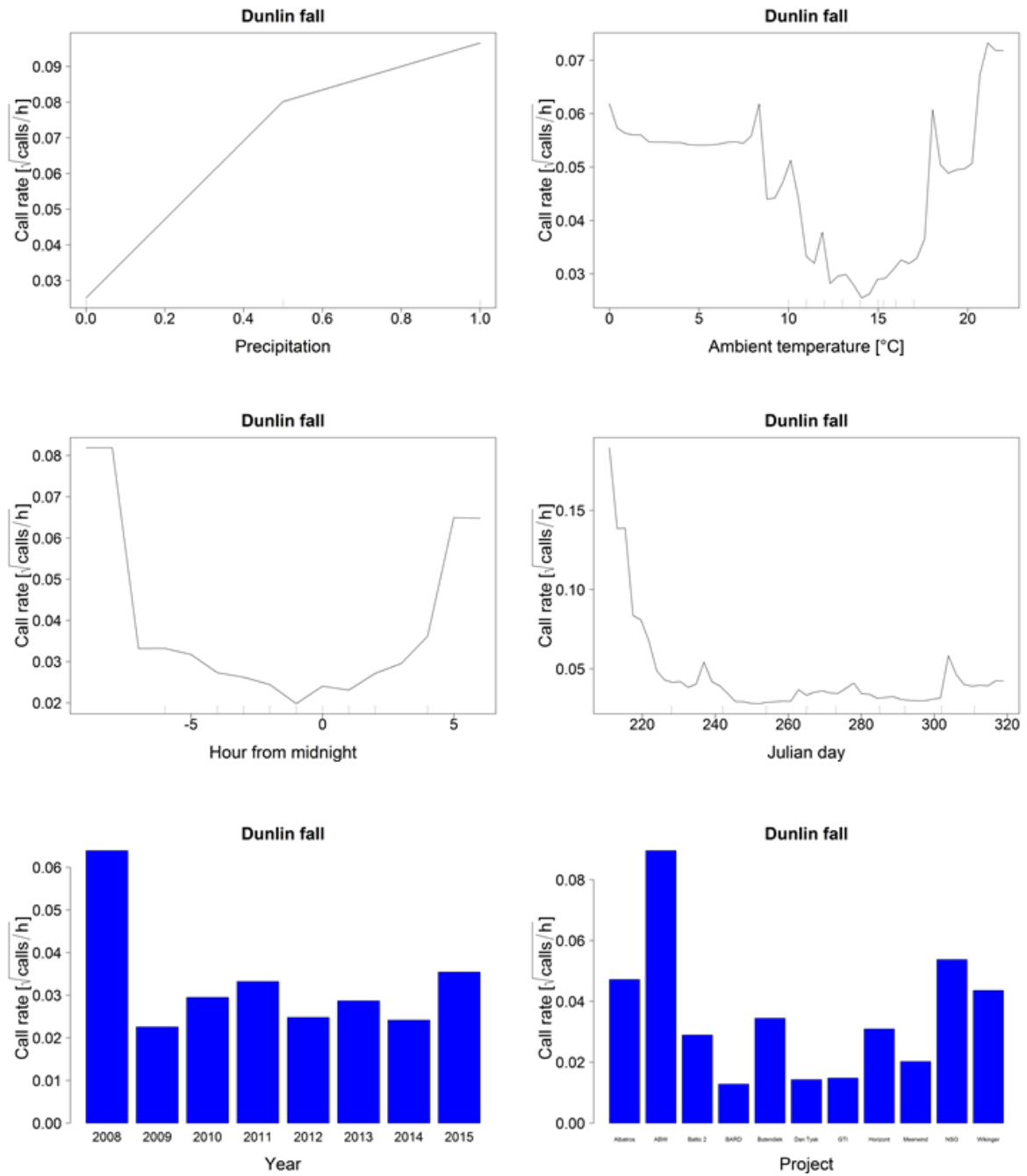


Figure A. 20 Dunlin fall, continued on next page.

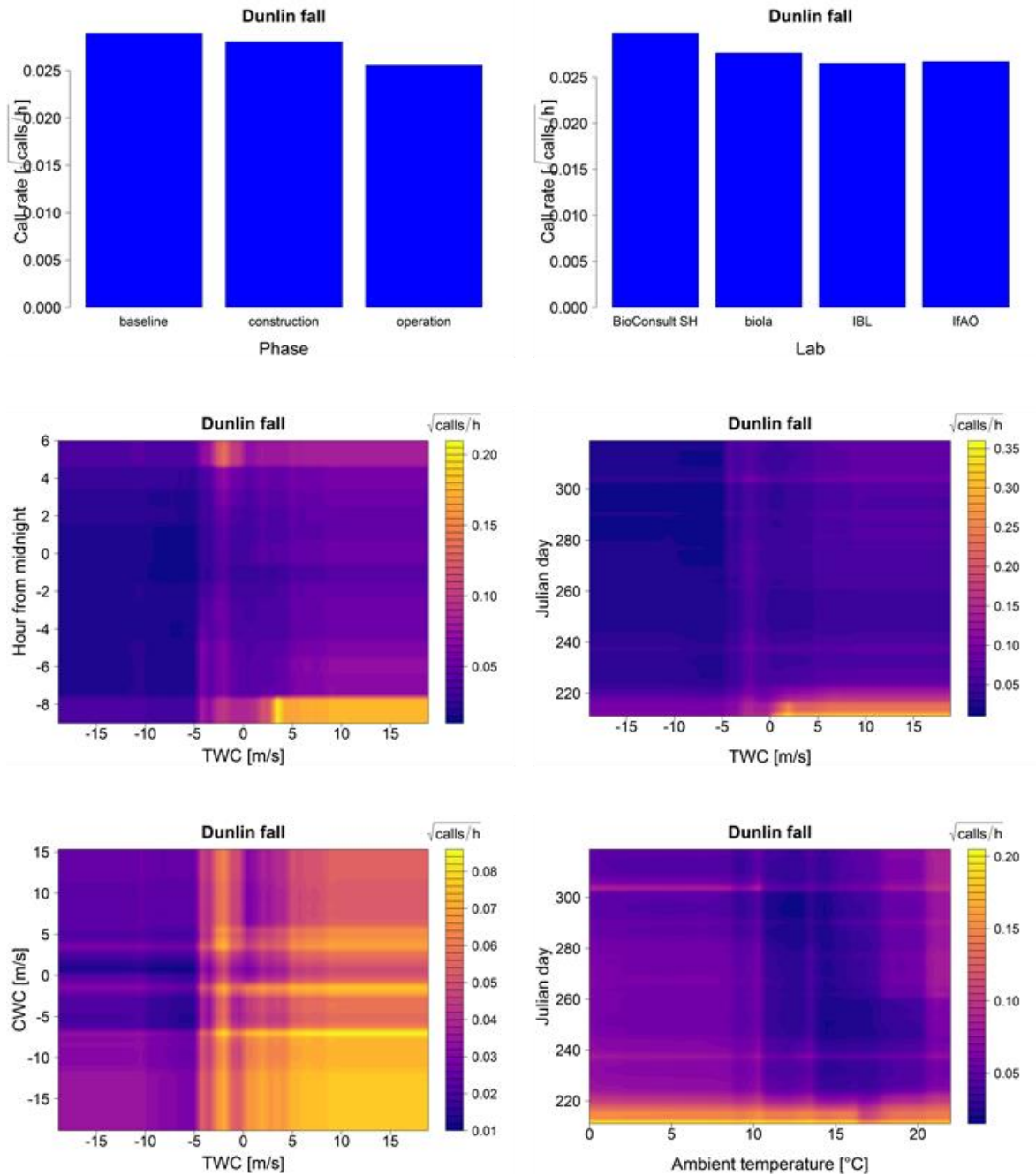


Figure A. 22 Dunlin fall: Top left panel shows the Standardized Error Variable Importance (%IncMSE) plot. Top right panel shows the multi-way importance plot. Below are the partial dependence plots for each variable included in the model (note the different scales of the partial effect on the y-axis). In the lower panels interaction plots are shown: TWC vs CWC, TWC vs Julian day, TWC vs hour from midnight and Julian day vs ambient temperature. Colours of the interaction plots represent the predicted bird call rate (square root transformed) for each combination of effects.

Blackbird

Spring

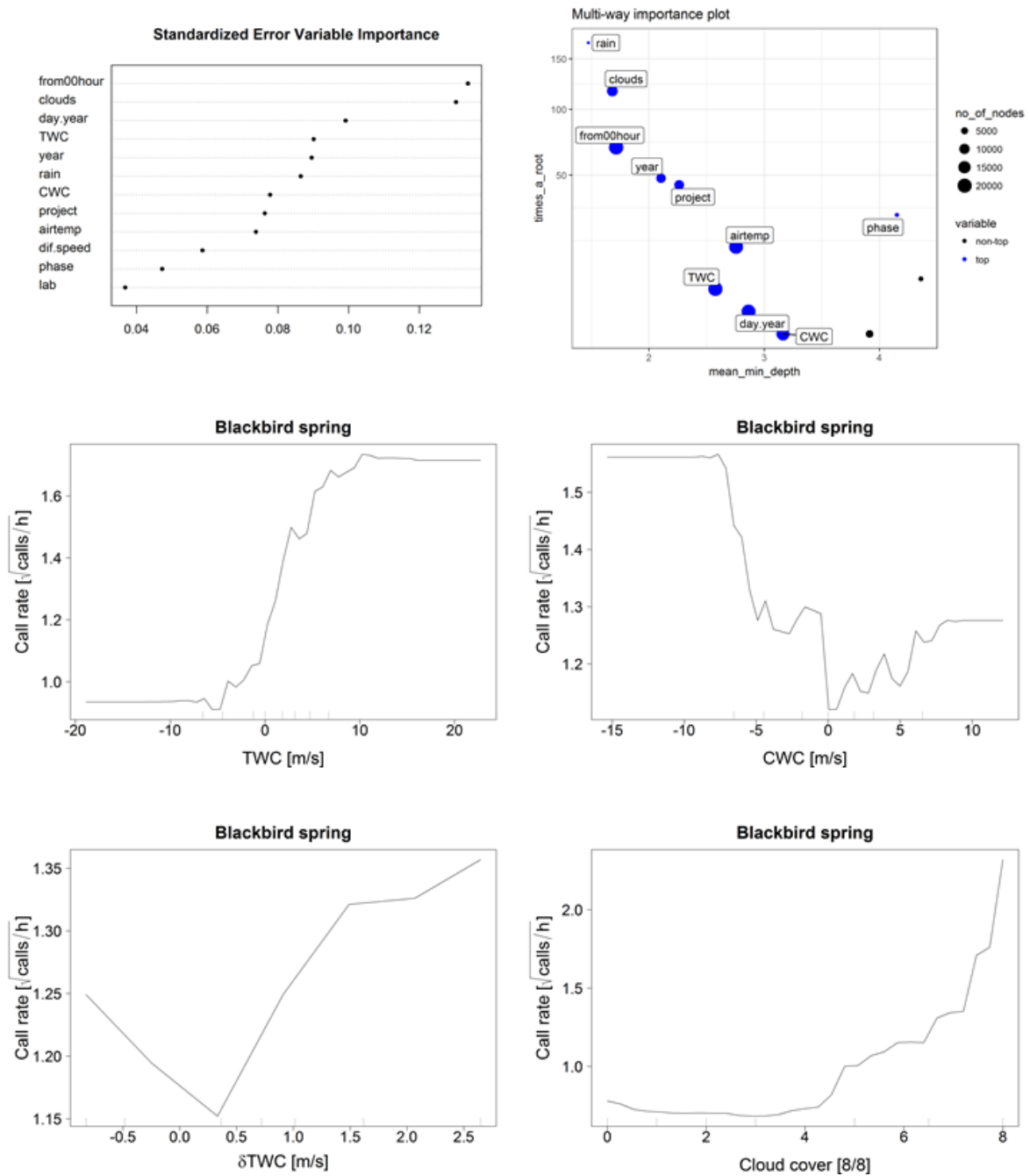


Figure A. 21 Blackbird spring, continued on next page.

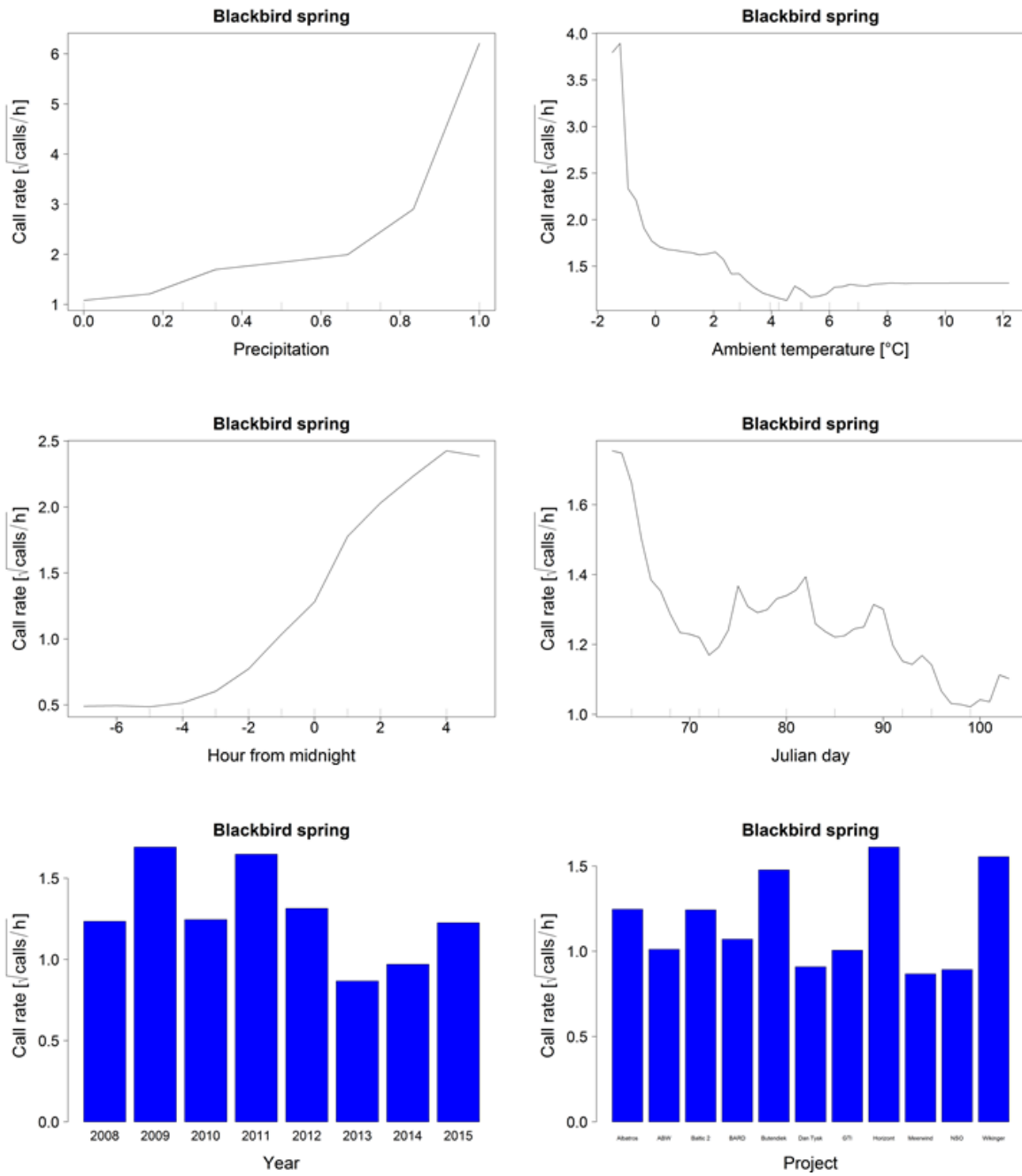


Figure A. 21 Blackbird spring, continued on next page.

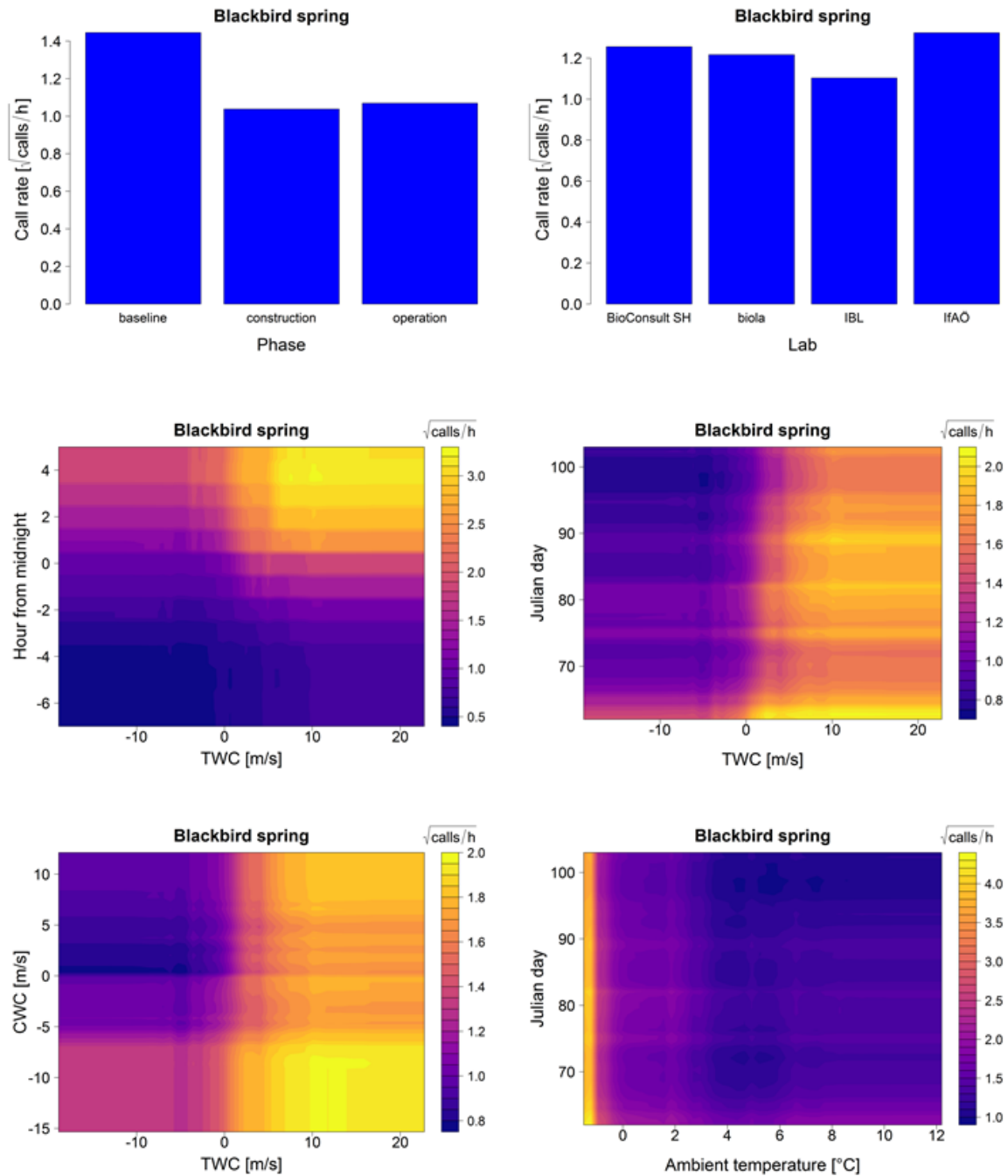


Figure A. 23 *Blackbird spring*: Top left panel shows the Standardized Error Variable Importance (%IncMSE) plot. Top right panel shows the multi-way importance plot. Below are the partial dependence plots for each variable included in the model (note the different scales of the partial effect on the y-axis). In the lower panels interaction plots are shown: TWC vs CWC, TWC vs Julian day, TWC vs hour from midnight and Julian day vs ambient temperature. Colours of the interaction plots represent the predicted bird call rate (square root transformed) for each combination of effects.

Fall

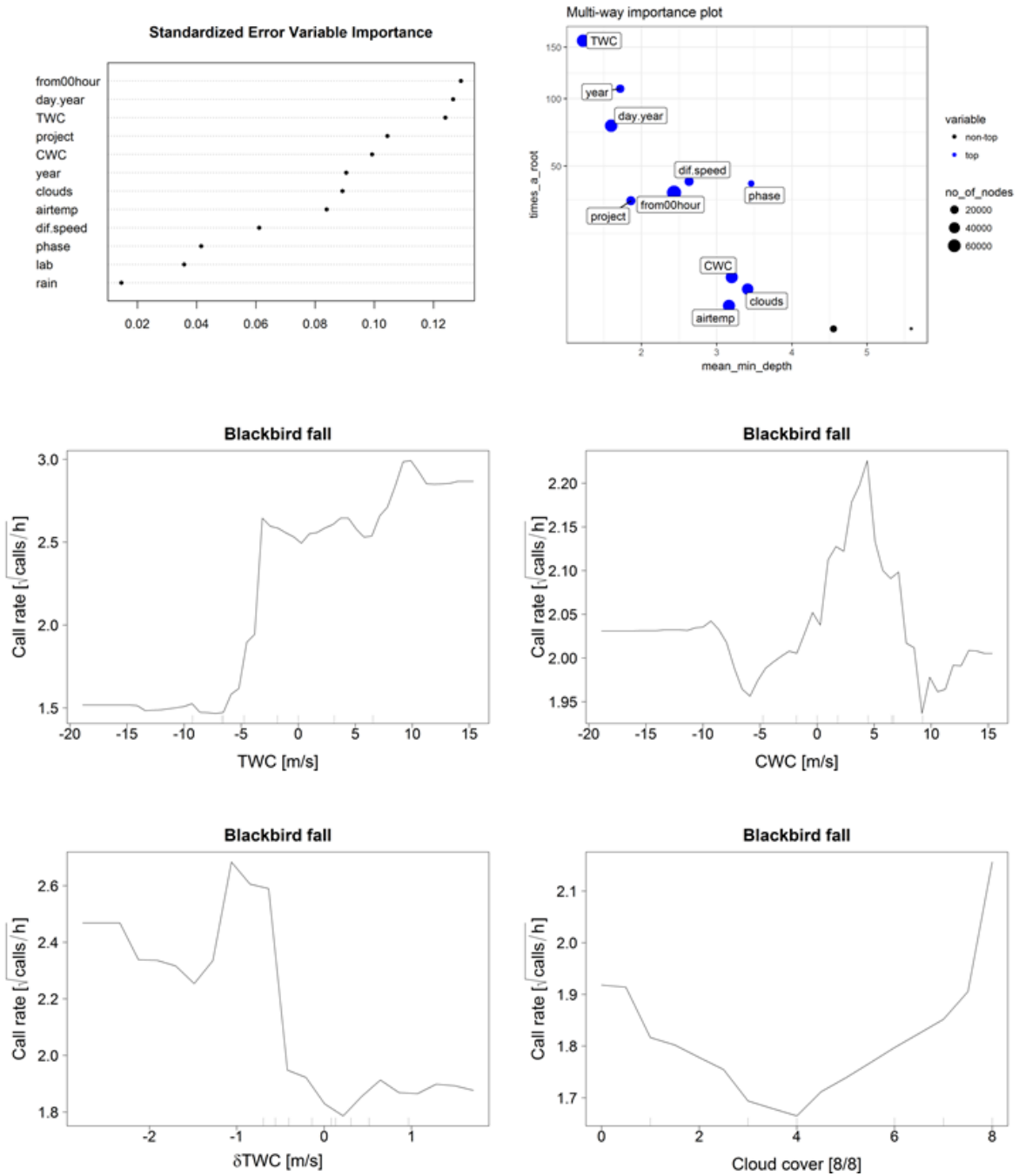


Figure A.22 Blackbird fall, continued on next page.

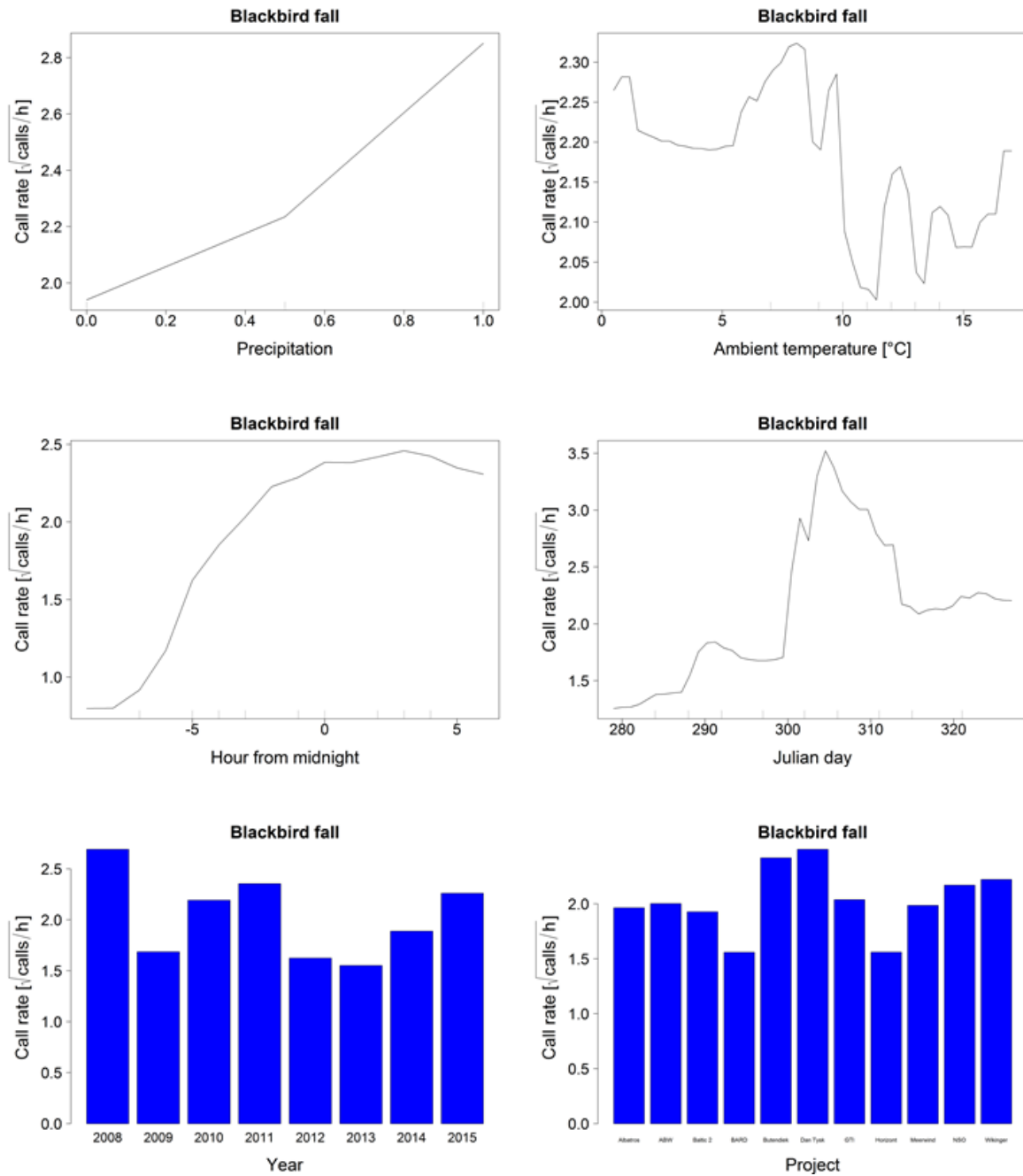


Figure A. 22 Blackbird fall, continued on next page.

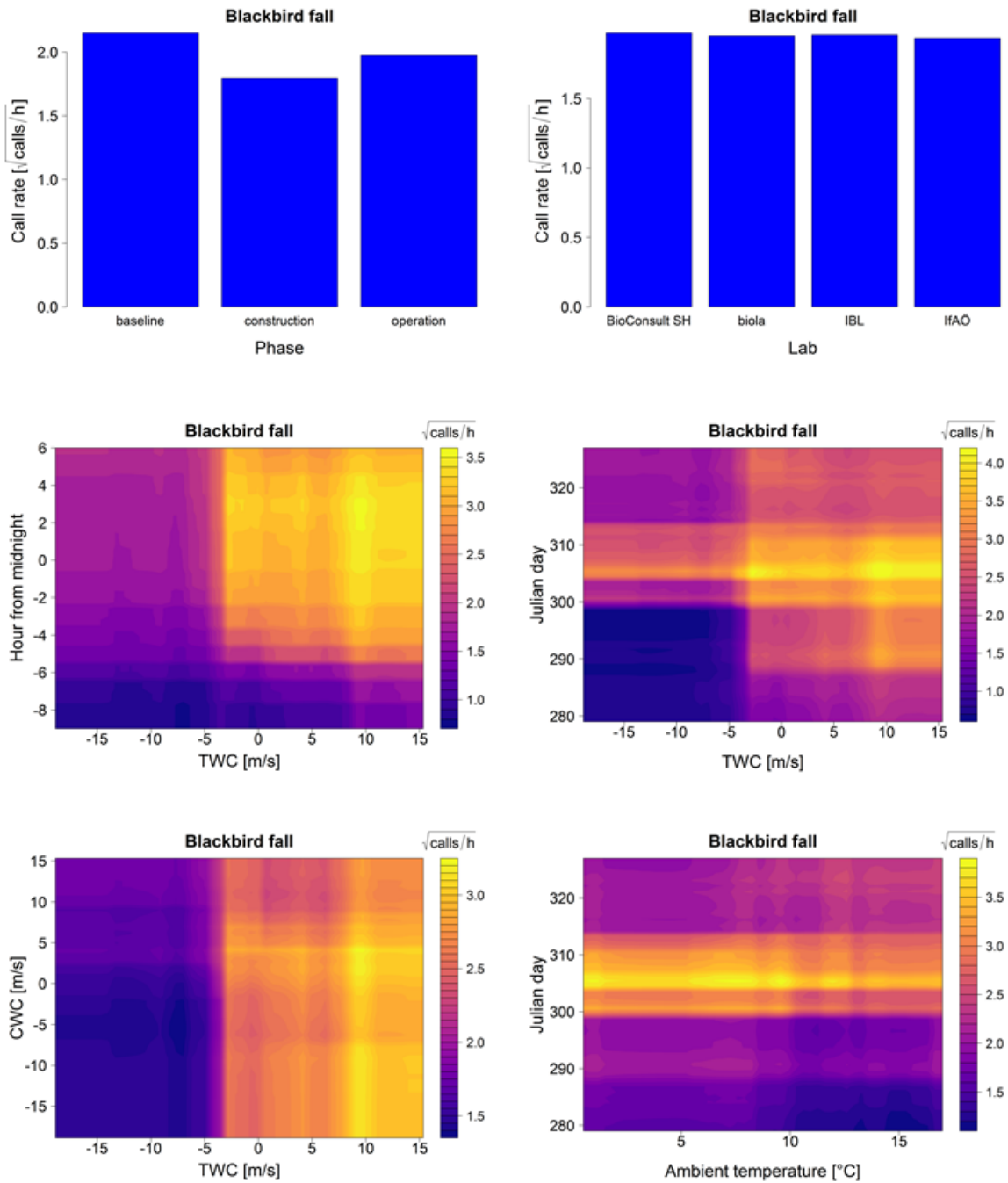


Figure A. 24 Blackbird fall: Top left panel shows the Standardized Error Variable Importance (%IncMSE) plot. Top right panel shows the multi-way importance plot. Below are the partial dependence plots for each variable included in the model (note the different scales of the partial effect on the y-axis). In the lower panels interaction plots are shown: TWC vs CWC, TWC vs Julian day, TWC vs hour from midnight and Julian day vs ambient temperature. Colours of the interaction plots represent the predicted bird call rate (square root transformed) for each combination of effects.

Redwing

Spring

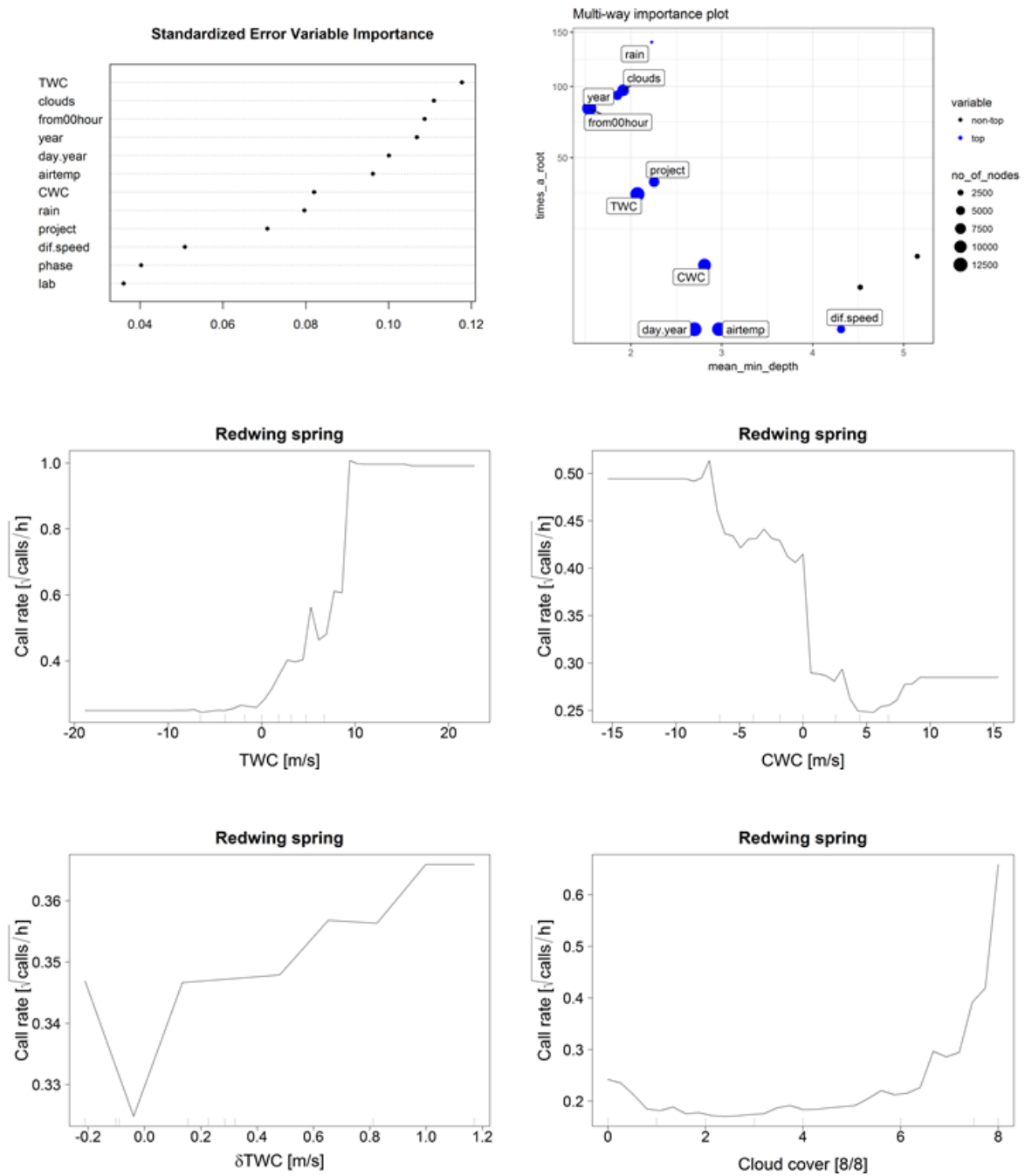


Figure A.23 Redwing spring, continued on next page.

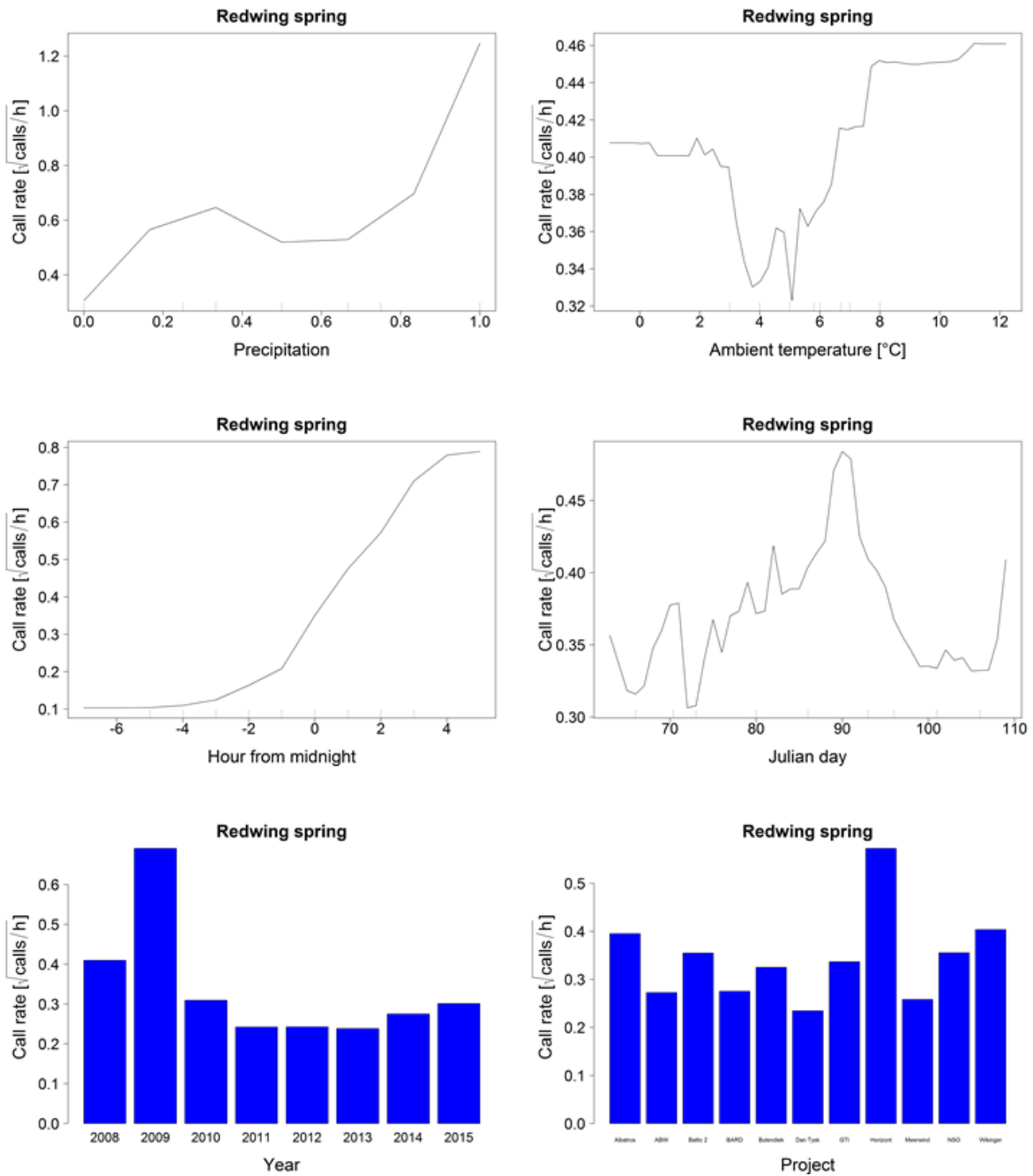


Figure A. 23 Redwing spring, continued on next page.

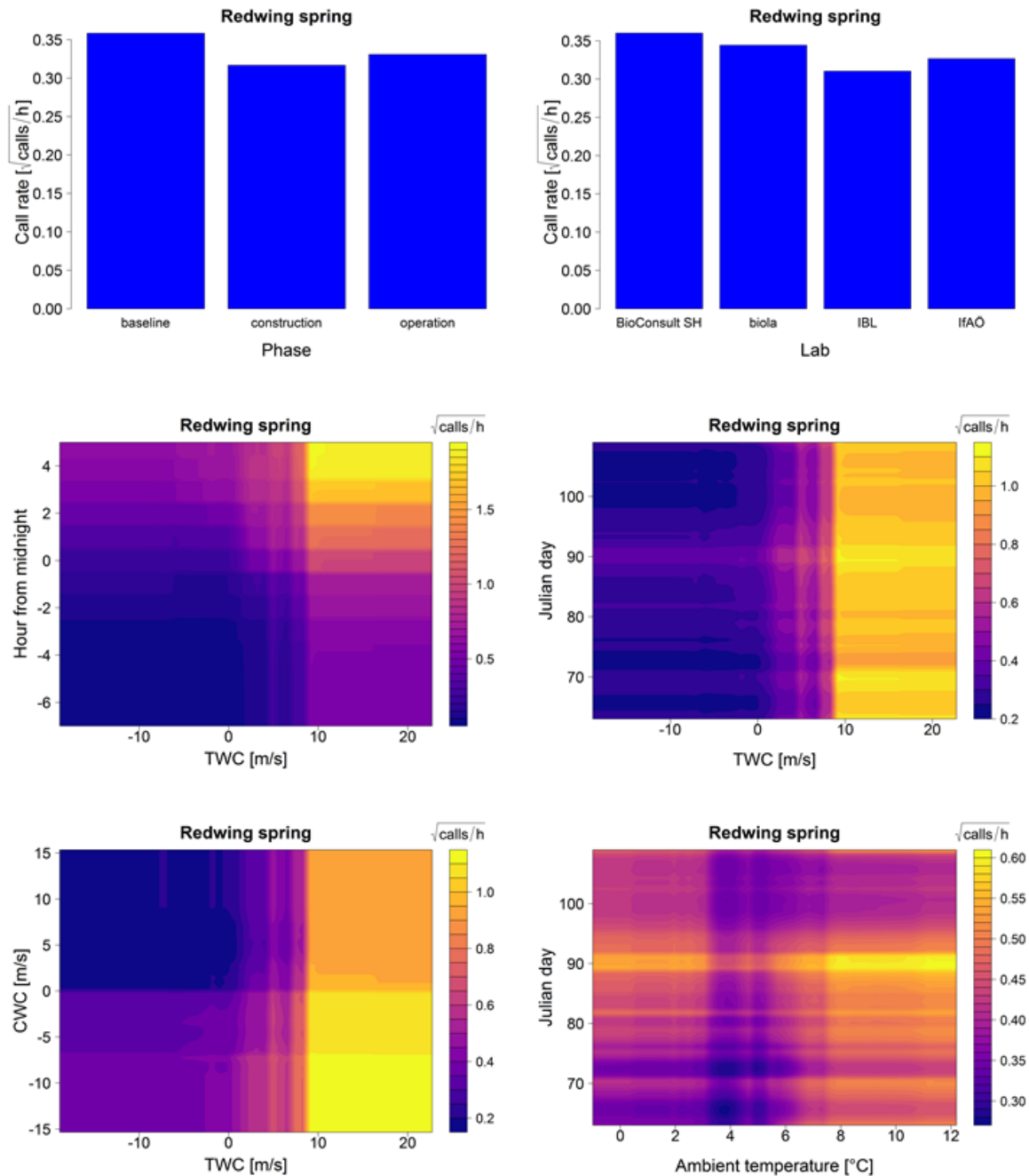


Figure A. 25 Redwing spring: Top left panel shows the Standardized Error Variable Importance (%IncMSE) plot. Top right panel shows the multi-way importance plot. Below are the partial dependence plots for each variable included in the model (note the different scales of the partial effect on the y-axis). In the lower panels interaction plots are shown: TWC vs CWC, TWC vs Julian day, TWC vs hour from midnight and Julian day vs ambient temperature. Colours of the interaction plots represent the predicted bird call rate (square root transformed) for each combination of effects.

Fall

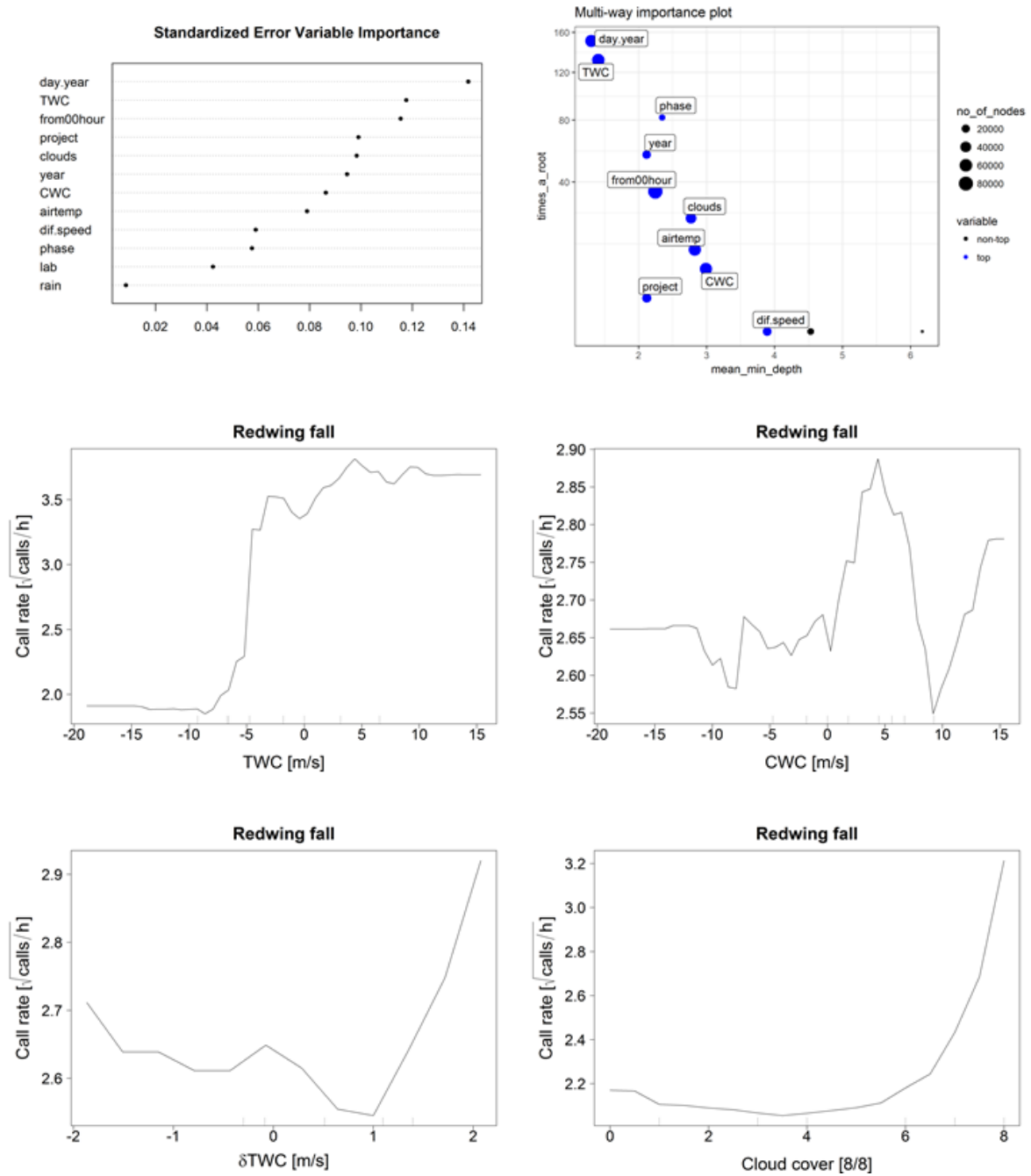


Figure A. 24 Redwing fall, continued on next page.

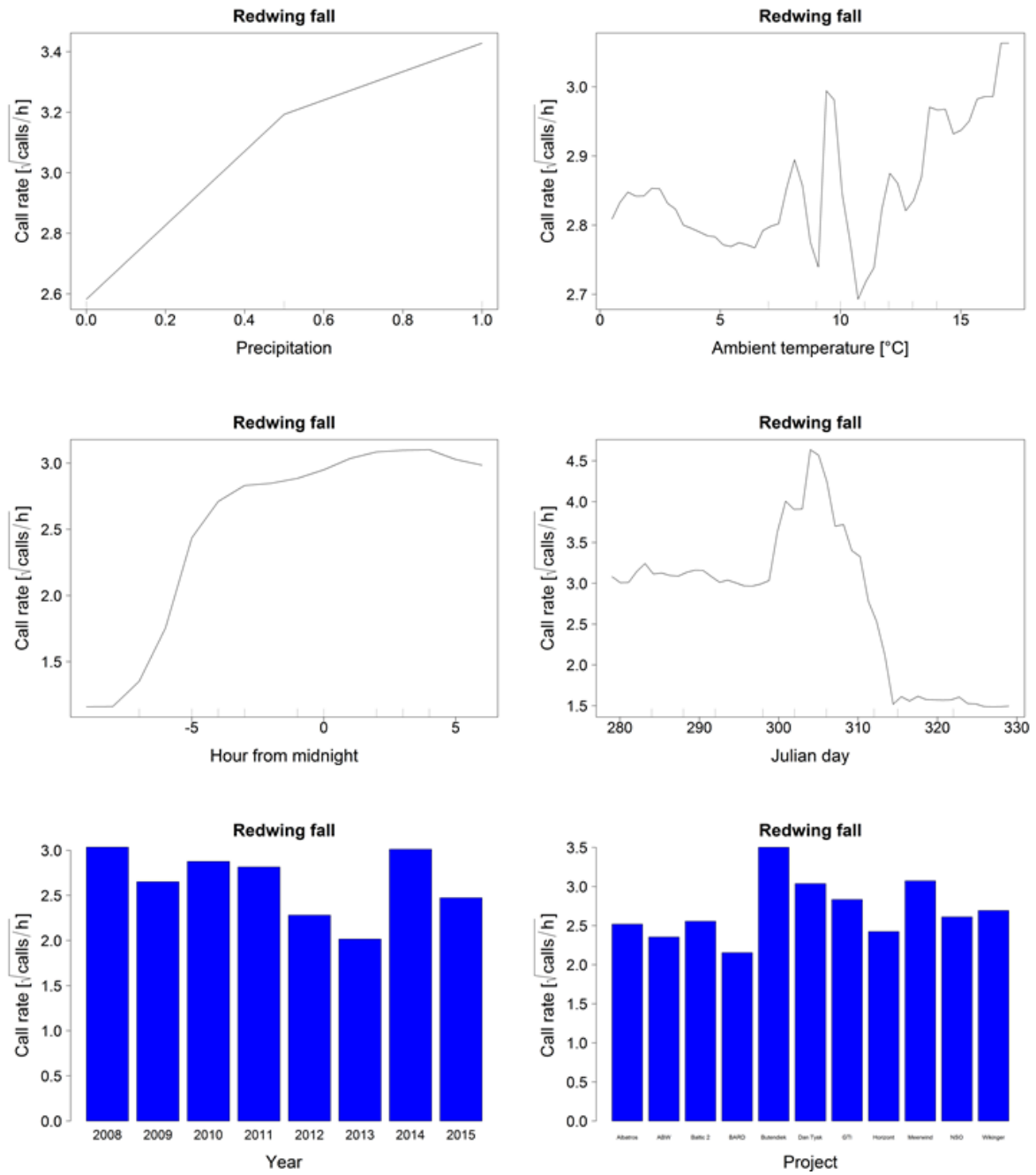


Figure A. 24 Redwing fall, continued on next page.

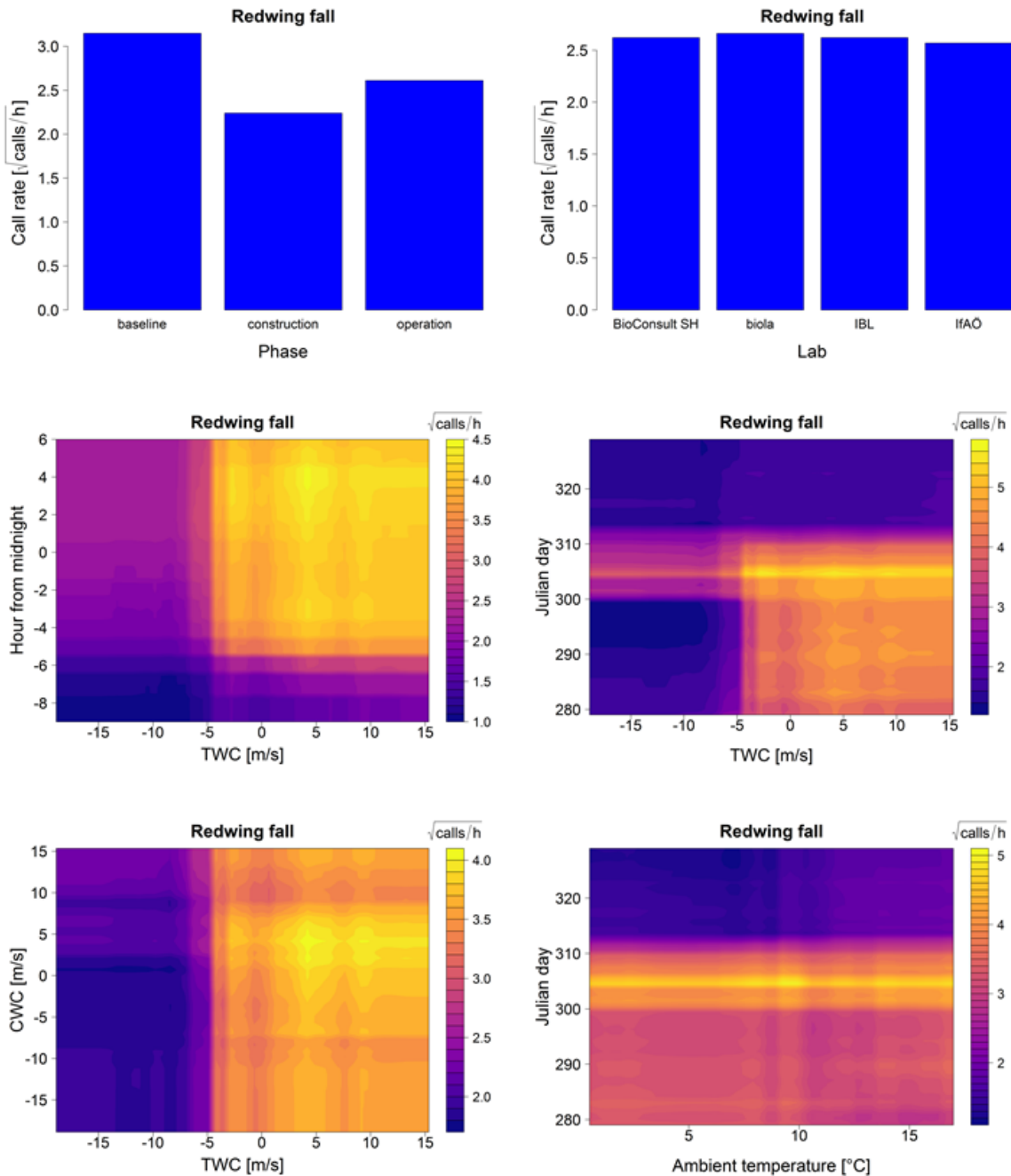


Figure A. 26 Redwing fall: Top left panel shows the Standardized Error Variable Importance (%IncMSE) plot. Top right panel shows the multi-way importance plot. Below are the partial dependence plots for each variable included in the model (note the different scales of the partial effect on the y-axis). In the lower panels interaction plots are shown: TWC vs CWC, TWC vs Julian day, TWC vs hour from midnight and Julian day vs ambient temperature. Colours of the interaction plots represent the predicted bird call rate (square root transformed) for each combination of effects.

Song Thrush

Spring

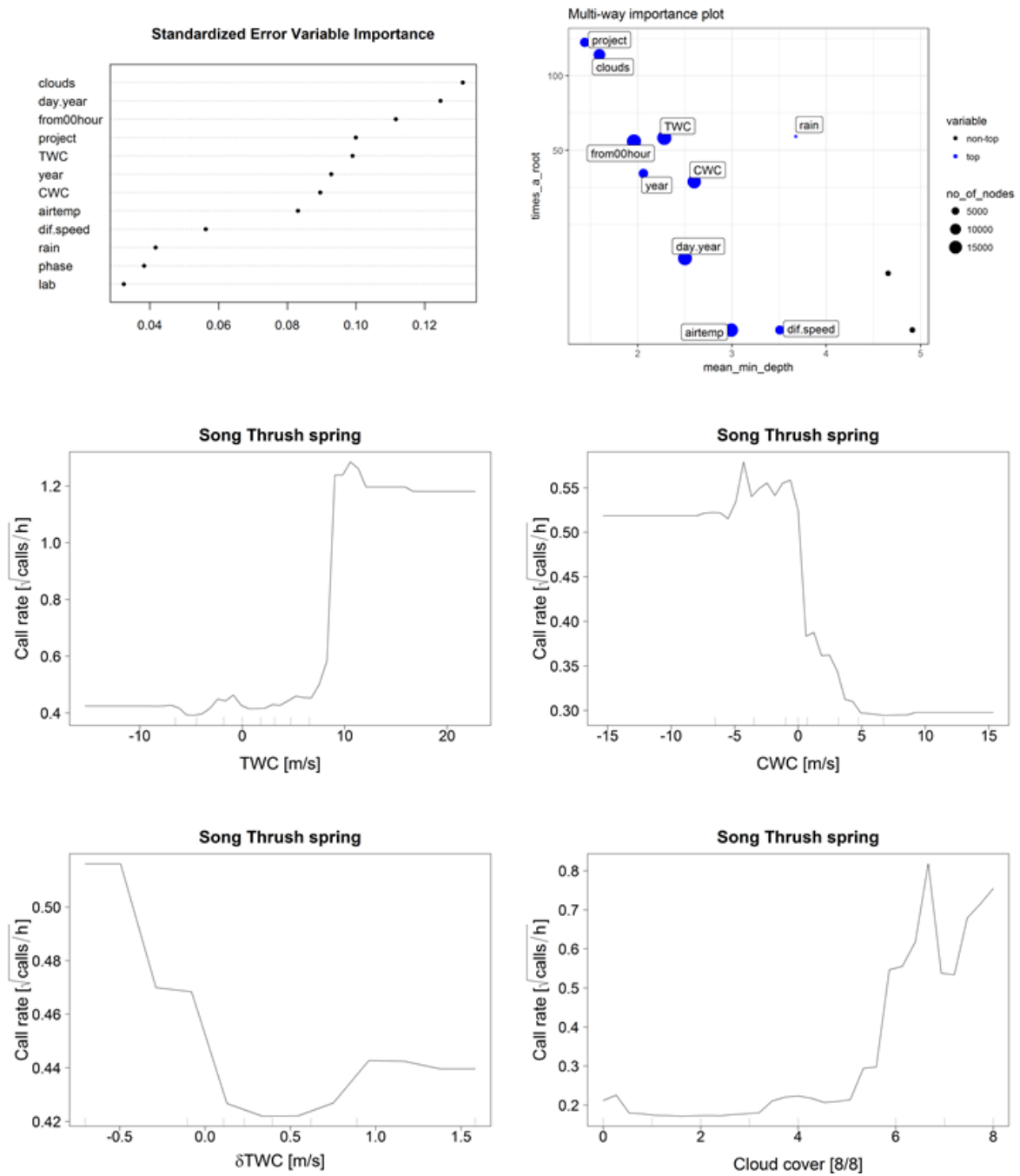


Figure A.25 Song Thrush spring, continued on next page.

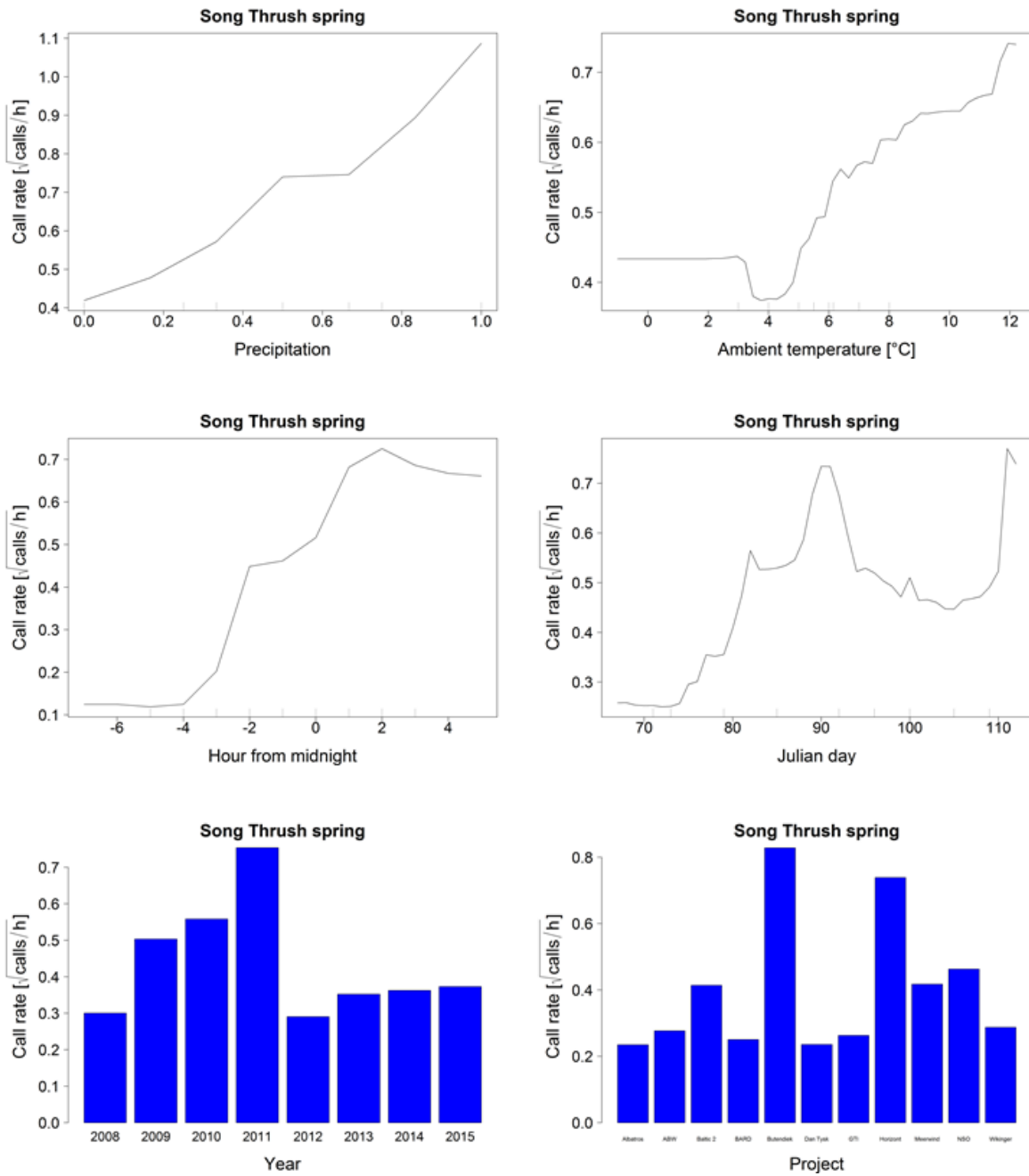


Figure A. 25 Song Thrush spring, continued on next page.

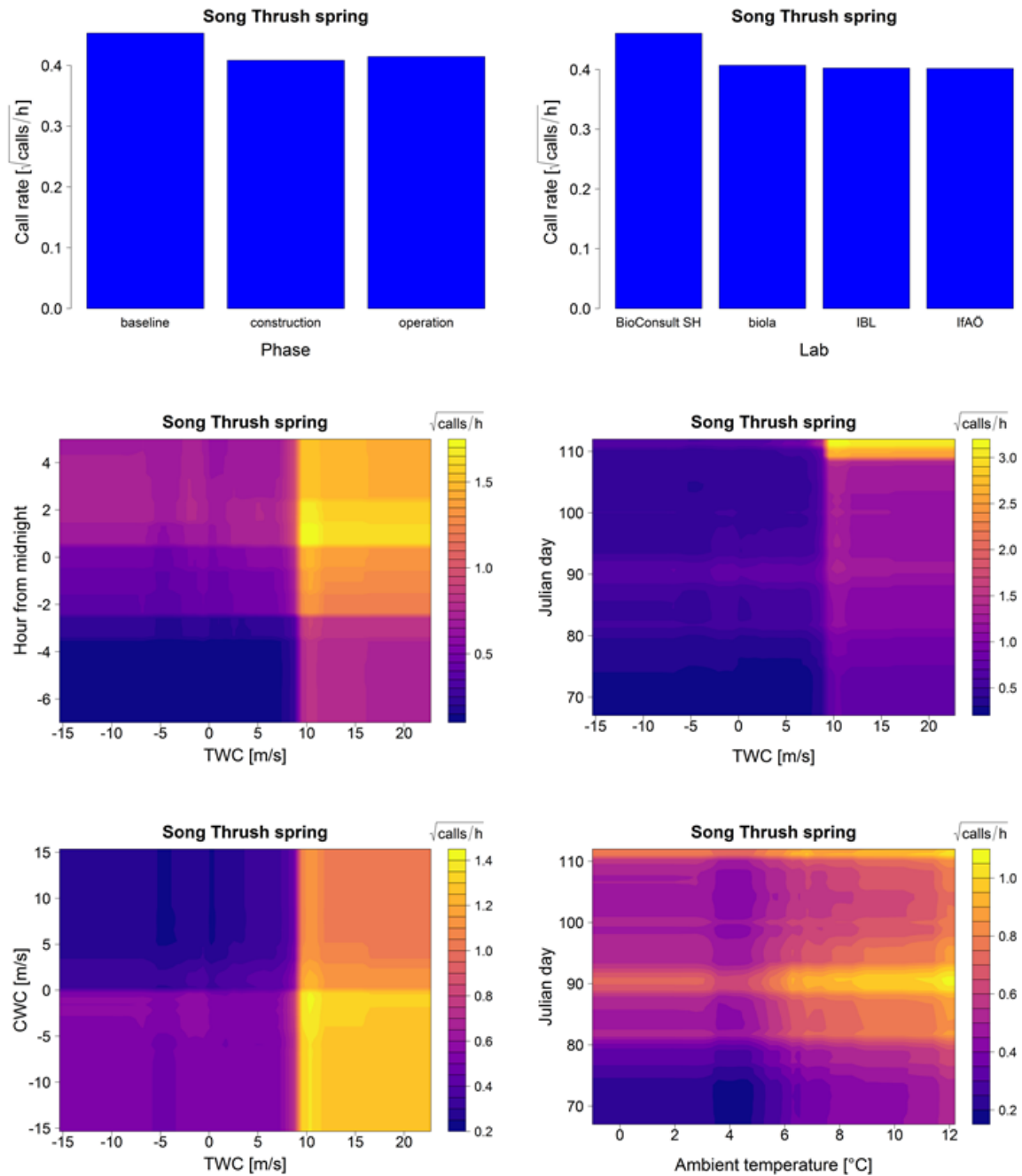


Figure A. 27 Song Thrush spring: Top left panel shows the Standardized Error Variable Importance (%IncMSE) plot. Top right panel shows the multi-way importance plot. Below are the partial dependence plots for each variable included in the model (note the different scales of the partial effect on the y-axis). In the lower panels interaction plots are shown: TWC vs CWC, TWC vs Julian day, TWC vs hour from midnight and Julian day vs ambient temperature. Colours of the interaction plots represent the predicted bird call rate (square root transformed) for each combination of effects.

Fall

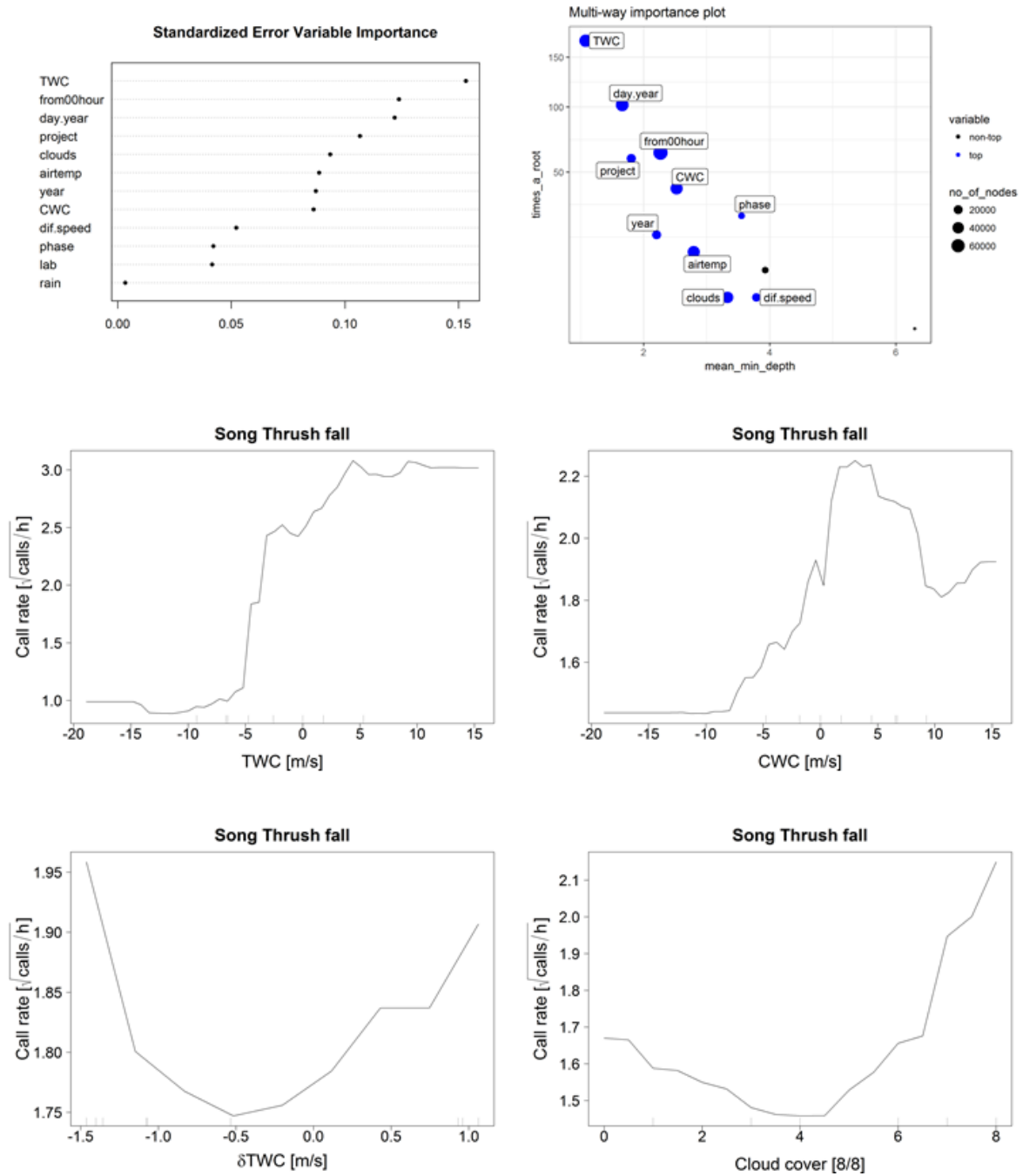


Figure A. 26 Song Thrush fall, continued on next page.

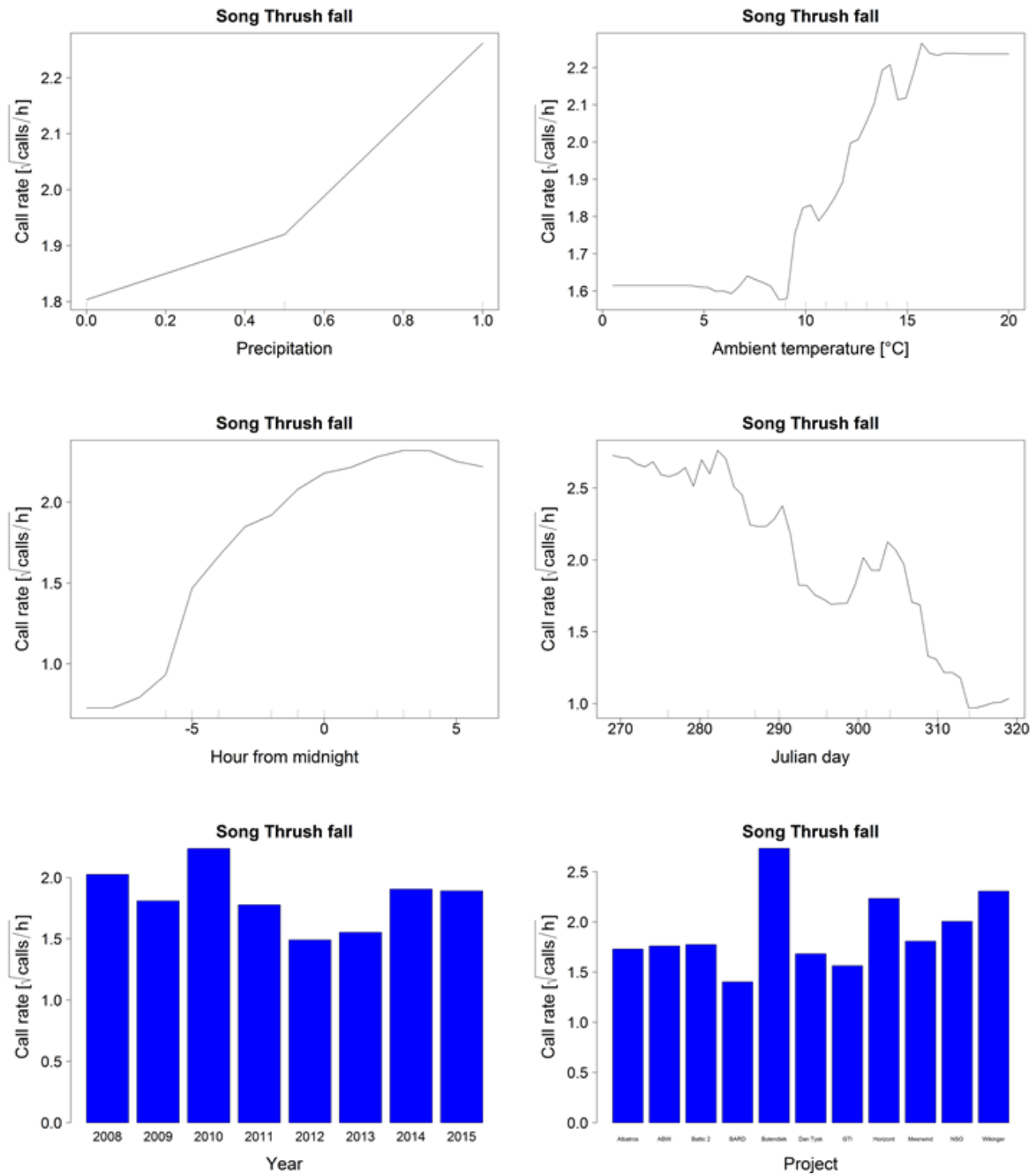


Figure A. 26 Song Thrush fall, continued on next page.

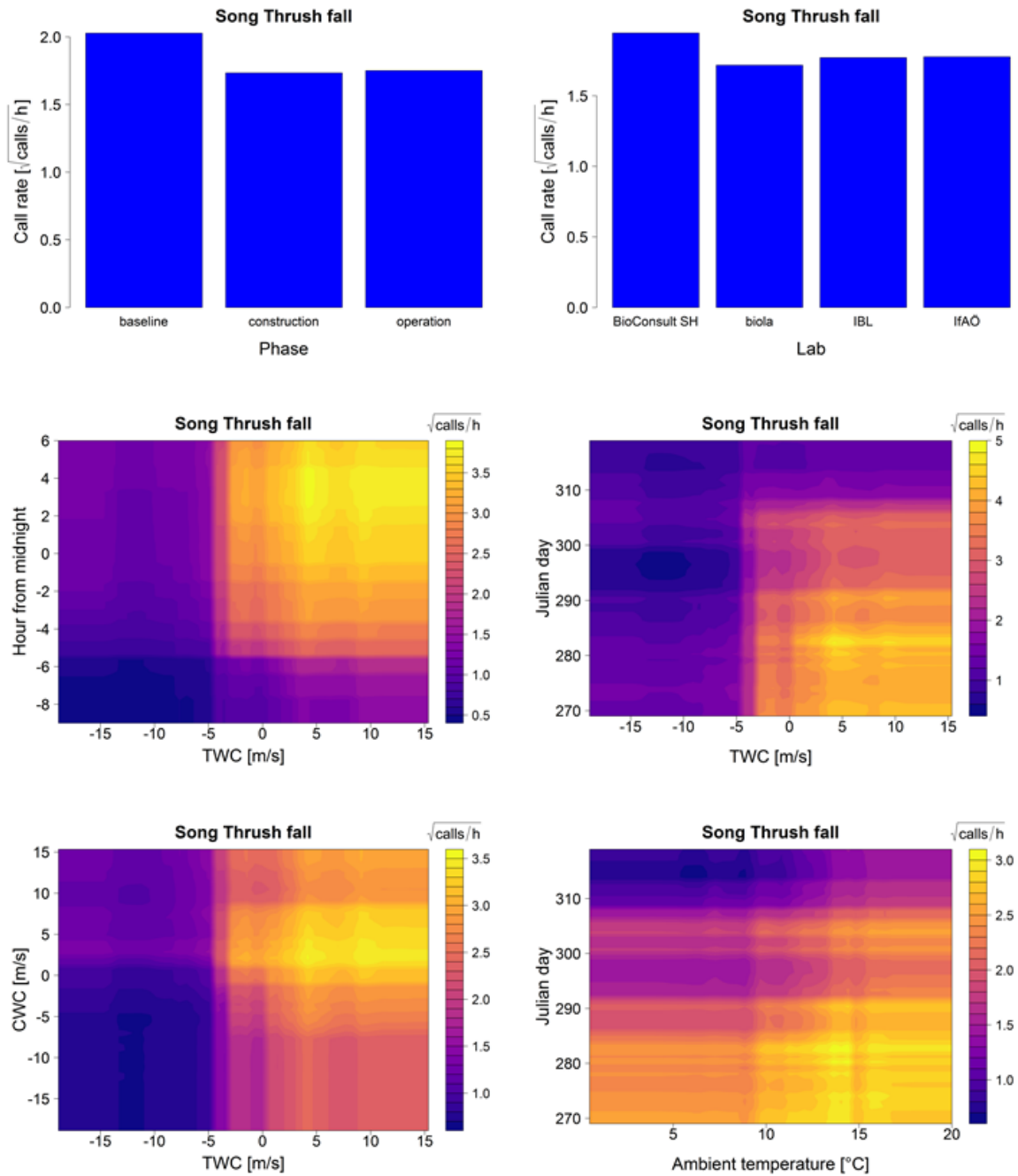


Figure A. 28 *Song Thrush fall*: Top left panel shows the Standardized Error Variable Importance (%IncMSE) plot. Top right panel shows the multi-way importance plot. Below are the partial dependence plots for each variable included in the model (note the different scales of the partial effect on the y-axis). In the lower panels interaction plots are shown: TWC vs CWC, TWC vs Julian day, TWC vs hour from midnight and Julian day vs ambient temperature. Colours of the interaction plots represent the predicted bird call rate (square root transformed) for each combination of effects.

Fieldfare

Spring

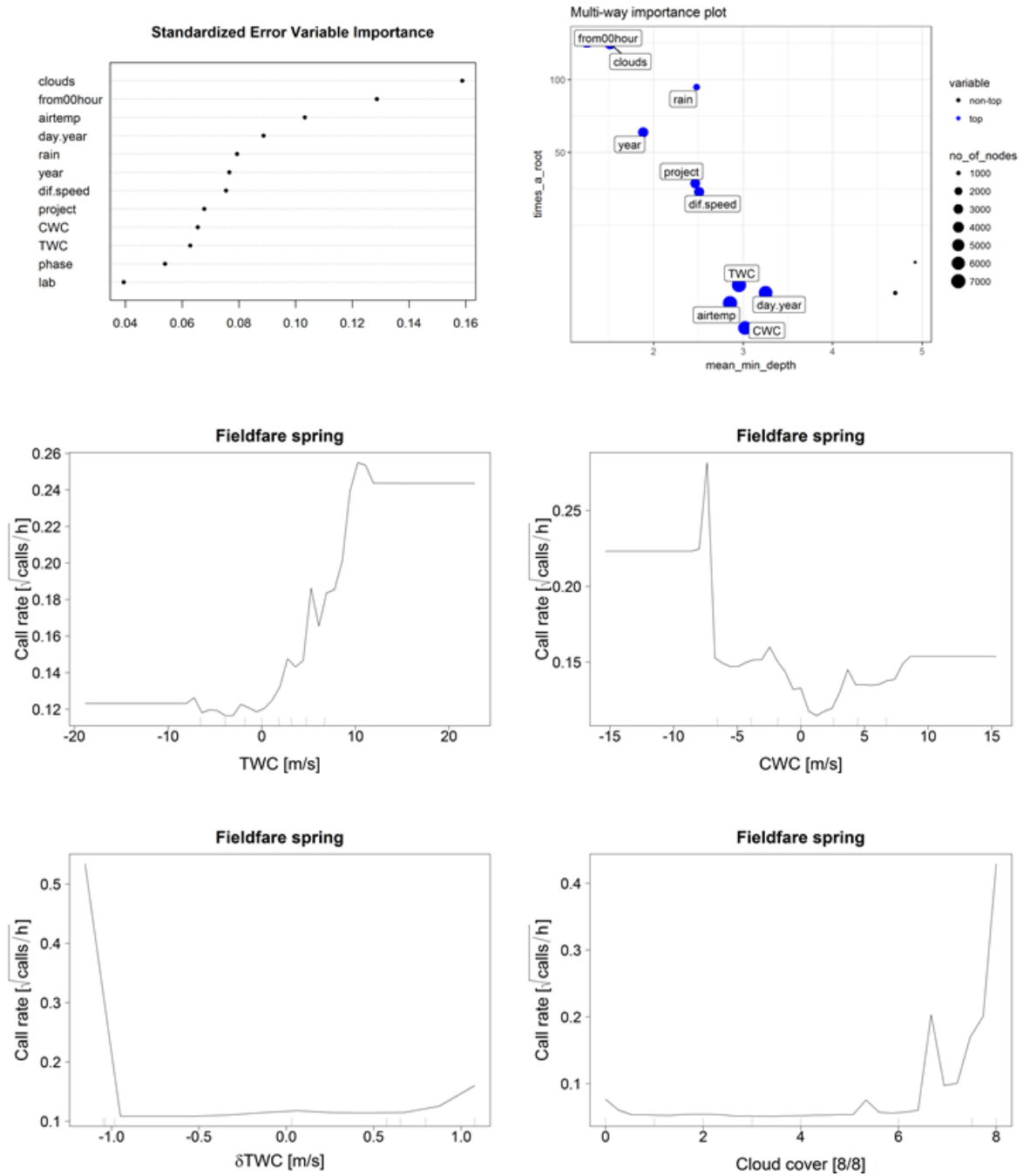


Figure A. 27 Fieldfare spring, continued on next page.

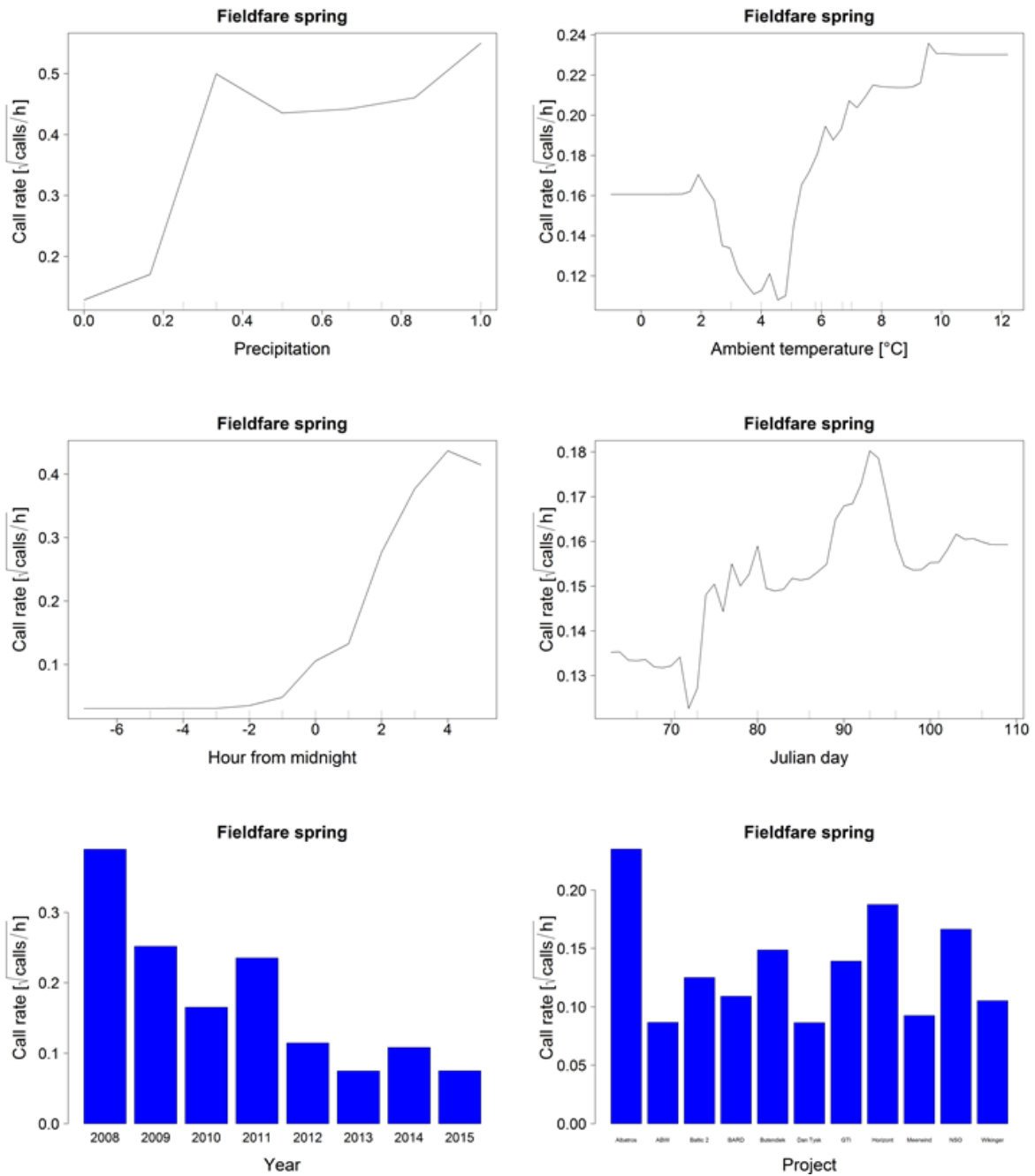


Figure A. 27 Fieldfare spring, continued on next page.

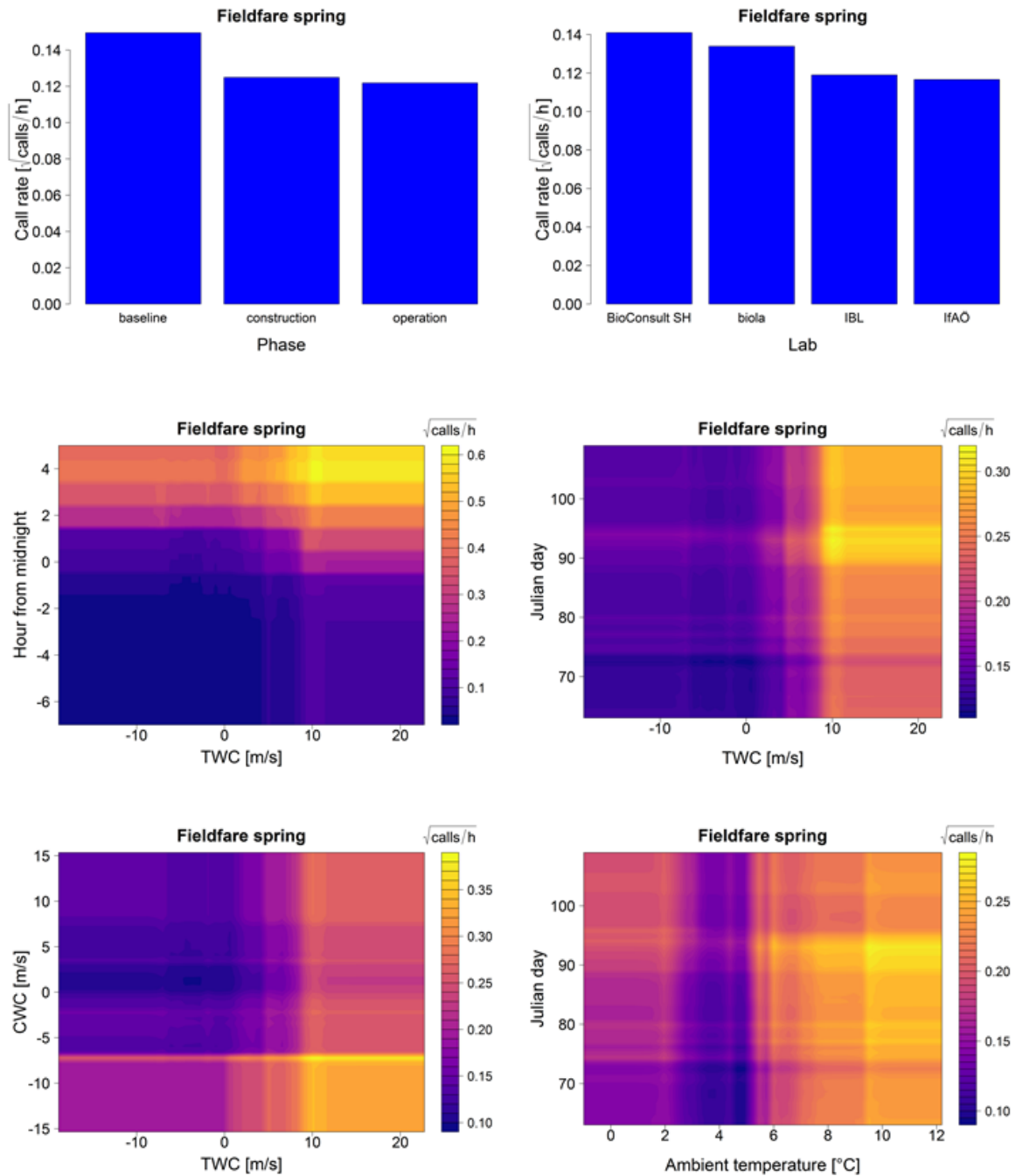


Figure A. 29 Fieldfare spring: Top left panel shows the Standardized Error Variable Importance (%IncMSE) plot. Top right panel shows the multi-way importance plot. Below are the partial dependence plots for each variable included in the model (note the different scales of the partial effect on the y-axis). In the lower panels interaction plots are shown: TWC vs CWC, TWC vs Julian day, TWC vs hour from midnight and Julian day vs ambient temperature. Colours of the interaction plots represent the predicted bird call rate (square root transformed) for each combination of effects.

Fall

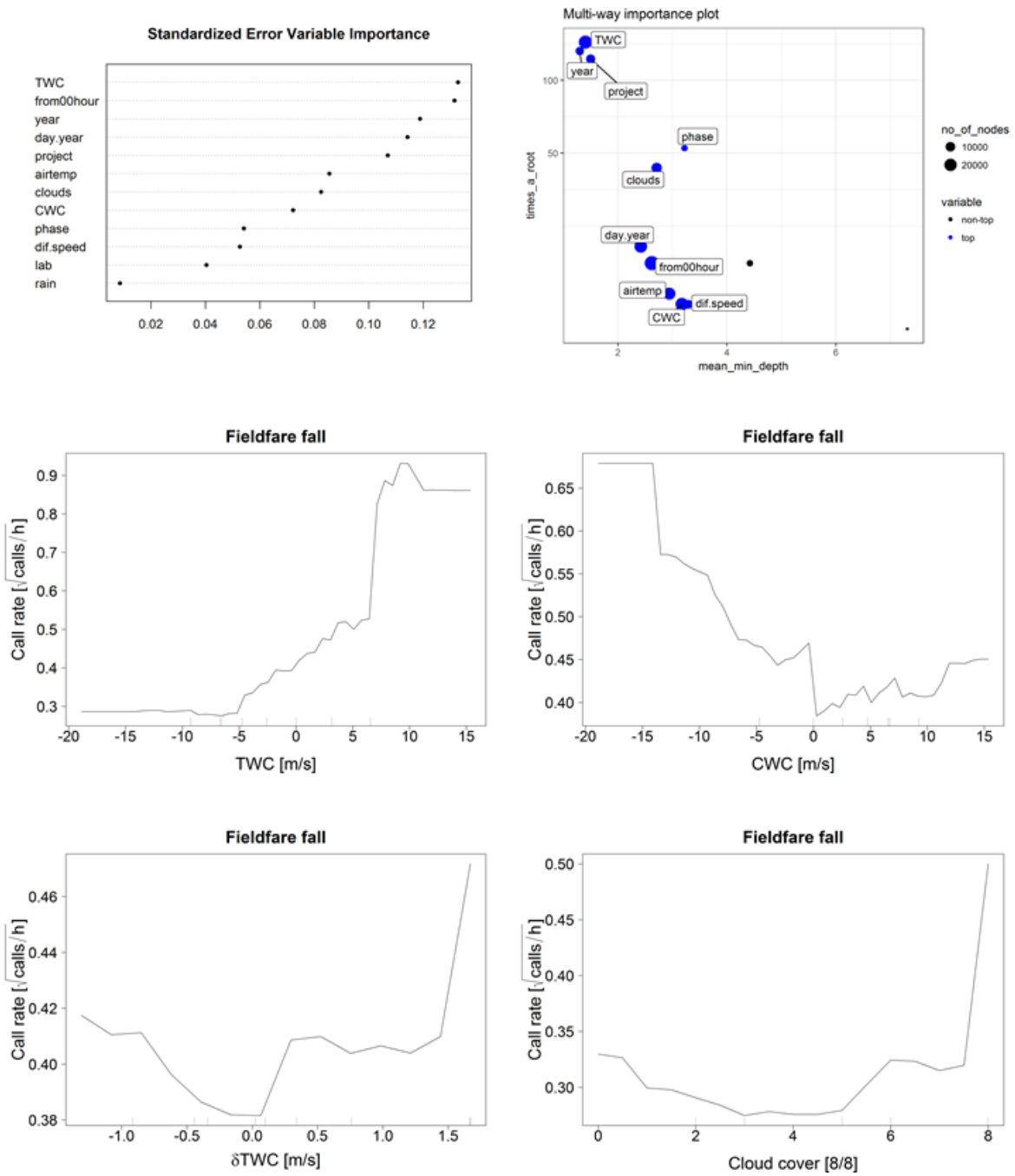


Figure A. 28 Fieldfare fall, continued on next page.

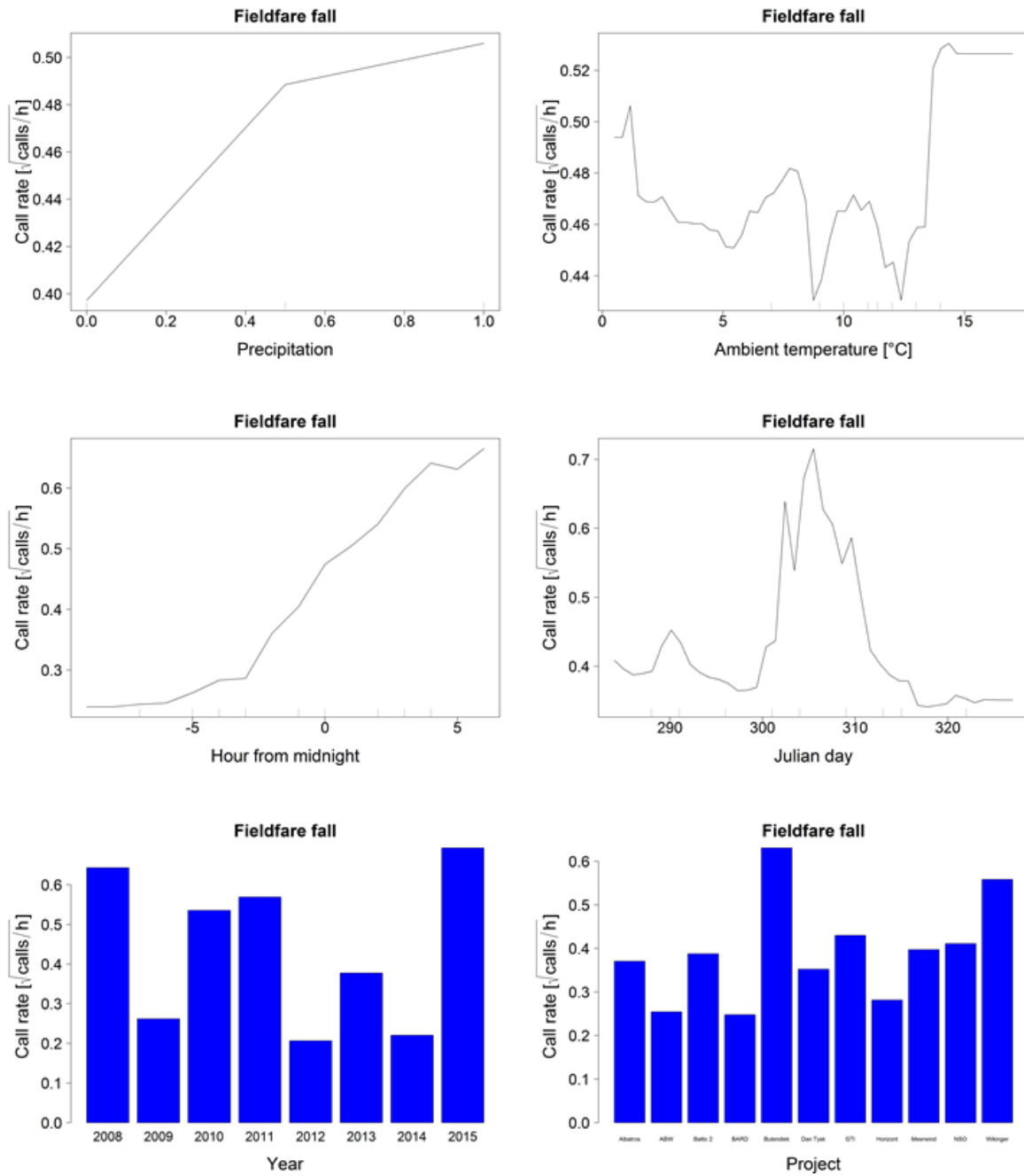


Figure A. 28 Fieldfare fall, continued on next page.

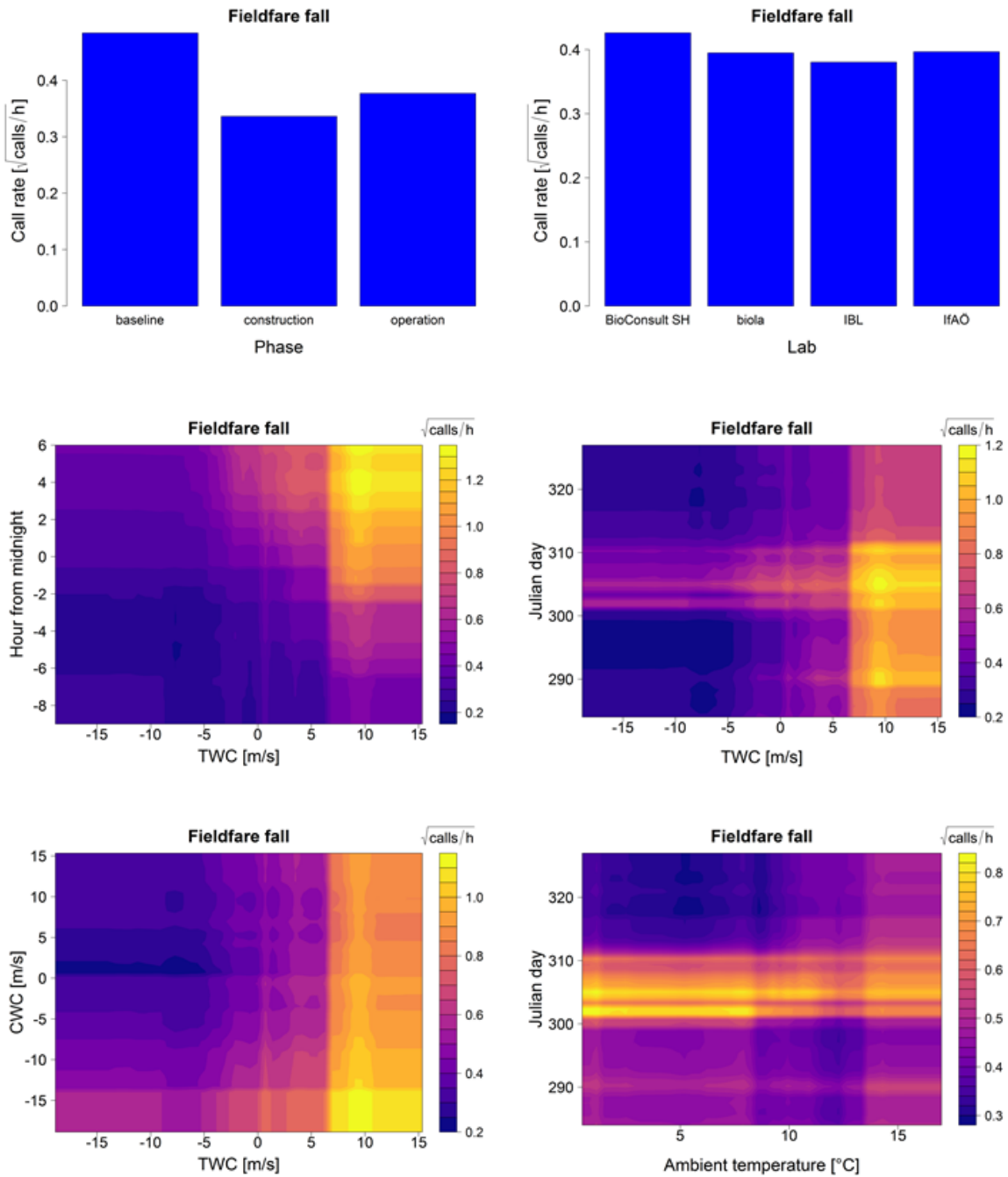


Figure A. 30 *Fieldfare fall*: Top left panel shows the Standardized Error Variable Importance (%IncMSE) plot. Top right panel shows the multi-way importance plot. Below are the partial dependence plots for each variable included in the model (note the different scales of the partial effect on the y-axis). In the lower panels interaction plots are shown: TWC vs CWC, TWC vs Julian day, TWC vs hour from midnight and Julian day vs ambient temperature. Colours of the interaction plots represent the predicted bird call rate (square root transformed) for each combination of effects.

Meadow Pipit

Spring

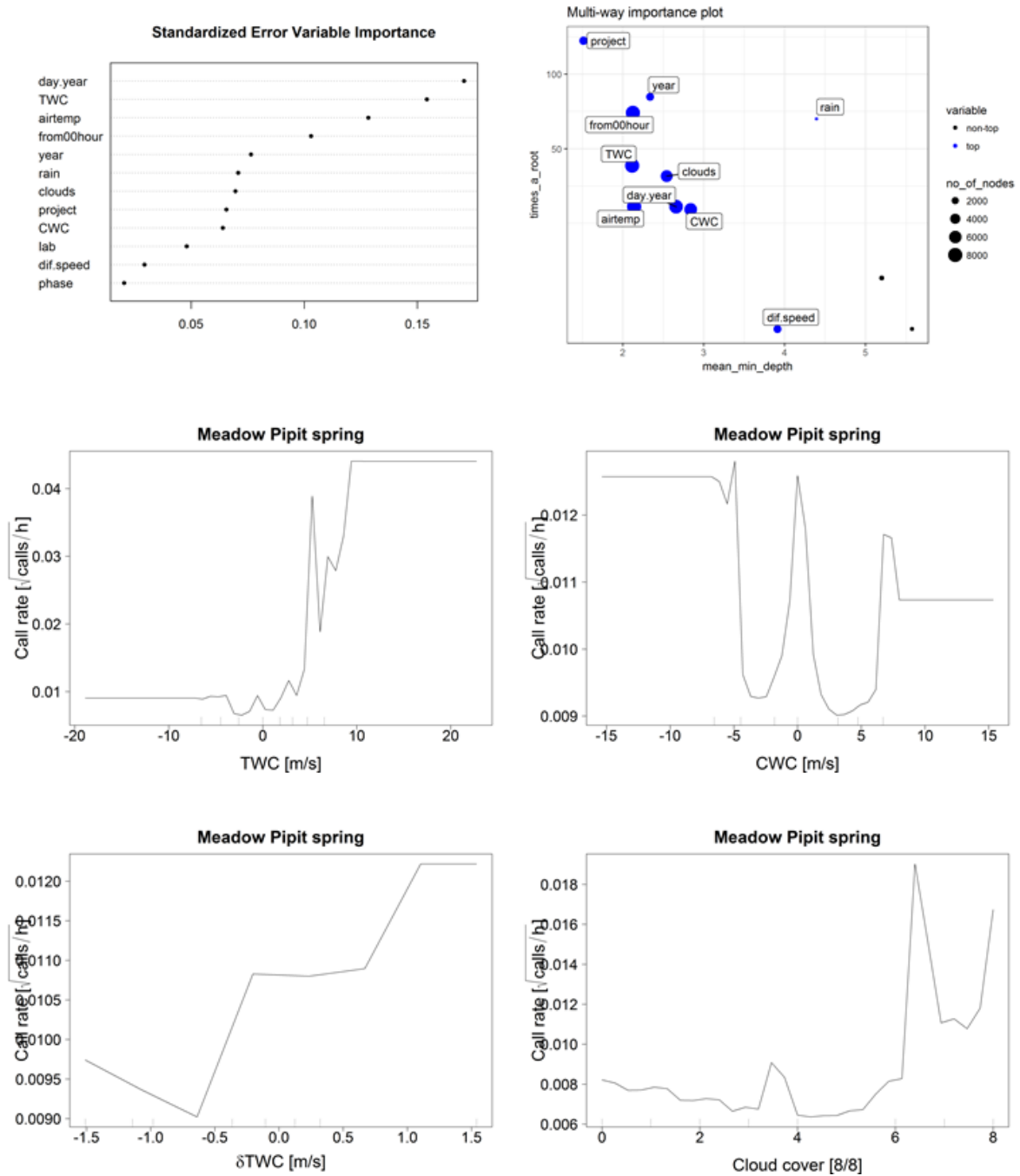


Figure A. 29 Meadow Pipit spring, continued on next page.

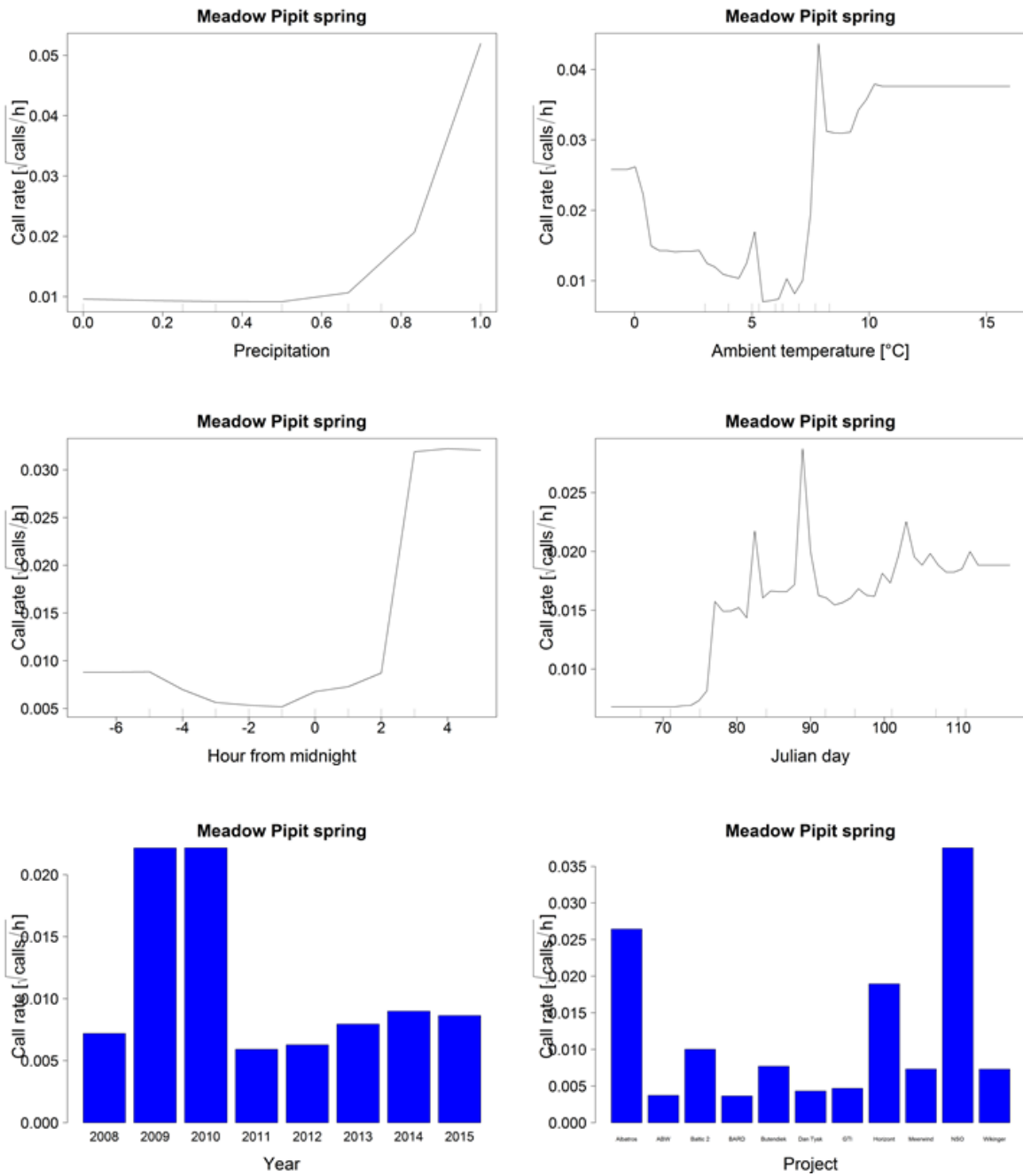


Figure A. 29 Meadow Pipit spring, continued on next page.

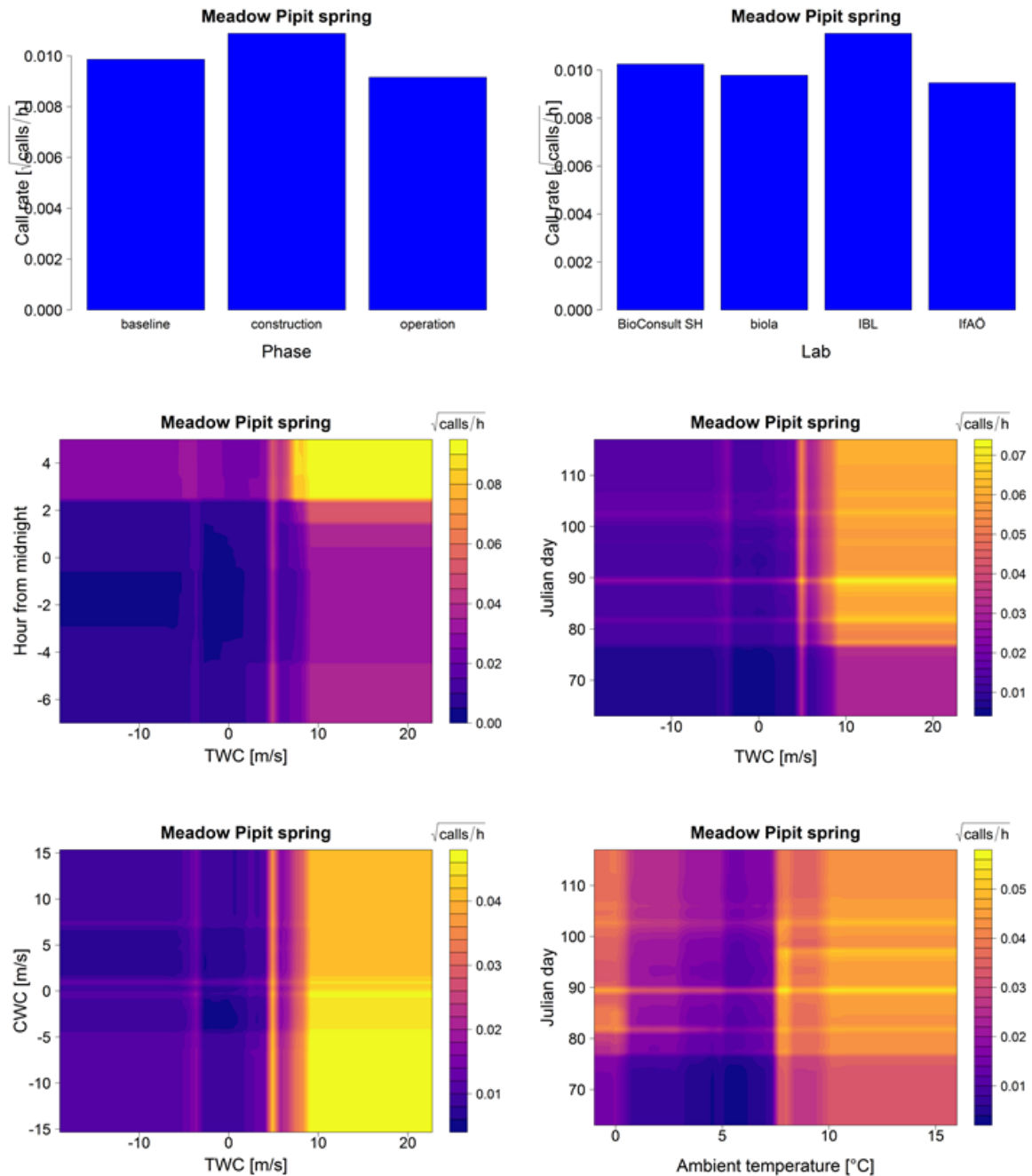


Figure A.31 Meadow Pipit spring: Top left panel shows the Standardized Error Variable Importance (%IncMSE) plot. Top right panel shows the multi-way importance plot. Below are the partial dependence plots for each variable included in the model (note the different scales of the partial effect on the y-axis). In the lower panels interaction plots are shown: TWC vs CWC, TWC vs Julian day, TWC vs hour from midnight and Julian day vs ambient temperature. Colours of the interaction plots represent the predicted bird call rate (square root transformed) for each combination of effects.

Fall

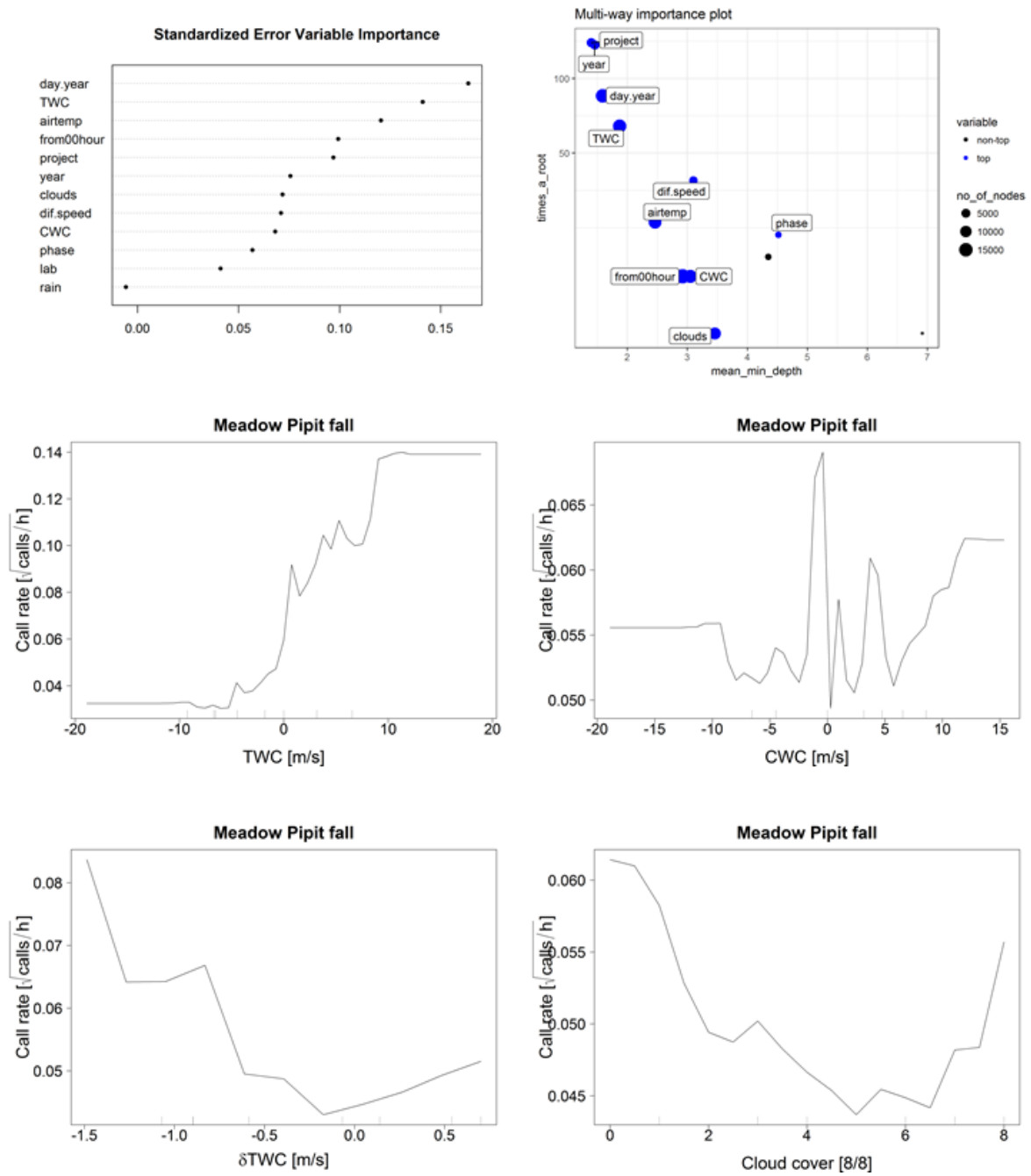


Figure A. 30 Meadow Pipit fall, continued on next page.

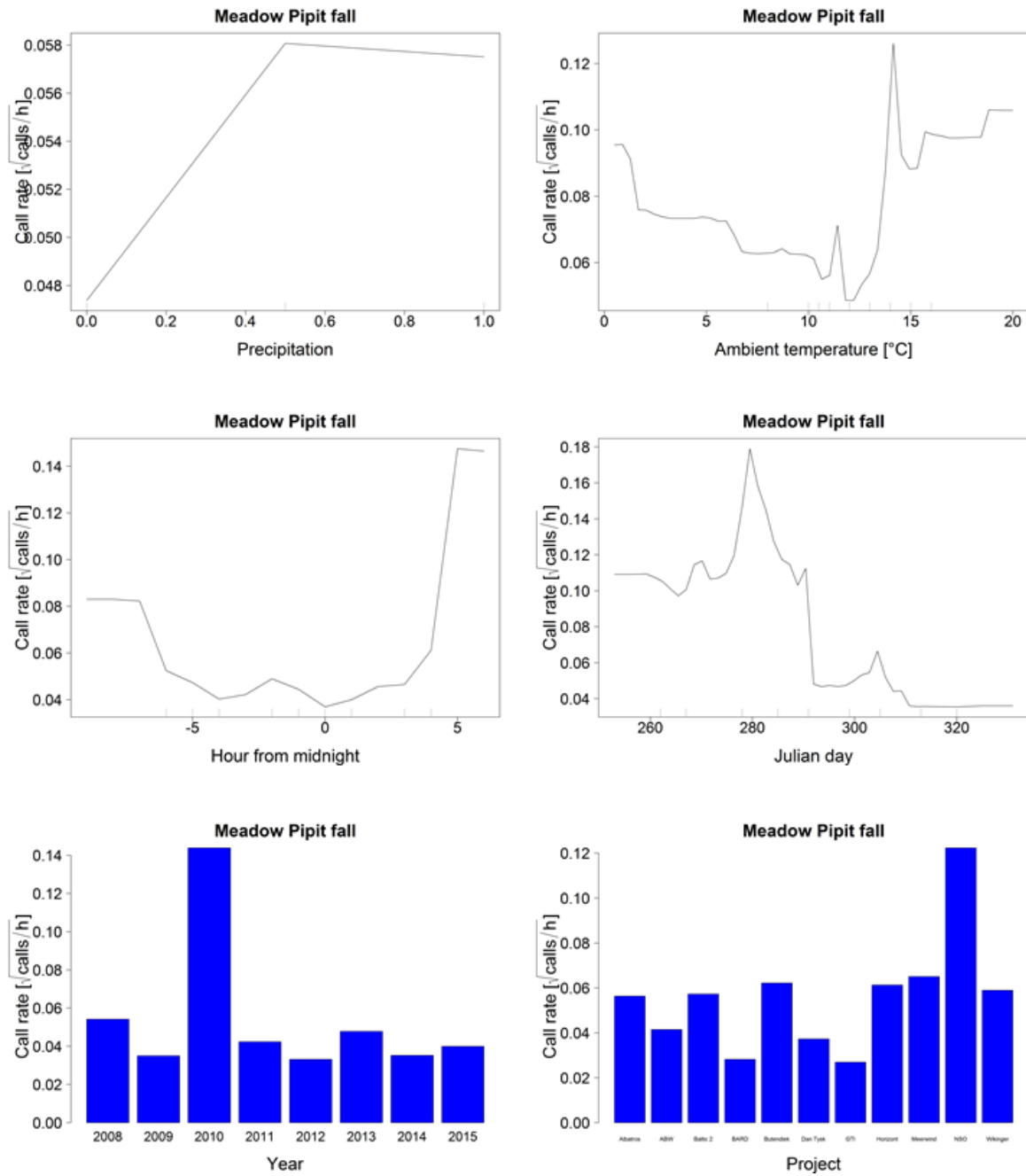


Figure A. 30 Meadow Pipit fall, continued on next page.

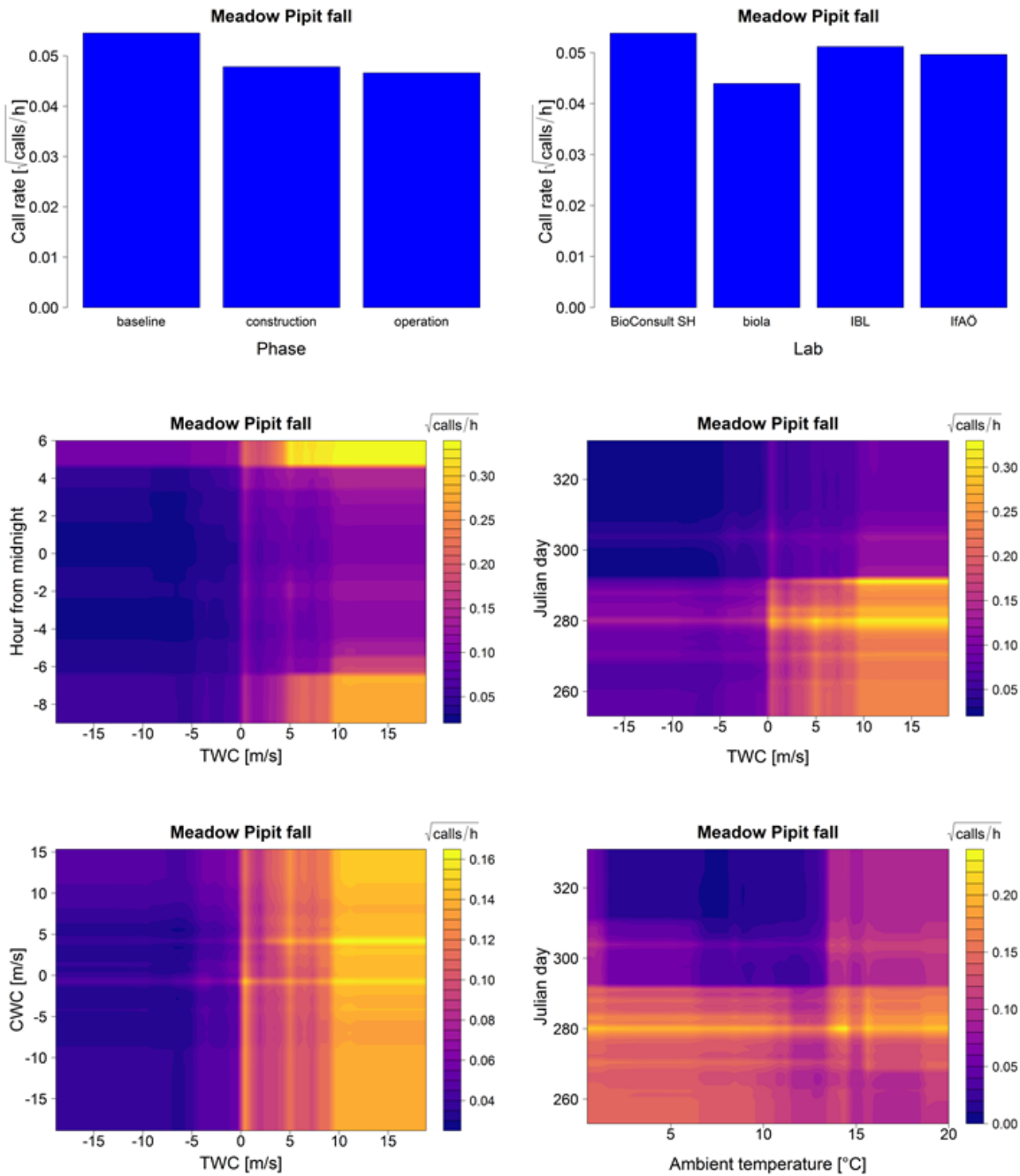


Figure A.32 Meadow Pipit fall: Top left panel shows the Standardized Error Variable Importance (%IncMSE) plot. Top right panel shows the multi-way importance plot. Below are the partial dependence plots for each variable included in the model (note the different scales of the partial effect on the y-axis). In the lower panels interaction plots are shown: TWC vs CWC, TWC vs Julian day, TWC vs hour from midnight and Julian day vs ambient temperature. Colours of the interaction plots represent the predicted bird call rate (square root transformed) for each combination of effects.

Skylark

Spring

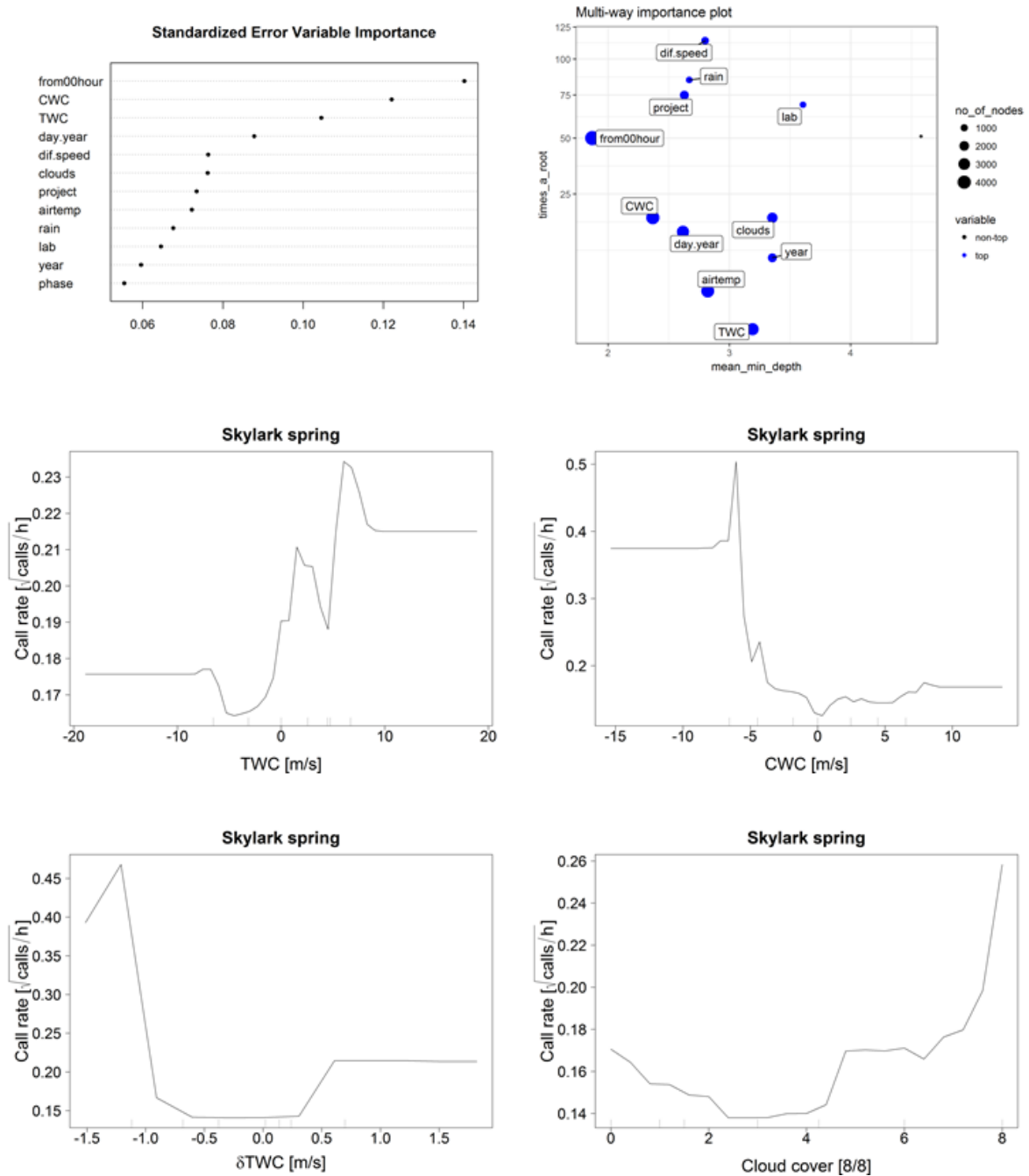


Figure A. 31 Skylark spring, continued on next page.

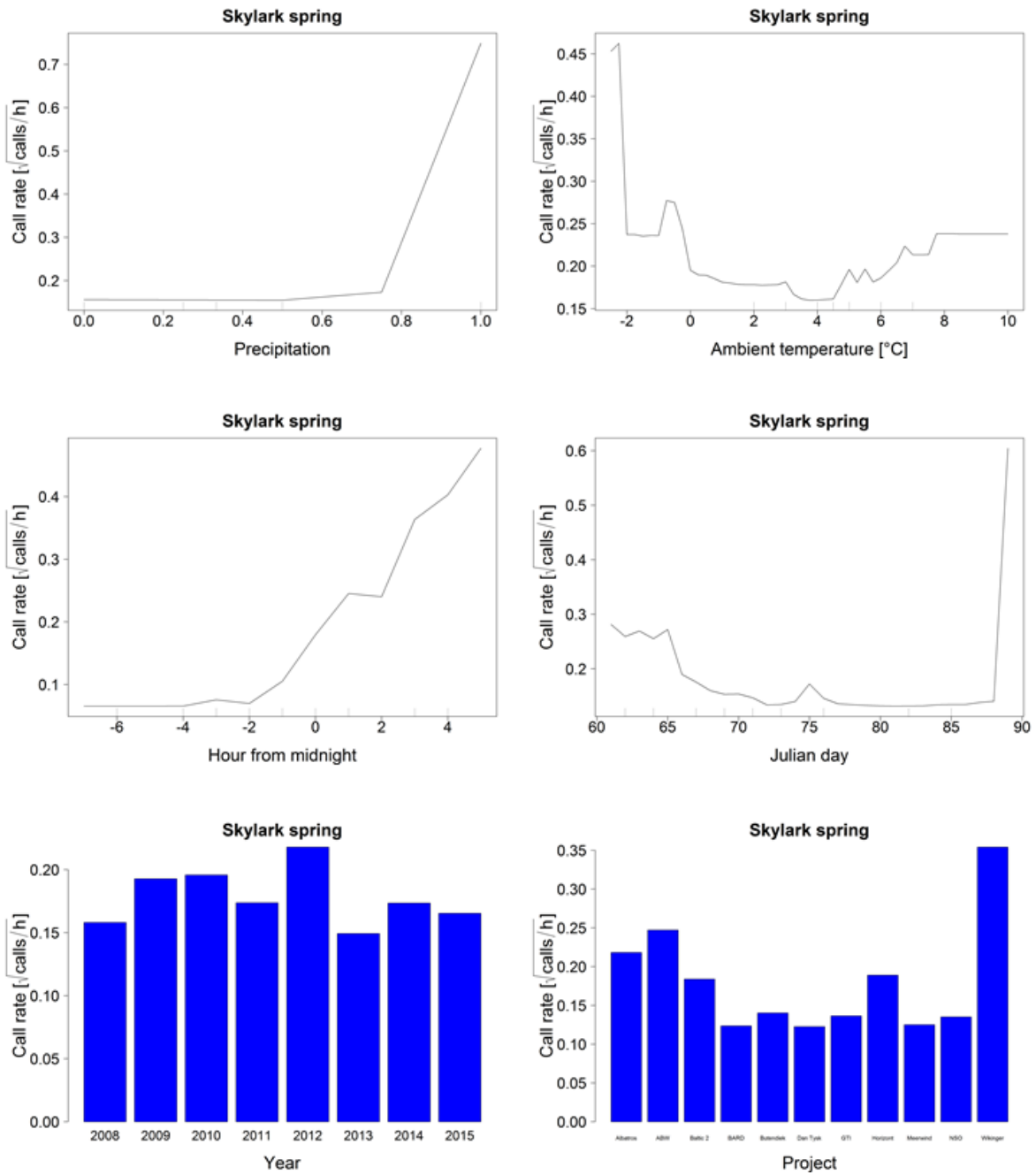


Figure A. 31 Skylark spring, continued on next page.

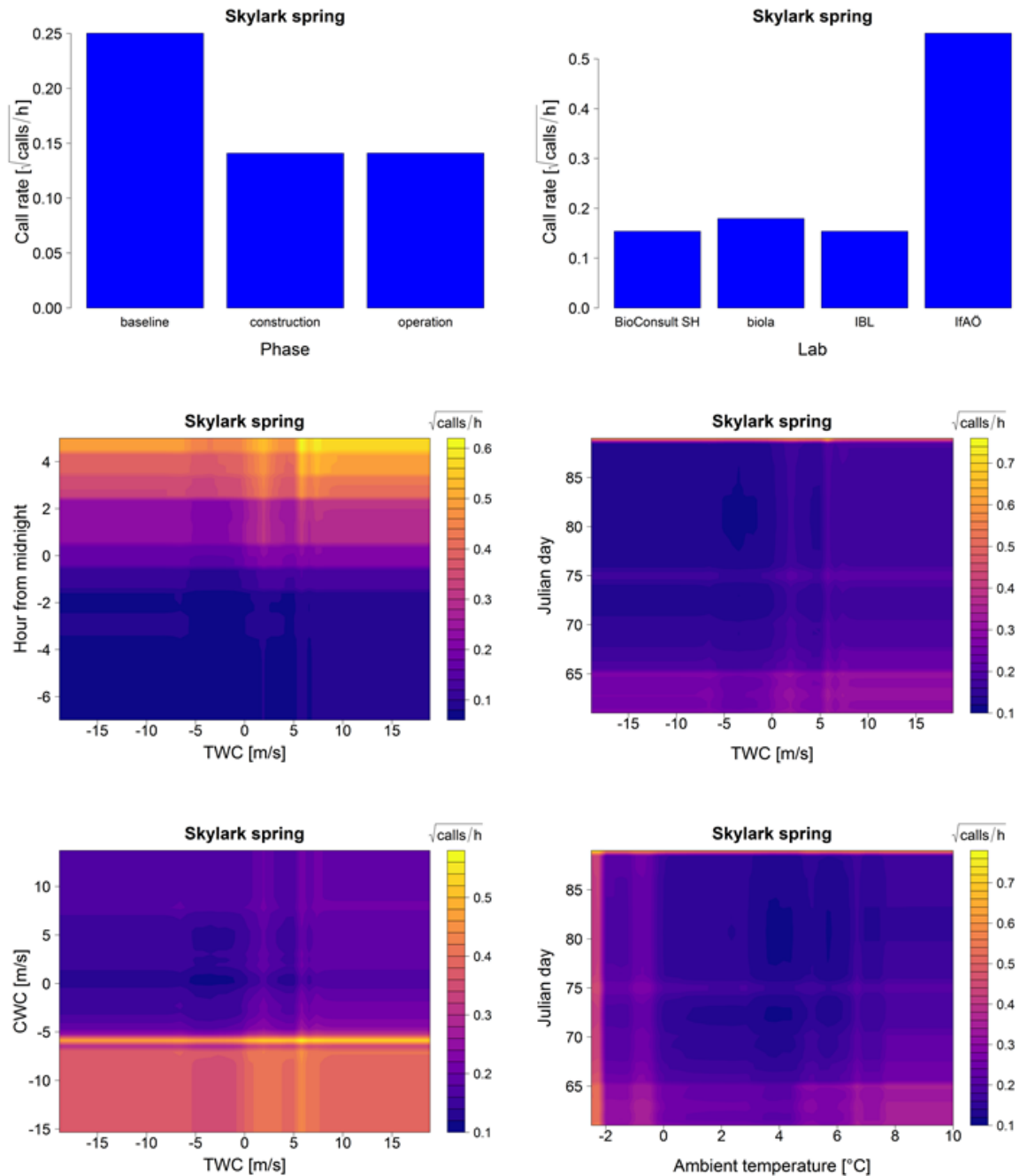


Figure A. 33 Skylark spring: Top left panel shows the Standardized Error Variable Importance (%IncMSE) plot. Top right panel shows the multi-way importance plot. Below are the partial dependence plots for each variable included in the model (note the different scales of the partial effect on the y-axis). In the lower panels interaction plots are shown: TWC vs CWC, TWC vs Julian day, TWC vs hour from midnight and Julian day vs ambient temperature. Colours of the interaction plots represent the predicted bird call rate (square root transformed) for each combination of effects.

Fall

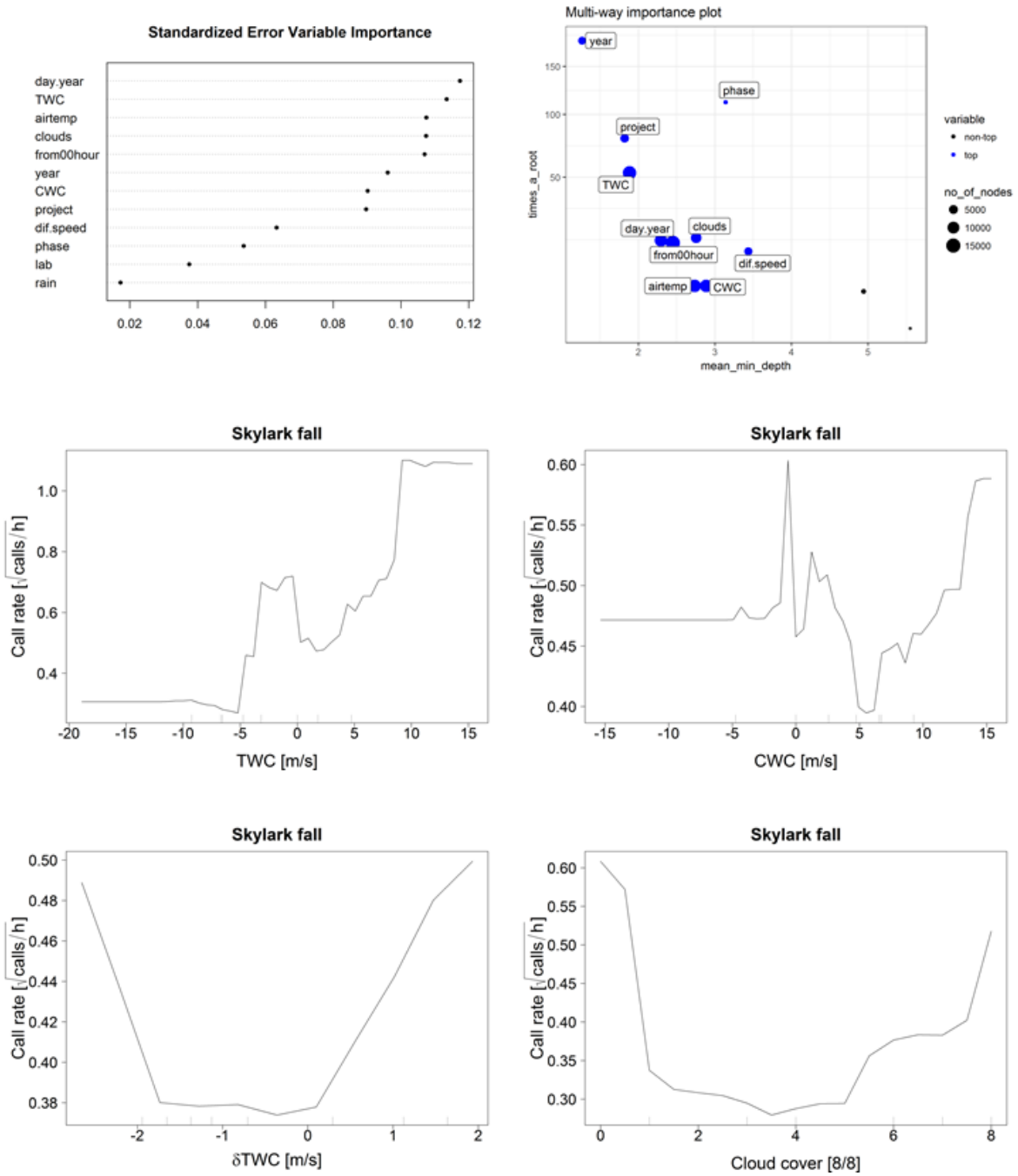


Figure A.32 Skylark fall, continued on next page.

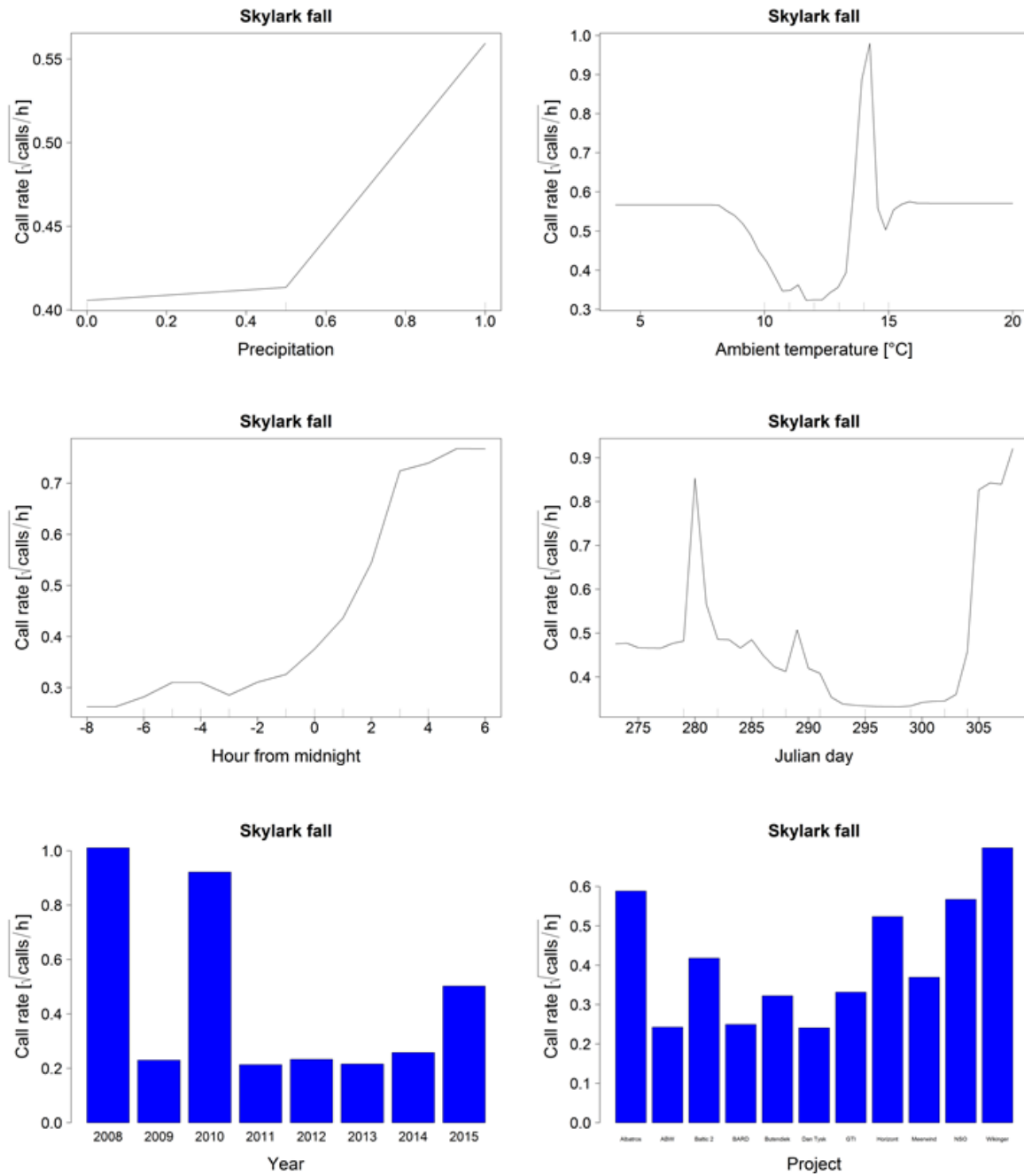


Figure A. 32 Skylark fall, continued on next page.

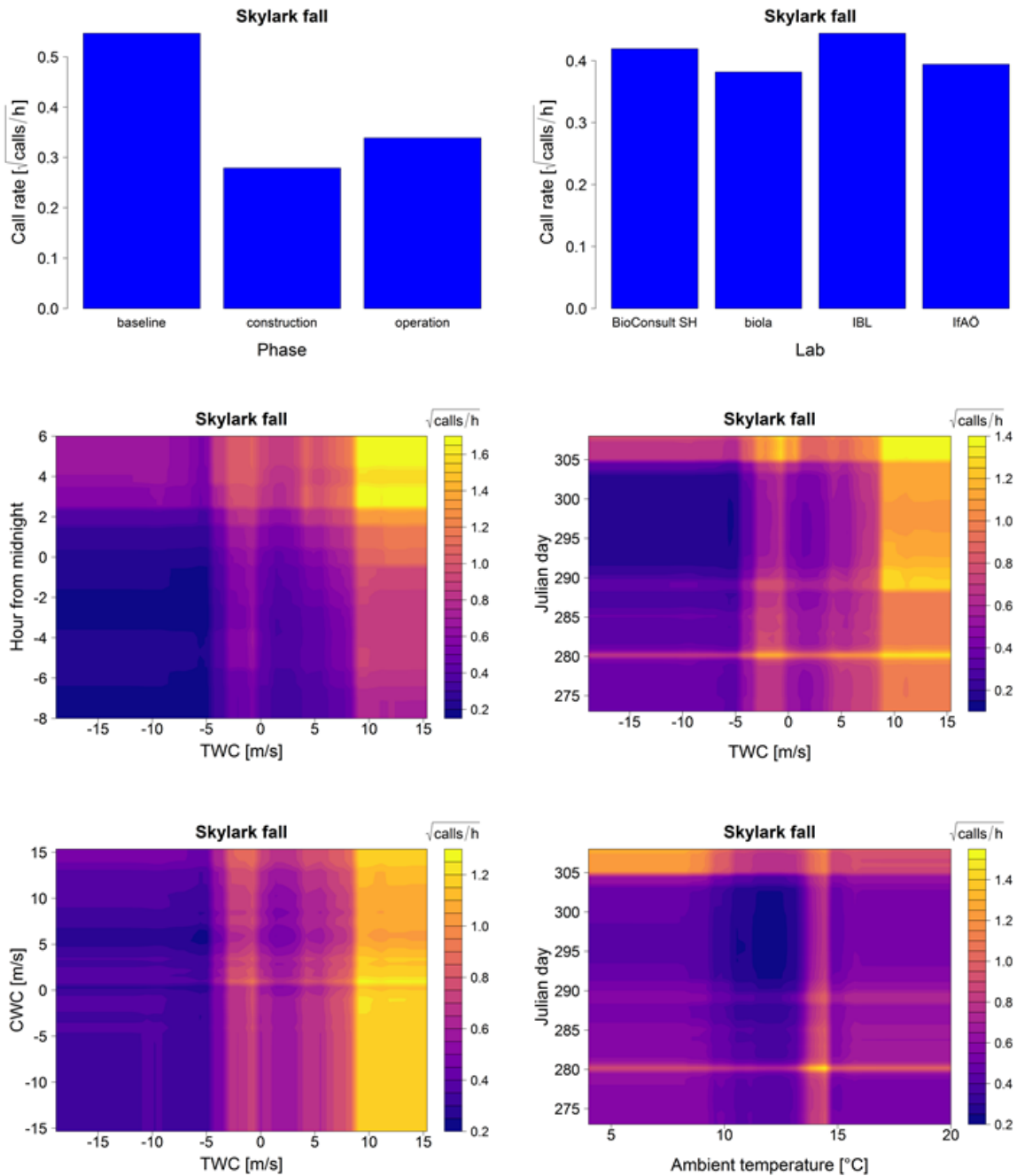


Figure A. 34 Skylark fall: Top left panel shows the Standardized Error Variable Importance (%IncMSE) plot. Top right panel shows the multi-way importance plot. Below are the partial dependence plots for each variable included in the model (note the different scales of the partial effect on the y-axis). In the lower panels interaction plots are shown: TWC vs CWC, TWC vs Julian day, TWC vs hour from midnight and Julian day vs ambient temperature. Colours of the interaction plots represent the predicted bird call rate (square root transformed) for each combination of effects.

Robin

Spring

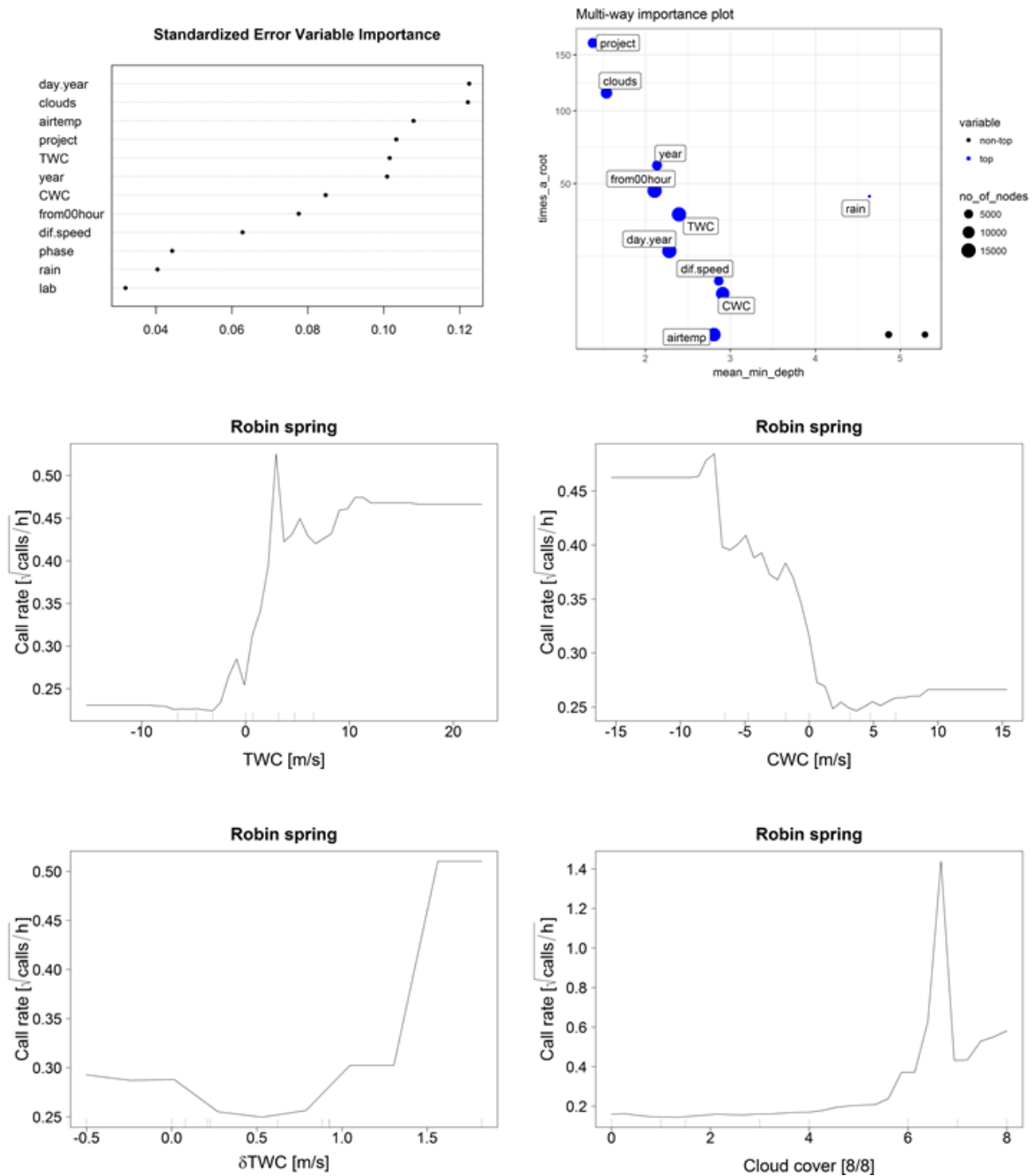


Figure A. 33 Robin spring, continued on next page.

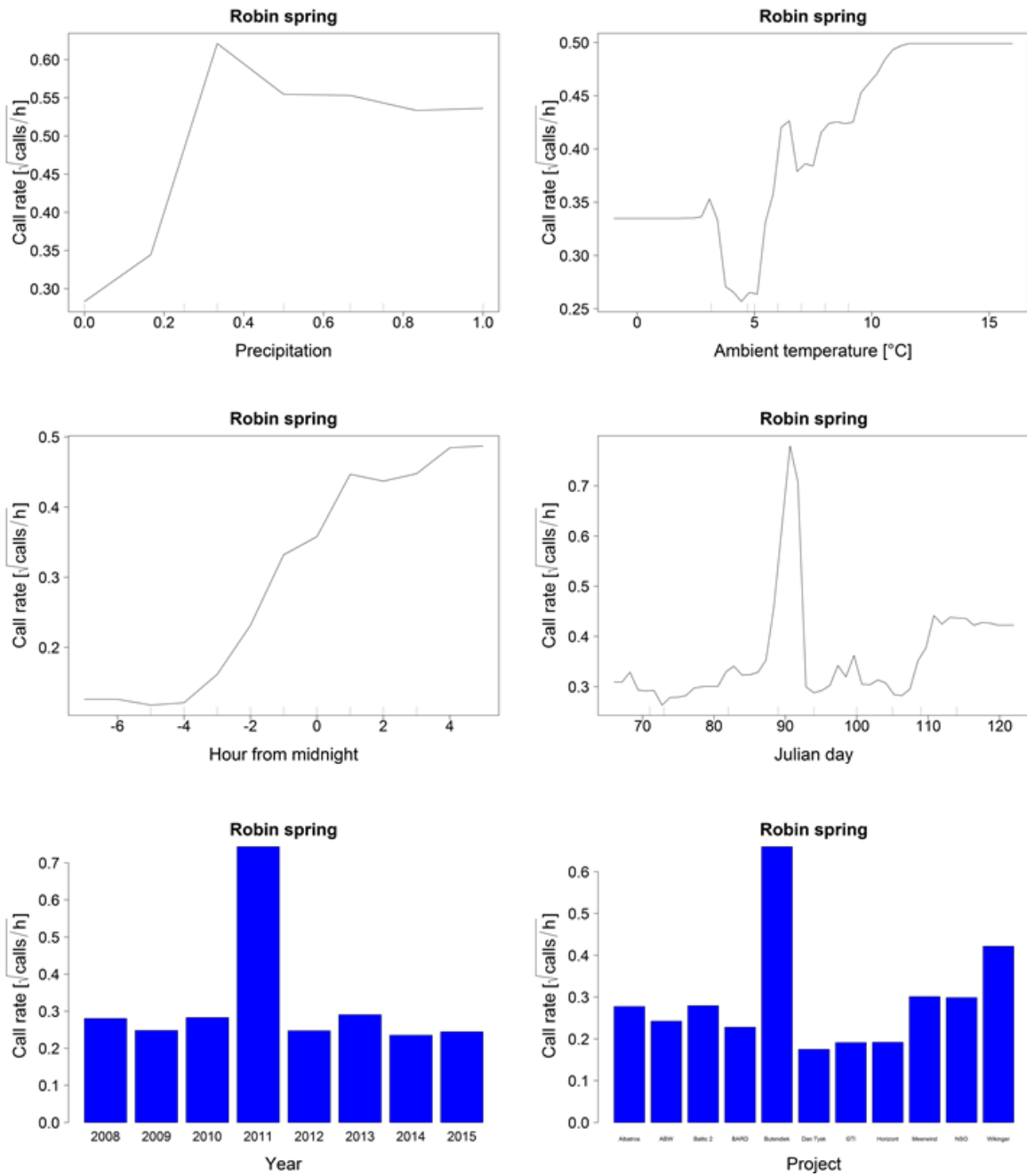


Figure A. 33 Robin spring, continued on next page.

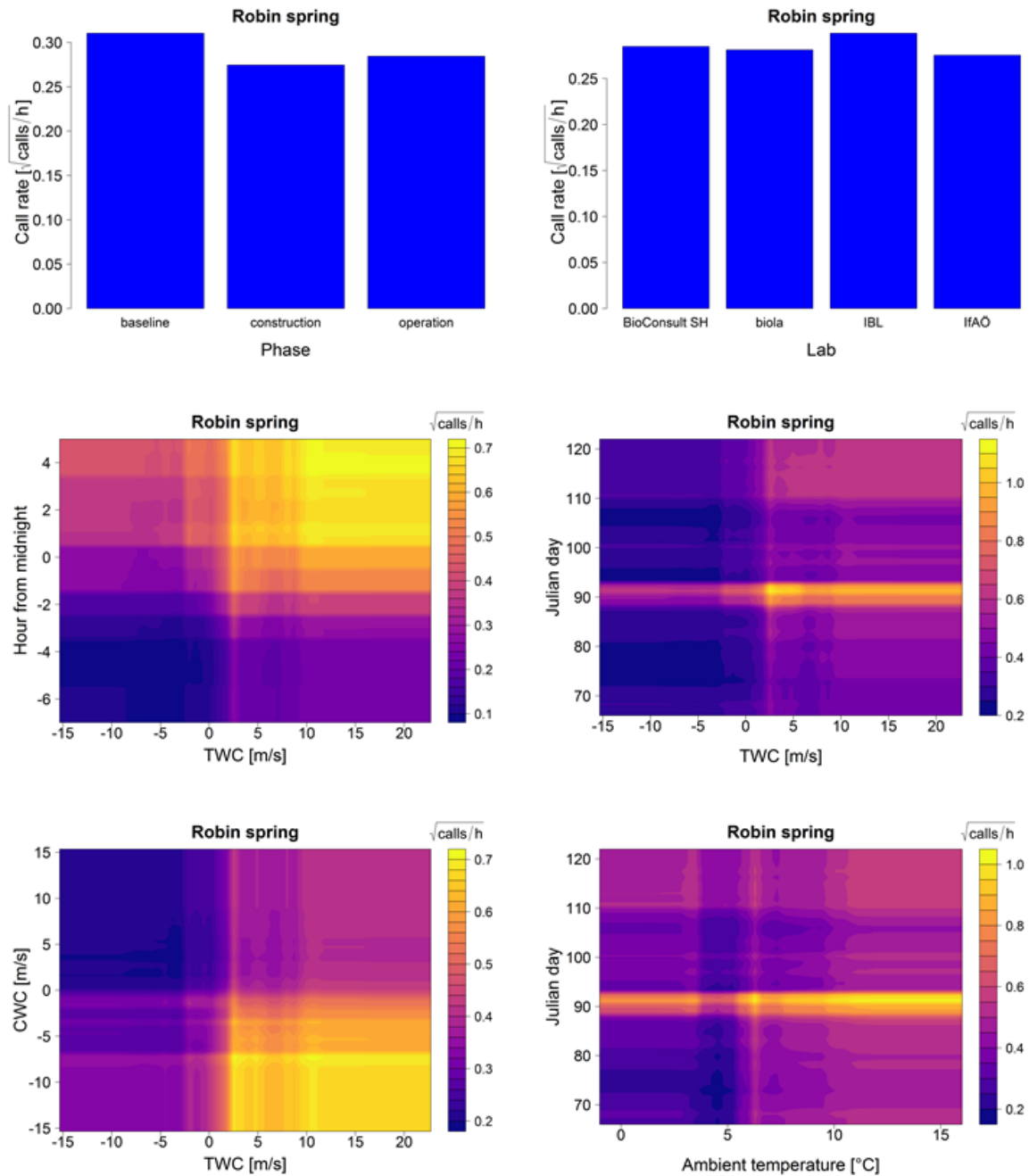


Figure A. 35 *Robin spring*: Top left panel shows the Standardized Error Variable Importance (%IncMSE) plot. Top right panel shows the multi-way importance plot. Below are the partial dependence plots for each variable included in the model (note the different scales of the partial effect on the y-axis). In the lower panels interaction plots are shown: TWC vs CWC, TWC vs Julian day, TWC vs hour from midnight and Julian day vs ambient temperature. Colours of the interaction plots represent the predicted bird call rate (square root transformed) for each combination of effects.

Fall

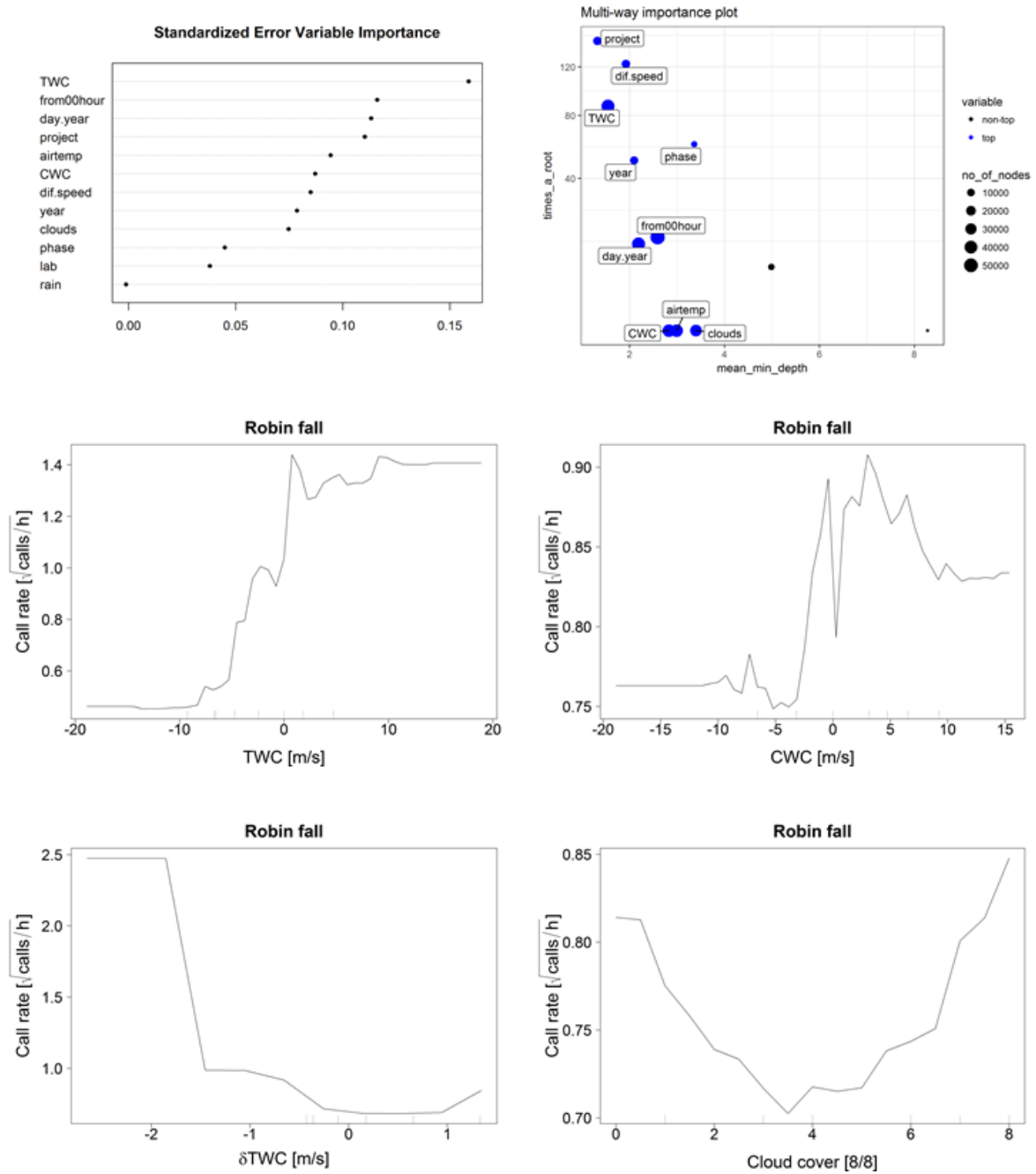


Figure A. 34 Robin fall, continued on next page.

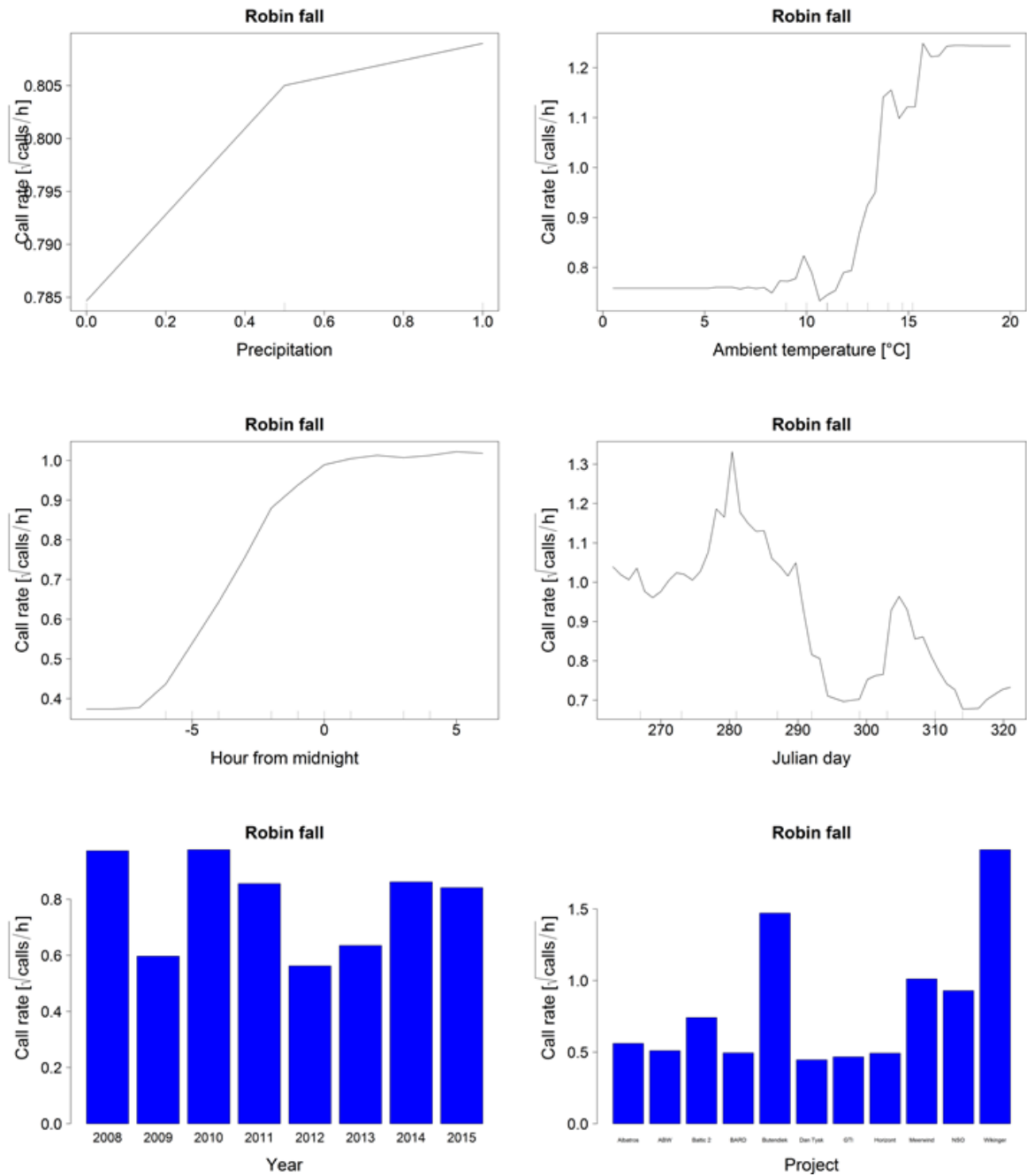


Figure A. 34 Robin fall, continued on next page.

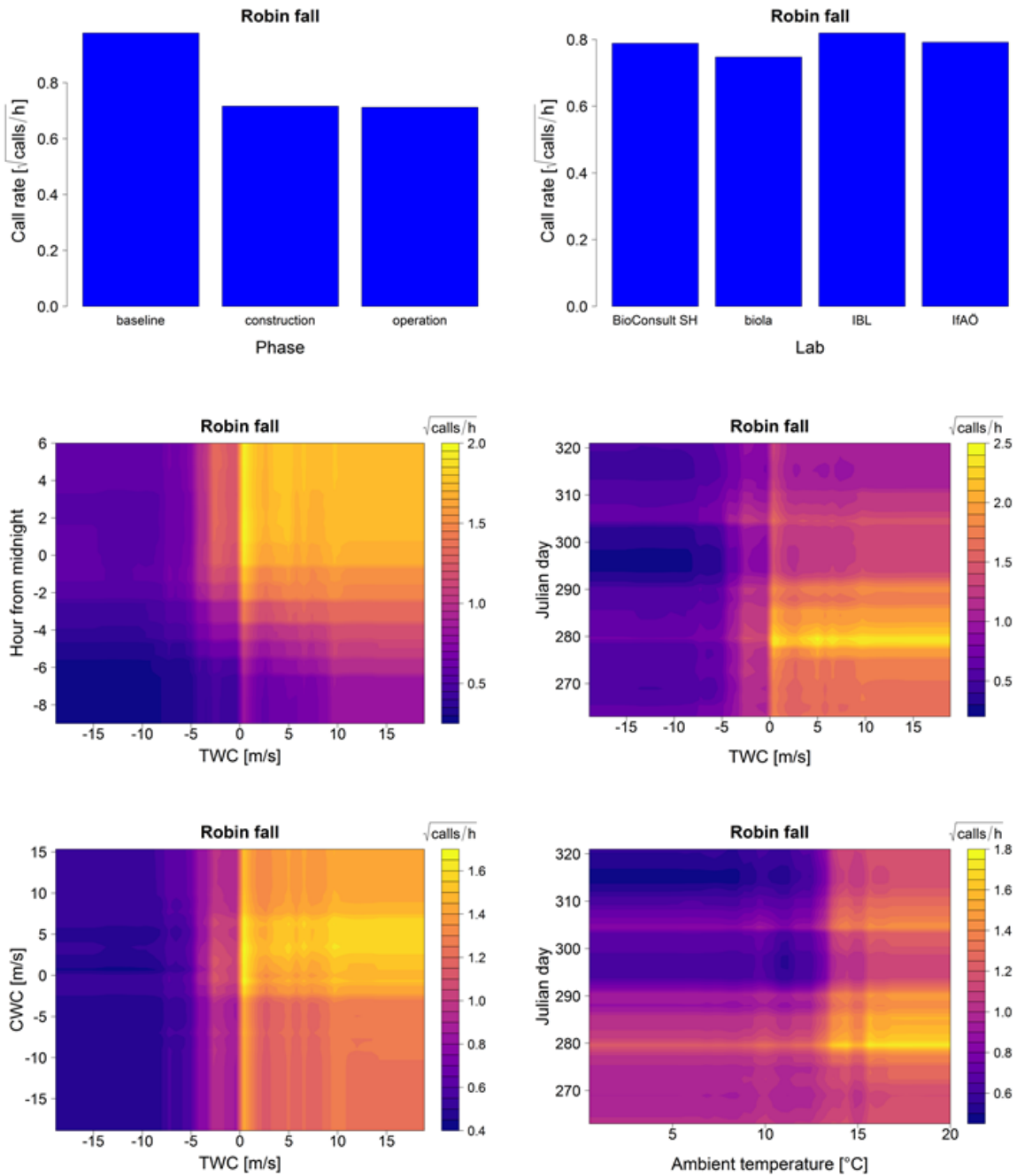


Figure A. 36 Robin fall: Top left panel shows the Standardized Error Variable Importance (%IncMSE) plot. Top right panel shows the multi-way importance plot. Below are the partial dependence plots for each variable included in the model (note the different scales of the partial effect on the y-axis). In the lower panels interaction plots are shown: TWC vs CWC, TWC vs Julian day, TWC vs hour from midnight and Julian day vs ambient temperature. Colours of the interaction plots represent the predicted bird call rate (square root transformed) for each combination of effects.

Starling

Spring

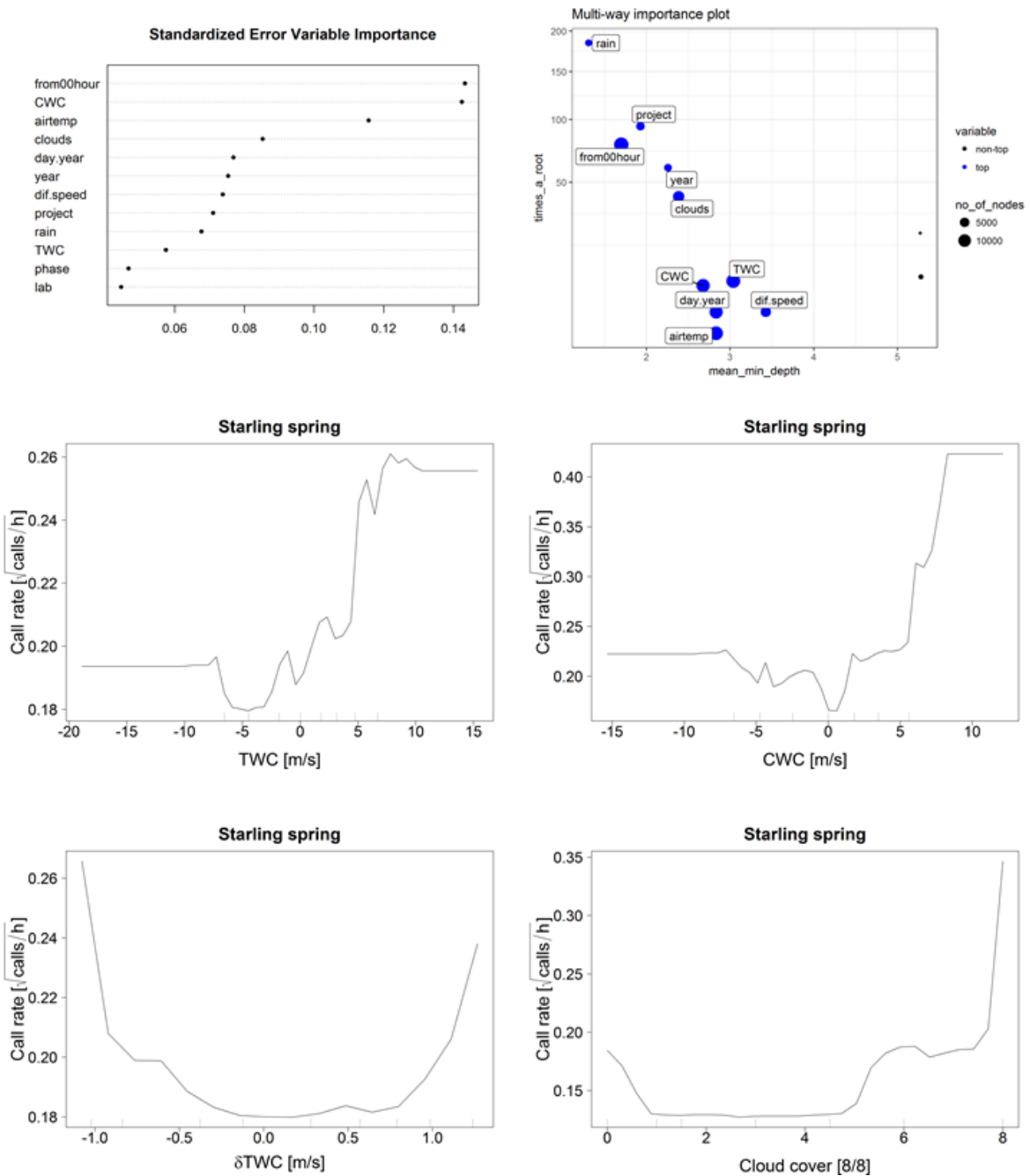


Figure A. 35 Starling spring, continued on next page.

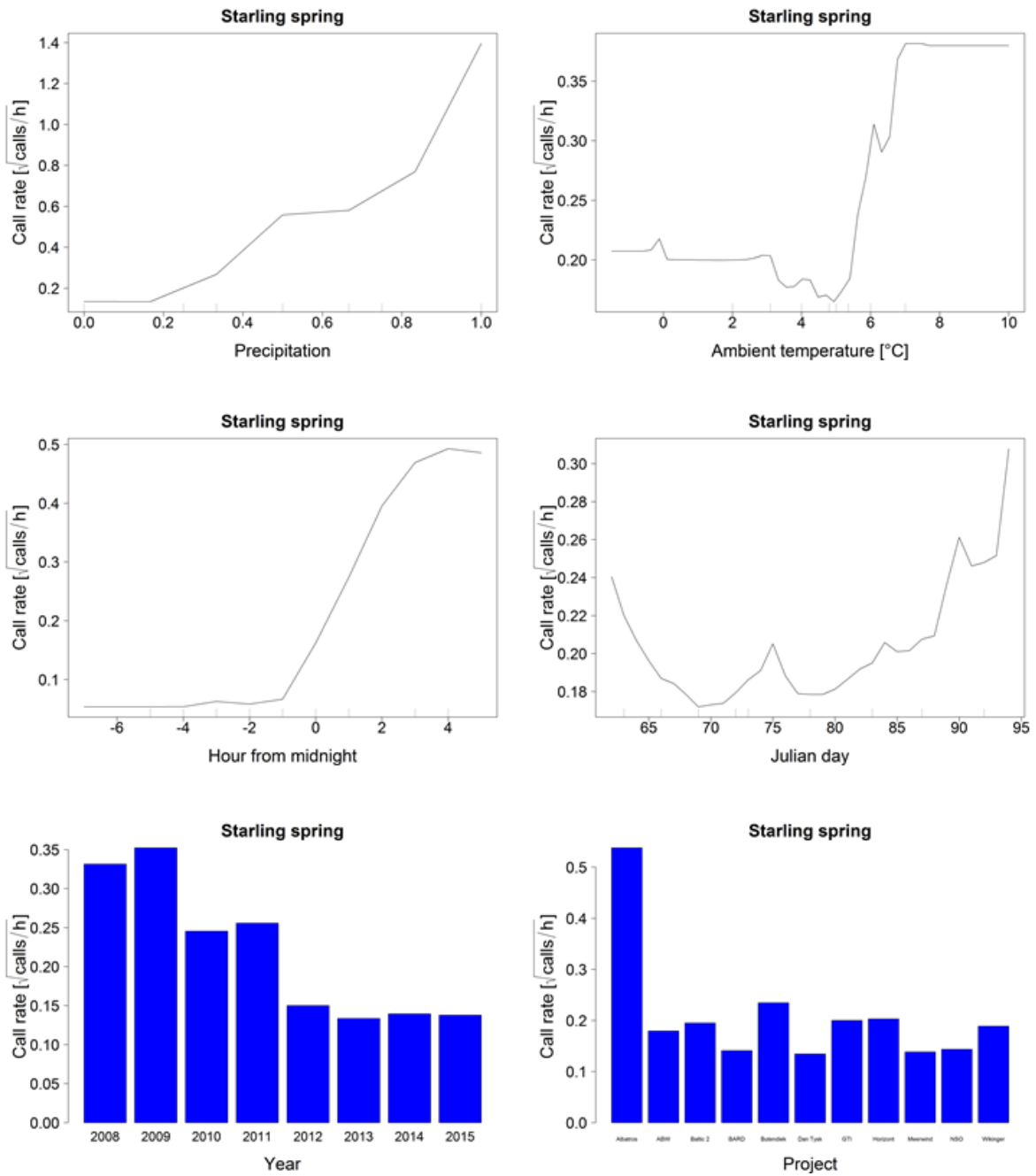


Figure A. 35 Starling spring, continued on next page.

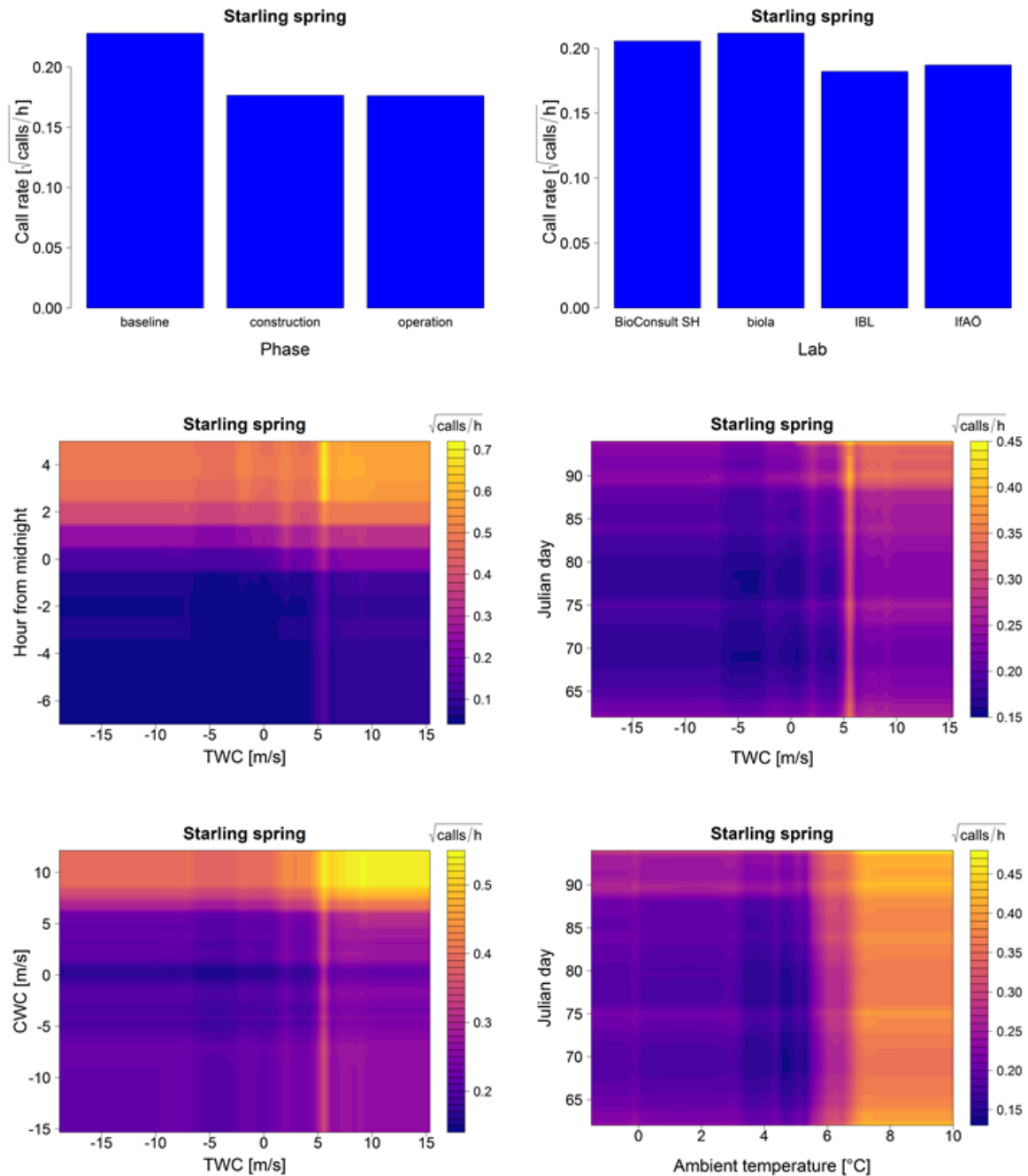


Figure A. 37 *Starling spring*: Top left panel shows the Standardized Error Variable Importance (%IncMSE) plot. Top right panel shows the multi-way importance plot. Below are the partial dependence plots for each variable included in the model (note the different scales of the partial effect on the y-axis). In the lower panels interaction plots are shown: TWC vs CWC, TWC vs Julian day, TWC vs hour from midnight and Julian day vs ambient temperature. Colours of the interaction plots represent the predicted bird call rate (square root transformed) for each combination of effects.

Fall

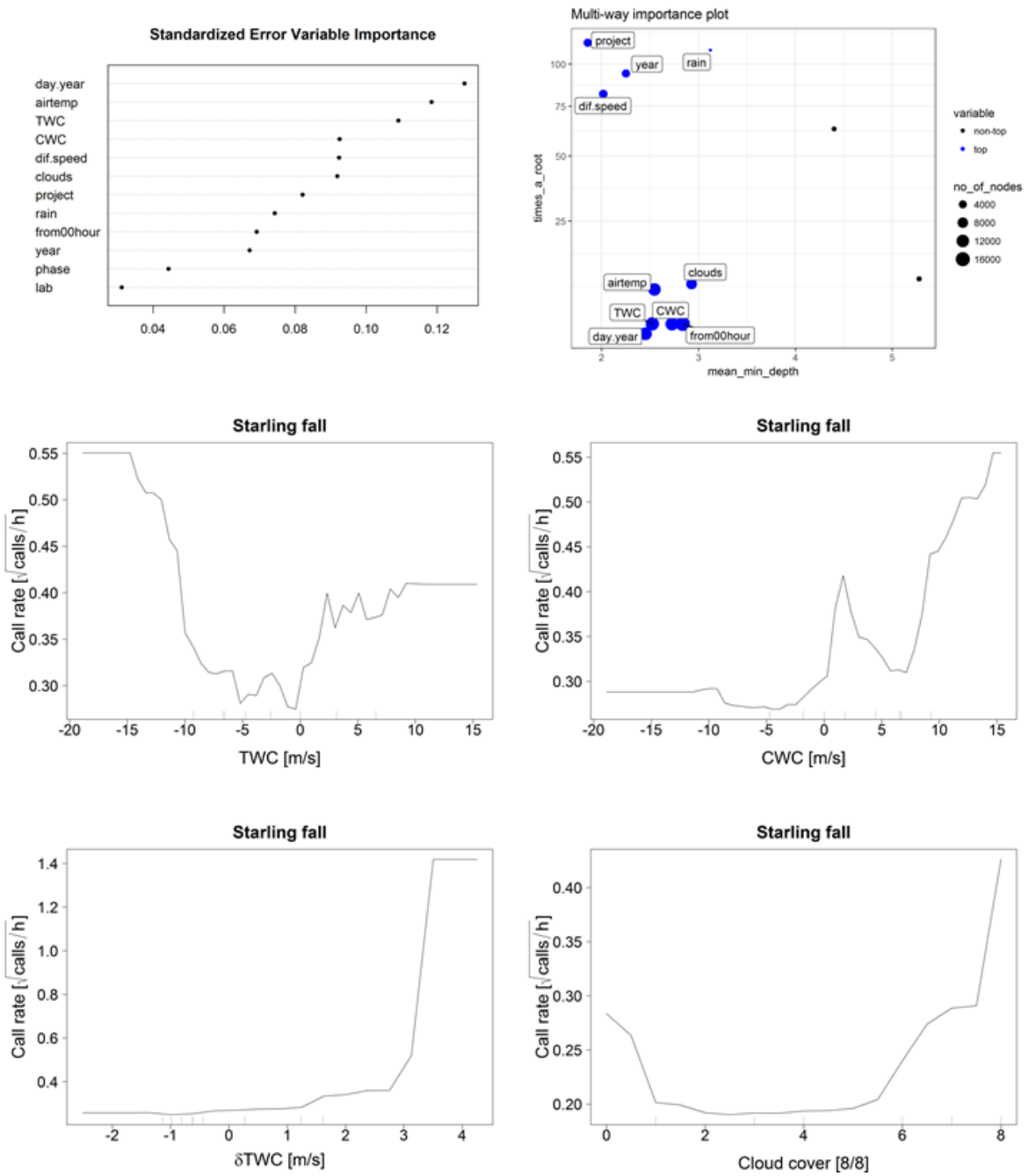


Figure A. 36 Starling fall, continued on next page.

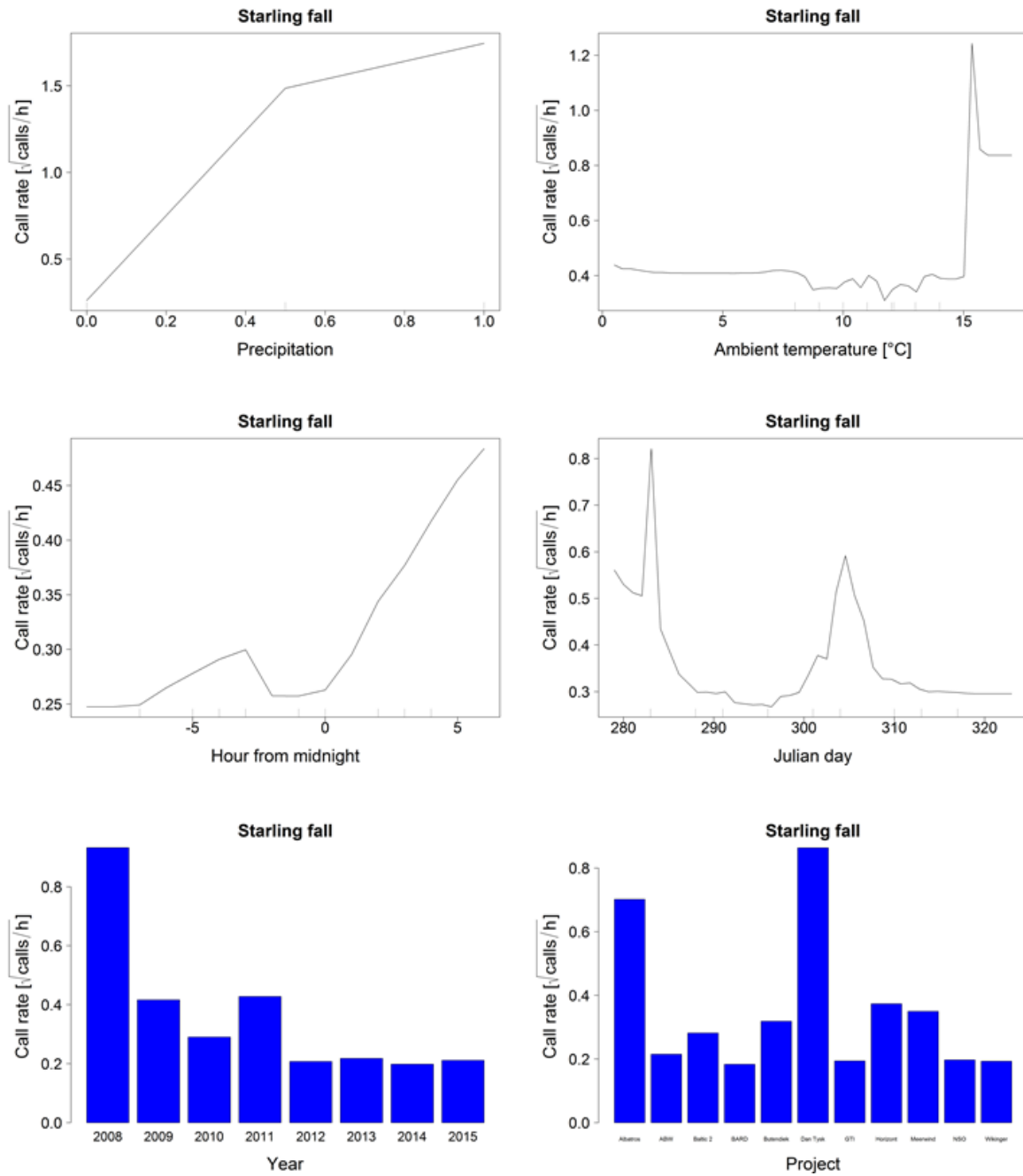


Figure A. 36 Starling fall, continued on next page.

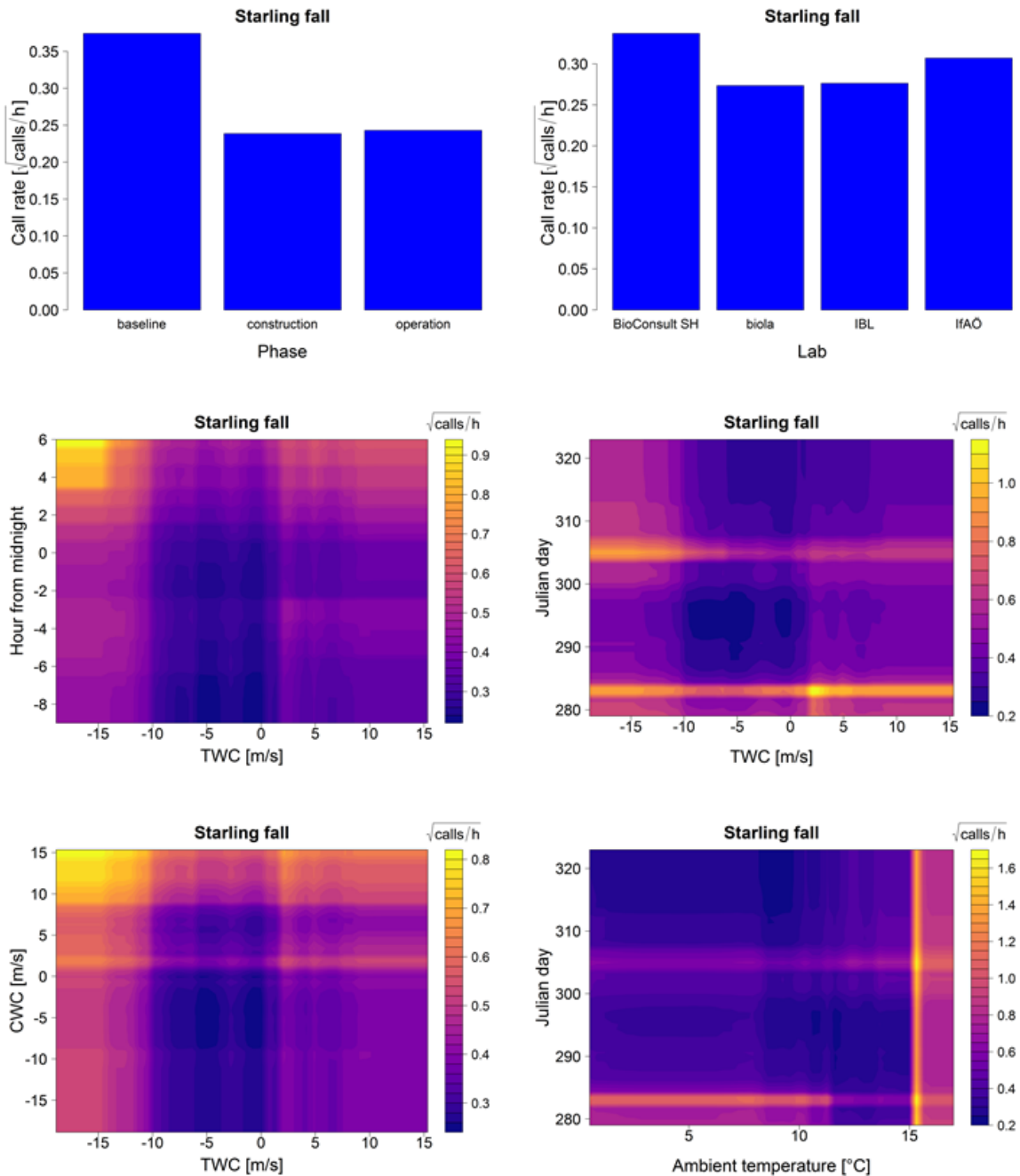


Figure A. 38 Starling fall: Top left panel shows the Standardized Error Variable Importance (%IncMSE) plot. Top right panel shows the multi-way importance plot. Below are the partial dependence plots for each variable included in the model (note the different scales of the partial effect on the y-axis). In the lower panels interaction plots are shown: TWC vs CWC, TWC vs Julian day, TWC vs hour from midnight and Julian day vs ambient temperature. Colours of the interaction plots represent the predicted bird call rate (square root transformed) for each combination of effects.